博士論文

Comprehensive Assessment of Urban Development and Its Environmental Implications Between China and Japan

中国と日本における都市発展及びその環境への影響

の総合評価に関する研究

北九州市立大学国際環境工学研究科

2020 年 9 月

彭　王崇彧

PENG WANGCHONGYU

Doctoral Thesis

Comprehensive Assessment of Urban Development and Its Environmental Implications Between China and Japan

September 2020

Wangchongyu PENG

The University of Kitakyushu

Faculty of Environmental Engineering

Deprtment of Architecture

Gao Laoratory

Preface

This study focused on the spatial effect impact on city development. Cities in China and Japan were selected for case study and further comparison analysis as the cities are in different city development phases. The issue of city development was investigated from multiple perspectives. Spatial dependence and spatial heterogeneity of urbanization or urban shrinkage were found through spatial analysis. The focus is set on exploring the characteristics and correlates of city development, and its impact on thermal environment for cities in China and Japan.

ACKNOWLEDGEMENTS

It is a great experience for me to come to Japan and follow Prof. Weijun GAO in the University of Kitakyushu. The past five years is very memorable time for me. I would like to extend heartfelt gratitude and appreciation to the people who helped me bring my study into reality.

Firstly, I would like to express the deepest appreciation to my advisor, Prof. Weijun GAO, for his great support and motivation for the work. His optimistic attitude and guidance have helped me greatly these years. In addition, Prof. Gao provides me a free space to develop my knowledge and teaches me how to become a matured researcher. Apart from the study, he also gives me much help and instruction for my daily life.

Also, I would like to express my thanks to all university clooeagues, especially Dr. Wei CHEN, Mr. Yujun YANG, Dr. Jinming JIANG, Mr. Rui WANG, Mr. He Wang, Dr. Yinqi ZHANG who give me the help, cooperation, and supports of reaseach and daily life in Japan. And thanks to all the members of Gao Laboratory, especially Dr. Jianan LIU, Ms. Danhua WU, Mr. Neng QU, Mr. Fanyue QIAN, Mr. Zhen YANG et al for their help and supporting during the study and life.

Finally, many thanks to my family for their love and encouragement which is beyond words.

COMPREHENSIVE ASSESSMENT OF URBAN DEVELOPMENT AND ITS ENVIRONMENTAL IMPLICATIONS BETWEEN CHINA AND JAPAN

ABSTRACT

The development of the city is the current main theme. However, there are great differences of the development stages among cities in the world. At present, China is mainly faced with uncoordinated development caused by rapid urbanization, large environmental problems, and obvious regional differences. Meanwhile, Japan is facing a serious problem of city shrinkage.

This study compares the urban development between China and Japan and its environmental impact through large scale and medium-small scale investigations. In addition, this study focused on exploring the role of spatial independence and spatial heterogeneity effect on urban development and its inner correlation with environment implications. Spatial dependence results from various spatial spillover effects, and spatial heterogeneity results from inherent differences between spatial units and variations over space. The spatial correlation analysis and semiparametric geographically weighted regression (SGWR) are adopted to reveal the spatial dependence and heterogeneity of city development and environment. Moreover, the differences of city development stages, driving forces, and environmental implications are evaluated and compared.

In chapter one, research background and significance of urban development and environmental implications is demonstrated. In addition, the importance of plan and evaluation of urban environment is analyzed and the previous study about this research is reviewed. Then the purpose of the study is proposed.

In chapter two, firstly, the concept and application of geographic information system (GIS) and remote sensing (RS) is introduced. In addition, theory, development history and application methods for ESDA are described. Finally, this thesis presents a loose-coupled urban development evaluation method considering the strength and weakness of both the GIS and RS. The requirement, conceptual framework and integration component for the association between GIS and RS is discussed.

In chapter three, we developed global, local, and mixed models to capture the spatiotemporal differences in determinants affecting urbanization in China based on national statistics data from 2005 to 2015. The correlation between the demographic, economic, infrastructure and social indexes and urbanization was revealed through quantitative analysis. PCGDP, GDPS, AFC, and EMBC, which refer to the economy development and urban infrastructure, were the critical spatially non-stationary correlates, with large estimated coefficients, affected the urbanization in different regions at different times. UPR, HIRE which refer to the demographic structure and educational resources

with large estimated coefficients, affected the urbanization spatially stationary. The findings contribute to improving our understanding of the situation and correlates of urbanization, and provide valuable information for governments and planners when developing effective coping strategies for sustainable city development.

In chapter four, we developed global, local, and mixed models to capture the spatiotemporal differences in determinants affecting city shrinkage in Japan based on national census data from 2005 to 2015. City shrinkage in Japan is a serious national problem, which showed a significant increasing positive spatial autocorrelation; Hokkaido, Tohoku, and Shikoku had the largest shrinking city clusters, and this phenomenon has already occurred in suburban areas around the Tokyo and Nagoya city clusters. The correlation between the demographic, economic, and social indexes and city shrinkage was revealed through quantitative analysis. Low fertility, ageing population, and industry changes, expressed by APR, UPR, and ECR, were the critical spatially non-stationary correlates, with large estimated coefficients, affected the city shrinkage in different regions at different times. The findings contribute to improving our understanding of the situation and correlates of city shrinkage, and provide valuable information for governments and planners when developing effective coping strategies for city regeneration.

In chapter five, the coupling coordination degree model make it possible to assess the comprehensive level of urbanization for cities in the Beijing city cluster from 2000 to 2017. The results suggest that those five indicators made the enormous contribution in evaluating the urbanization level, and determining the coupling coordination degree of urbanization. Besides, the results reveal that the coordinated urbanization in the region from 'barely coordination' to 'medium coordination' to 'good coordination'. This study can provide useful information for understanding the current level of urbanization and promoting sustainable development in the future. In the foreseeable future, the comprehensive urbanization process in the Beijing city cluster will be the main component of China's urbanization. Our empirical analysis for the 13 cities in the Beijing city cluster illustrated that the coupling coordination urbanization model is a useful tool which contribute to improve the understanding of the urbanization process and help with management policies and strategies for comprehensive development of urbanization for cities and balanced development for the region.

In chapter six, we first applied global and local Moran's tests to investigate the population change since the city plan with the concept of compact city come out. The results the change is not spatially dependent. However, according to the results of local Moran's I statistics, there are six main regions with their own characteristics of population shrinkage and expansion. The shrinkage and expansion of the six main regions in Kitakyushu have some similarities, but the differences are larger. The government wish the compact city model to creates benefits that are attractive to modern urbanites. The desired benefits include shorter commute times, reduced environmental impact of the community, and reduced consumption of fossil fuels and energy.

In chapter seven, we developed RF models to downscale the MODIS LST products during eight periods in Fukuoka, Japan. Then we captured the spatial correlation between the population, the LULC, and the LSTs, and explored the cooling effect potential of the urban blue-green spaces. The downscaled LST results showed good fitting performance of the RF model. With such downscaling methods, analysis on the SUHI and its correlates could be spatial-temporal precisely in a cloudy, rainy area using remote sensing data. We found the LULC could have an impact on the LST of its surrounding neighbors, and which also is the basis for investigating the cooling effect of the urban blue-green spaces. Through zonal statistics, the forest and sea could significantly mitigate the UHI in its approximate 1 km buffer zone, while the mitigation effect of the water and the grassland on the UHI are less spectacular compared with the forest and sea. The findings contribute to improving our understanding of the spatial temporal variation and the correlates of UHI, and provide valuable information for governments and planners to developing effective coping migration strategies for the UHI considering the perspective of the local environment.

In chapter eight, the urban development process in China and Japan is summarized. From 2005 to 2015, the economic factors have a little spatially stationary impact both in China and Japan. In addition, the social factors have great spatially non-stationary impact on urbanization of cities in China while the effect is global and little in Japan. Moreover, strong evidence showing that urban heat island was related to city size that the intensity varies spatially with a sequence of mega-city > large-city > mid-city; whilst it varies temporally with a course of summer > winter and daytime > nighttime through differences of SUHI through time. Also, significant increases both in extent and magnitude of SUHI were observed for the 60 cities. In the foreseeable future, the comprehensive urbanization process in several main city clusters will be the main component of China's urbanization, while cities in Japan will face increasing urban shrinkage phenomena.

In chapter nine, the whole summary of each chapter has been presented.

CONTENTS

Chapter 3. Spatial temporal assessment of urbanization of China

Chapter 4. Spatial temporal determinants of city shrinkage in Japan

Chapter 5. Comprehensive evaluation of urbanization process in Beijing city cluster

Chapter 8. Comparison of urban development and thermal environment in China and Japan

Chapter 9. Conclusion

CONTENTS OF FIGURES

CONTENTS OF TABLES

Chapter 1. Previous study and purpose of the study

1.1. Introduction

As of 2019, more than half of the world's population is living in urban areas, and the rate is expected to reach 65% by 2030 and 70% by 2050 [1]. With the rapid development of information networks, the global mobility of capital and labor has increased, and large-scale urbanization movements have begun around the world [2]. For developed countries, it has entered the post-urbanization stage. And most developing countries are still in the period of excessive urbanization from the beginning to rapid development. In recent years, there has been a positive understanding of urban development, which has been incorporated into the national development policy [3].

At the turn of the century in 2000, there are 371 cities with a population of over 1 million worldwide. By 2018, the number of the cities with at least 1 million inhabitants has increased to 548, and by 2030, 706 cities are expected to have at least 1 million inhabitants. Cities with a population of more than 10 million are often referred to as megacities. The number of megacities globally is expected to be 33 in 2018 and 43 by 2030. In 2018, 48 cities had a population between 5 and 10 million. By 2030, 10 of them are expected to become megacities. Between 2018 and 2030, there will be 13 in Asia and 10 in Africa. In 2030, the population of 66 cities is expected to be between 5 and 10 million inhabitants. Most cities in the world have fewer than 5 million inhabitants. Asia has the largest population in the world, with most countries being the developing countries (Fig. 1-1) [4]. In the next decades, population growth will be the most noticeable, and corresponding strategies are urgently needed to deal with related problems.

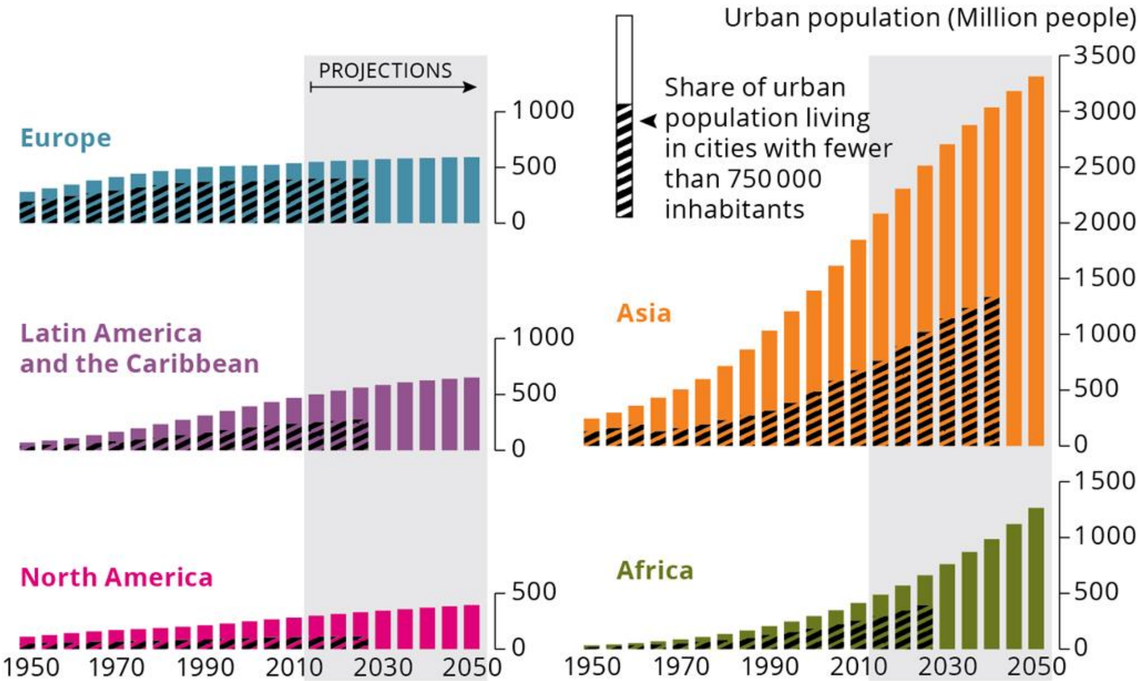

Fig. 1-1 Urban trends by world regions, 1950-2050

(Source: UN World urbanization prospects: The 2012 revision)

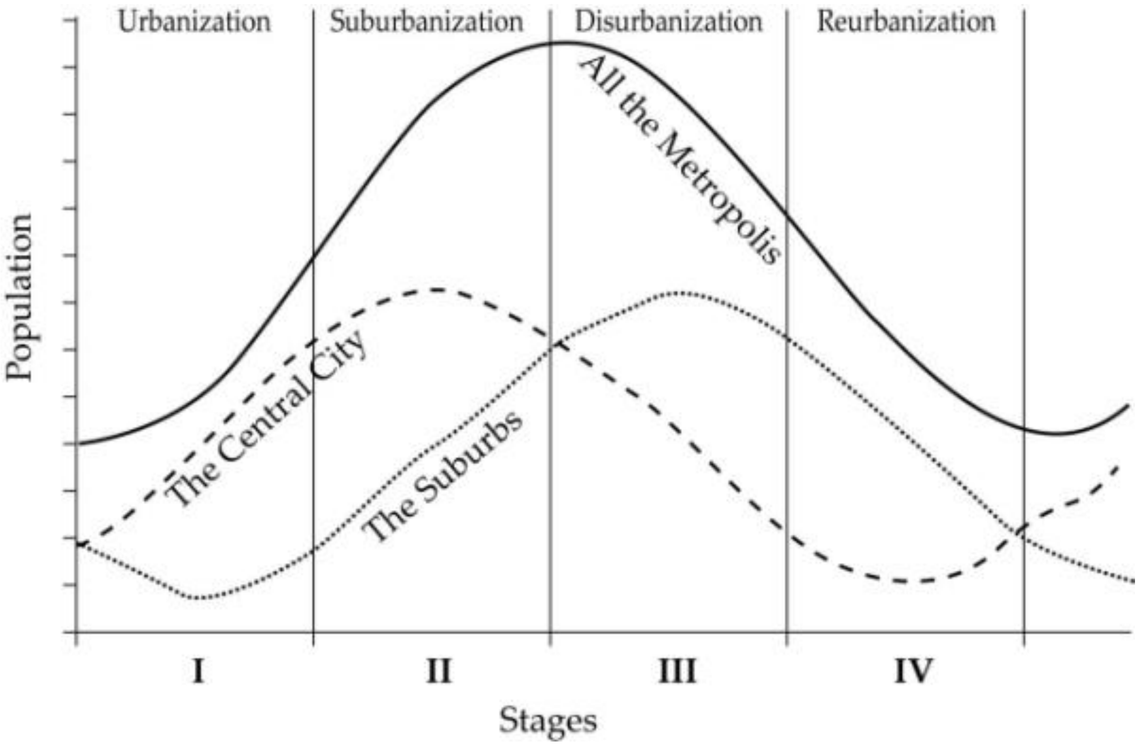

Fig. 1-2 City development model

(Source: Berg, L. van den, Klassenn, L.H., Rossi, A. and Vijverberg, C.H.T. (1982). Urban Europe: a Study of Growth and Decline, vol 1: Oxford: Pergamon)

Berg et al. (1982) portrayed the evolutionary course of a metropolitan region in four phases (Fig 1-2) [5]. In the first phase, urbanization, the central city occupies a dominant position. It has achieved a positive immigration balance and has become the main node of regional employment. In the second stage, suburbanization is the shift of the focus of population and land-intensive uses to the suburbs. However, the central city is still the core of employment in the region. In the third stage, de-urbanization, the metropolis tends to split into many urban centers, some of which are located on the edge of the city [6]. At this stage, the metropolis has lost its compact node structure, and population and employment in the central city and its surrounding suburbs have tended to decline. The fourth stage, re-urbanization, although in the theoretical stage before theory, is considered by Berg et al. (1982) as a remedy for the split structure of the metropolis. The fourth phase is now more likely refers to a strict re-urbanization strategy aimed at reviving their original metropolitan core to become a high-density, function-intensive "compact city"[7].

With the development of urbanization, there are many urban phenomena occurred. This includes population issues, environmental issues, social issues and many other aspects. Each city is facing or will face some of these problems during its development. Meanwhile, these problems are gradually intensifying with the development of the city and have aroused widespread concern. Cities at different stages of urban development, are facing with many different problems. Therefore, it is necessary to analyze the problems and their causes facing cities at different development stages, and explore countermeasures to provide effective responses to the government and policymakers.

1.2. Research background and significance

1.2.1 Introduction of urbanization and city shrinkage

Urbanization is a population movement phenomenon that people shift from rural area to an urban area. The phenomenon is having a massive impact on the economic, social, environmental landscape all over the world. While the process of urbanization keeping going on, more and more problems occur that we are required to make it process on a more sustainable and equitable path [1].

Urbanization took place over a period of several decades in Europe countries and North America countries. And it is happening in East Asia only a few years. It's an essential role for urban policy makers that they take the responsibility for making all the residents living in the urban areas a better living environment [2]. Urban growth and sprawl have severely altered the biophysical environment. Rapid urbanization has significant influence on different aspects of the quality of life and research in determining the patterns of urbanization and quantifying their impacts is the need of the hour. Unplanned urbanization an urban sprawl will directly affect the land use and land cover of the area. The changes in land cover include loss of agricultural lands, loss of forest lands, increase of barren area, an increase of impermeable surface of the area because of the built-up area. For the sustainable urban eco-systems, the amount of land required for growing the vegetation can be estimated from these studies. For a city being built, it will be really hard to change the urban form and land use patterns of the city. If there is something defective of the urban form, it will cost a large sum of money and years to undo the mistakes.

The process of urbanization provides people in urban areas a better living environment and working opportunities. East Asia has a numerous population, and a large amount of developing countries. Therefore, we can foresee a fast expansion of urban areas where millions of East Asia people will have the chance to leave extreme poverty behind and to prosper in the coming decades.

Urbanization is not easy to evaluate due to the processing of urbanization itself is very complicated and confused to understand, the scholars around the world would like to judge the level of urbanization by many parameters such as the urban population, the economic index, the energy usage, also the urban facilities construction, etc. Urbanization reflected in every regard of a city, to have a comprehensive understanding of urbanization of a city, it is necessary to do the analysis from many different parts of the urban development and have a comprehensive assessment of the city development [3].

However, city shrinkage, as the antithesis of urbanization, is an ongoing extreme phenomenon not only in developed countries, but also emerging in some fast-urbanizing countries [11, 12]. City shrinkage is characterized by population loss, economic downturn, and inefficient land use [13-15]. Especially in the developed world, with a background of globalization and de-industrialization, many large cities are considered shrinking cities or will be shrinking cities [16-19]. Research on the city shrinkage not only provides solutions for the affected regions, but also alerts fast-urbanizing areas about future problems.

The process of city shrinkage occurs within a complex system, so studies on city shrinkage considered many aspects. Many studies focused on the policies and response to city shrinkage and called for local corresponding strategies for the sustainable development of the cities. For example, by assessing four policy responses to city shrinkage in Europe, improving the quality of life of local citizens is the optimal strategy for local government [20]; by identifying the shortcomings of the local government response to city shrinkage as lack of transparency and lack of understanding of best practices, the development of local adaptation policies in shrinking cities is required [21]. Some scholars focused on exploring the factors driving city shrinkage. The driving factors vary from demographics, economy, society, and policies at global and local levels. For example, socio-spatial inequalities were found to more strongly influence city shrinking compared with economic factors in the American Rust Belt [22]; falling birth rates and the effects of German reunification were the main factors affect shrinkage in Germany [23]. The demographic change, which refers to the ageing population and low birth rate, is the primary cause of city shrinkage in Japan [12]; the economic level and population structure are highly related to city shrinkage in China [24].

1.2.2 Trends of urban development implications

Increasing inequality in and among cities: Inequality has become a major trend that has an impact on achieving the New Urban Agenda and the Sustainable Development Goals. The gap between rich and poor is currently at its highest level in the past 30 years; since the 1980s, the highest-income 1% share of global economic growth has doubled the poorest 50%. At the city level, 75% of the world ’s cities have higher income inequality than they did 20 years ago. Inequality in cities is more pronounced than in rural areas, and women, youth and the elderly are particularly affected by inequality. The New Urban Agenda and the 2030 Agenda for Sustainable Development seek to address inequality by leaving no one behind, which requires the provision of equal infrastructure and basic services and adequate and affordable housing, and promotes productive employment and decent work for everyone. On the other hand, due to the different functions and different development levels of cities in urban agglomerations, the city gaps in some urban agglomerations have gradually widened. How to achieve collaborative development has become an important issue.

Population aging is happening all over the world: Globally, the population aged 60 and above is growing at a rate of 3.3% per year, faster than any other age group. Planning for the aging of the urban population requires innovation to meet the increasing demand for health care, leisure, transportation, housing and other facilities for the elderly, and to respond to the impact of social protection and pension schemes. This phenomenon is particularly prominent in Japan. Japan’s population has continued to decline in recent years. The low birth rate, strict naturalization policy, and the extension of life expectancy brought by the advanced medical system have made Japan's aging rate increase very quickly. The shrinking population in Japanese cities is also due to the primary cause of the population structure.

Urban expansion and low-density development: As the urban population increases, the land area occupied by the city increases at a faster rate. On average, the growth rate of urban land area is twice that of the urban population. This has led to a decrease in density and a more scattered urbanization model, manifested in the disordered expansion of cities. Low-density development not only wastes resources, but also increases travel distance and energy consumption, increases the cost of providing infrastructure, reduces the economic effects of agglomeration, and reduces urban productivity.

Environmental implications: Climate change is one of the biggest challenges that cities must deal with. Urban energy 60% to 80% of source consumption and produce up to 70% of anthropogenic greenhouse gas emissions. Cities are also extremely vulnerable to climate change and extreme weather events. Therefore, climate change is not only a global issue but also a local issue. Cities play a vital role in addressing climate change and achieving the goals of the Paris Agreement. To address the impact of climate change on cities, partnerships have been established. The New Urban Agenda and the 2030 Agenda for Sustainable Development provide many opportunities for developing strategies to mitigate and adapt to climate change, especially through environmental sustainability and resilient urban development. In cities around the world, there are large differences in environmental issues, such as the water pollution, air pollution, etc. The environmental problems facing cities in developing countries are much more complicated than those in developed countries. For example, the PM2.5 problem in China in recent years has rarely been affected in other countries. Kitakyushu City in Japan has caused serious air and water pollution due to urban development, but through effective management, these environmental problems have been effectively improved. Different the other environmental implications, the urban heat island (UHI) is a kind of environmental implication that all the cities are facing. The UHI effect refers to the city's "high temperature" caused by a large number of artificial heat generation, high heat storage bodies such as buildings and roads, and the reduction of green space. The temperature in the city is significantly higher than that in the surrounding suburbs. On the near-surface temperature map, the suburban air temperature changes little, and the urban area is a high-temperature area, like an island protruding from the sea. Because this island represents a high-temperature urban area, it is called the urban heat island. The main factors that form the urban heat island effect include urban underlying surface, artificial heat source, water vapor influence, air pollution, green space reduction, population migration and many other factors. The distribution of UHI is often correlate to the urban rain island (URI), urban dry island (UDI), urban fog island (UFI), and urban pollution island (UPI). This study investigated the impact of urban development on the urban environment through the analyst of UHI.

1.2.3 Research Significance

Urban development refers to the process of the change and growth of the city's status and role, its attractiveness, and its radiant power within a certain region. It is a process to meet the multi-level needs of the growing urban population. Including quantitative expansion and qualitative improvement. The quantitative expansion is manifested by the increase in the number of cities and the expansion of scale, that is, the improvement of the level of urbanization; the improvement of quality is manifested by the strengthening of urban functions and the improvement of modernization. Urban development, from a spatial perspective, is a unique form of settlement that exists in a country or region. As a gathering point of regional economy, technology, politics, production, population, information, transportation, culture, etc., the city has a certain attraction to its surrounding area, and the city continues to produce radiation to the surrounding area during its operation. As previous studies on policy responses to urbanization and urban shrinkage illustrate the local strategies are more effective and required than corresponding global policies, understanding the local driving factors from the global level is essential for policies makers and actors to better respond to this phenomenon. Most previous studies did not take the spatial effects into consideration, this significance of the urban research needs to be explored in terms of spatial effects.

Spatial dependence results from various spatial spillover effects, and spatial heterogeneity results from inherent differences between spatial units and variations over space [25, 26]. Ordinary least squares (OLS) regression can be used to assess the general correlates of city shrinkage where the correlates are spatially stationary [24]. However, local adaptation strategies are required to identify the spatial heterogeneity of city shrinkage. Geographically weighted regression (GWR) has become an increasingly essential tool for revealing local variables' effects on the dependent variable over a geographical area [27-30]. In the GWR model, all the explanatory variables are spatially non-stationary. The semiparametric geographically weighted regression (SGWR) model, which is a mix of OLS and GWR models, is useful in situations where certain explanatory variables influencing the response are global while others are local [31]. Compared with the traditional OLS and GWR models, the SGWR model is usually more interpretive [32-34]. As shrinking cities may have several similar characteristics, which are better considered as spatially stationary impact factors, the SGWR model could be more appropriate for modeling the driving factors of urban development.

1.3. Review of previous study

1.3.1 Study on urban development

During the past few decades, the world was undergoing fast pace urbanization, particularly in China [37,38]. With the continuous rural-urban migration and urban expansion, more mega cities, large cities have emerged continuously in China. However, there are quite differences in urbanization level according to cities in China [39, 40]. Along with the rapid urbanization and modernization, built-up areas replaced with natural landscapes, and thus many environmental issues occurred, such as water and air pollution, increase in greenhouse gas, increase in fossil fuel energy consumption, and urban heat islands [41-43]. The most significant environmental implications of urbanization are water-air pollution, increase in energy consumption, and the urban heat island (UHI). Numerous studies have found that urbanization has a significant effect on the environment and urban quality [44-46]. With increasing closely economic and traffic connection among cities, three principal urban agglomerations emerged in China, including the Yangtze River Delta Region, the Peral River Delta Region, and the Beijing city clyster (also known as Beijing-Tianjin-Hebei Region) [47]. The urban built-up areas and the urban environment form a complex system with multiple feedback loops. Hence, it is essential to study the urbanization process and its impact on the urban environment on the urban agglomeration scale instead of a signal city for maintaining a good quality of urbanization and better urban planning strategies.

Within systems theory, a complex system refers to its constituent elements cannot explain the overall characteristics for their nonlinear links [48]. Previous studies showed urbanization process is a complex system which is inappropriate to evaluate only using population, such economy factors and social infrastructure factors are also essential parts for urbanization evaluation [49-52]. At present, there are several methods applied to assess urbanization including AHP, fuzzy comprehensive evaluation method, entropy method, gray relational analysis, and so on [53-56]. The entropy method is a useful tool according to the abstraction and quantitative difficulty of urbanization impact factors. Information entropy is defined as the measurement of the degree of order that higher entropy indicates more information, and lower entropy indicates less information. The urbanization coupling coordination model treats demographic urbanization, economic development, and social development as three subsystems that interact with each other nonlinearly. The three subsystems are considered as independent but integrated systems. The coordination statement between subsystems is an indicator of sustainable development, providing a standard for judging whether the system is tending to higher-order [57].

1.3.2 Study on urban heat island

With urban development, environmental implications become essential issues for urban planning. Panel data and monitoring stations data were the primary sources for evaluation of environmental implications such as water pollution and air pollution. However, remote sensing (RS) and GIS technologies enable large-scale research of the UHI which are increasingly used in recent UHI studies [58]. Compared with the traditional method for UHI studies of observing meteorological data, which has the limitation that the local meteorological observation points are not able to represent the whole study region, the RS based studies provided high resolution of spatial-temporal information. There are several RS datasets used in UHI studies, including NOAA AVHRR [59], ASTER [60,61], MODIS [62], and Landsat series [63,64]. However, there are many limitations of the satellite remote sensing approach. One of the most significant weaknesses of remote sensing data is that the data accuracy could affect by could cover. Therefore, two possible solutions including choosing cloud-free images or constructing temporally composited data are mainly adopted to decrease the impact of clouds [60, 65-67]. Hence, Moderate Resolution Imaging Spectroradiometer (MODIS) LST products have become an increasingly important source in UHI studies for providing land surface temperature (LST) images with 1 km spatial resolution and high temporal resolution (per day) which decrease the clouds impact and make temporal UHI studies available.

1.4. Purpose of this study

This study focuses on evaluation of urban development and its environmental implications. Cities and regions in different urban development stage were taken into consideration with the integration of geographic information system and remote sensing. Based on the previous study and theory analysis, the explanatory spatial data analysis methods were applied in the study. Fig. 1-3 is the research flow.

✧ Previous study

In chapter one, research background and significance of urban development and environmental implications are investigated. In addition, the importance of evaluation of urban environment is analysis and the previous study about this research is reviewed. Finally, Purpose of this study is proposed.

✧ Study methods

In chapter two, firstly, the concept and application of GIS and RS is introduced. In addition, the application and principle of explanatory spatial data analysis are described. The requirement, of integration component for the association between GIS and RS is discussed.

✧ Numerical analysis of urban development

In chapter three, as the urbanization and land sprawl had drawn more and more attention, it is meaningful and useful to have an investigation of the urbanization in China. The investigation of urbanization can help us to get a comprehensive understanding of the urban land use and land cover variation during the years. After the investigation, not only can we get the advantages and benefit from the development, but also present the imbalance and weakness to remind us what we should do for our city to get a better condition. The investigation of urbanization also can let us know the urban development trend where more attention should be paid to make sure the steady development of the city from a global view.

In chapter four, the population change ratio derived from national census data in 2005, 2010, and 2015 was selected as the city shrinkage index, and a total of 1647 municipalities in Japan were selected as study objects. The objectives of this study were to (1) investigate the spatiotemporal distributions and patterns of shrinking cities in Japan; (2) reveal the interrelationship between city shrinkage and demographic, economy, and social indexes on global and local scales; and (3) compare the determinants across different regions from a global view. The findings illustrate the local determinants of city shrinkage in Japan, improve the understanding of the situation and the factors driving city shrinkage, provide valuable information for governments and planners developing effective coping strategies on the global and local levels, and hopefully will draw the attention of fast-developing countries to this possible future issue.

In chapter five, we took the Beijing city cluster as a local case of urbanization study, which is locating on the North China Plain, being the economic and cultural center in north China. There are in total 13 cities with quite differences in urbanization level in the region. This research is structured as follows: after presenting study area, data and methods, we will evaluate the urbanization process and it coupling coordination degree for the 13 cities in the Beijing city cluster from 2000 to 2017. Then the surface urban heat island (SUHI), one of the environmental implications, will be investigated utilizing two indicators from SUHI magnitude and extent aspects for the 13 cities in summer and winter both in daytime and nighttime from 2000 to 2017. Then, four cities in the core area of the region are selected for analyzing the impact of urbanization effect on SUHI.

In chapter six, we explored the spatial population change patterns and its impact factors in Kitakyushu from a local level. As the first city plan based on the compact city idea was issued in 2003, the study period was selected from 2000 to 2015. The objectives of this study were to (1) investigate the spatiotemporal distributions and patterns of population change in Kitakyushu; (2) reveal the interrelationship between urban shrinkage and aggregation and demographic, economy, and social indexes on global and local scales; and (3) compare the determinants across different regions. The findings illustrate the local determinants of urban shrinkage in Kitakyushu, improve the understanding of the situation and the factors driving city shrinkage, provide valuable information for governments and planners developing effective coping strategies on the global and local levels, and hopefully will draw the attention of other cities to this possible future issue.

✧ Numerical analysis of urban heat island

In chapter seven, one of the most urbanized areas, Fukuoka prefecture (Japan) was selected as the study area. The main objectives are first to investigate the UHI in this area during summer and winter both in the daytime and nighttime; second to explore the spatial correlation between the population, the LULC and the LSTs; and third to explore the urban cooling effect of the urban blue-green spaces. For the following reasons, we developed RF models to downscale the LSTs in the area with MODIS LST products from 1 km spatial resolution to 250 m: (1) the area is cloudy and rainy during the years that remote sensors with the low temporal resolution are not applicable for this area for the discontinuous time-series observations for the same area and high possibility of the images with high cloud cover; (2) various studies concluded the urban cooling effect of the water bodies and green spaces was relate to its size, and the affected distance is less than 1 km; and (3) the RF models for downscaling LSTs have better fitting performance than the other methods. The study contributes to illustrate the spatial correlates of LSTs, improve the understanding of the situation and the factors driving UHI, provide valuable information for governments and planners developing effective coping strategies on the UHI, and hopefully will draw the attention of the urbanizing cities.

✧ Discussion of urban development and thermal environment between China and Japan

In chapter eight, we took sixty cities in China and Japan as targets to compare the urbanization and UHI, one of the most severe environmental implications. The main purpose of this chapter is to have a comprehensive understanding of the numerical analysis chapters, to have a comparison and better understanding of urban development similarities and differences in China and Japan.

✧ Conclusion

In chapter nine, a conclusion of the whole study is summarized.

Previous study	**Chapter one** Previous study and purpose of the study	
Theoretical survey	**Chapter two** Theories and methods of urban development assessment	
Urban development assessment	**Chapter three** Spatial temporal assessment of urbanization in China	**Chapter four** Spatial temporal assessment of city shrinkage in Japan
	Chapter five Comprehensive urbanization assessment of Beijing city cluster	**Chapter six** Correlation analysis of population change and urban vitality in Kitakyushu
Environmental implication assessment	**Chapter seven** Spatial temporal analysis of thermal environmental implications based on remote sensing	
Comparative analysis	**Chapter eight** Comparison of urban development and thermal environment in China and Japan	
Conclusion	**Chapter nine** Conclusion and prospect	

Fig. 1-3 Research flow

Reference

[1] Nations U. 2018 revision of world urbanization prospects. United Nations Department of Economic and Social Affairs; 2018.

[2] Nations U. The worlds cities in 2018 data booklet. United Nations Department of Economic and Social Affairs; 2018.

[3] Habitat U N. State of the world's cities 2012/2013: Prosperity of cities[M]. Routledge, 2013.

[4] Nations U. 2012 revision of world urbanization prospects. United Nations Department of Economic and Social Affairs; 2018.

[5] Berg, L. van den, Klassenn, L.H., Rossi, A. and Vijverberg, C.H.T. (1982). Urban Europe: a Study of Growth and Decline, vol 1: Oxford: Pergamon

[6] Johnson, J. H. (1974). "Geographical Processes at the Edge of the City". In Johanson, J.H., Suburban Growth. London: Wiley, 1-16.

[7] Shachar, A. (1997). "A Metropolitan Approach in Planning the Urbanized Area of Tel Aviv". In Nachmias, D. and Nahum, G. (editors), Tel Aviv-Yafo, Social Processes and Public Policy. Tel Aviv: Ramot Press, Tel Aviv University, 305-319.

[11] Haase A, Rink D, Grossmann K, Bernt M, Mykhnenko V. Conceptualizing urban shrinkage. Environment and Planning A. 2014;46:1519-34.

[12] Mallach A, Haase A, Hattori KJC. The shrinking city in comparative perspective: Contrasting dynamics and responses to urban shrinkage. 2017;69:102-8.

[13] Hattori K, Seike Y, Yoshida Z, Hamaguchi S, Yamada H, Suzuki N, et al. Shrinkage of tokamak current channel by external ergodization. 1984;121:368-73.

[14] He SY, Lee J, Zhou T, Wu DJC. Shrinking cities and resource-based economy: The economic restructuring in China's mining cities. 2017;60:75-83.

[15] Hospers G-JJUdi. Coping with shrinkage in Europe's cities and towns. 2013;18:78-89.

[16] Großmann K, Bontje M, Haase A, Mykhnenko VJC. Shrinking cities: Notes for the further research agenda. 2013;35:221-5.

[17] Haase D, Haase A, Kabisch N, Kabisch S, Rink DJEM, Software. Actors and factors in land-use simulation: The challenge of urban shrinkage. 2012;35:92-103.

[18] Haase DJN, Culture. Urban ecology of shrinking cities: an unrecognized opportunity? 2008;3:1-8.

[19] Rieniets TJN, Culture. Shrinking cities: causes and effects of urban population losses in the twentieth century. 2009;4:231-54.

[20] Hospers G-JJEPS. Policy responses to urban shrinkage: From growth thinking to civic engagement. 2014;22:1507-23.

[21] Syssner JJARdEsDyDR. Planning for shrinkage? Policy implications of demographic decline in Swedish municipalities. 2016:7-31.

[22] Sadler RC, Lafreniere DJ. Racist housing practices as a precursor to uneven neighborhood change in a post-industrial city. Housing Studies. 2017;32:186-208.
[23] Wiechmann T, Pallagst KMJIjou, research r. Urban shrinkage in Germany and the USA: A comparison of transformation patterns and local strategies. 2012;36:261-80.
[24] Zhang Y, Fu Y, Kong X, Zhang FJSC, Society. Prefecture-level city shrinkage on the regional dimension in China: spatiotemporal change and internal relations. 2019;47:101490.
[25] Anselin L. The Moran scatterplot as an ESDA tool to assess local instability in spatial association: Regional Research Institute, West Virginia University Morgantown, WV; 1993.
[26] Anselin LJGa. Lagrange multiplier test diagnostics for spatial dependence and spatial heterogeneity. 1988;20:1-17.
[27] Brunsdon C, Fotheringham AS, Charlton MEJGa. Geographically weighted regression: a method for exploring spatial nonstationarity. 1996;28:281-98.
[28] Fotheringham AS, Brunsdon C, Charlton M. Geographically weighted regression: the analysis of spatially varying relationships: John Wiley & Sons; 2003.
[29] Fotheringham AS, Charlton ME, Brunsdon CJE, A p. Geographically weighted regression: a natural evolution of the expansion method for spatial data analysis. 1998;30:1905-27.
[30] Van Donkelaar A, Martin RV, Spurr RJ, Burnett RTJEs, technology. High-resolution satellite-derived PM2.5 from optimal estimation and geographically weighted regression over North America. 2015;49:10482-91.
[31] Mei CL, He SY, Fang KT. A note on the mixed geographically weighted regression model. Journal of Regional Science. 2004;44:143-57.
[32] Jin C, Xu J, Huang ZJHI. Spatiotemporal analysis of regional tourism development: A semiparametric Geographically Weighted Regression model approach. 2019;87:1-10.
[33] Li W, Cao Q, Lang K, Wu JJSotTE. Linking potential heat source and sink to urban heat island: Heterogeneous effects of landscape pattern on land surface temperature. 2017;586:457-65.
[34] Zhao Q, Wentz EA, Fotheringham S, Yabiku ST, Hall SJ, Glick JA, et al. Semi-parametric Geographically Weighted Regression (S-GWR): a Case Study on Invasive Plant Species Distribution in Subtropical Nepal. 2016.
[35] Hattori K, Kaido K, Matsuyuki MJC. The development of urban shrinkage discourse and policy response in Japan. 2017;69:124-32.
[36] Frey WH. Migration and depopulation of the metropolis: regional restructuring or rural renaissance? American Sociological Review. 1987:240-57.
[37] Pallagst K. Shrinking cities in the United States of America. The Future of Shrinking Cities: Problems, Patterns and Strategies of Urban Transformation in a Global Context Los Angeles (University of California). 2009:81-8.
[38] J. Klugman, *A sourcebook for poverty reduction strategies*. World Bank Washington, DC, 2002.

[39] A. R. dos Santos *et al.*, "Spatial and temporal distribution of urban heat islands," *Science of the Total Environment,* vol. 605, pp. 946-956, 2017.

[40] Q. Chen and Z. Song, "Accounting for China's urbanization," *China Economic Review,* vol. 30, pp. 485-494, 2014.

[41] B. Qin and Y. Zhang, "Note on urbanization in China: Urban definitions and census data," *China Economic Review,* vol. 30, pp. 495-502, 2014.

[42] J. A. Foley *et al.*, "Global consequences of land use," *science,* vol. 309, no. 5734, pp. 570-574, 2005.

[43] L. Zhou *et al.*, "Evidence for a significant urbanization effect on climate in China," *Proceedings of the National Academy of Sciences,* vol. 101, no. 26, pp. 9540-9544, 2004.

[44] H.-M. Zhu, W.-H. You, and Z.-f. Zeng, "Urbanization and CO2 emissions: A semi-parametric panel data analysis," *Economics Letters,* vol. 117, no. 3, pp. 848-850, 2012.

[45] N. B. Grimm *et al.*, "The changing landscape: ecosystem responses to urbanization and pollution across climatic and societal gradients," *Frontiers in Ecology and the Environment,* vol. 6, no. 5, pp. 264-272, 2008.

[46] S. Peng *et al.*, "Surface urban heat island across 419 global big cities," *Environmental science & technology,* vol. 46, no. 2, pp. 696-703, 2011.

[47] D. Zhou, S. Zhao, L. Zhang, and S. Liu, "Remotely sensed assessment of urbanization effects on vegetation phenology in China's 32 major cities," *Remote Sensing of Environment,* vol. 176, pp. 272-281, 2016.

[48] X. Zhu *et al.*, "The inhabited environment, infrastructure development and advanced urbanization in China's Yangtze River Delta Region," *Environmental Research Letters,* vol. 11, no. 12, 2016.

[49] R. Gallagher and T. Appenzeller, "Beyond reductionism," *Science,* vol. 284, no. 5411, pp. 79-80, 1999.

[50] M. Chen, D. Lu, and L. Zha, "The comprehensive evaluation of China's urbanization and effects on resources and environment," *Journal of Geographical Sciences,* vol. 20, no. 1, pp. 17-30, 2010.

[51] M. Chen, D. Lu, and H. Zhang, "Comprehensive evaluation and the driving factors of China's urbanization," *Acta Geographica Sinica,* vol. 64, no. 4, pp. 387-398, 2009.

[52] L. Guo-ping, "The analysis and evaluation of the compatible relationship between industrialization and urbanization in China," *Areal Research and Development,* vol. 5, no. 002, 2008.

[53] Y. Sakieh, B. J. Amiri, A. Danekar, J. Feghhi, and S. Dezhkam, "Scenario-based evaluation of urban development sustainability: an integrative modeling approach to compromise between urbanization suitability index and landscape pattern," *Environment, Development and Sustainability,* vol. 17, no. 6, pp. 1343-1365, 2015.

[54] A. Beskese, H. H. Demir, H. K. Ozcan, and H. E. Okten, "Landfill site selection using fuzzy AHP and fuzzy TOPSIS: a case study for Istanbul," *Environmental Earth Sciences,* vol. 73, no. 7, pp. 3513-

3521, 2015.

[55] Y. Liu, R. Li, and X. Song, "Grey associative analysis of regional urbanization and eco-environment coupling in China," *Acta Geographica Sinica,* vol. 2, pp. 237-247, 2005.

[56] S. Wang, H. Ma, and Y. Zhao, "Exploring the relationship between urbanization and the eco-environment—A case study of Beijing–Tianjin–Hebei region," *Ecological Indicators,* vol. 45, pp. 171-183, 2014.

[57] G. Yan-bing, "Comprehensive assessment on ecological risk of Hexi Corridor urbanization based on normal cloud model and entropy weight," *Journal of Arid Land Resources and Environment,* vol. 26, no. 5, pp. 169-173, 2012.

[58] K. P. Gallo and T. W. Owen, "Satellite-based adjustments for the urban heat island temperature bias," *Journal of applied meteorology,* vol. 38, no. 6, pp. 806-813, 1999.

[59] J. A. Sobrino, J. C. Jiménez-Muñoz, P. J. Zarco-Tejada, G. Sepulcre-Cantó, and E. de Miguel, "Land surface temperature derived from airborne hyperspectral scanner thermal infrared data," *Remote Sensing of Environment,* vol. 102, no. 1-2, pp. 99-115, 2006.

[60] D. R. Streutker and N. F. Glenn, "LiDAR measurement of sagebrush steppe vegetation heights," *Remote Sensing of Environment,* vol. 102, no. 1-2, pp. 135-145, 2006.

[61] L. Liu and Y. Zhang, "Urban heat island analysis using the Landsat TM data and ASTER data: A case study in Hong Kong," *Remote Sensing,* vol. 3, no. 7, pp. 1535-1552, 2011.

[62] R. Pu, P. Gong, R. Michishita, and T. Sasagawa, "Assessment of multi-resolution and multi-sensor data for urban surface temperature retrieval," *Remote Sensing of Environment,* vol. 104, no. 2, pp. 211-225, 2006.

[63] J. Quan, Y. Chen, W. Zhan, J. Wang, J. Voogt, and M. Wang, "Multi-temporal trajectory of the urban heat island centroid in Beijing, China based on a Gaussian volume model," *Remote Sensing of Environment,* vol. 149, pp. 33-46, 2014.

[64] P. Fu and Q. Weng, "Consistent land surface temperature data generation from irregularly spaced Landsat imagery," *Remote Sensing of Environment,* vol. 184, pp. 175-187, 2016.

[65] Q. Weng and P. Fu, "Modeling annual parameters of clear-sky land surface temperature variations and evaluating the impact of cloud cover using time series of Landsat TIR data," *Remote Sensing of Environment,* vol. 140, pp. 267-278, 2014.

[66] B. N. Holben, "Characteristics of maximum-value composite images from temporal AVHRR data," *International journal of remote sensing,* vol. 7, no. 11, pp. 1417-1434, 1986.

[67] P. J. Sellers *et al.*, "A global 1 by 1 NDVI data set for climate studies. Part 2: The generation of global fields of terrestrial biophysical parameters from the NDVI," *International Journal of Remote Sensing,* vol. 15, no. 17, pp. 3519-3545, 1994.

Chapter 2. Theories and methods of urban development assessment

2.1 Introduction

The development of cities takes place in a very complex system. Although cities can be investigated through the population, economy, and other aspects, the endogenous of these factors cannot be avoided. In addition, the First Law of Geography, according to Waldo Tobler, is "everything is related to everything else, but near things are more related than distant things" [1]. This law makes the evaluation of urban development require more complex and in-depth consideration, because compared with the model developed based on the general panel data, the relevant model of a city or a region often require a spatial model which takes the location and the neighbors into consideration to make the evaluation more accurate. Besides, due to the large scale of a city or a region, there are great differences among the statistics data quality, the statistics caliber and standard of the urban related data. The timeliness, accuracy, and reliability of data are all essential issues to be considered in model design. Hence, especially for a city or a region, how to evaluate the spatial-temporal development require the most appropriate model design with the data source, processing, and analysis methods. In this context, this paper presents works done by integrating a Geographic Information System (GIS) and Remote Sensing (RS) to evaluate the urbanization and urban shrinkage (two types of urbanization), and urban heat island, one of the biggest urban environmental issues, in China and Japan both from global and local level.

GIS is a computer system for collection, storage, analysis and display of spatial information, and a common technology for processing and analyzing geographic data. During the integration process of water quality model and GIS, GIS is a powerful tool for spatial discretization, parameterization and visualization of water quality model. Geographic information systems are utilized in multiple technologies, processes, techniques and methods. It is attached to various operations and numerous applications, that relate to: engineering, planning, management, transport/logistics, insurance, telecommunications, and business [2]. Therefore, GIS is at the foundation of location-enabled services, that rely on geographic analysis and visualization.

Exploratory Spatial Data Analysis (ESDA), which is based on GIS technologies, includes a series of spatial analyst methods. ESDA are developed to statistically analyze spatial data and mine necessary knowledge of features' spatial structure and correlation [3-5]. Before applying these measures, it is necessary to at first define the spatial correlation between proximate features by Spatial Weight Matrix [6] and test if there is a statistically significant spatial correlation by Global Moran's I [7-9]

RS is the acquisition of information about an object or phenomenon without making physical contact with the object and thus in contrast to on-site observation, especially the Earth [10]. In current usage, RS refers to the use of satellite- or aircraft-based sensor technologies to detect and classify objects on Earth, including on the surface and in the atmosphere and oceans. RS is used in numerous fields, including geography, land surveying, urban planning and most Earth science disciplines [11, 12]. The advantage of RS is accurate multi-attribute data. However, the spatial, temporal, spectral, and radiometric resolution of the RS data could significantly affect the choice of optimal RS for a specified study.

2.2 Theories and applications of Geographic Information System

2.2.1 Theories and development of GIS

GIS is a computer system for collection, storage, analysis and display of spatial information, and a common technology for processing and analyzing geographic data. During the integration process of water quality model and GIS, GIS is a powerful tool for spatial discretization, parameterization and visualization of water quality model. Geographic information systems are utilized in multiple technologies, processes, techniques and methods. It is attached to various operations and numerous applications, that relate to: engineering, planning, management, transport/logistics, insurance, telecommunications, and business [13]. Therefore, GIS is at the foundation of location-enabled services, that rely on geographic analysis and visualization. Still, many refer to "geographic information system" as GIS even though it doesn't cover all tools connected to topology. In the strictest sense, the term describes any information system that integrates, stores, edits, analyzes, shares, and displays geographic information. In a more generic sense, GIS applications are tools that allow users to create interactive queries (user created searches), analyze spatial information, edit data, maps, and present the results of all these operations. Geographic Information Science is the science underlying the geographic concepts, applications and systems, taught in degree and GIS Certificate programs at many universities [14].

"Geographic information system", was first raised by Roger Tomlinson, who is known as the father of GIS, in 1968 [15]. Tomlinson also led the first computerized GIS on the Canada Geographic Information System in early 1960s. It was called the Canada Geographic Information System (CGIS) and was used to store, analyze, and manipulate data collected for the Canada Land Inventory. The system was used to simulate the land capability for rural Canada by mapping information about soils, agriculture, recreation, wildlife, waterfowl, forestry and land use.

CGIS was an improvement over "computer mapping" applications as it provided capabilities for overlay, measurement, and digitizing/scanning. It supported a national coordinate system that spanned the continent, coded lines as arcs having a true embedded topology and it stored the attribute and locational information in separate files [16]. CGIS lasted into the 1990s and built a large digital land resource database in Canada. It was developed as a mainframe-based system in support of federal and provincial resource planning and management. Its strength was continent-wide analysis of complex datasets [17].

Nowadays, many disciplines have benefited from GIS technologies [18]. The active GIS market has led to low costs and continuous improvements in hardware and software for GIS components. These developments, in turn, are driving wider applications of the technology in science, government, business and industry, including real estate, public health, crime mapping, national defense, sustainable development, natural resources, landscape architecture, archaeology, community planning, transportation and logistics. GIS have also branched out into location services (LBS).LBS USES GPS to use a mobile device to display their location (the nearest restaurant, gas station, fire hydrant), a mobile device (friends, children, a police car) or send their location back to a central server for display or other processing based on their location in relation to a fixed base station. These services continue to evolve as GPS capabilities are integrated with increasingly powerful mobile electronics.

2.2.2 Panel data analysis

In statistics and econometrics, panel data are multi-dimensional data involving measurements over time. Panel data contain observations of multiple phenomena obtained over multiple time periods for the same firms or individuals [19, 20]. Analysis methods based on panel data include correlation, regression, etc. However, most methods ignore the potential spatial effect between the variables.

Pearson correlation analysis

In this study, three analyst methods have been applied. Firstly, the Pearson correlation analysis, is applied to reveal the linear correlation between two variables [21]. The magnitude of the correlation is evaluated by the Pearson correlation coefficient, which is also refers to Pearson's R. The value of Pearson's r is between +1 to -1, where 1 refers to a total positive correlation, -1 refers to a total negative correlation, and 0 refers to no linear correlation. And it can be calculated through the following Eq. 2-1.

$$\rho_{X,Y} = \frac{cov(X,Y)}{\sigma_X \sigma_Y} \qquad (\text{Eq. } 2-1)$$

where cov is the covariance, X and Y are two variables, σ is the standard deviation.

Multivariate ordinary least squares (OLS) regression

Secondly, multivariate ordinary least squares (OLS) regression is developed to find the relationship between a dependent variable and all the explanatory variables [21]. The traditional OLS model considers all explanatory variables are global and spatially stationary. Moreover, an OLS model can be expressed as follows:

$$y_i = \beta_0 + \sum_{j=1}^{p} \beta_j x_j + \varepsilon_i \qquad (\text{Eq. } 2-2)$$

where β_0 represents the intercept, β_j represents the regression coefficient for the explanatory variable x_j, ε_i represents the error term.

The determination coefficient (R^2) is defined as a ratio of explained variance to the total variance of the dependent variable y and is used to represent the degree of fit between the predicted value and the actual value. R^2 is the square of the correlation coefficient and the value of R^2 is between 0 and 1, with values close to 1 indicating a good degree of fit. However, this is a biased estimate of the population R^2, and will never decrease if additional regressors are added, even if they are irrelevant. That is to say, in a regression analysis, the degree of fit can keep increase when adding variables constantly, while the improvement of the model is spurious. To penalize the addition non-significant variables, which means adding a non-significant variable can not increase the model fit, adjusted R^2 is designed to limit the explanatory power of non-significant explanatory variables in the model. The adjusted R^2 can be calculated through the following equation:

$$Adjusted\ R^2 = 1 - \frac{n-1}{n-p}(1-R^2) \qquad (\text{Eq. } 2-3)$$

Moreover, there are several criterions can also be applied to select the optimal model, such as Akaike Information Criterion (AIC), Bayesian Information Criterion (BIC), and Cross Validation (CV) [22-24]. The optimal model will be different when choose a different criterion. The selection of the criterions will be introduced later.

Coupling Coordination Degree Model

Within systems theory, a complex system refers to its constituent elements cannot explain the overall characteristics for their nonlinear links [25]. Previous studies showed urbanization process is a complex system which is inappropriate to evaluate only using population, such economy factors and social infrastructure factors are also essential parts for urbanization evaluation [26-29]. At present, there are several methods applied to assess urbanization including AHP, fuzzy comprehensive evaluation method, entropy method, gray relational analysis, and so on [29-34]. The entropy method is a useful tool according to the abstraction and quantitative difficulty of urbanization impact factors. Information entropy is defined as the measurement of the degree of order that higher entropy indicates more information, and lower entropy indicates less information. The urbanization coupling coordination model treats demographic urbanization, economic development, and social development as three subsystems that interact with each other nonlinearly. The three subsystems are considered as independent but integrated systems. The coordination statement between subsystems is an indicator of sustainable development, providing a standard for judging whether the system is tending to higher-order [35].

The entropy method was used to determine the weight of each indicator. The information entropy represents the disorder of a system and varies by index. Compared to expert weighting model and analytic hierarchy process (AHP), the entropy method can avoid the effect by subjective weight determination [36, 37]. The steps for calculating the weights of the indicators are showing as follows:

The proportion P_{ij} of the indicator *j* in year *i*: $P_{ij} = \frac{X_{ij}}{\sum_{i=1}^{n} X_{ij}}$ (Eq. 2 − 4)

Information entropy E_j for the indicator *j*: $E_j = -\frac{1}{\ln n}\sum_{i=1}^{n}(P_{ij} \times \ln(P_{ij}))$ (Eq. 2 − 5)

Entropy redundancy D_j: $D_j = 1 - E_j$ (Eq. 2 − 6)

Weight W_j of the indicator *j*: $W_j = \frac{D_j}{\sum_{j=1}^{m} D_j}$ (Eq. 2 − 7)

Evaluation of the indicator *j* in year *i*: $Y_{ij} = W_j \times X_{ij}$ (Eq. 2 − 8)

Index for composition systems in year *i*: $Y_i = \sum_{j=1}^{m} Y_{ij}$ (Eq. 2 − 9)

Where n is the total number of observations; m is the number of indicators.

As urbanization promote the urban population migration, economic growth, and social infrastructure development, coordinated development is a big issue in regional research. As urbanization is a multi-component process, the coupling coordination degree model can be utilized to understand the comprehensive urbanization level. Coupling coordination refers to two or more systems can influence each other through interactive mechanisms [35]. The coupling coordination degree were calculated as follows:

The coupling degree: $C = \left\{ \frac{\prod Y_i}{\left[\frac{(\sum Y_i)}{n}\right]^n} \right\}^{\frac{1}{n}}$ (Eq. 2 − 10)

Comprehensive coupling coordinated development evaluation index: $T = \sum w_i Y_i$ (Eq. 2 − 11)

The degree of coupling coordination: $D = \sqrt{C \times T}$ (Eq. 2 − 12)

Where C is the coupling degree of urbanization; Y_i is the index system i; T is the comprehensive coupling coordinated development evaluation index; w_i denote the contribution of index system i; D is the coupling coordination degree.

2.2.3 Explanatory spatial data analysis in GIS

ESDA are developed to statistically analyze spatial data and mine necessary knowledge of features' spatial structure and correlation [38, 39]. Before applying these measures, it is necessary to at first define the spatial correlation between proximate features by Spatial Weight Matrix [40] and test if there is a statistically significant spatial correlation by Moran's I tests [41].

Spatial Weight Matrix

Spatial statistics integrate space and spatial relationships directly into their mathematics. The spatial weight matrix is designed to measure the spatial relationships. There are a multitude of weighting possibilities (also refers to kernel types) including inverse distance, fixed distance, K nearest neighbors, contiguity, and spatial interaction. The choice of kernel type varies with different research scales.

The software GWR 4 allows four kernel types, including adaptive bi-square, adaptive Gaussian, fixed bi-square, fixed Gaussian (Table 2-1), according to the GWR 4 manual.

Table 2-1. Four kernel type options available in GWR4

Kernel type	Equation
Fixed Gaussian	$w_{ij} = \exp\left(\frac{-d_{ij}^2}{\theta^2}\right)$
Fixed bi-square	$w_{ij} = \begin{cases} \left(1 - \frac{d_{ij}^2}{\theta^2}\right)^2 & d_{ij} < \theta \\ 0 & d_{ij} > \theta \end{cases}$
Adaptive bi-square	$w_{ij} = \begin{cases} \left(1 - \frac{d_{ij}^2}{\theta_{i(k)}}\right)^2 & d_{ij} < \theta \\ 0 & d_{ij} > \theta \end{cases}$
Adaptive Gaussian	$w_{ij} = \exp\left(\frac{-d_{ij}^2}{\theta_{i(k)}^2}\right)$

Notes: i is the regression point index; j is the locational index;

w_{ij} is the weight value of observation at location j for estimating the coefficient at location i.

d_{ij} is the Euclidean distance between i and j;

θ is a fixed bandwidth size defined by a distance metric measure.

$\theta_{i(k)}$ is an adaptive bandwidth size defined as the k th nearest neighbour distance.

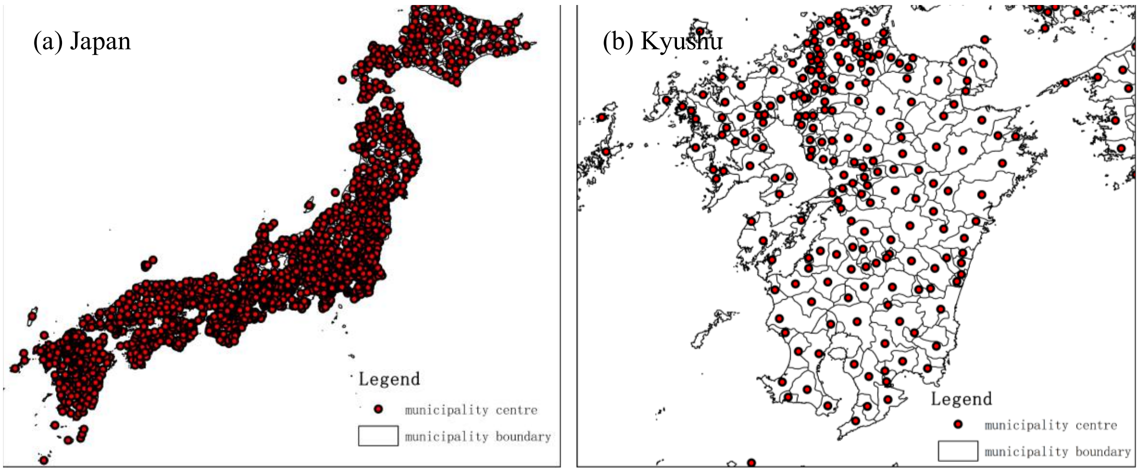

Fig. 2-1 The distribution of Japan's municipalities center (a) Japan, (b) Kyushu.

The adaptive Bi-square kernel, which narrow the bandwidth where data are dense but allows it to spread where data are spread, has a clear-cut range where kernel weighting is non-zero. And it has been widely used in studies take the city as a unit. For example, Lee et al. (2019) studied the spatial differences of obesity prevalence determinants of America cities through GWR models with the adaptive kernel [42]. Cheng et al.(2019) studied the correlates of regional tourism development of cities in Jiangsu, China, through SGWR models with adaptive Bi-square kernel [43]. For example, as

Fig. 2-1 shows, the centre points of Japan's municipalities are scattered). It can be checked with distribution of the municipalities in Kyushu (Fig. 2-1(b)) The municipalities in the north part of Kyushu are more dense than the south part. So, an adaptive bi-square kernel can be applied in this case.

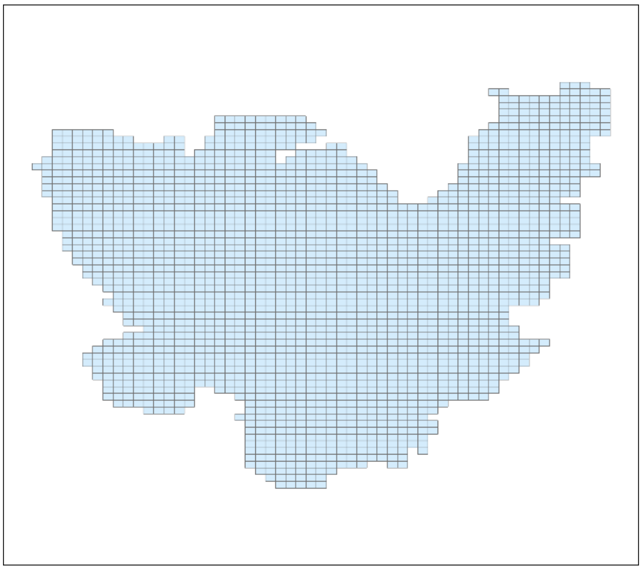

Fig. 2-2 250m fishnet of Kitakyushu.

The fixed Gaussian kernel, which bandwidth is fixed, is suitable to regular distribution. This type can apply in spatial analysis with RS data or fishnet data. As Fig. 2-2 shows, when the unit of a spatial analysis is regular fishnet, a fixed type is more suitable.

Spatial autocorrelation analysis

Spatial autocorrelation statistics are used to measure a fundamental property of geographic data: the degree of interdependence between data at one location and data at other locations. This dependence is usually called spatial dependence. Due to the influence of spatial interaction and spatial diffusion, geographic data may no longer be independent from each other, but related to each other. For example, many spatially separated markets are viewed as a set. If markets are close enough to exchange and flow goods, the price and supply of goods may be spatially related rather than independent. In fact, the closer markets are, the closer and more correlated commodity prices will be.

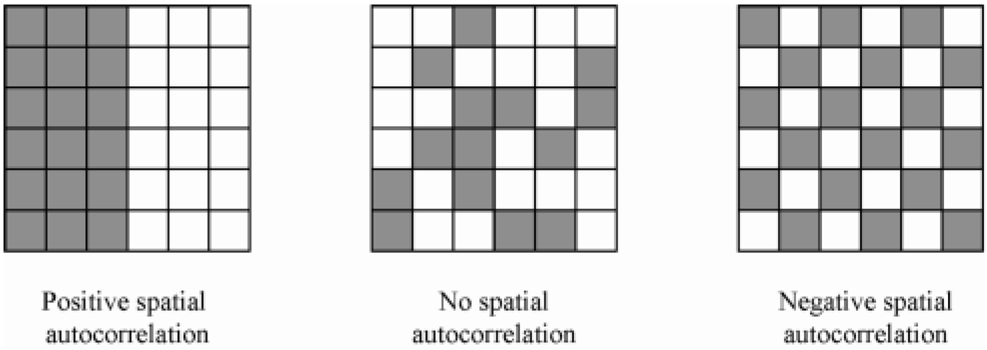

Fig. 2-3 Spatial autocorrelation types and samples.

Fig. 2-3 shows three spatial autocorrelation types and samples. The positive spatial autocorrelation and negative spatial correlation refers the spatial dependence, Spatial dependence results from various spatial spillover effects, and spatial heterogeneity results from inherent differences between spatial units and variations over space [43, 44]. OLS regression can be used to assess the general correlation between dependent variable and explanatory variables where the correlates are spatially stationary. However, local adaptation strategies are often required to identify the spatial heterogeneity. Hence, the spatial autocorrelation analysis is an important measure and precondition of ESDA.

Generally, the global and local Moran’s I tests (univariate) are the most widely used approach to evaluate the spatial autocorrelation. Specifically, the global Moran’s I. Global Moran’s I, which is a rational number ranging from –1 to 1 after normalized variance was selected for spatial autocorrelation analysis for its widely used to reveal the global spatial autocorrelation. Global Moran’s I > 0 indicates positive spatial correlation where the larger the value, the stronger the spatial correlation; global Moran’s I < 0 indicates negative spatial correlation, where the smaller the value, the larger the spatial difference; and global Moran's I = 0 indicates a random space. In this study, a larger absolute value indicates greater spatial agglomeration (positive value) or differentiation (negative value). The global Moran’s I can be calculated with the following equation:

$$I = \frac{n}{S_o}\frac{\sum_{i=1}^{n}\sum_{j=1}^{n} w_{i,j} z_i z_j}{\sum_{i=1}^{n} z_i^2} \qquad (\text{Eq. } 2-13)$$

Where z_i is the deviation between element i and its mean value $(x_i - \bar{x})$, $w_{i,j}$ is the spatial weight between element i and j, n is the total number of the elements, S_o is the aggregation of all spatial weights.

However, the global Moran’s I can only reflect spatial autocorrelation but does not identify the location and type of spatial clusters [45]. The Local Moran’s I can be applied to identify the local differences and similarities among neighboring municipalities. The local indicators of spatial association (LISA) can be determined using local Moran's I [46]. The local Moran’s I can be calculated with the following equations:

$$I_i = \frac{x_i - \bar{x}}{S_i^2} \sum_{j=1, j \neq i}^{n} w_{i,j} (x_i - \bar{x}) \qquad \text{(Eq. 2-14)}$$

$$S_i^2 = \frac{\sum_{j=1, j \neq i}^{n} (x_i - \bar{x})}{n-1} \qquad \text{(Eq. 2-15)}$$

Generally, four clustering/outlier types are classified using the local Moran's I including (1) high-high cluster (HH), (2) high-low outlier (HL), (3) low-high outlier (LH), and (4) low-low outlier (LL). HH and LL reflect positive spatial correlation; HL and LH reflect negative spatial correlation.

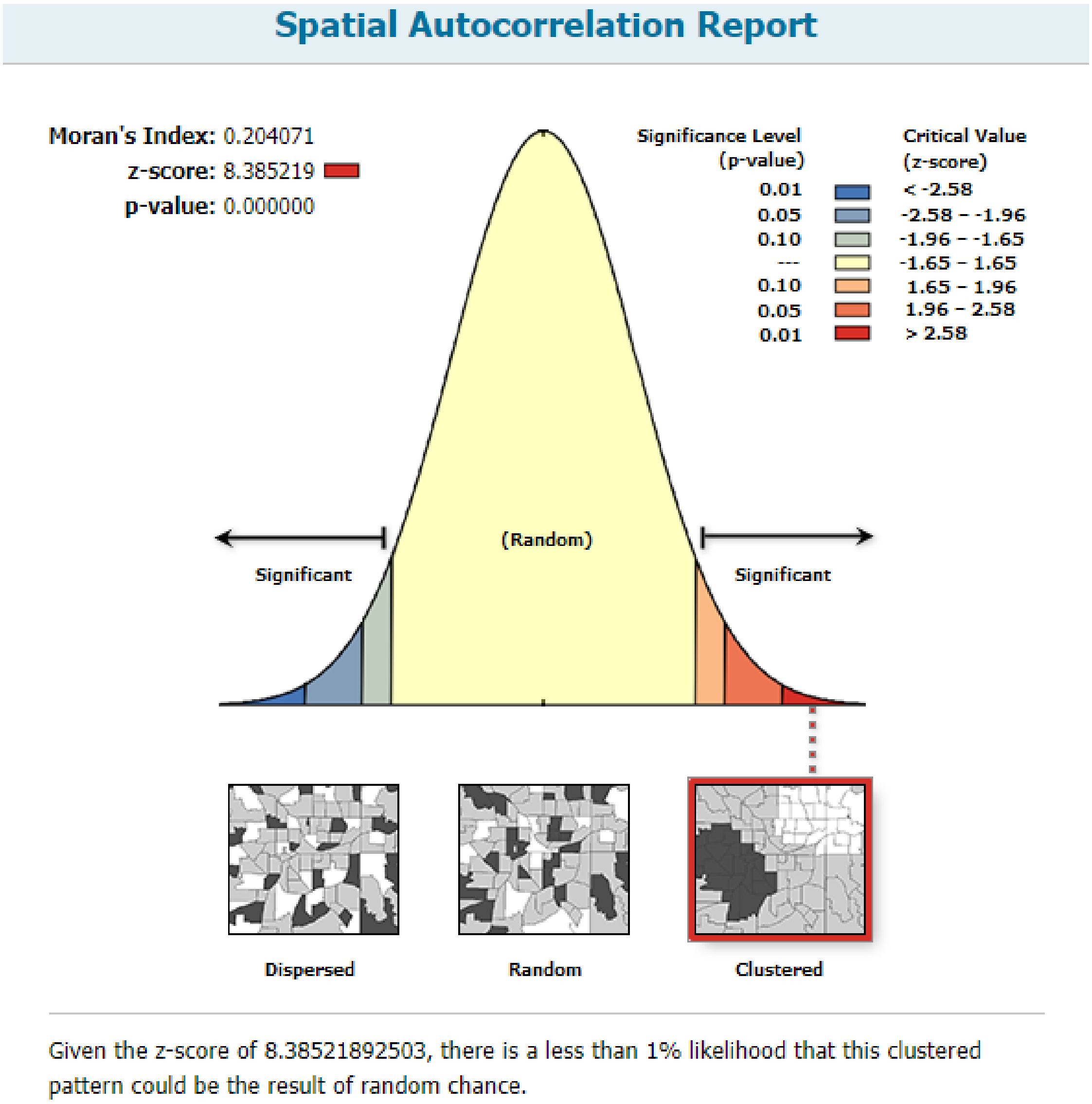

Fig. 2-4 Sample of autocorrelation analysis report.

As Fig. 2-4 shows the sample of autocorrelation analysis report. The z-score and p-value are two parameters which are used to measure the significant level of a Moran's I test. The z-score is calculated through T-test.

Moreover, as an extension of univariate global and local Moran's I tests, bivariate global and local Moran's I tests have been developed to reveal the spatial correlation between two variables. It is typically considered to be the correlation between one variable and the spatial lag of another variable。 However, this does not take into account the inherent correlation between the two variables. More precisely, the bivariate spatial correlation is between x_i and $\sum_{j=1}^{n} w_{i,j} y_j$, but does not take into account the correlation between x_i and y_j at the same location. The bivariate Moran's I can be calculated through the following equation:

$$I_B = \frac{\sum_{i=1}^{n}\sum_{j=1}^{n} w_{i,j} y_j \times x_i}{\sum_{i=1}^{n} x_i^2} \qquad (\text{Eq. } 2-16)$$

Meanwhile, the spatial weight matrix can significantly affect the results of Moran's I. The selection of the optimal spatial weight matrix has been mentioned before.

Geographically weighted regression

However, in this study, due to the spatial differences in demographics, economy, and society, the GWR model, which considers spatial heterogeneity, could be a better model for reducing the error caused by spatial non-stationary. The GWR model is an extension of the OLS regression model that has been applied to multidisciplinary studies such as meteorology, sociology, and economics, to effectively reveal the spatial heterogeneity. In a GWR model, spatial heterogeneity is investigated in the model fit where the spatial locations of data are incorporated. A local linear regression model for each feature in the dataset was calibrated using a different weighting of observations [48]. The parameter in this model is a single function that represents the spatial location that is derived by weighting all neighboring observations based on a decreasing function of distance [49]. A GWR model can be expressed as:

$$y_i = \beta_0(u_i, v_i) + \sum_{j=1}^{p} \beta_j(u_i, v_i)\, x_{ij} + \varepsilon_i \qquad (\text{Eq. } 2-17)$$

where (u_i, v_i) represents the coordinates of location *i*, $\beta_0(u_i, v_i)$ represents the intercept, $\beta_j(u_i, v_i)$ represents the local regression coefficient for the explanatory variable x_j at location *i*, and represents the error term. They are estimated using the local weighted least squares method. A GWR model assumes all the factors are non-stationary and focuses on the differences in the spatial effect of the variables. However, due to population change in Japan being caused by complex factors, the possibility always exists that several global explanatory variables could contribute to explain the population change in Japan. The semiparametric geographically weighted regression (SGWR) model, which is an extension of traditional GWR model, can be applied to meet the requirements of the model and allow some parameters to be global variables and others to be local [50-52]. An SGWR model can be expressed as follows:

$$y_i = \sum_{k=1}^{q} \beta_k\, x_k + \sum_{j=1}^{p} \beta_j(u_i, v_i)\, x_{ij} + \varepsilon_i, \qquad (\text{Eq. } 2-18)$$

where k represents the global variables and j represents the local variables. We applied the SGWR model to investigate the spatial impact factors of population change in Japan, using an adaptive bi-square kernel type to calculate the weight matrix. We used an adaptive rather than a fixed kernel because regression points (the center of each municipalities) were irregularly scattered over the study area, and adaptive kernel allows the dataset to be large enough for each local regression [53].

In a GWR model, the accuracy is profoundly affected by the bandwidth, which refers to the number of nearest neighbors of municipality i. The corrected Akaike information criterion (AICc) method [54, 55] and the cross-validation (CV) method are two methods often applied to determine the bandwidth. Compared with the CV method, the AICc method can quickly and effectively solve the problem considering the differences in the degree of freedom of different models. Therefore, in this study, the smallest AICc was selected for the appropriate bandwidth determination [50]. The selection of the optimal SGWR model with the smallest AICc based on an iterative process was processed using GWR 4 software [56]. The AICc value can be calculated through the follow equation:

$$AIC = 2k - 2\ln(\hat{l}) \qquad (\mathrm{Eq.}\, 2-19)$$

$$AICc = AIC + \frac{2k^2+2k}{n-k-1} \qquad (\mathrm{Eq.}\, 2-20)$$

where k is the number of estimated parameters in the model, $\hat{l}$ is the maximum value of the likelihood function for the model, n denotes the sample size. Thus, AICc is essentially AIC with an extra penalty term for the number of parameters.

2.3 Theories and applications of Remote Sensing

2.3.1 Theories and development of RS

RS is the acquisition of information about an object or phenomenon without making physical contact with the object and thus in contrast to on-site observation, especially the Earth. In current usage, RS refers to the use of satellite- or aircraft-based sensor technologies to detect and classify objects on Earth, including on the surface and in the atmosphere and oceans. RS is used in numerous fields, including geography, land surveying, urban planning and most Earth science disciplines. The advantage of RS is accurate multi-attribute data. However, the spatial, temporal, spectral, and radiometric resolution of the RS data could significantly affect the choice of optimal RS for a specified study.

The development of artificial satellites in the latter half of the 20th century allowed remote sensing to progress to a global scale as of the end of the Cold War. Instrumentation aboard various Earth observing and weather satellites such as Landsat, the Nimbus and more recent missions such as RADARSAT and UARS provided global measurements of various data for civil, research, and military purposes. Space probes to other planets have also provided the opportunity to conduct remote sensing studies in extraterrestrial environments, synthetic aperture radar aboard the Magellan spacecraft provided detailed topographic maps of Venus, while instruments aboard SOHO allowed studies to be performed on the Sun and the solar wind, just to name a few examples.

Recent developments include, beginning in the 1960s and 1970s with the development of image processing of satellite imagery. Several research groups in Silicon Valley including NASA Ames Research Center, GTE, and ESL Inc. developed Fourier transform techniques leading to the first notable enhancement of imagery data. In 1999 the first commercial satellite (IKONOS) collecting very high resolution imagery was launched [57].

In recent years, with the development of the remote sensing techniques, we are able to get the information about the world through many remote sensing sources. The Landsat series datasets are the most popular remote sensing sources which released by NASA and it is available for public freely. In this study, we used Landsat 5 and Landsat 8 series images. Landsat 5 was a low Earth orbit satellite launched on March 1, 1984 to collect imagery of the surface of Earth. A continuation of the Landsat Program, Landsat 5 was jointly managed by the U.S. Geological Survey (USGS) and the National Aeronautics and Space Administration (NASA). Data from Landsat 5 was collected and distributed from the USGS's Center for Earth Resources Observation and Science (EROS). Landsat 8 is an American Earth observation satellite launched on February 11, 2013. It is the eighth satellite in the Landsat program; the seventh to reach orbit successfully. Originally called the Landsat Data Continuity Mission (LDCM), it is a collaboration between NASA and the United States Geological Survey (USGS). NASA Goddard Space Flight Center in Greenbelt, Maryland, provided development, mission systems engineering, and acquisition of the launch vehicle while the USGS provided for development of the ground systems and will conduct on-going mission operations.

As for the remote sensing, with several decades' development, the remote sensing has traditionally been the province of Earth scientists and the national security community. Early civilian satellite instruments were designed largely to meet the needs of weather forecasting, earth systems science and natural resource management. Social science applications were, generally speaking, not even considered. However, since the late 1980s, this began to change as a number of social scientists began to apply remote sensing imagery to understand the underlying social processes such as deforestation, desertification and urbanization. Among the research in urbanization, the scientists had used the remote sensing imagery to help get the land use/cover change and sustainability trajectories, monitoring changes and urban growth over time, classification of urban areas, population dynamic, etc. In addition, there are lots of academic research which is about the urban heat island studies by using the remote sensing data to get the distribution imagery and to analysis the cause of formation, it has already been proven that the remote sensing data are an edge tool applied in the urban studies.

2.3.2 Applications of RS data

Remote sensing applications in the field of optics may require consideration of different categories of models from precision to approximate modeling. In addition to targeted objectives, it may be recommended to look for practical radiative transport models that will provide quick solutions to the inverse problem. However, the computational efficiency of these models is unlikely to be a core issue rather than assessing the potential of the information contained in satellite images. In general, a pixel in a satellite image will be characterized by several features at four resolutions: space, spectrum, Angle, and time. When selecting methods for processing data, particular attention will be paid to the extent of the information provided by these different resolutions. In a sense, in order to reduce physics, it is best to emphasize some assumptions. For example, in the case of medium or even coarse scale resolution, a statistic-based approach is preferable to a physics-based approach, which is intended in theory to provide an accurate model of the signal. In terms of spectral resolution, the narrower the band available, the more options there are for describing biogeochemical processes.

2.3.3 Introduction and pre-processing of RS data

Landsat series data are one of the most widely used RS datathe basic data originated from Landsat 5 and Landsat 8 series images. Landsat 5 launched on March 1, 1984 and was decommissioned on June 5, 2013. Landsat 5 images consist 7 bands; the specific parameters were shown as Table 2-2. Landsat 8 launched on February 11, 2013 which carries 2 main load: OLI (Operational Land Imager) and TIRS (Thermal Infrared Sensor), shown as Table 2-3.

The application of remote sensing is mainly determined by the four resolutions of the data source. The most important are the temporal resolution and spatial resolution. For example, when utilizing remote sensing data analyzing the urban heat island, different from investigating the UHI using air temperature data from the local meteorological observations or in-situ measurements, the land surface temperature (LST) is another critical parameter for the investigation and assessment of the UHI. The LST could be obtained or retrieved from the thermal infrared remote sensors, which enables surface urban heat island (SUHI) studies over large-scale spaces. However, for the quite differences between the spatial and temporal resolution, the remote sensors have their respective characteristics and applicability. In general, the high spatial resolution sensors have a low temporal resolution, whilst the low spatial resolution sensors have a high temporal resolution.

For example, the spatial resolution of Landsat TIRS is 100 m but the temporal resolution is 16 day; The spatial resolution of the Moderate Resolution Imaging Spectroradiometer (MODIS) LST images is 1 km but the temporal resolution is twice a day. Hence, downscaling the spatial resolution of LST images from coarser to finer resolution became a mainstream method to improve the application of the LSTs.

The Moderate Resolution Imaging Spectroradiometer (MODIS) is a payload imaging sensor that was launched into Earth orbit by NASA in 1999 on board the Terra (EOS AM) satellite, and in 2002 on board the Aqua (EOS PM) satellite. The instruments capture data in 36 spectral bands ranging in wavelength from 0.4 μm to 14.4 μm and at varying spatial resolutions (2 bands at 250 m, 5 bands at 500 m and 29 bands at 1 km). Together the instruments image the entire Earth every 1 to 2 days (Table 2-4).

Table 2-2. Landsat 5 bands parameters

Band number	Band	Spectrum (μm)	Resolution (m)
B1	Blue	0.45—0.52	30
B2	Green	0.52—0.60	30
B3	Red	0.63—0.69	30
B4	Near IR	0.76— 0.90	30
B5	SW IR	1.55—1.75	30
B6	LW IR	10.40 —12.5	120
B7	SW IR	2.08 —2.35	30

Table 2-3 Landsat 8 bands parameters

Load	Band number	Band	Spectrum (μm)	Resolution (m)
OLI	B1	Coastal	0.433–0.453	30
	B2	Blue	0.450–0.515	30
	B3	Green	0.525–0.600	30
	B4	Red	0.630–0.680	30
	B5	NIR	0.845–0.885	30
	B6	SWIR 1	1.560–1.660	30
	B7	SWIR 2	2.100–2.300	30
	B8	Pan	0.500–0.680	15
	B9	Cirrus	1.360–1.390	30
TIRS	B10	TIRS 1	10.6-11.2	100
	B11	TIRS 2	11.5-12.5	100

Table 2-4 MODIS bands parameters

Band	Wavelength	Resolution	Primary use
1	620–670	250	Land/cloud/aerosols boundaries
2	841–876	250	
3	459–479	500	Land/cloud/aerosols properties
4	545–565	500	
5	1230–1250	500	
6	1628–1652	500	
7	2105–2155	500	
8	405–420	1000	Ocean color phytoplankton biogeochemistry
9	438–448	1000	
10	483–493	1000	
11	526–536	1000	
12	546–556	1000	
13	662–672	1000	
14	673–683	1000	
15	743–753	1000	
16	862–877	1000	
17	890–920	1000	Atmospheric water vapor
18	931–941	1000	
19	915–965	1000	
20	3.660–3.840	1000	Surface/cloud temperature
21	3.929–3.989	1000	
22	3.929–3.989	1000	
23	4.020–4.080	1000	
24	4.433–4.498	1000	Atmospheric temperature
25	4.482–4.549	1000	
26	1.360–1.390	1000	Cirrus clouds water vapor
27	6.535–6.895	1000	
28	7.175–7.475	1000	
29	8.400–8.700	1000	Cloud properties
30	9.580–9.880	1000	Ozone
31	10.780–11.280	1000	Surface/cloud temperature
32	11.770–12.270	1000	
33	13.185–13.485	1000	Cloud top altitude
34	13.485–13.785	1000	
35	13.785–14.085	1000	
36	14.085–14.385	1000	

2.4 Integration methods of urban development and environmental implication assessments

2.4.1 Requirements for the comprehensive assessment for urban sustainable development

Building a green ecological city is an objective requirement of sustainable development. "Sustainable development" as a global development strategy has been increasingly valued by governments in today's world. Humans have the right to pursue a healthy and wealthy life, but in the process of development, they should adhere to the harmony and unity of the environment, society, and economy, rather than relying on investment in people’s to pursue economic development by depleting resources, destroying ecology, and polluting the environment. When creating and pursuing development and consumption in this world, contemporary people should strive to equalize their opportunities with those of future generations, and cannot allow contemporary people to blindly pursue short-term ultra-high-speed development and consumption and deprive future generations of what they should Reasonably enjoy equal opportunities for development and consumption. Specifically, sustainable development is to enable the coordinated development of the environment, economy, and society, the effective use of resources, and the orderly progress of urban and rural development. It can be seen from this that it is of great significance to take the road of sustainable development, build a city with coordinated economic and environmental development, protect the natural environment, and organize social life efficiently.

The city is one of the main carriers of human settlement and the center of human economic, political and spiritual activities. City is not only an entity of material environment, but also an entity of social cultural environment. Compared with the natural environment, the social environment is a deeper and more complex environmental system, which involves many aspects such as social order, social politics, social security system, social public places, social life and so on. A good social environment is a higher-level pursuit. Historically, many developing regions have blindly pursued the improvement of the physical environment and ignored the improvement of the overall social environmental quality, which has led to the spread of social ugliness and high crime rates. Even the political situation is turbulent, and examples of restricting social progress are numerous and the lessons are tremendous. Therefore, creating a good social environment and promoting the ecologicalization of the social environment is an indispensable aspect of building a green ecological city. It can be seen from this that the green ecological city is an objective requirement for sustainable development and has strong vitality. Its construction is not a temporary thing and requires our continuous efforts. Therefore, its construction has no ultimate. People must respect nature, return to nature, and build a green ecological city in which population, economy, environment, and social services are coordinated. It is common to mankind. Ideal pursuit.

There are three terms similar to urban sustainability, sustainable city and ecological city. These three terms are from different perspectives (that is, urban sustainable development emphasizes the development process of things, urban sustainability and sustainable cities pay more attention to the conditions and status of things development. Eco-city is the environmental ecology of urban sustainable development It expresses the application of sustainable development ideas in urban development, and their connotations are exactly the same for how cities evolve towards sustainable development.) Since the proposition of urban sustainable development has been proposed, different scholars have different from the angle, the connotation was discussed in depth.

Since its birth, the city has been the main place for human activities. It has accumulated material, capital, and technology within a certain geographical area, and has gradually evolved into the center of economic activity, and has achieved unprecedented prosperity and development. But at the same time, a series of serious problems appeared in the city. First of all, the urban population has increased from 10% of the world 's total population in 1800 to 15% in 1900, and is expected to reach 50% in 2000. The increasing size of cities will cause tremendous pressure on the earth. Secondly, the interaction and accumulation of urban environmental, economic and social problems in different historical periods and stages make cities that are already very serious problems more vulnerable. Therefore, in this sense, only if cities embark on the road of sustainable development, can there be sustainable development of the country and the world.

As urban development being a complex system, the internal parameters of the system are potentially endogenous. Within systems theory, a complex system refers to its constituent elements cannot explain the overall characteristics for their nonlinear links. Previous studies showed urbanization process is a complex system which is inappropriate to evaluate only using population, such economy factors and social infrastructure factors are also essential parts for urbanization evaluation. Therefore, if only single index is used to evaluate urban development, the evaluation will usually be incomplete, while multi-index evaluation will often be over-interpreted due to endogeneity. Hence, the evaluation methods of urban development should be rigorous.

2.4.2 Conceptual framework of GIS-RS integration

3S technology is Remote sensing techniques (Remote sensing, RS), geographical information system (the Geography information systems, GIS) and Global positioning system (Global positioning systems, GPS) collectively, space technology, sensor technology, satellite positioning and navigation technology and computer technology, communication technology, the combination of multidisciplinary highly integration of spatial information acquisition, processing, management, analysis and expression, transmission and application of modern information technology.

Nowadays, RS impact has become the main information source of GIS, and as a core component of GIS, GIS is an effective means of managing and analyzing spatial data, helping to improve the utilization value of images. The integration of remote sensing and GIS has gradually become a trend and development trend. In the past, many people proposed the concept of remote sensing and GIS integration, but this only stops at the mutual support between image raster format and vector data format. By choice, this integration becomes more multifaceted and includes the mutual support of various software.

There is a natural connection between remote sensing and GIS, and they can complement each other. Remote sensing is an effective tool for spatial data collection and classification, and GIS is an effective tool for managing and analyzing spatial data. The two are the main components of spatial information and have a natural connection. Remote sensing has the ability to collect spatial information dynamically and in multiple phases. Remote sensing images have become the main information source of GIS. As the core component of GIS, remote sensing images are an ideal way to provide timely information. In the case of disasters, remote sensing images are the only geographic information that we can obtain immediately; in areas lacking maps, remote sensing images are even the only information we can obtain; in many industries of spatial information, leaving remote sensing images, GIS is not complete. On the other hand, remote sensing to obtain rich and massive spatial data depends on the effective management and sharing of GIS. At the same time, it uses the powerful spatial analysis function of GIS to extract deeper thematic information and comprehensively enhance the use value of images. The application mode of remote sensing data is also gradually changing, and it has gradually changed from pure background maps and basic data to more professional and in-depth thematic information. For example, in precision agriculture, the crop area and growth information obtained by remote sensing can be directly used in GIS production estimation models. Remote sensing and GIS will not only integrate data, but also from the entire software architecture system, so as to achieve complementary advantages, further improve the operability of GIS software, improve the efficiency of spatial and image analysis, and effectively save system costs.

With the rapid development of the spatial information market, the combination of remote sensing data and GIS is becoming increasingly close. The integration of remote sensing and GIS has gradually become a trend and development trend.

2.5 Summary

In this chapter, firstly, the concept and application of GIS and RS is introduced. In addition, theory, development history and application methods for ESDA are described. Finally, this thesis presents a loose-coupled urban development evaluation method considering the strength and weakness of both the GIS and RS. The requirement, conceptual framework and integration component for the association between GIS and RS is discussed.

Reference

[1] Tobler, Waldo R. "A computer movie simulating urban growth in the Detroit region." Economic geography 46.sup1 (1970): 234-240.

[2] Maliene V, Grigonis V, Palevičius V, Griffiths S (2011). "Geographic information system: Old principles with new capabilities". Urban Design International. 16 (1): 1–6.

[3] Wise S, Haining R, Ma J. Regionalisation tools for the exploratory spatial analysis of health data[M]//Recent developments in spatial analysis. Springer, Berlin, Heidelberg, 1997: 83-100.

[4] Le Gallo, Julie, and Cem Ertur. "Exploratory spatial data analysis of the distribution of regional per capita GDP in Europe, 1980–1995." Papers in regional science 82.2 (2003): 175-201.

[5] Anselin, Luc. "Interactive techniques and exploratory spatial data analysis." (1996).

[6] Seya, Hajime, Yoshiki Yamagata, and Morito Tsutsumi. "Automatic selection of a spatial weight matrix in spatial econometrics: Application to a spatial hedonic approach." Regional Science and Urban Economics 43.3 (2013): 429-444.

[7] Tiefelsdorf, Michael, and Barry Boots. "The exact distribution of Moran's I." Environment and Planning A 27.6 (1995): 985-999.

[8] Fortin, M. J., Drapeau, P., & Legendre, P. (1990). Spatial autocorrelation and sampling design in plant ecology. In Progress in theoretical vegetation science (pp. 209-222). Springer, Dordrecht.

[9] Boots, Barry, and Michael Tiefelsdorf. "Global and local spatial autocorrelation in bounded regular tessellations." Journal of Geographical Systems 2.4 (2000): 319-348.

[10] Campbell, James B., and Randolph H. Wynne. Introduction to remote sensing. Guilford Press, 2011.

[11] Richards, John A., and J. A. Richards. Remote sensing digital image analysis. Vol. 3. Berlin et al.: Springer, 1999.

[12] Voogt, James A., and Tim R. Oke. "Thermal remote sensing of urban climates." Remote sensing of environment 86.3 (2003): 370-384.

[13] Djindjian, François. "GIS usage in worldwide archaeology." (1998).

[14] Ovalles, Cesar, and Carl E. Rechsteiner Jr. Analytical Methods in Petroleum Upstream Applications. CRC Press, 2015.

[15] "The 50th Anniversary of GIS". ESRI.

[16] "GIS Hall of Fame – Roger Tomlinson". URISA.

[17] Tim Foresman 1997 The History of GIS (Geographic Information Systems): Perspectives from the Pioneers. (Prentice Hall Series in Geographic Information Science) Prentice Hall PTR; 1st edition (10 November 1997), 416 p.

[18] Campagna, Michele, ed. GIS for sustainable development. Crc Press, 2005.

[19] Baltagi, Badi H. (2008). Econometric Analysis of Panel Data (Fourth ed.). Chichester: John Wiley & Sons.

[20] Davies, A.; Lahiri, K. (1995). "A New Framework for Testing Rationality and Measuring Aggregate Shocks Using Panel Data". Journal of Econometrics. 68 (1): 205–227.

[21] Zou, Kelly H., Kemal Tuncali, and Stuart G. Silverman. "Correlation and simple linear regression." Radiology 227.3 (2003): 617-628.

[22] Sakamoto, Yosiyuki, Makio Ishiguro, and Genshiro Kitagawa. "Akaike information criterion statistics." Dordrecht, The Netherlands: D. Reidel 81 (1986).

[23] Chen, Scott, and Ponani Gopalakrishnan. "Speaker, environment and channel change detection and clustering via the bayesian information criterion." Proc. DARPA broadcast news transcription and understanding workshop. Vol. 8. 1998.

[24] Kohavi, Ron. "A study of cross-validation and bootstrap for accuracy estimation and model selection." Ijcai. Vol. 14. No. 2. 1995.

[25] Gallagher, Richard, Tim Appenzeller, and Dennis Normile. "Beyond reductionism." Science 284.5411 (1999): 79.

[26] Chen, M., Lu, D., Zha, L., 2010. The comprehensive evaluation of China's urbanization and effects on resources and environment. Journal of Geographical Sciences 20, 17-30.

[27] Chen, M., Lu, D., Zhang, H., 2009. Comprehensive evaluation and the driving factors of China's urbanization. Acta Geographica Sinica 64, 387-398.

[28] Guo-ping, L., 2008. The analysis and evaluation of the compatible relationship between industrialization and urbanization in China. Areal Research and Development 5.

[29] Sakieh, Y., Amiri, B.J., Danekar, A., Feghhi, J., Dezhkam, S., 2015. Scenario-based evaluation of urban development sustainability: an integrative modeling approach to compromise between urbanization suitability index and landscape pattern. Environment, Development and Sustainability 17, 1343-1365.

[30] Beskese, A., Demir, H.H., Ozcan, H.K., Okten, H.E., 2015. Landfill site selection using fuzzy AHP and fuzzy TOPSIS: a case study for Istanbul. Environmental Earth Sciences 73, 3513-3521.

[31] Chen, M., Lu, D., Zhang, H., 2009. Comprehensive evaluation and the driving factors of China's urbanization. Acta Geographica Sinica 64, 387-398.

[32] Liu, Y., Li, R., Song, X., 2005. Grey associative analysis of regional urbanization and eco-environment coupling in China. Acta Geographica Sinica 2, 237-247.

[33] Wang, S., Ma, H., Zhao, Y., 2014. Exploring the relationship between urbanization and the eco-environment—A case study of Beijing–Tianjin–Hebei region. Ecological Indicators 45, 171-183.

[34] Yan-bing, G., 2012. Comprehensive assessment on ecological risk of Hexi Corridor urbanization based on normal cloud model and entropy weight. Journal of Arid Land Resources and Environment 26, 169-173.

[35] Li, Y., Li, Y., Zhou, Y., Shi, Y., Zhu, X., 2012. Investigation of a coupling model of coordination between urbanization and the environment. Journal of environmental management 98, 127-133.

[36] Wang, J., Zhang, J.-s., 2001. Comparing several methods of assuring weight vector in synthetical evaluation. JOURNAL-HEBEI UNIVERSITY OF TECHNOLOGY 30, 52-57.
[37] Zheng, W., Tian, Q., 2009. The Application of Entropy Method and AHP in Weight Determining [J]. Computer Programming Skills & Maintenance 22, p19-20.
[38] Haining, Robert, Stephen Wise, and Jingsheng Ma. "Exploratory spatial data analysis." Journal of the Royal Statistical Society: Series D (The Statistician) 47.3 (1998): 457-469.
[39] Dou, Yi, et al. "An empirical study on transit-oriented low-carbon urban land use planning: Exploratory Spatial Data Analysis (ESDA) on Shanghai, China." Habitat International 53 (2016): 379-389.
[40] Getis, Arthur, and Jared Aldstadt. "Constructing the spatial weights matrix using a local statistic." Geographical analysis 36.2 (2004): 90-104.
[41] Goodchild, M. W., and JH McD Whitaker. "A petrographic study of the Rotliegendes sandstone reservoir (Lower Permian) in the Rough gas field." Clay Minerals 21.4 (1986): 459-477.
[42] Lee, Kyung Hee, et al. "Proximity to parks and natural areas as an environmental determinant to spatial disparities in obesity prevalence." Applied Geography 112 (2019): 102074.
[43] Jin, Cheng, Jing Xu, and Zhenfang Huang. "Spatiotemporal analysis of regional tourism development: A semiparametric Geographically Weighted Regression model approach." Habitat International 87 (2019): 1-10.
[44] Anselin L. The Moran scatterplot as an ESDA tool to assess local instability in spatial association: Regional Research Institute, West Virginia University Morgantown, WV; 1993.
[45] Anselin LJGa. Lagrange multiplier test diagnostics for spatial dependence and spatial heterogeneity. 1988;20:1-17.
[46] Anselin LJGa. Local indicators of spatial association—LISA. 1995;27:93-115.
[47] Forey E, Lortie CJ, Michalet R. Spatial patterns of association at local and regional scales in coastal sand dune communities. Journal of Vegetation Science. 2009;20:916-25.
[48] Brunsdon C, Fotheringham A, Charlton MJC, Environment, Systems U. Geographically weighted summary statistics—a framework for localised exploratory data analysis. 2002;26:501-24.
[49] Shi H, Laurent EJ, LeBouton J, Racevskis L, Hall KR, Donovan M, et al. Local spatial modeling of white-tailed deer distribution. 2006;190:171-89.
[50] Fotheringham AS, Brunsdon C, Charlton M. Geographically weighted regression: the analysis of spatially varying relationships: John Wiley & Sons; 2003.
[51] Jin C, Xu J, Huang ZJHI. Spatiotemporal analysis of regional tourism development: A semiparametric Geographically Weighted Regression model approach. 2019;87:1-10.
[52] Local spatiotemporal modeling of house prices: A mixed model approach. 2016;68:189-201.
[53] Feuillet T, Salze P, Charreire H, Menai M, Enaux C, Perchoux C, et al. Built environment in local relation with walking: Why here and not there? Journal of Transport & Health. 2016;3:500-12.

[54] Bozdogan HJP. Model selection and Akaike's information criterion (AIC): The general theory and its analytical extensions. 1987;52:345-70.
[55] Sakamoto Y, Ishiguro M, Kitagawa GJD, The Netherlands: D. Reidel. Akaike information criterion statistics. 1986;81.
[56] Nakaya T, Fotheringham S, Charlton M, Brunsdon C. Semiparametric geographically weighted generalised linear modelling in GWR 4.0. 2009.
[57] NASA website https://www.nasa.gov/

Chapter 3. Spatial temporal assessment of urbanization of China

3.1 Introduction

Urbanization is a population movement phenomenon that people shift from rural area to an urban area. The phenomenon is having a massive impact on the economic, social, environmental landscape all over the world. While the process of urbanization keeping going on, more and more problems occur that we are required to make it process on a more sustainable and equitable path [1].

Urbanization took place over a period of several decades in Europe countries and North America countries. And it is happening in East Asia only a few years. It's an essential role for urban policy makers that they take the responsibility for making all the residents living in the urban areas a better living environment [2]. Urban growth and sprawl have severely altered the biophysical environment [3, 5]. Rapid urbanization has significant influence on different aspects of the quality of life and research in determining the patterns of urbanization and quantifying their impacts is the need of the hour. Unplanned urbanization an urban sprawl will directly affect the land use and land cover of the area. The changes in land cover include loss of agricultural lands, loss of forest lands, increase of barren area, an increase of impermeable surface of the area because of the built up area. For the sustainable urban ecosystems the amount of land required for growing the vegetation can be estimated from these studies [6 - 9]. For a city being built, it will be really hard to change the urban form and land use patterns of the city. If there is something defective of the urban form, it will cost a large sum of money and years to undo the mistakes.

The process of urbanization provides people in urban areas a better living environment and working opportunities. East Asia has a numerous population, and a large amount of developing countries. Therefore, we can foresee a fast expansion of urban areas where millions of East Asia people will have the chance to leave extreme poverty behind and to prosper in the coming decades.

Urbanization is not easy to evaluate due to the processing of urbanization itself is very complicated and confused to understand, the scholars around the world would like to judge the level of urbanization by many parameters such as the urban population, the economic index, the energy usage, also the urban facilities construction, etc. Urbanization reflected in every regard of a city, to have a comprehensive understanding of urbanization of a city, it is necessary to do the analysis from many different parts of the urban development and have a comprehensive assessment of the city development [5, 6].

As the urbanization and land sprawl had drawn more and more attention, it is meaningful and useful to have an investigation of the urbanization in China. The investigation of urbanization can help us to get a comprehensive understanding of the urban land use and land cover variation during the years. After the investigation, not only can we get the advantages and benefit from the development, but also present the imbalance and weakness to remind us what we should do for our city to get a better condition. The investigation of urbanization also can let us know the urban development trend where more attention should be paid to make sure the steady development of the city.

3.1 Introduction

Urbanization is a population movement phenomenon that people shift from rural area to an urban area. The phenomenon is having a massive impact on the economic, social, environmental landscape all over the world. While the process of urbanization keeping going on, more and more problems occur that we are required to make it process on a more sustainable and equitable path [1].

Urbanization took place over a period of several decades in Europe countries and North America countries. And it is happening in East Asia only a few years. It's an essential role for urban policy makers that they take the responsibility for making all the residents living in the urban areas a better living environment [2]. Urban growth and sprawl have severely altered the biophysical environment [3, 5]. Rapid urbanization has significant influence on different aspects of the quality of life and research in determining the patterns of urbanization and quantifying their impacts is the need of the hour. Unplanned urbanization an urban sprawl will directly affect the land use and land cover of the area. The changes in land cover include loss of agricultural lands, loss of forest lands, increase of barren area, an increase of impermeable surface of the area because of the built up area. For the sustainable urban ecosystems the amount of land required for growing the vegetation can be estimated from these studies [6 - 9]. For a city being built, it will be really hard to change the urban form and land use patterns of the city. If there is something defective of the urban form, it will cost a large sum of money and years to undo the mistakes.

The process of urbanization provides people in urban areas a better living environment and working opportunities. East Asia has a numerous population, and a large amount of developing countries. Therefore, we can foresee a fast expansion of urban areas where millions of East Asia people will have the chance to leave extreme poverty behind and to prosper in the coming decades.

Urbanization is not easy to evaluate due to the processing of urbanization itself is very complicated and confused to understand, the scholars around the world would like to judge the level of urbanization by many parameters such as the urban population, the economic index, the energy usage, also the urban facilities construction, etc. Urbanization reflected in every regard of a city, to have a comprehensive understanding of urbanization of a city, it is necessary to do the analysis from many different parts of the urban development and have a comprehensive assessment of the city development [5, 6].

As the urbanization and land sprawl had drawn more and more attention, it is meaningful and useful to have an investigation of the urbanization in China. The investigation of urbanization can help us to get a comprehensive understanding of the urban land use and land cover variation during the years. After the investigation, not only can we get the advantages and benefit from the development, but also present the imbalance and weakness to remind us what we should do for our city to get a better condition. The investigation of urbanization also can let us know the urban development trend where more attention should be paid to make sure the steady development of the city.

Therefore, this chapter investigate the urbanization process in China, with population change ratio as the index reflect urbanization. Moreover, the interrelationship between urbanization and social-economic-demographic factors is explored with ESDA.

3.2 Study area, methods, and materials

3.2.1 General information of urbanization in China

China's urbanization process is mainly concentrated after the implementation of the reform and opening up policy. Before the 1980s, due to China's low economic level and population control, urbanization has not achieved healthy and sound development, and the rural economy once occupied a dominant position in China [8]. With the rapid development of the Chinese economy since the 1980s, a large number of people have poured into cities, and the level of urbanization in China has been unprecedentedly developed.

According to six censuses in mainland China in 1953, 1964, 1982, 1990, 2000 and 2010, the urbanization rates were 12.84%, 17.58%, 20.43%, 25.84%, 35.39% and 49.68%, respectively [10, 11]. According to data from the National Bureau of Statistics in 2019, China's urbanization rate reached over 60% in 2018, of which the urban permanent population was over 800 million (Fig. 3-1).

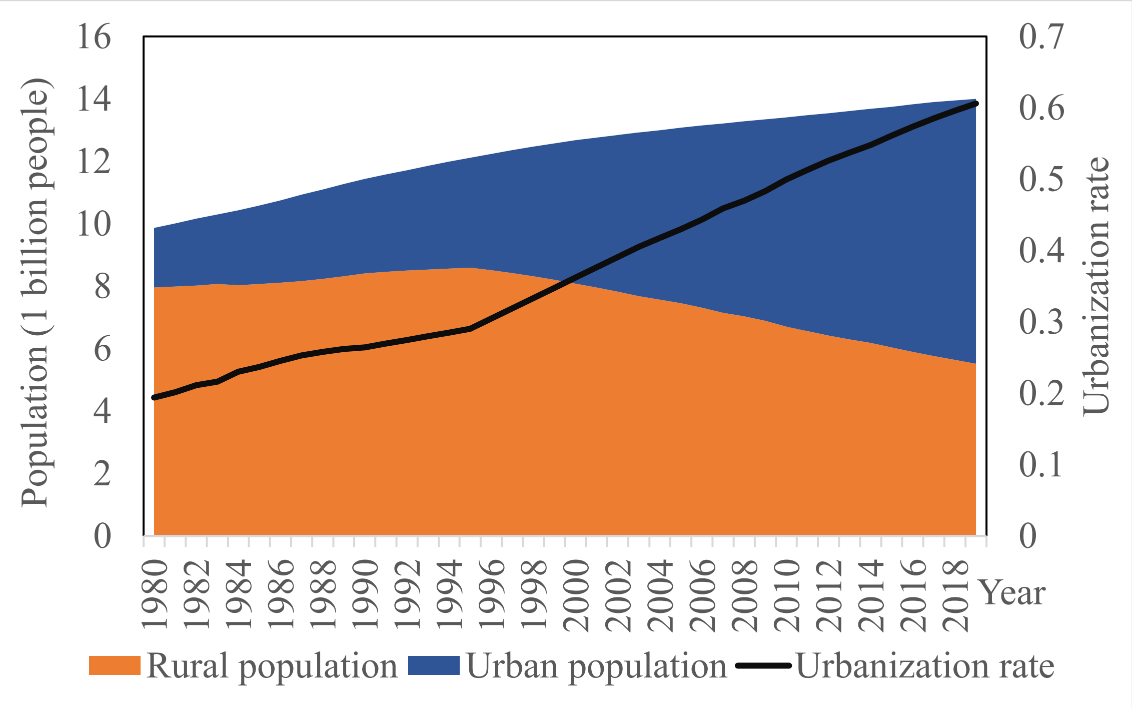

Fig. 3.1 Variation of population and urbanization rate from 1980 to 2019

China's urbanization accounted for 17.9% of the urban population from 1978 to 56.15% in 2015, and formed the Chinese urban agglomeration represented by the three major urban agglomerations of the Pearl River Delta, Yangtze River Delta, and Beijing city cluster. The process of urbanization has led to large-scale population movements and economic exchanges [13 - 15]. The resident population of the Pearl River Delta urban agglomeration, the Yangtze River Delta urban agglomeration and the Beijing-Tianjin-Hebei urban agglomeration accounts for 23.4% of the total population of prefecture-level and above cities in the country. The three major urban agglomerations received a net inflow of more than 60 million people. China has actually entered the urban era.

China is currently in the fastest period of urbanization, with the urbanization rate increasing at an annual rate of nearly 2%. The government plans to make the urban population account for 70% of the country 's total population in the next ten years, reaching about 900 million in number. The urban and industrial regions produced a huge urban arc that stretched from Harbin in the northeast to Beijing to Shanghai [8]. Due to the uneven development and migration within China, a large number of people have migrated to eastern China, especially in the eastern coastal areas, where the degree of urbanization is significantly higher than in the western regions. China is traditionally divided into 8 regions [12]. These 8 regions differ greatly in urbanization and economic level construction, which also causes a certain flow direction of population movement. Although the boundaries of regions are beginning to blur due to the expansion of urban agglomerations, there are still large differences in the overall situation [16 - 18].

Fig. 3.2 The schematic diagram of the eight economic zones of China

(Data source: Zeng, Liangen, et al.)

In this chapter, due to the lack of statistical data of some cities or regions, we have chosen various cities in China as the research object. The distribution of the selected cities is shown in Fig. 3-3. The cities with missing data are mainly distributed in the western region. In addition, the statistical calibers of Taiwan, Hong Kong and Macau are quite different from the mainland of China, so the cities in these three regions are not included in the chapter.

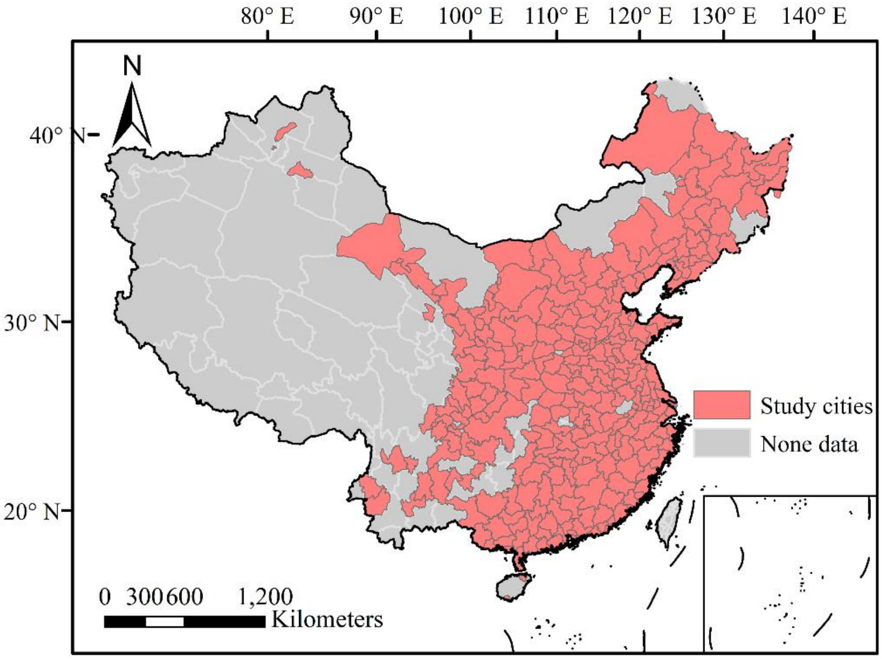

Fig. 3-3 Spatial distribution of study cities

According to the “Notice on Adjusting the Standards for City Size Division” issued by the State Council in November 2014, the city size division standard uses the urban permanent population as the statistical standard. The cities selected in this chapter are mainly large-mega cities, and it can be observed that the number of megalopolis in China has been increasing in recent years (Table 3-1).

Table 3-1 City level division and numbers of city

City level	Population	Numbers in 2005	Numbers in 2010	Numbers in 2015
Megalopolis	> 10 million	8	9	12
Mega city	5 – 10 million	76	77	74
Large city	1 – 5 million	187	186	187
Medium city	0.5 – 1 million	8	8	6
Small city	< 0.5 million	4	3	3

Unlike Japan, whose population is declining, the population of China is increasing, so the overall population of the city is also increasing. This chapter selects the permanent population as the evaluation index rather than the registered population. There are several reasons for this. On the one

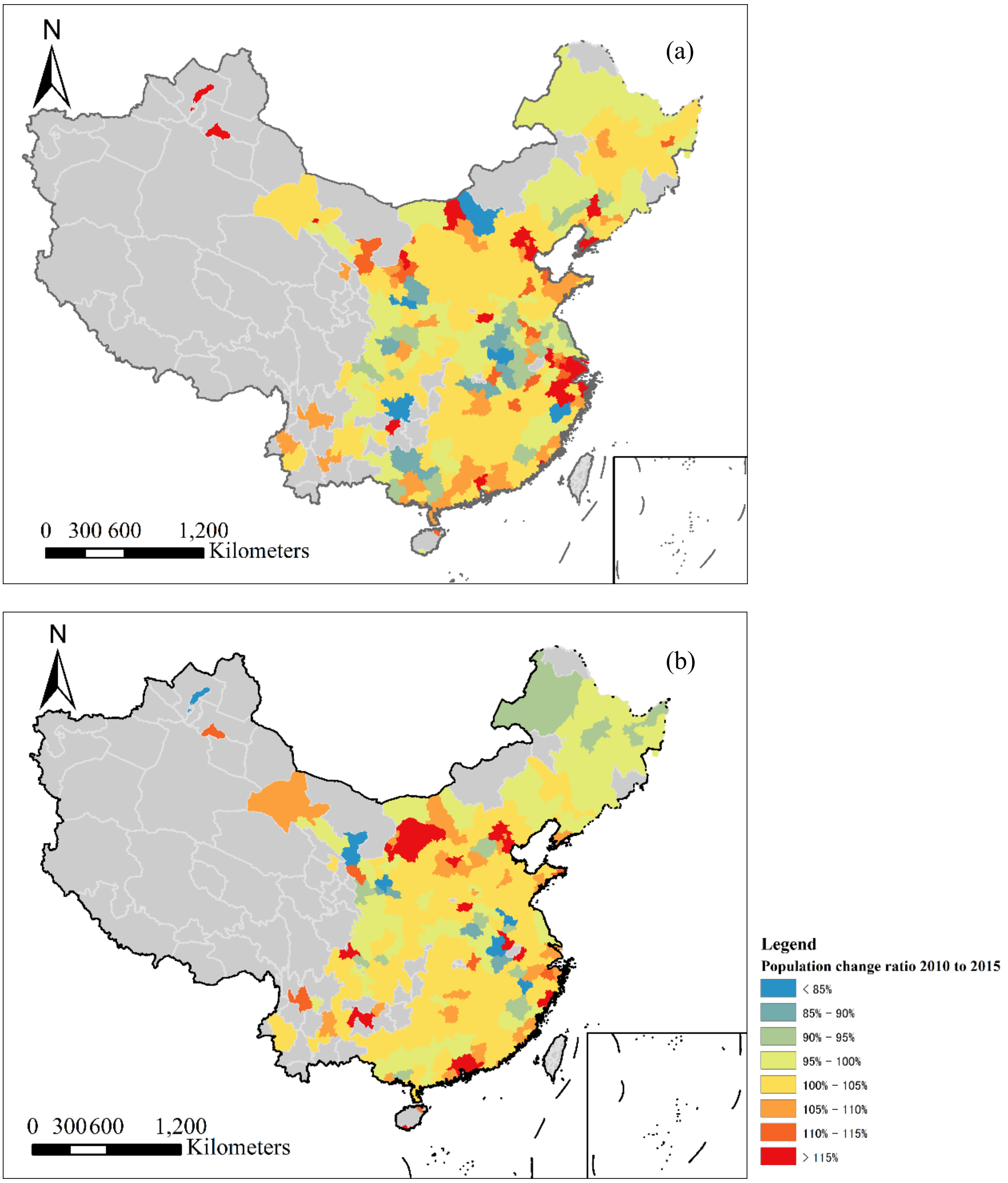

Fig. 3-4 Spatial distribution of population change ratio from (a) 2005 to 2010, (b) 2010 to 2015.

hand, the hukou policies of mega cities and megalopolis are more complicated. A resident in a big city needs to meet many conditions to meet the household registration standard, which results in many people living and working in the big city, but they cannot register local household. This means that when the registration population is used as an evaluation index, it is difficult to accurately evaluate the urbanization level of the city. On the other hand, Statistical caliber of economic and social indicators in the city statistical yearbook used later is calculated based on the resident population, such as GDP. Moreover, in the following chapters, for the evaluation of shrinking cities in Japan, etc., the population indicators are all permanent population. This is also easy for comparison analysis later.

Table 3-2. The ratio of urbanization cities classified by city level

Type	**City level**				
	Megalopolis	Mega city	Large city	Medium city	Small city
Continuous shrinkage	8.3% (1)	14.9% (11)	23.0% (43)	0% (0)	0% (0)
Temporal increase	16.7% (2)	24.3% (18)	29.9% (56)	50.0% (3)	66.7% (2)
Continuous increase	75.0% (9)	60.8% (45)	47.1% (88)	50.0% (3)	33.3% (1)

Note: Numbers in bracket refers to the counts of cities

Since the population of China kept increase, the urbanization become an increasingly national trend which is badly in need of investigation. Targeting on for China will improve the understanding of mechanisms for the population migration. According to the China City Statistical Yearbook data in 2005, 2010, and 2015, 51.6% cities experienced continuous population increase, and 28.6% cities experienced temporal population increase during 2005 to 2015, while only 19.8% cities population continuously decrease during the period. Specifically, urbanization was occurring at a higher rate in megalopolis (75.0%), and mega city (60.8%). However, urbanization is not only a phenomenon for big cities, but medium-small cities are also facing population increase in China, indicating a great process of urbanization in China (Table 3-2.).

3.2.2 Analysis Method and Research Flow

Usually, causal pathways can only be suggested by theoretical background, not by statistical analyses. As the pervious study concluded the driving factors of China urbanization are relate to demographic economic and social factors, we applied regression analysis to reveal the degree of those factors affect the urbanization in Japan. Three kinds of models have been used in this chapter including OLS, GWR, and SGWR. Some methods have been introduced in Chapter 2.

In this chapter, the methods have mentioned were designed to model the correlation between population change ratio and its potential related factors. Specially, the traditional OLS model considers all explanatory variables are global and spatially stationary. In a GWR model, all explanatory variables are local and spatially non-stationary. Spatial heterogeneity is investigated in the model fit where the spatial locations of data are incorporated. A local linear regression model for each feature in the dataset was calibrated using a different weighting of observations. The parameter in this model is a single function that represents the spatial location that is derived by weighting all neighboring observations based on a decreasing function of distance. In a SGWR model, as the integration of OLS and GWR models, some variables are global and spatially stationary, while the rest variables are local and spatially non-stationary.

In a GWR or an SGWR model, the accuracy is profoundly affected by the bandwidth, which refers to the number of nearest neighbors of city i. The corrected Akaike information criterion (AICc) method and the CV method are two methods often applied to determine the bandwidth. Compared with the CV method, the AICc method can quickly and effectively solve the problem considering the differences in the degree of freedom of different models. Therefore, in this study, the smallest AICc was selected for the appropriate bandwidth determination. The selection of the optimal SGWR model with the smallest AICc based on an iterative process was processed using GWR 4 software.

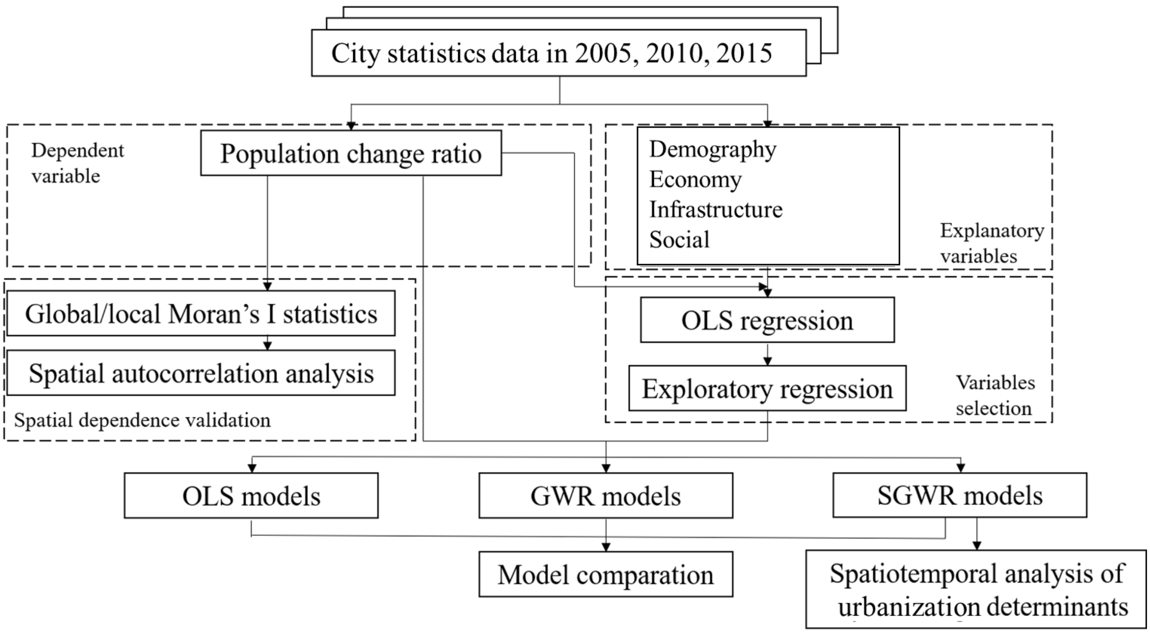

Fig. 3-5 Research flow of assessment of the determinants of urbanization in China.

The research flow of the assessment of the spatial temporal determinants of urbanization in China is shown in Fig. 3-5. We divided two study periods to discuss the temporal variation of the determinants of urbanization. The two study periods are from 2005 to 2010, and from 2010 to 2015. As urbanization was primary referring the population increase of urban area, we select the population change ratio as the dependent variable, we collected China City Statistics Yearbook data in 2006, 2011, and 2016 from the portal site of the Official Statistics of China. Then the population change ratio of each city in the two study periods was calculated as the dependent variable.

In order to ensure the applicability of GWR and SGWR models, which is to validate the spatial dependence of population change in China, both the global and local Moran's tests were conducted to reveal the spatial autocorrelation of population change ratio. Moreover, the process could also help with investigation of spatial patterns of urbanization in China.

Table 3-3. Classification, name, and description for explanatory variables for urbanization evaluation in China.

Classification	**Variable**	**Description**
Demographic factors	TP	Total population (people)
	UPR	Urban population rate (%)
Economic development and structure factors Economic factors	NE	Average number of employed staff and workers (people)
	WE	Average wage of employed staff and workers (CHY)
	UR	Unemployment rate (%)
	PCGDP	Per capita GDP (CHY/people)
	SIGDP	Secondary industry as percentage to GDP (%)
	TIGDP	Tertiary industry as percentage to GDP (%)
	GDPS	Secondary and tertiary as percentage to GDP (%)
City infrastructure development	BUA	Built up area (m^2)
	AFC	Amount of foreign capital actually utilized (CHY)
	IFA	Investment in fixed assets (CHY)
	EMBC	Expenditure for maintaining and building cities (CHY)
	ACPR	Area of paved road (m^2)
Social development	HIRE	Regular institutions of higher education
	NHHC	Numbers of hospitals and health centers
	GCA	Green covered area as % of completed area (%)

The demography factors, economy level and structure, city infrastructure level and social development level were found to be vitally essential issues for urban development, which are directly connected with urbanization (Table 3-3). The data were also collected from China City Statistics Yearbook and derived from Statistical Observations of Municipalities from 2006 to 2016. The explanatory variables consisted of 17 variables from four urban sub-systems. In the demographic urbanization sub-systems, TP refers to the size of a municipality; UPR refers to the population structure; in the economic sub-systems, NE, WE, UR, and PCGDP refer to the economy level of local resident and local government; BUA, AFC, IFA, EMBC, ACPR refers to the city infrastructure development; HIRE, NHHC, and GCA refers to the social development level from educational, medical, and welfare aspects.

In a regression model, multicollinear variables will significantly affect the regression results and distort the model, while non-significant variables will make the model more complex. Hence, we applied OLS regression and explanatory regression to exclude the multicollinear variables and non-significant variables.

After validation of the spatial dependence of population change ratio, and selection of the explanatory variables, the correlation between the dependent variable and the explanatory variables were formulated through OLS, GWR, and SGWR models.

3.3 Spatial autocorrelation analysis of population changes patterns in China

In this chapter, the population change in China from 2005 to 2010, and 2010 to 2015 was confirmed to be positive spatially clustered with the global Moran's I for the 2 study periods being 0.204, and 0.316 respectively (Table 3-4). To further understand the spatial features of population change, the Local Moran's I was applied. The LISA maps of population change shown in Fig. 3-6 revealed the local spatial cluster of the population change. During the 2 study periods, a large number of cities showed spatial clustering characteristics, especially in the Beijing city cluster, Yangtze river delta, Pearl river delta, and the western part. The results showed the LL cluster areas concentrated in western city cluster from 2005 to 2015, central city cluster from 2005 to 2010, and northeast city cluster from 2010 to 2015, while the HH cluster areas concentrated in the Beijing city cluster, Yangtze river delta, Pearl river delta from 2005 to 2015. Meanwhile, Chongqing city belongs to the HL outlier areas existed next to the LL cluster in the western city cluster, which indicate the population inflow to Chongqing and Chongqing has a population attraction to surrounding cities. Besides, for the three main HH cluster surrounded by cities belong to the LH outlier indicate the agglomeration of cities has caused population shrinkage in the surrounding areas of the urban agglomeration and population growth in the main central cities.

Table 3-4. Global Moran's I results for population change in China.

Study period	Global Moran's I	Z-score	P value
2005-2010	0.204	6.39	<0.01
2010-2015	0.316	8.15	<0.01

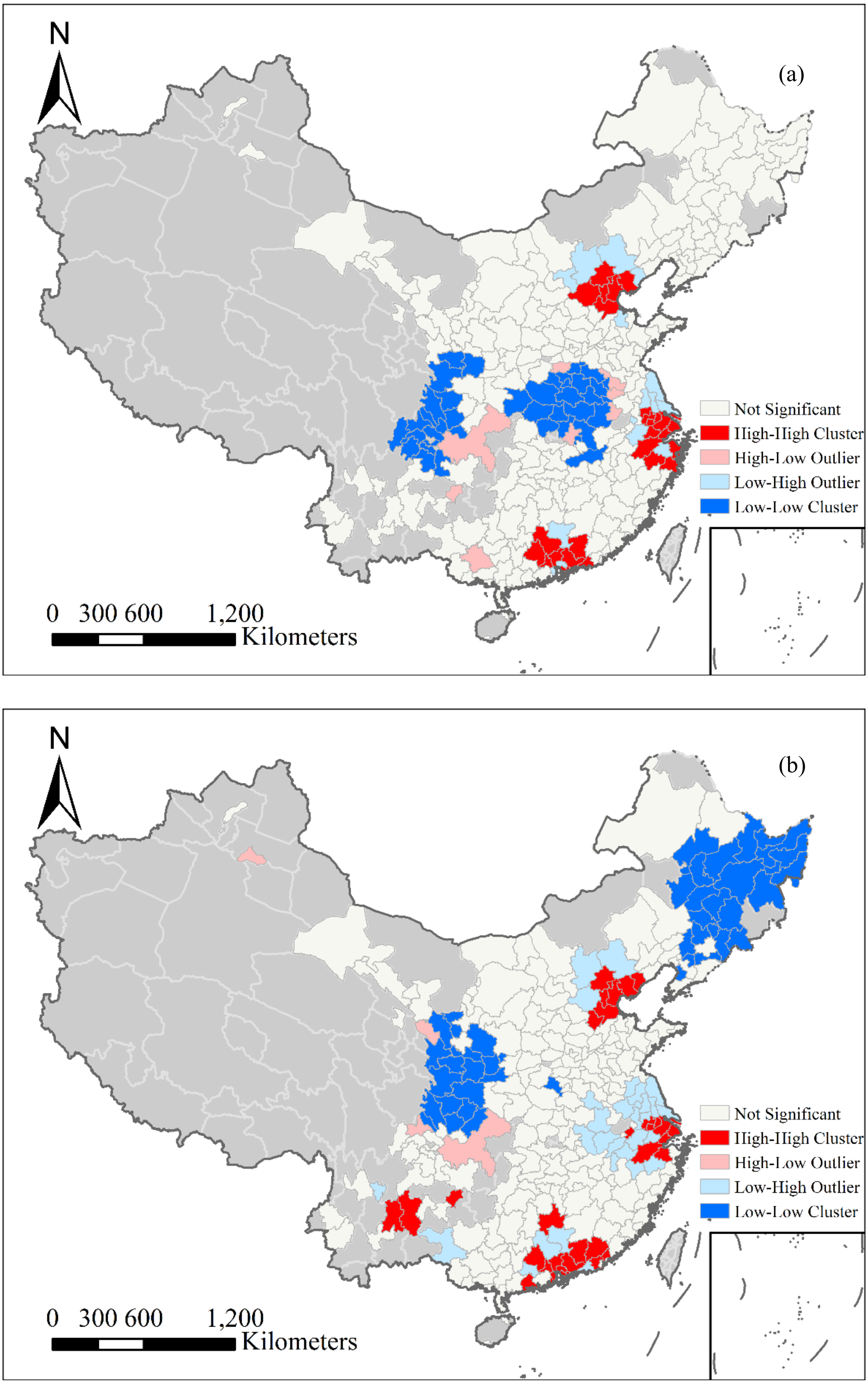

Fig. 3-6 LISA cluster maps of population change in China
(a) from 2005 to 2010; (b) from 2010 to 2015.

Through the global/local Moran’s I statistics, the results indicated the population change patterns did have spatial autocorrelation. City clusters centered in Beijing, Shanghai, and Guangzhou were shown as the spatial agglomeration of population growth municipalities, while cities in the western region, central region, and northeast region were shown as the spatial agglomeration of shrinking cities. The unbalanced regional economic scale and urban development degree are essential factors leading to population mobility, which in turn accelerates the population outflow in small cities. These results revealed that significant correlation between urbanization and city spatial distribution, and the increasing urbanization process in China. This finding also showed the spatial dependency of population change.

3.4 Regression results

3.4.1 Variable selection

To eliminate the multicollinearity of the data, which could produce a distorted or inaccurate model, the variance inflation factor (VIF) for each explanatory variable was calculated, and the variables with a VIF value over 5 were sequentially excluded from the final model until no more VIF > 5 were found [19]. In this procedure, shown in Table 3-4 and Table 3-5, 8 explanatory variables including TP, NE, BUA, IFA, ACPR, and NHHC, which had significant multicollinearity with the population change ratio, were therefore excluded from the final model. Then, exploratory regression was conducted to exclude the non-significant variables of the population change at a 95% confidence level. In this procedure, SIGDP, TIGDP, and GCA was excluded. After testing the spatial autocorrelation of population change, multivariate OLS regression and exploratory regression were conducted to test the relationship between population change and selected explanatory variables. All the variables were first normalized to ensure the variables were normally distribution or approximated normal distribution.

The results showed that no local multicollinearity existed among the remaining variables. Therefore, after removing the variables redundancy or non-significance, eight explanatory variables, including UPR, WE, UR, PCGDP, GDPS, AFC, EMBC, and RIHE, were screened out for both study periods, which suggests the general correlates of urbanization remain unchanged. After screening out the variables, the OLS model was reformulated with the eight explanatory variables. These variables were then used for the corresponding GWR and SGWR models.

Table 3-5. Variance inflation factor (VIF) value of variables selection procedure of the China urbanization model study period 2005 to 2010.

Iteration	TP	UPR	NE	WE	UR	PCGDP	SIGDP	TIGDP	GDPS	BUA	AFC	IFA	EMBC	ACPR	RIHE	NHHC	GCA
1 (keep all)	20.53	2.58	7.41	9.28	4.01	5.62	4.72	2.96	3.9	7.48	9.92	8.99	3.57	6.62	5.67	20.75	1.21
2 (remove TP)	-	2.57	7.4	7.31	3.91	5.24	4.21	2.95	3.87	7.47	7.84	8.91	3.51	6.6	5.57	18.71	1.21
3 (remove NHHC)	-	2.57	7.29	7.1	3.81	5.15	4.09	2.94	3.85	7.46	7.15	8.89	3.5	6.59	5.41	-	1.21
4 (remove IFA)	-	2.56	7.18	5.18	3.65	4.98	1.24	2.91	1.78	7.46	5.45	-	3.46	6.51	4.08	-	1.2
5 (remove BUA)	-	2.54	7.09	4.81	3.51	4.52	1.24	2.87	1.74	-	4.91	-	3.45	6.48	3.87	-	1.2
6 (remove NE)	-	2.52	-	1.18	3.41	4.18	1.21	2.85	1.68	-	4.86	-	3.44	6.37	3.81	-	1.19
7 (remove ACPR)	-	2.51	-	1.18	3.21	3.91	1.19	2.81	1.51	-	4.71	-	3.44	-	3.71	-	1.18

Table 3-6. Variance inflation factor (VIF) value of variables selection procedure of the China urbanization model study period 2010 to 2015.

Iteration	TP	UPR	NE	WE	UR	PCGDP	SIGDP	TIGDP	GDPS	BUA	AFC	IFA	EMBC	ACPR	RIHE	NHHC	GCA
1 (keep all)	6.73	2.31	11.38	3.53	1.17	3.66	4.72	2.96	3.9	28.09	5.93	11.85	10.77	13.33	5.92	11.65	11.89
2 (remove BUA)	6.71	2.3	11.08	7.31	3.91	5.24	4.21	2.95	3.87	-	7.84	8.91	7.91	12.18	5.57	11.45	4.95
3 (remove ACPR)	6.65	2.29	10.84	7.1	3.81	5.15	4.09	2.94	3.85	-	7.15	8.89	5.89	-	5.18	10.98	4.81
4 (remove NHHC)	6.61	2.24	10.15	6.92	3.68	4.91	3.94	2.62	3.78	-	6.66	8.84	5.67	-	5.12	-	4.71
5 (remove NE)	6.48	1.84	-	6.56	3.25	4.53	3.78	2.22	3.38	-	6.65	8.81	5.27	-	5.07	-	4.62
6 (remove IFA)	6.41	1.57	-	6.14	3.15	4.43	3.31	1.79	2.88	-	6.41	-	4.97	-	4.91	-	4.41
7 (remove TP)	-	1.11	-	5.86	3.07	4.22	3.01	1.31	2.64	-	6.39	-	4.82	-	4.67	-	4.02

3.4.2 Global and local analysis of urbanization in China

After screening out the variables, the global model based on the OLS regression procedure was reformulated using the six variables. The results revealed the intercorrelation between population change and municipality parameters, as shown in Table 3-7.

Table 3-7. Municipality parameters estimated coefficient for the global model (China).

Study period	Intercept	UPR	WE	UR	PCGDP	GDPS	AFC	EMBC	RIHE	Adjust R^2
2005-2010	14.39*	2.49*	7.07*	-0.61	0.90	4.67*	11.81*	20.88*	8.31*	0.623
2010-2015	16.28*	3.16*	0.99*	-0.85	0.10	8.34*	14.94*	9.22*	11.06*	0.528

Note: * $p < 0.05$.

The results showed that the global model for population change from 2010 to 2015 was moderate (adjusted coefficient of determination (R^2) = 0.527), which indicates the eight parameters could explain the population change during 2005–2010 to a certain extent. The adjusted R^2 of the global model for population change from 2010 to 2015 was 0.640, indicating a substantially adequate explanation of the population change. The results also revealed that AFC and EMBC had the greatest coefficient values, which suggests the urban infrastructure construction has the most significant effect on population change compared with the other parameters. Moreover, RIHE, with high positive coefficients, had significantly positive effects on population change compared with the other parameters, which indicating the social development have a positive effect on population inflow.

Table 3-8. Municipality parameters estimated coefficient for the GWR model (China study period from 2005 to 2010).

Variable	Min	Mean	Max	STD	Range
UPR	-4.05	2.82	13.41	4.40	17.46
WE	-.923	1.07	10.22	3.60	19.45
UR	-7.15	0.91	7.35	3.75	14.49
PCGDP	-15.46	0.99	28.54	9.24	44.10
GDPS	-5.45	11.83	27.52	8.75	32.97
AFC	-45.52	4.46	43.47	22.30	88.99
EMBC	-21.07	20.37	34.03	10.46	55.10
RIHE	-2.76	10.94	26.86	6.74	29.61

Table 3-9. Municipality parameters estimated coefficient for the GWR model
(China study period from 2010 to 2015).

Variable	Min	Mean	Max	STD	Range
UPR	-10.1	-0.77	8.50	4.49	18.61
WE	-6.78	4.87	16.22	5.24	22.99
UR	-5.54	7.8	22.8	8.51	28.35
PCGDP	-18.91	2.41	14.3	8.1	33.21
GDPS	-4.84	14.58	40.13	12.55	44.98
AFC	-13.7	19.3	59.97	19.19	73.67
EMBC	-27.24	25.03	82.71	28.24	109.95
RIHE	-11.31	6.47	19.41	9.12	30.72

Comparably, the various indicators of the economy sub-system have more or less affected the attractiveness of the city to the population, while the urban infrastructure construction and some indicators in the social development system have an impact on the urban population mobility. This shows that on the one hand, China's economic development is accompanied by the urbanization process, and in the current urbanization process, people are more inclined to choose cities with advantages in specific urban indicators, such as education resources, urban construction investment funds, etc.

Considering the spatial heterogeneity and spatial autocorrelation of population change, GWR was applied to fit a local population change model. shows the parameter coefficients for the local model of the two study periods. Compared with the first study period, the variation range and the number of mild outliers of the parameters increased. The effects of the parameters could be positive or negative for different regions (Table 3-8, Table 3-9).

3.4.3 Assessment of urbanization in China through SGWR models

Considering the global model explained the population change to some degree whereas the local model improved the accuracy, the SGWR models were developed to consider both the spatial stationarity and non-stationarity for the parameters affecting population change. An iterative process was used to determine whether a parameter was a global or local variable. The most fitted SGWR model was based on the AICc; the model with the smallest AICc value was selected, which refers to the best fitting result. In this procedure, UPR, WE, PCGDP were selected as global variables, and UPR, APR, and ECR remained local variables for both models (Table 3-10).

Table 3-10. Determination of parameters for the SGWR models (China).

Study Period	Explanatory Variable							
	UPR	**WE**	**UR**	**PCGDP**	**GDPS**	**AFC**	**EMBC**	**RIHE**
2005–2010	Global	Global	Global	Local	Local	Local	Local	Global
2010–2015	Global	Global	Global	Local	Local	Local	Local	Global

As shown in Table 3-11, the adjusted R^2 for the two local models were 0.528 and 0.815, respectively, which are higher than the global models, suggesting that considering the parameter influences to be spatially non-stationary is more representative than considering them to be spatially stationary. The fitting results of the SGWR model improved compared with the global and local models. The R^2 of the SGWR model was the largest compared to the other two models. The AICc value of the SGWR model for the first study period decreased by 155.43, and 136.96 compared with the OLS and GWR models, respectively. For the second study period, the AICc value decreased by 114.36 and 114.35, respectively. Combined with the value of the bandwidth and residual square, we found that the SGWR model was optimal for both study periods, which indicates the population change in China displayed spatially stationary and non-stationary parameters. In addition, in the first study period from 2005 to 2010, the adjusted R^2 of OLS model is greater than the GWR model. From this point, the OLS model is better, but this is a misunderstanding, which only means that the value predicted by the OLS model is closer to the original value. In comparison of AICc values, the GWR model is still better.

Table 3-11. Accuracy evaluation for the global, local, and SGWR model (China).

Parameter	2005–2010			2010–2015		
	OLS	**GWR**	**SGWR**	**OLS**	**GWR**	**SGWR**
Bandwidth	-	138	58	-	135	84
Residual squares	342.85	351.75	142.93	337.18	336.17	169.99
AICc	2858.84	2840.37	2703.41	2827.54	2827.55	2713.20
Adjusted R^2	0.640	0.622	0.805	0.527	0.528	0.718

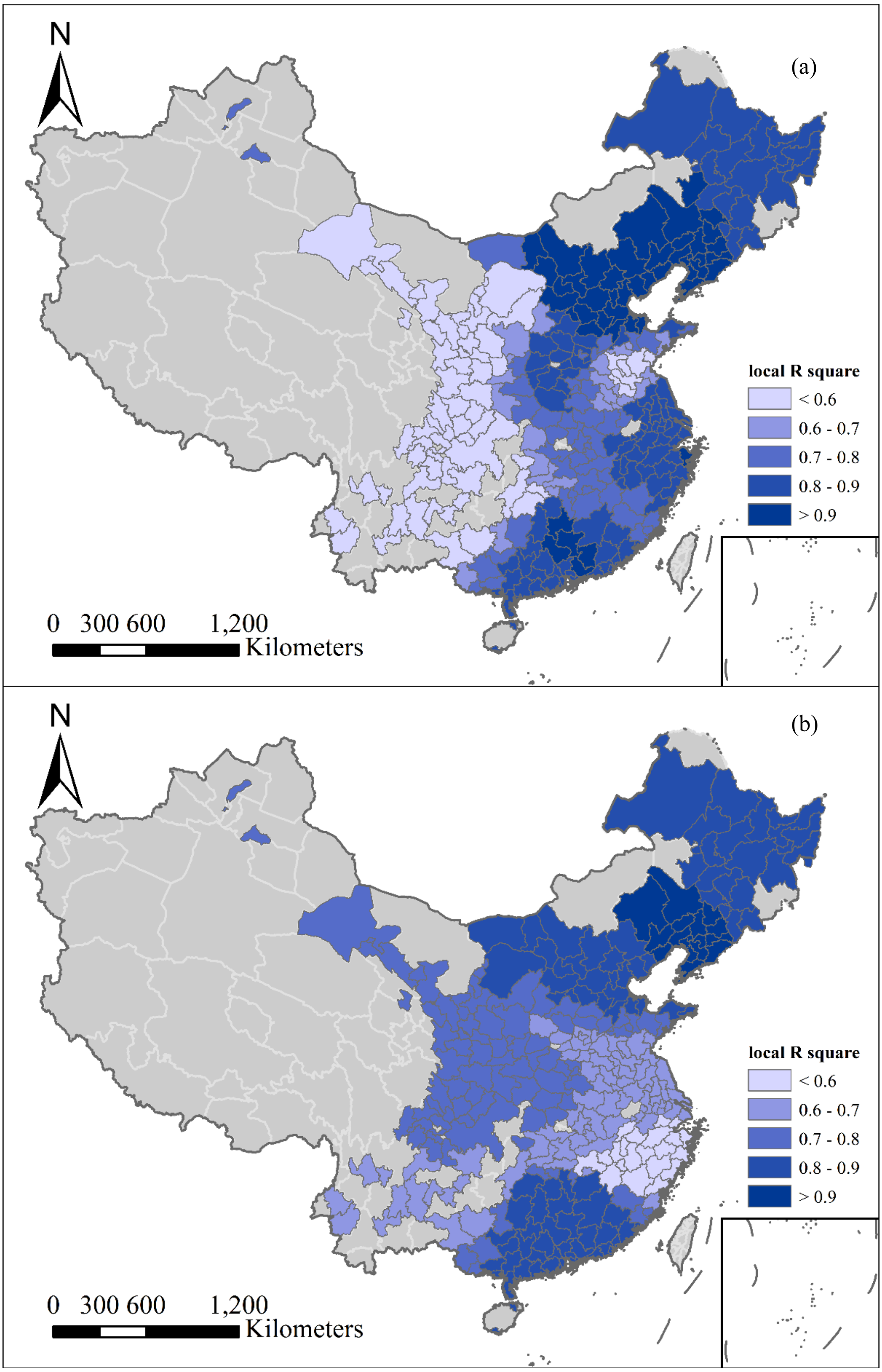

Fig. 3-7 Local R^2 of urbanization in China based on SGWR

(a) from 2005 to 2010; (b) from 2010 to 2015.

As Fig. 3-7 shown the local R^2 of the SGWR models, for the first study period from 2005 to 2010, the values of local R^2 for northeast region, coastal regions except Shandong province were relatively larger, especially in and around the Beijing city cluster and the Pearl river delta region. However, the values of local R^2 for the western regions and Shandong province were relatively smaller. Conversely, from 2010 to 2015, the local R^2 for the western regions were higher than before, while R^2 for the Zhejiang province decreased.

For PCGDP, GDPS, AFC, and EMBC found to be non-stationary spatial correlates affect the population change, the local coefficients of each variable and the spatial characteristics of city shrinkage correlates were analyzed. The t-test was conducted to pick out the coefficients of the local variables which passed the significance level of 0.05.

Fig. 3-8 depicts the local coefficients of PCGDP from 2005 to 2010, and from 2010 to 2015, PCGDP had a significant positive effect in 51 and 74 cities ($p < 0.05$) for the two study periods, respectively. The results indicated that from 2005 to 2010, the ratio of the per capita GDP mainly affected the population change around the eastern coastal region, whereas from 2010 to 2015, the per capita GDP affected areas were scattered and extended to southern coastal region, and Xinjiang province. PCGDP remained correlated with the population change in most parts of eastern coastal region from 2005 to 2015.

There is a great correlation between the economic level and the level of urbanization. China's urban economic development in the Yangtze River Delta and Pearl River Delta regions is relatively high. Even the small and medium-sized cities in the region have the highest GDP per capita. In these cities, it can be seen that the estimated impact coefficient of per capita GDP is positive, indicating its positive effect on population attraction. On the other hand, for the Yangtze River Delta, cities with the largest estimated coefficients are gradually extending inwards, which may actually be due to the impact of the expansion of the Yangtze River Delta region. Initially, the cities in the Yangtze River Delta region were centered on Shanghai, with Nanjing and Hangzhou as sub-centers, covering only about 20 cities in Shanghai, Jiangsu Province, and Zhejiang Province. In recent years, with the continuous development of urbanization in China, the Yangtze River Delta region has expanded to cover the entire province of Jiangsu and Zhejiang and covers most cities in Anhui Province.

Fig. 3-9 depicts the local coefficients of GDPS from 2005 to 2010, and from 2010 to 2015, GDPS had a significant positive effect on population change for the two study periods, respectively. The results indicated that from 2005 to 2010, the ratio of the GDPS mainly affected the population change around the central region, whereas from 2010 to 2015, the GDPS affected areas were extended to the eastern coastal region and west region. This may be due to changes in the attractiveness of population movements caused by regional differences and changes in industrial structure.

Fig 3-10 shows the coefficient of the amount of foreign capital actually utilized effect on population change from 2005 to 2010 and from 2010 to 2015. Compared with the PCGDP and GPDS indicators in the economic system, the influence of AFC on population changes has expanded a lot. In the first study period, AFC has a greater impact on the urbanization of central regional cities, followed by eastern coastal regional cities, and northeastern regional cities. In addition, in some cities in the west and southwest regions, negative correlation effects can be observed. This means that the influence of the area is negative. Cities in these regions have invested a lot of foreign capital, but the urban population is losing. This may be because city construction takes a certain amount of time to see the effect with the impact of this hysteresis. In the second period of time, the impact of AFC on the population mobility of these cities became positive, which just shows that the investment in urban construction.

In the second time period, it can be seen that the AFC's influence has expanded to the west and south. Due to the policies of the “Belt and Road” initiative and the development of the western region, the western region has attracted a large amount of foreign capital and continuously introduced talents. The coastal cities in the east and south are more attractive to talents due to their outgoing economy, so the impact of AFC is also positive.

Fig. 3-11 shows the spatial distribution of the local EMBC coefficient from 2005 to 2010 and from 2010 to 2015. The local ECR coefficient was found to be spatially non-stationary, and the differences between the two study periods in the region varied. Generally, the impact of EMBC on population mobility is similar to that of AFC, and some cities have negative estimates. This can also be attributed to the lag of urban construction for population mobility.

On the whole, the impact of urban infrastructure on urbanization is positive and negative, while the impact of the economic system is positive. However, the estimated coefficient of urban infrastructure indicators is much larger than the estimated coefficient of economic factors.

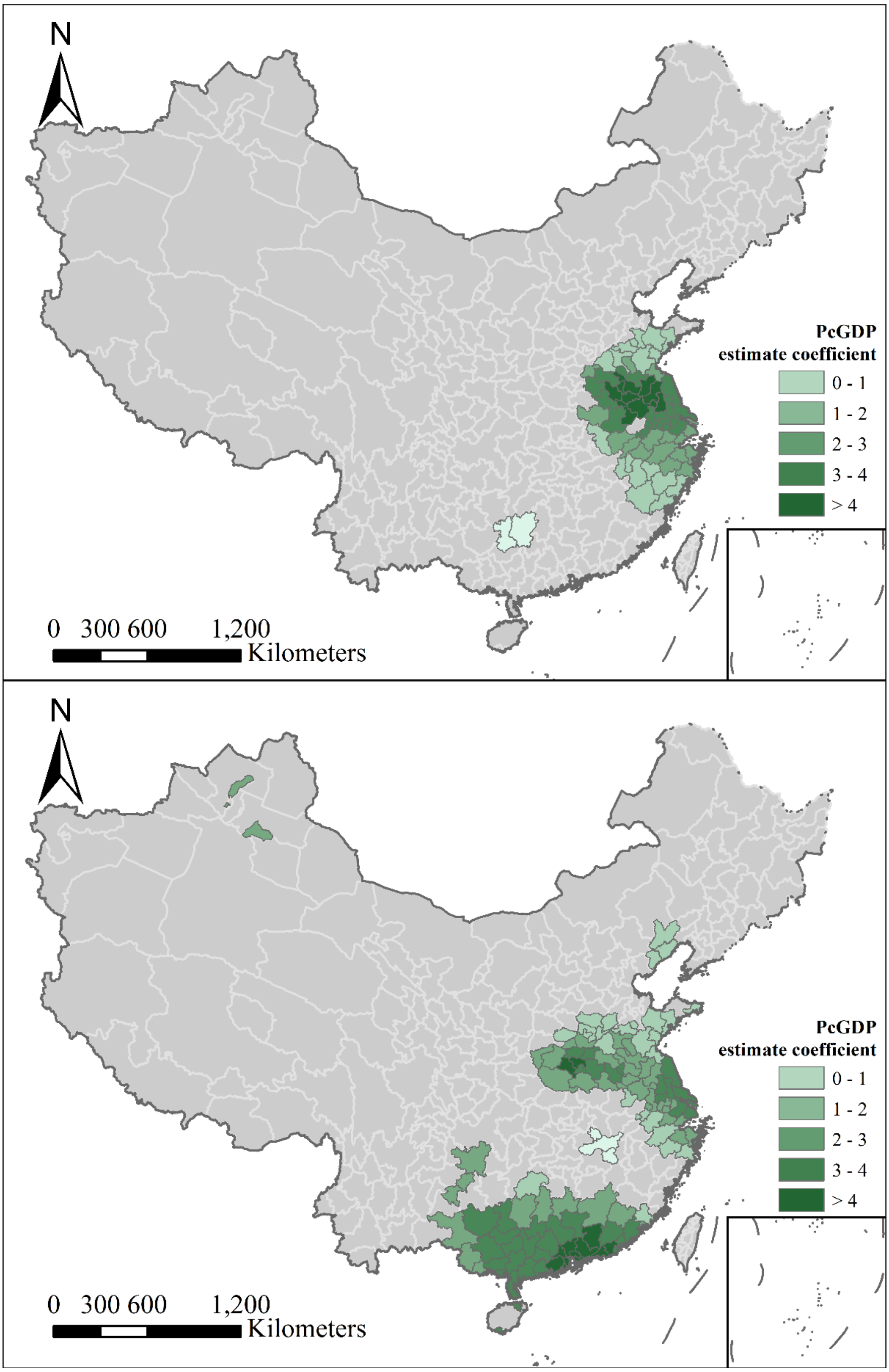

Fig. 3-8 Local estimated coefficient of per capita GDP

(a) from 2005 to 2010 and (b) from 2010 to 2015.

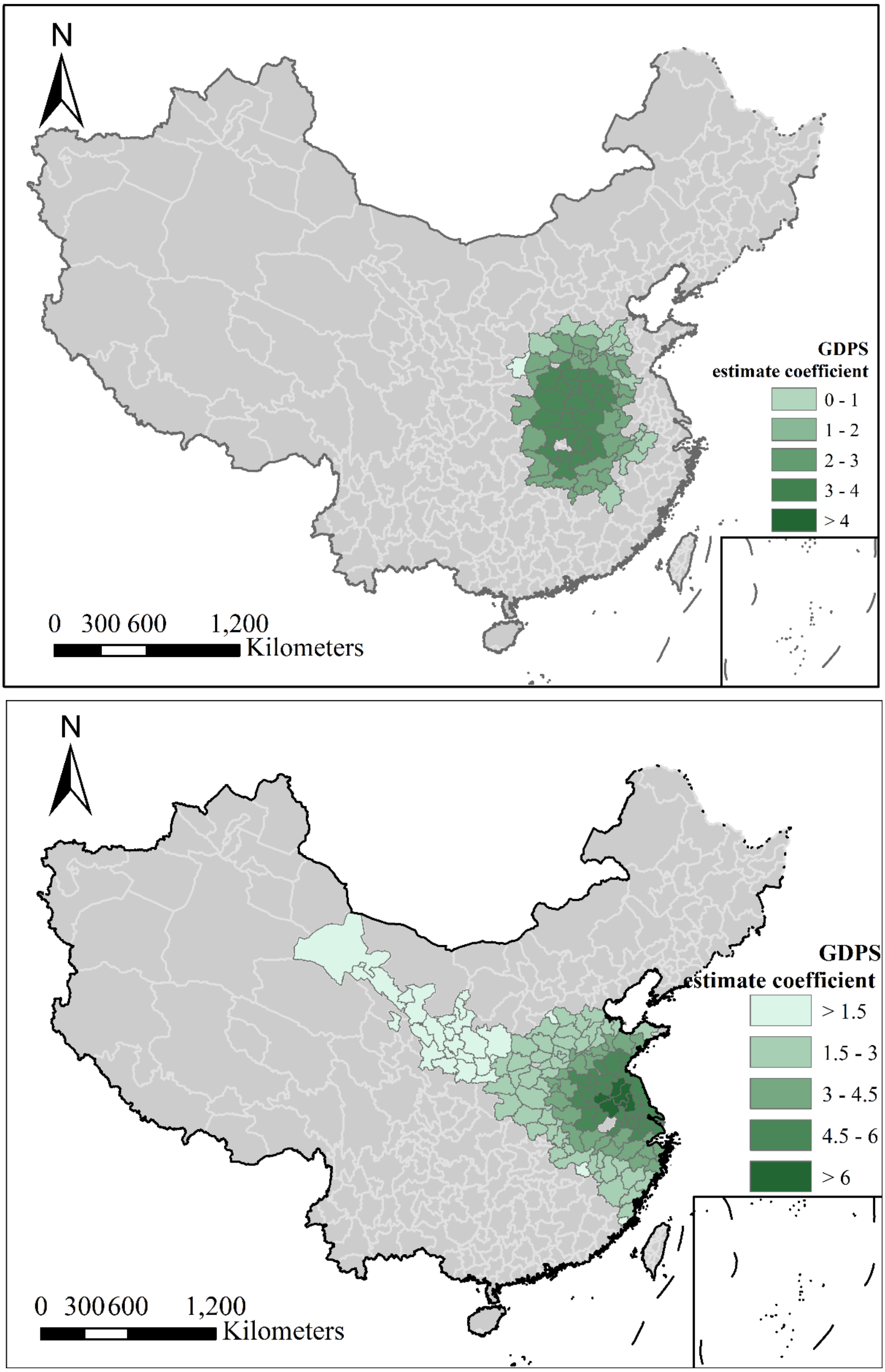

Fig. 3-9 shows the coefficient of the GDPS

(a) from 2005 to 2010 and (b) from 2010 to 2015

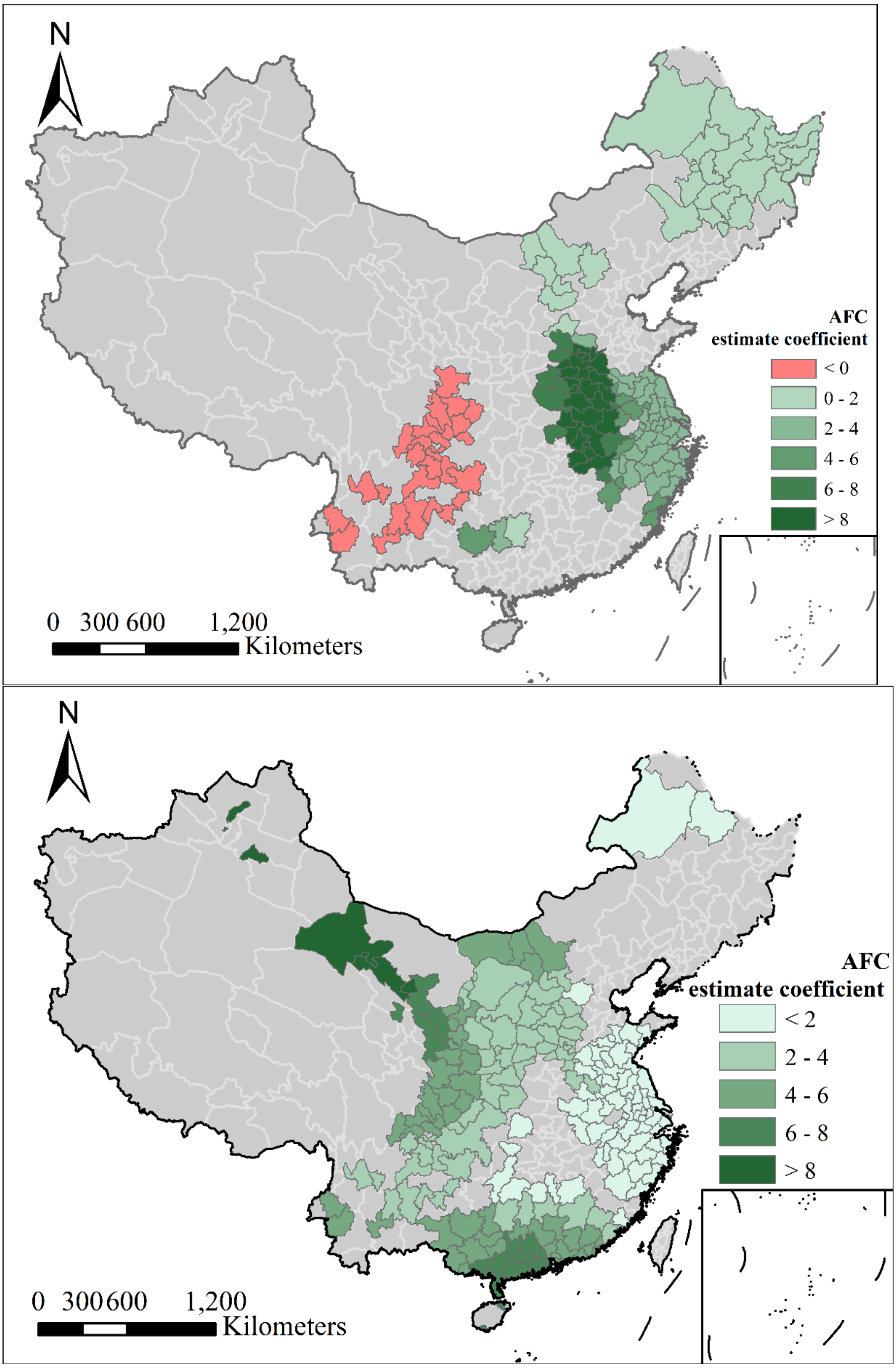

Fig. 3-10 Local estimated coefficient of AFC

(a) from 2005 to 2010 and (b) from 2010 to 2015.

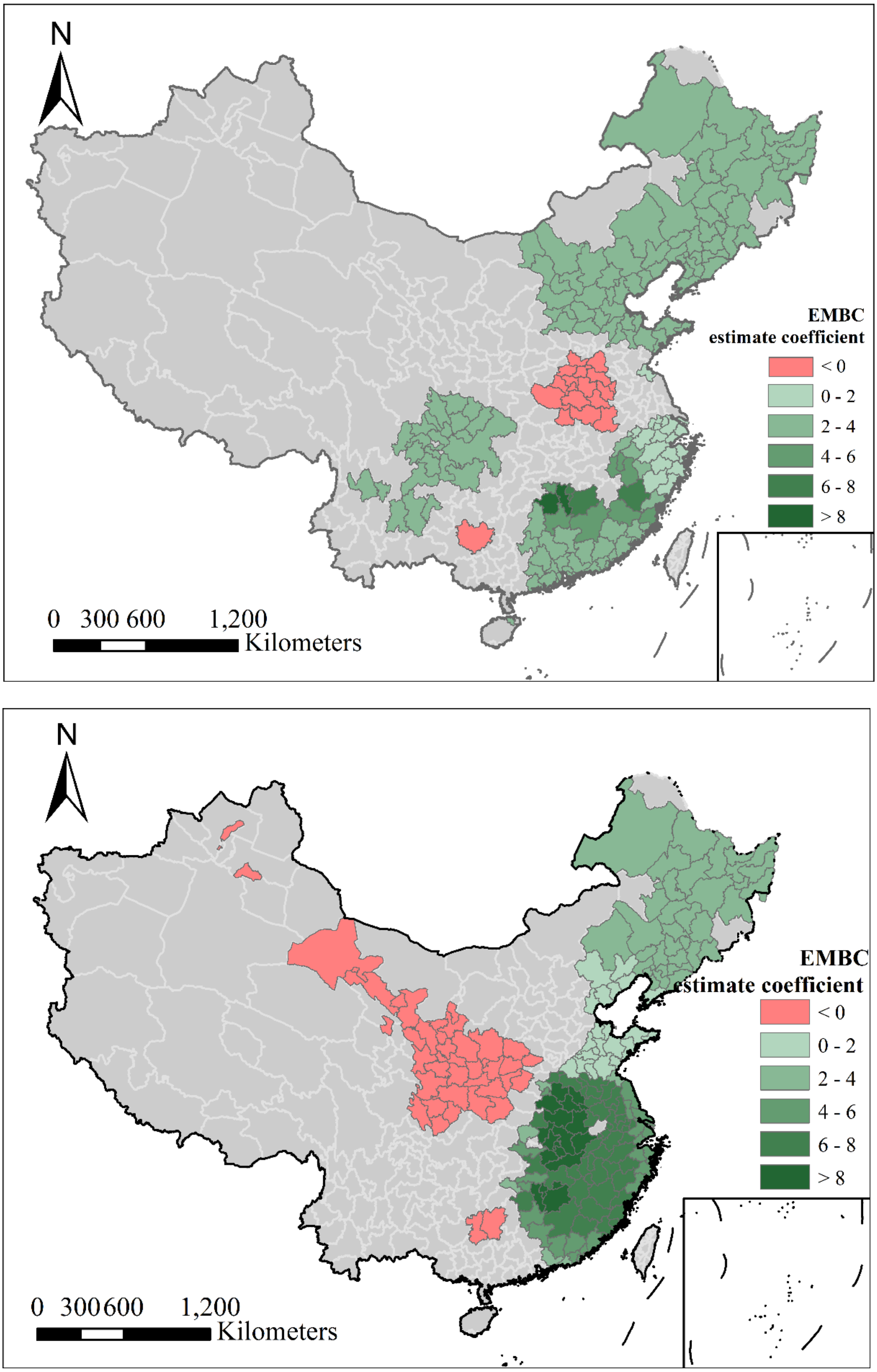

Fig. 3-11 Local estimated coefficient of EMBC

(a) from 2005 to 2010 and (b) from 2010 to 2015.

Other studies explained urbanization in China as being due to the economy development, and industrialization at a global level. However, few studies focused on the quantitative differences of determinates that contribute to urbanization. As the global and local Moran's I statistics showed spatial aggregation for the population change ratio, we considered the variables to have spatially stationary or non-stationary effects on urbanization in China, and encouraging us to explore the regional differences in urbanization from 2005 to 2015. The results revealed the spatial dependency and spatial heterogeneity of urbanization in China, and showed PCGDP and GDPS, which refers to economy development, dominated urbanization in the cities which are belongs to the economically developed region in China; AFC and EMBC, which refers to the urban infrastructure development dominated urbanization in most cities in China with negative or positive effect. Moreover, the demographic and social development factors impact on various cities in China can be considered to be spatially stationary, which means that the consideration of these factors for the movement of population is rarely affected by their spatial location. From the perspective of the impact coefficient, HIRE, which refers to the educational resources, AFC and EMBC, which refer to the urban construction, are the key factors influencing urbanization in China from 2005 to 2015.

3.5 Summary

In this chapter, we developed OLS, GWR, and SGWR models to capture the spatiotemporal differences in determinants affecting urbanization in China based on national statistics data from 2005 to 2015. The spatial dependence of the urbanization in China has been confirmed through both global and local Moran's I tests.

Our findings are as follows: (1) Urbanization in China showed a significant increasing positive spatial autocorrelation. (2) Compared with traditional OLS and GWR models, the SGWR models, which consider spatial dependence and heterogeneity, are more interpretive in the explanation of urbanization. (3) The correlation between the demographic, economic, infrastructure and social indexes and urbanization was revealed through quantitative analysis. PCGDP, GDPS, AFC, and EMBC, which refer to the economy development and urban infrastructure, were the critical spatially non-stationary correlates, with large estimated coefficients, affected the urbanization in different regions at different times. (4) UPR, HIRE which refer to the demographic structure and educational resources with large estimated coefficients, affected the urbanization spatially stationary. The findings contribute to improving our understanding of the situation and correlates of urbanization, and provide valuable information for governments and planners when developing effective coping strategies for sustainable city development.

The limitation of this study is the insufficient consideration of the endogenous data. It can be seen from the results that China's urbanization and economic development are inseparable. Economic development has attracted population inflows while population inflows have accelerated economic development. Indicators such as urban construction can be regarded as lagging variables, and educational resources (universities) as relatively stable indicators can be considered as not endogenous to the flow of population. But the economic impact may cause some misinterpretation of the results.

Reference

[1] Quigley, J. M. (2009). Urbanization, agglomeration, and economic development. Urbanization and growth, 115.

[2] Nations U. 2018 revision of world urbanization prospects. United Nations Department of Economic and Social Affairs; 2018.

[3] Zlotnik, H. (2017). World urbanization: trends and prospects. In New Forms of Urbanization (pp. 43-64). Routledge.

[4] Champion, T. (2001). Urbanization, suburbanization, counterurbanization and reurbanization. Handbook of urban studies, 160, 1.

[5] Chen, M., Liu, W., & Tao, X. (2013). Evolution and assessment on China's urbanization 1960–2010: under-urbanization or over-urbanization?. Habitat International, 38, 25-33.

[6] Bertinelli, L., & Black, D. (2004). Urbanization and growth. Journal of Urban Economics, 56(1), 80-96.

[7] Chen, J. (2007). Rapid urbanization in China: A real challenge to soil protection and food security. Catena, 69(1), 1-15.

[8] Zhang, K. H., & Shunfeng, S. (2003). Rural–urban migration and urbanization in China: Evidence from time-series and cross-section analyses. China Economic Review, 14(4), 386-400.

[9] Chan, K. W., & Xu, X. (1985). Urban population growth and urbanization in China since 1949: reconstructing a baseline. The China Quarterly, 104, 583-613.

[10] National Geophysical Data Center. http://ngdc.noaa.gov/eog/

[11] National Bureau of Statistics of China. http://data.stats.gov.cn/.

[12] Liangen, Zeng & Lu, Jingyan & Liu, Yenping & Zhou, Yang & Hu, Haoyu. (2019). Analysis of Regional Differences and Influencing Factors on China’s Carbon Emission Efficiency in 2005–2015. Energies.

[13] Chen, J., Guo, F., & Wu, Y. (2011). One decade of urban housing reform in China: Urban housing price dynamics and the role of migration and urbanization, 1995–2005. Habitat International, 35(1), 1-8.

[14] Li, S. M. (2004). Population migration and urbanization in China: A comparative analysis of the 1990 population census and the 1995 national one percent sample population survey. International Migration Review, 38(2), 655-685.

[15] Ling, L. I. (2001). Internal population migration in China since the economic reforms: A review [J]. Geographical Research, 4(10).

[16] Wang, X. R., Hui, E. C. M., & Sun, J. X. (2017). Population migration, urbanization and housing prices: Evidence from the cities in China. Habitat International, 66, 49-56.

[17] Chan, K. W. (2010). Population, migration and the Lewis turning point in China. China Labor Economics, (1), 3.

[18] Wang, G. X., & Lu, Q. (2007). Migration of rural population in recent years in China. Scientia Geographica Sinica, 27(5), 630-635.
[19] Hair JF, Sarstedt M, Ringle CM, Mena JAJJotaoms. An assessment of the use of partial least squares structural equation modeling in marketing research. 2012;40:414-33.

Chapter 4. Spatial temporal determinants of city shrinkage in Japan

4.1 Introduction

As of 2019, more than half of the world's population is living in urban areas, and the rate is expected to reach 70% by 2050 [1]. Due to rapid urbanization, many environmental effects have become severe and are receiving people's attention, such as air pollution and urban heat islands. However, city shrinkage, as the antithesis of urbanization, is an ongoing extreme phenomenon not only in developed countries, but also emerging in some fast-urbanizing countries [2, 3]. City shrinkage is characterized by population loss, economic downturn, and inefficient land use [4-6]. Especially in the developed world, with a background of globalization and de-industrialization, many large cities are considered shrinking cities or will be shrinking cities [7-10]. Research on the city shrinkage not only provides solutions for the affected regions, but also alerts fast-urbanizing areas about future problems.

The process of city shrinkage occurs within a complex system, so studies on city shrinkage considered many aspects. Many studies focused on the policies and response to city shrinkage and called for local corresponding strategies for the sustainable development of the cities. For example, by assessing four policy responses to city shrinkage in Europe, improving the quality of life of local citizens is the optimal strategy for local government [11]; by identifying the shortcomings of the local government response to city shrinkage as lack of transparency and lack of understanding of best practices, the development of local adaptation policies in shrinking cities is required [12]. Some scholars focused on exploring the factors driving city shrinkage. The driving factors vary from demographics, economy, society, and policies at global and local levels. For example, socio-spatial inequalities were found to more strongly influence city shrinking compared with economic factors in the American Rust Belt [13]; falling birth rates and the effects of German reunification were the main factors affect shrinkage in Germany [14]. The demographic change, which refers to the ageing population and low birth rate, is the primary cause of city shrinkage in Japan [3]; the economic level and population structure are highly related to city shrinkage in China [15]. Although spatial dependence and spatial heterogeneity were confirmed to exist in the city shrinkage spatial distribution [15], previous studies mainly focused on investigating local driving factors of single cities or global driving factors for regions or countries. As studies on policy responses to city shrinkage illustrate the local strategies are more effective and required than corresponding global policies, understanding the local driving factors from the global level is essential for policies makers and actors to better respond to this phenomenon.

Spatial dependence results from various spatial spillover effects, and spatial heterogeneity results from inherent differences between spatial units and variations over space [16, 17]. Ordinary least squares (OLS) regression can be used to assess the general correlates of city shrinkage where the correlates are spatially stationary [15]. However, local adaptation strategies are required to identify the spatial heterogeneity of city shrinkage. Geographically weighted regression (GWR) has become an increasingly essential tool for revealing local variables' effects on the dependent variable over a geographical area [18-21]. In the GWR model, all the explanatory variables are spatially non-stationary. The semiparametric geographically weighted regression (SGWR) model, which is a mix of OLS and GWR models, is useful in situations where certain explanatory variables influencing the response are global while others are local [22]. Compared with the traditional OLS and GWR models, the SGWR model is usually more interpretive [23-25]. As shrinking cities may have several similar characteristics, which are better considered as spatially stationary impact factors, the SGWR model could be more appropriate for modeling the driving factors of city shrinkage.

Following the Meiji restoration, the population of Japan, characterized by urbanization, continued to quickly increase. The population increased from 34 million in 1868 to 128 million in 2008. However, with strict immigration rules, low fertility, and the ageing society, after 2008, the population began to decrease, and many cities became shrinking cities. Compared to other countries experiencing city shrinkage, Japan urban shrinkage is particularly serious. This phenomenon has already significantly influenced the sustainable social development even in large urban agglomerations such as Tokyo and Nagoya [3,26]. Studies on Japan are helpful for understanding the process and mechanism of city shrinkage. As city shrinkage was first proposed to occur due to migration and depopulation [27], population loss is the most indicative phenomenon of a shrinking city [28]. The population change ratio is the most often used indicator to represent the degree of city shrinkage [15, 28-31].

In this chapter, the population change ratio derived from national census data in 2005, 2010, and 2015 was selected as the city shrinkage index, and a total of 1647 municipalities in Japan were selected as study objects. The objectives of this study were to (1) investigate the spatiotemporal distributions and patterns of shrinking cities in Japan; (2) reveal the interrelationship between city shrinkage and demographic, economy, and social indexes on global and local scales; and (3) compare the determinants across different regions. The findings illustrate the local determinants of city shrinkage in Japan, improve the understanding of the situation and the factors driving city shrinkage, provide valuable information for governments and planners developing effective coping strategies on the global and local levels, and hopefully will draw the attention of fast-developing countries to this possible future issue.

This chapter is organized as the following. In Chapter 4.2 the methods and the materials are introduced, and general information of city shrinkage in Japan is discussed. The investigation of spatial distribution patterns of shrinking cities is presented in Chapter 4.3. And the spatial temporal determinants of city shrinkage is explored through regression analysis in Chapter 4.4. The Chapter 4.5 is the summary.

4.2 Study area, methods, and materials

4.2.1 Study area and general information of city shrinkage in Japan

Japan is a highly developed country, having the world's third-largest gross domestic product (GDP) [32]. The total population of Japan was about 127 million and the urbanization rate was about 93% according to the National Census in 2015. Japan consists of four main islands, including Hokkaido, Honshu, Shikoku, and Kyushu from north to south, and about 6848 surrounding islands. Japan has 47 prefectures, and each prefecture consists of numerous municipalities, with 1741 in total as of October 2016. Japan is traditionally divided into eight regions, and each region includes several prefectures, excluding Hokkaido (Fig. 4-1). Four types of municipalities exist in Japan: cities, towns, villages, and special wards (the ward in Tokyo). Cities with a certain population are labeled core cities (over 200,000 residents) or designated cities (over 700,000 residents) [31]. In this study, a total of 1647 municipalities on the 4 main islands and surrounding isolated islands were selected as the study items (Okinawa prefecture was excluded). The municipalities were further classified into four categories based on population (Table 4-1.).

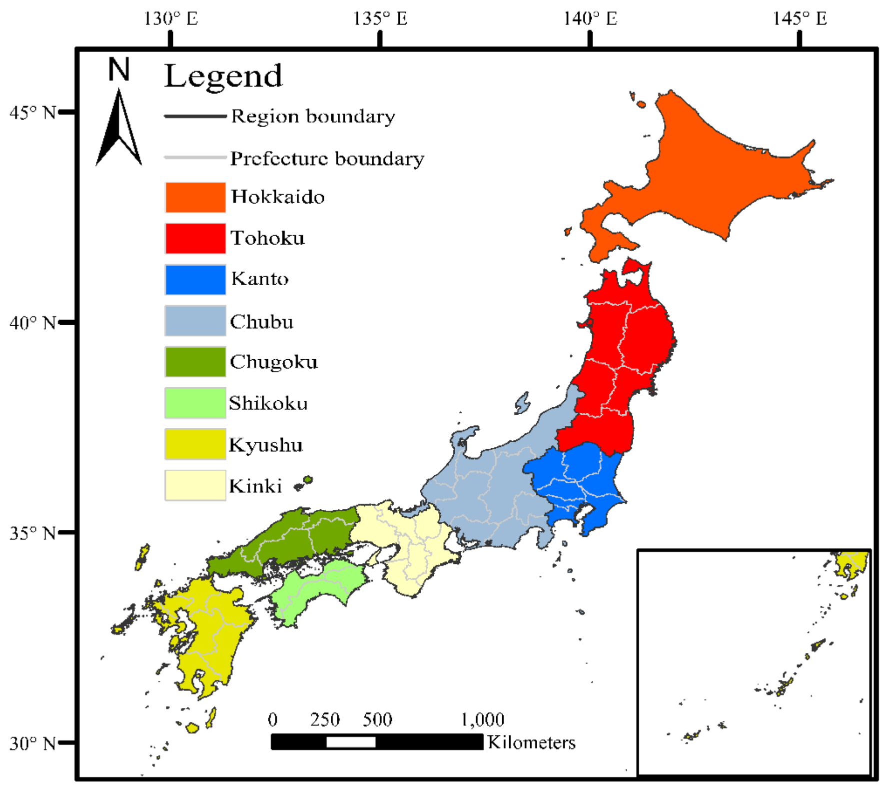

Fig.4-1 Regions of Japan, from north to south: Hokkaido, Tohoku, Kanto, Chubu, Kinki, Chugoku, Shikoku, and Kyushu.

Table 4-1. Municipalities level classification.

Category	Description	Number
Large city	Population over 700,000	21
Medium city	Population between 200,000 and 700,000	89
Small city	City population below 200,000	631
Town/village	Municipality type is town or village	906

Compared to countries such as the United States and China, where the population is growing and city shrinkage is only happening in local suburban cities or local regions [14, 29], the situation of city shrinkage in Japan is more severe and requires investigation. However, the population of Japan declined since 2008, and the rate of decline kept increasing, which makes the city shrinkage become an increasingly national severe problem which is badly in need of countermeasures. Targeting on for Japan will improve the understanding of mechanisms for the city shrinkage. According to the National Census data in 2005, 2010, and 2015, 71.9% municipalities experienced continuous shrinkage, and 13.6% municipalities experienced temporal shrinkage, while only 14.5% municipalities population continuously increased during the period. Specifically, city shrinkage was occurring at a higher rate in towns or villages (80.8%), and small cities (70.4%). However, city shrinkage is not only a phenomenon for local or small municipalities, but 56 big-medium cities are also facing population loss in Japan, indicating an extreme situation of city shrinkage in Japan (Table 4-2.). Regionally, the city shrinkage was extreme in Shikoku, Hokkaido, Tohoku, and Chugoku (Table 4-3.). The unbalanced economic scale and development degree are essential factors leading to population mobility, which in turn accelerates the aging population and low fertility in small municipalities.

Table 4-2. The ratio of shrinking cities classified by municipalities level

Type	Municipality level			
	Large city	Medium city	Small city	Town/village
Continuous shrinkage	14.3% (3)	27.0% (24)	70.4% (444)	80.8% (732)
Temporal shrinkage	19.0% (4)	28.1% (25)	14.4% (91)	10.9% (99)
Continuous increase	66.7% (14)	44.9% (40)	15.2% (96)	8.3% (75)

Note: Numbers in bracket refers to the counts of municipalities

Table 4-3. The ratio of shrinking cities classified by region

Type	Area							
	Hokkaido	Tohoku	Kanto	Chubu	Kinki	Chugoku	Shikoku	Kyushu
Continuous shrinkage	89.4% (160)	88.2% (194)	52.0% (146)	66.0% (225)	68.4% (134)	82.1% (87)	90.2% (83)	75.0% (174)
Temporal shrinkage	7.3% (13)	6.4% (14)	19.6% (55)	17.9% (61)	15.8% (31)	8.5% (9)	4.4% (4)	13.8% (32)
Continuous increase	3.4% (6)	5.5% (12)	28.5% (80)	16.1% (55)	15.8% (31)	9.4% (10)	5.4% (5)	11.2% (26)

Note: Numbers in bracket refers to the counts of municipalities

4.2.2 Analysis Method and Research Flow

Usually, causal pathways can only be suggested by theoretical background, not by statistical analyses. As the pervious study concluded the primary driving factors of Japan city shrinkage are demographic factors such as low birth rate and aging society, we applied regression analysis to reveal the degree of those factors affect the city shrinkage in Japan. Three kinds of models have been used in this chapter including OLS, GWR, and SGWR. Some methods have been introduced in Chapter 2.

In this chapter, the methods have mentioned were designed to model the correlation between population change ratio and its potential related factors. Specially, the traditional OLS model considers all explanatory variables are global and spatially stationary. In a GWR model, all explanatory variables are local and spatially non-stationary. Spatial heterogeneity is investigated in the model fit where the spatial locations of data are incorporated. A local linear regression model for each feature in the dataset was calibrated using a different weighting of observations. The parameter in this model is a single function that represents the spatial location that is derived by weighting all neighboring observations based on a decreasing function of distance. In a SGWR model, as the integration of OLS and GWR models, some variables are global and spatially stationary, while the rest variables are local and spatially non-stationary.

In a GWR or an SGWR model, the accuracy is profoundly affected by the bandwidth, which refers to the number of nearest neighbors of municipality i. The corrected Akaike information criterion (AICc) method and the cross-validation method are two methods often applied to determine the bandwidth. Compared with the CV method, the AICc method can quickly and effectively solve the problem considering the differences in the degree of freedom of different models. Therefore, in this study, the smallest AICc was selected for the appropriate bandwidth determination. The selection of the optimal SGWR model with the smallest AICc based on an iterative process was processed using GWR 4 software.

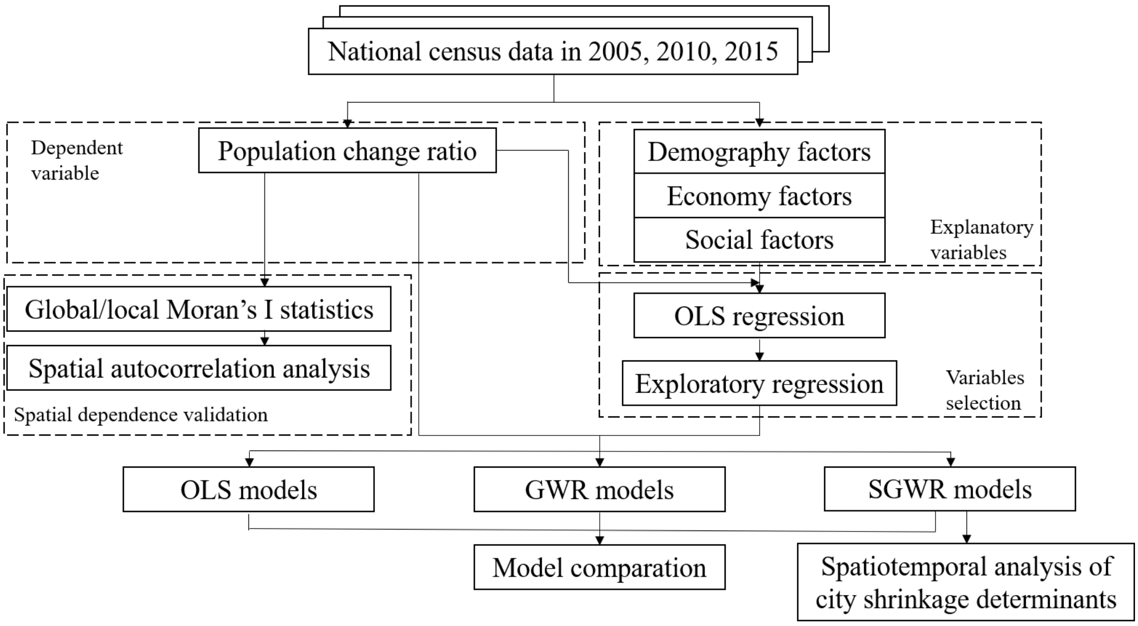

Fig. 4-2 Research flow of assessment of the determinants of city shrinkage in Japan.

The research flow of the assessment of the spatial temporal determinants of city shrinkage in Japan is shown in Fig.4-2. We divided two study periods to discuss the temporal variation of the determinants of city shrinkage. The two study periods are from 2005 to 2010, and from 2010 to 2015. As population loss was primary variable for evaluating a city is shrinking or expanding in most previous studies, we collected the national census data in 2005, 2010, and 2015 from the portal site of the Official Statistics of Japan. Then the population change ratio of each municipalities in the two study periods was calculated as the dependent variable.

In order to ensure the applicability of GWR and SGWR models, which is to validate the spatial dependence of population change in Japan, both the global and local Moran's tests were conducted to reveal the spatial autocorrelation of population change ratio. Moreover, the process could also help with investigation of spatial patterns of city shrinkage in Japan.

The age structure, economy level, and social development level were found to be vitally essential issues for urban regeneration, which are directly connected with urban shrinking. Multiple commonly used demographic, economic, and social indicators were selected as the explanatory variables for analysis (Table 4-4) [15, 33, 34]. The data were downloaded and derived from Statistical Observations of Municipalities from 2006 to 2016. The explanatory variables consisted of 15 variables from 3 urban sub-systems. In the demographic sub-systems, TP refers to the size of a municipality; UPR, APR, and FPR refer to the age and population structure; in the economic sub-systems, CT and GR refer to the income of local resident and local government, respectively; ECR refers to the industry changes;

STIER and STIWR refer to the local industry structure; UR refers to local poverty; in the social sub-systems, SN refers to the local education resources; HN and DN refer to the local medical level; and NEF and NNC refer to the local social welfare level, respectively.

Table 4-4. Classification, name, and description for explanatory variables.

Classification	**Variable**	**Description**
Demographic factors	TP	Total population (people)
	UPR	Underage population ratio (age < 15)
	APR	Aging population ratio (age ≥ 65)
	FPR	Foreign population ratio
Economic factors	CT	Per capita taxes (JPY/people)
	GR	Government revenue (million JPY)
	ECR	Numbers of enterprise change ratio
	STIER	Secondary and tertiary industry enterprises ratio
	STIWR	Secondary and tertiary industry workers ratio
	UR	Unemployment rate
Social factors	SN	Number of primary and secondary schools
	HN	Number of hospitals and clinics
	DN	Number of doctors (per 10,000 people)
	NEF	Number of elderly facilities
	NNC	Number of nursery centers

In a regression model, multicollinear variables will significantly affect the regression results and distort the model, while non-significant variables will make the model more complex. Hence, we applied OLS regression and explanatory regression to exclude the multicollinear variables and non-significant variables.

After validation of the spatial dependence of population change ratio, and selection of the explanatory variables, the correlation between the dependent variable and the explanatory variables were formulated through OLS, GWR, and SGWR models.

4.3 Spatial autocorrelation analysis of population change patterns

In this chapter, the population change in Japan from 2005 to 2010, and 2010 to 2015 was confirmed to be positive spatially clustered with the global Moran's I for the 2 study periods being 0.462, and 0.615 respectively (Table 4-5). To further understand the spatial features of population change, the Local Moran's I was applied. The LISA maps of population change shown in Fig. 4-3 revealed the local spatial cluster of the population change. During the 2 study periods, a large number of municipalities showed spatial clustering characteristics. The results showed the LL cluster areas concentrated in Hokkaido, Tohoku, Shikoku, and Kinki, while the HH cluster areas concentrated around Tokyo city cluster in the central area of Kanto, Osaka city cluster in the south-west of Kinki, Nagoya city cluster in the south-west of Chubu, and the Fukuoka city cluster in the north of Kyushu. Meanwhile, the LH outlier areas existed around Tokyo city cluster and Nagoya city cluster, which indicate the city shrinkage was happening in the suburban areas around large urban agglomerations already. Besides, from 2010 to 2015, the number of cities in the HH cluster and LL cluster increased by 54 and 15 respectively compared with the period from 2005 to 2010. These results revealed that significant correlation between city shrinkage and spatial distribution, and the increasing city shrinkage phenomenon.

Table 4-5. Classification, name, and description for explanatory variables.

Study period	Global Moran's I	Z-score	P value
2005-2010	0.462	23.10	<0.01
2010-2015	0.615	30.67	<0.01

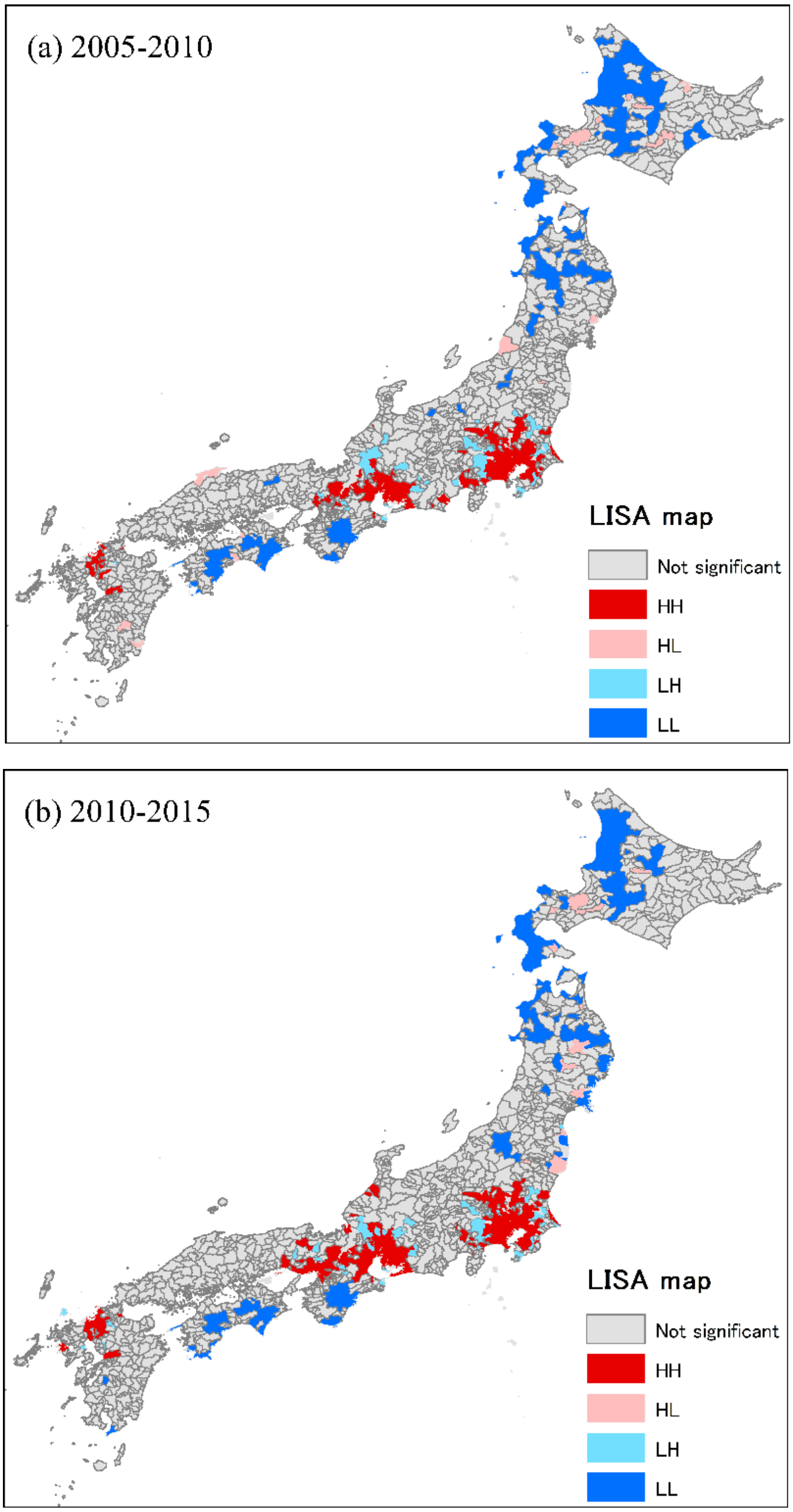

Fig. 4-3 LISA cluster maps of population change (a) from 2005 to 2010; (b) from 2010 to 2015.

Through the global/local Moran's I statistics, the results indicated the population change patterns did have spatial autocorrelation. City clusters centered in Tokyo, Osaka, Nagoya, and Fukuoka were shown as the spatial agglomeration of population growth municipalities, while municipalities in Hokkaido, Tohoku, Shikoku were shown as the spatial agglomeration of shrinking cities. The unbalanced regional economic scale and urban development degree are essential factors leading to population mobility, which in turn accelerates the aging population and low fertility in small municipalities.

4.4 Regression results

4.4.1 Variable selection

In this procedure, shown in Table 4-6 and Table 4-7, 8 explanatory variables including TP, CT, GR, STIER, SN, HN, DN, and NEF, which had significant multicollinearity with the population change, were therefore excluded from the final model. Then, exploratory regression was conducted to exclude the non-significant variables of the population change at a 95% confidence level. In this procedure, UR was excluded. After testing the spatial autocorrelation of population change, multivariate OLS regression and exploratory regression were conducted to test the relationship between population change and selected explanatory variables. All the variables were first normalized to ensure the variables were normally distribution or approximated normal distribution. Then, to eliminate the multicollinearity of the data, which could produce a distorted or inaccurate model, the variance inflation factor (VIF) for each explanatory variable was calculated, and the variables with a VIF value over 5 were sequentially excluded from the final model until no more VIF > 5 were found [35]. In this procedure, 8 explanatory variables including TP, CT, GR, STIER, SN, HN, DN, and NEF, which had significant multicollinearity with the population change, were therefore excluded from the final model. Then, exploratory regression was conducted to exclude the non-significant variables of the population change at a 95% confidence level. In this procedure, UR was excluded. The results showed that no local multicollinearity existed among the remaining variables. Therefore, after removing the variables redundancy or non-significance, 6 explanatory variables, including UPR, APR, FPR, ECR, STIWR, and NNC, were screened out for both study periods, which suggests the general correlates of city shrinkage remain unchanged. After screening out the variables, the OLS model was reformulated with the 6 explanatory variables. These variables were then used for the corresponding GWR and SGWR models.

Table 4-6. Variance inflation factor (VIF) value of variables selection procedure of the model study period 2005 to 2010.

Iteration	**TP**	**UPR**	**APR**	**FPR**	**CT**	**GR**	**ECR**	**STIER**	**STIWR**	**UR**	**SN**	**HN**	**DN**	**NEF**	**NNC**
1 (keep all)	208.95	3.62	4.98	1.28	167.45	33.62	1.25	47.16	2.40	1.84	12.61	25.56	14.10	8.65	4.61
2 (remove CT)	52.01	2.98	4.02	1.21	-	32.10	1.24	45.64	2.03	1.31	12.44	25.00	13.73	8.29	4.14
3 (remove TP)	-	2.97	4.01	1.21	-	29.75	1.24	30.78	2.02	1.21	12.41	23.99	13.50	8.29	4.09
4 (remove STIER)	-	2.96	3.91	1.18	-	25.10	1.24	-	1.78	1.21	12.01	22.84	12.71	7.87	4.08
5 (remove GR)	-	2.93	3.90	1.18	-	-	1.24	-	1.74	1.21	9.10	20.08	12.62	7.66	3.64
6 (remove HN)	-	2.93	3.77	1.18	-	-	1.21	-	1.68	1.20	8.22	-	10.08	7.39	3.62
7 (remove DN)	-	2.91	3.59	1.18	-	-	1.19	-	1.51	1.20	6.80	-	-	6.70	3.61
8 (remove SN)	-	2.88	3.52	1.17	-	-	1.18	-	1.49	1.20	-	-	-	6.08	3.54
9 (remove NEF)	-	2.82	3.50	1.16	-	-	1.18	-	1.48	1.19	-	-	-	-	1.19

Table 4-7. Variance inflation factor (VIF) value of variables selection procedure of the model study period 2010 to 2015.

Iteration	TP	UPR	APR	FPR	CT	GR	ECR	STIER	STIWR	UR	SN	HN	DN	NEF	NNC
1 (keep all)	211.51	1.51	4.53	1.07	169.83	17.78	2.03	48.41	2.03	1.72	26.22	13.50	15.35	10.24	1.28
2 (remove CT)	42.80	1.51	4.46	1.07	-	16.12	1.17	42.25	1.81	1.26	11.75	12.78	13.10	9.90	1.28
3 (remove TP)	-	1.50	4.28	1.07	-	15.72	1.15	22.38	1.77	1.16	11.42	11.95	13.02	9.87	1.27
4 (remove STIER)	-	1.48	4.29	1.07	-	15.53	1.14	19.76	1.74	1.16	11.30	11.84	10.13	9.75	1.27
5 (remove GR)	-	1.44	4.27	1.07	-	-	1.11	-	1.64	1.16	10.80	11.11	8.02	9.46	1.26
6 (remove HN)	-	1.31	4.30	1.07	-	-	1.10	-	1.63	1.16	8.82	-	7.31	8.84	1.26
7 (remove NEF)	-	1.28	4.29	1.06	-	-	1.10	-	1.62	1.15	7.13	-	6.44	-	1.25
8 (remove SN)	-	1.25	4.28	1.06	-	-	1.09	-	1.54	1.15	-	-	6.21	-	1.25
9 (remove DN)	-	1.21	4.08	1.06	-	-	1.08	-	1.44	1.14	-	-	-	-	1.24

4.4.2 Global and local analysis of city shrinkage in Japan

After screening out the variables, the global model based on the OLS regression procedure was reformulated using the six variables. The results revealed the intercorrelation between population change and municipality parameters, as shown in Table 4-8.

Table 4-8. Municipality parameters estimated coefficient for the global model (Japan).

Study period	**Intercept**	**UPR**	**APR**	**FPR**	**ECR**	**STIWR**	**NNC**	**Adjust R^2**
2005-2010	-3.556*	1.262*	-2.907*	0.315*	1.029*	0.040	0.855*	0.512
2010-2015	-5.343*	2.147*	-1.727*	0.125	1.204*	0.211*	0.727*	0.715

Note: * $p < 0.05$.

The results showed that the global model for population change from 2005 to 2010 was moderate (adjusted coefficient of determination (R^2) = 0.512), which indicates the six parameters could explain the population change during 2005–2010 to a certain extent. The adjusted R^2 of the global model for population change from 2010 to 2015 was 0.715, indicating a substantially adequate explanation of the population change. The results also revealed that APR had a negative coefficient value, which suggests the ageing population ratio has the most significant adverse effect on population change compared with the other parameters. With high positive coefficients, UPR and ECR had significantly positive effects on population change compared with the other parameters. STIWR was found to be non-significant in the first study period, and FPR was found to be non-significant in the second study period. Comparably, the estimated coefficient of UPR increased, indicating an increasing effect of low fertility on city shrinkage. Conversely, the effect of ageing population was found to decrease as the absolute value of APR decreased.

Considering the spatial heterogeneity and spatial autocorrelation of population change, GWR was applied to fit a local population change model. Figure 4 shows the parameter coefficients for the local model of the two study periods. Compared with the first study period, the variation range and the number of mild outliers of the parameters increased. The effects of the parameters could be positive or negative for different regions. Figure 5 shows the variation in parameters' t-values for the local model. Most observations of UPR, APR, ECR, and NNC reached the 0.05 significance level for the first study period, whereas most observations of UPR, APR, and ECR reached the 0.05 significance level for the second study period.

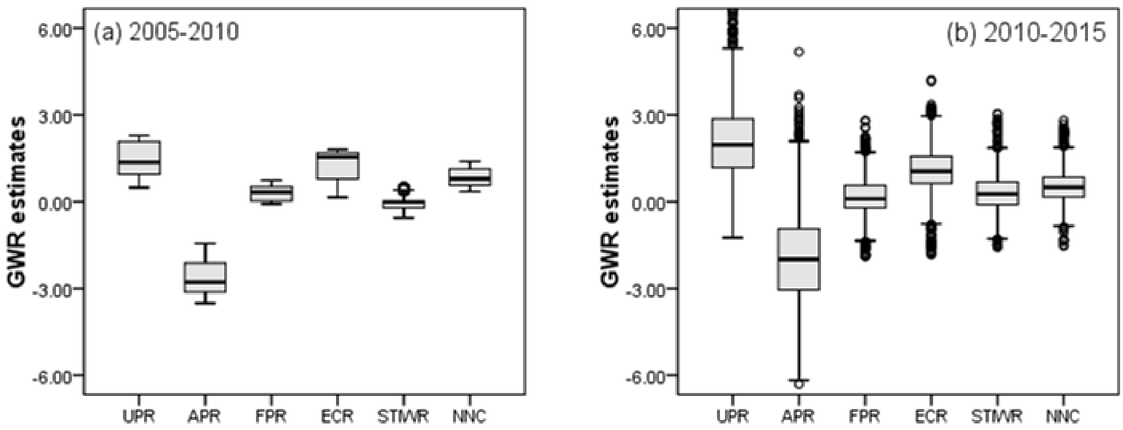

Fig. 4-4 Parameters estimated coefficients for the local model (**a**) from 2005 to 2010 and (**b**) from 2010 to 2015.

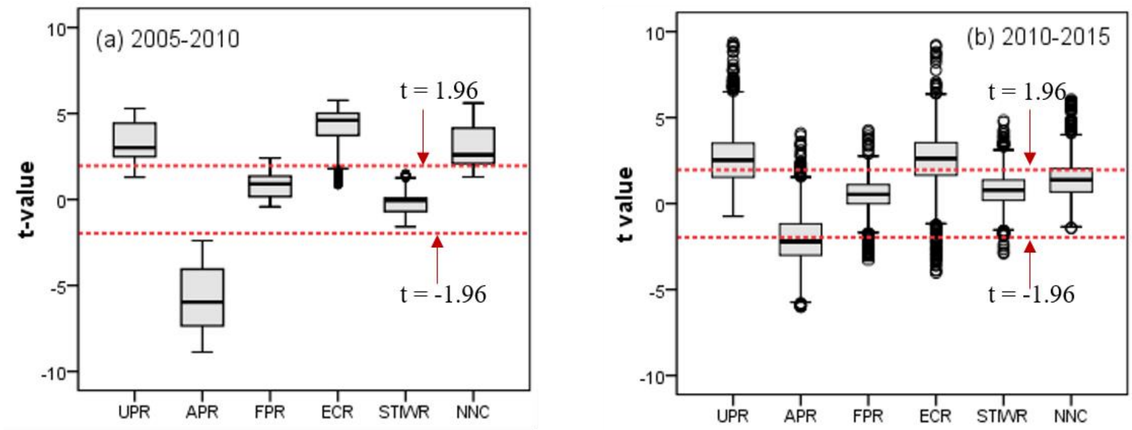

Fig. 4-5 The t-value of the parameters for the local model (**a**) from 2005 to 2010 and (**b**) from 2010 to 2015.

4.4.3 Assessment of city shrinkage in Japan through SGWR models

Considering the global model explained the population change to some degree whereas the local model improved the accuracy, the SGWR models were developed to consider both the spatial stationarity and non-stationarity for the parameters affecting population change. An iterative process was used to determine whether a parameter was a global or local variable. The most fitted SGWR model was based on the AICc; the model with the smallest AICc value was selected, which refers to the best fitting result. In this procedure, FPR, STIWR, and NNC were selected as global variables, and UPR, APR, and ECR remained local variables for both models (Table 4-9).

Table 4-9. Determination of parameters for the SGWR models (Japan).

Study Period	Explanatory Variable					
	UPR	APR	FPR	ECR	STIWR	NNC
2005–2010	Local	Local	Global	Local	Global	Global
2010–2015	Local	Local	Global	Local	Global	Global

As shown in Table 4-10, the adjusted R^2 for the two local models were 0.528 and 0.815, respectively, which are higher than the global models, suggesting that considering the parameter influences to be spatially non-stationary is more representative than considering them to be spatially stationary. The fitting results of the SGWR model improved compared with the global and local models. The R^2 of the SGWR model was the largest compared to the other two models. The AICc value of the SGWR model for the first study period decreased by 47.40, and 10.05 compared with the OLS and GWR models, respectively. For the second study period, the AICc value decreased by 527.43 and 111.89, respectively. Combined with the value of the bandwidth and residual square, we found that the SGWR model was optimal for both study periods, which indicates the population change in Japan displayed spatially stationary and non-stationary parameters.

Table 4-10. Accuracy evaluation for the global, local, and SGWR model.

Parameter	2005–2010			2010–2015		
	OLS	GWR	SGWR	OLS	GWR	SGWR
Bandwidth	-	341	201	-	87	66
Residual squares	395.17	373.21	369.09	157.46	80.94	77.27
AICc	−5245.55	−5282.90	−5292.95	−6761.06	−7176.80	−7288.49
Adjusted R^2	0.512	0.528	0.532	0.715	0.815	0.818

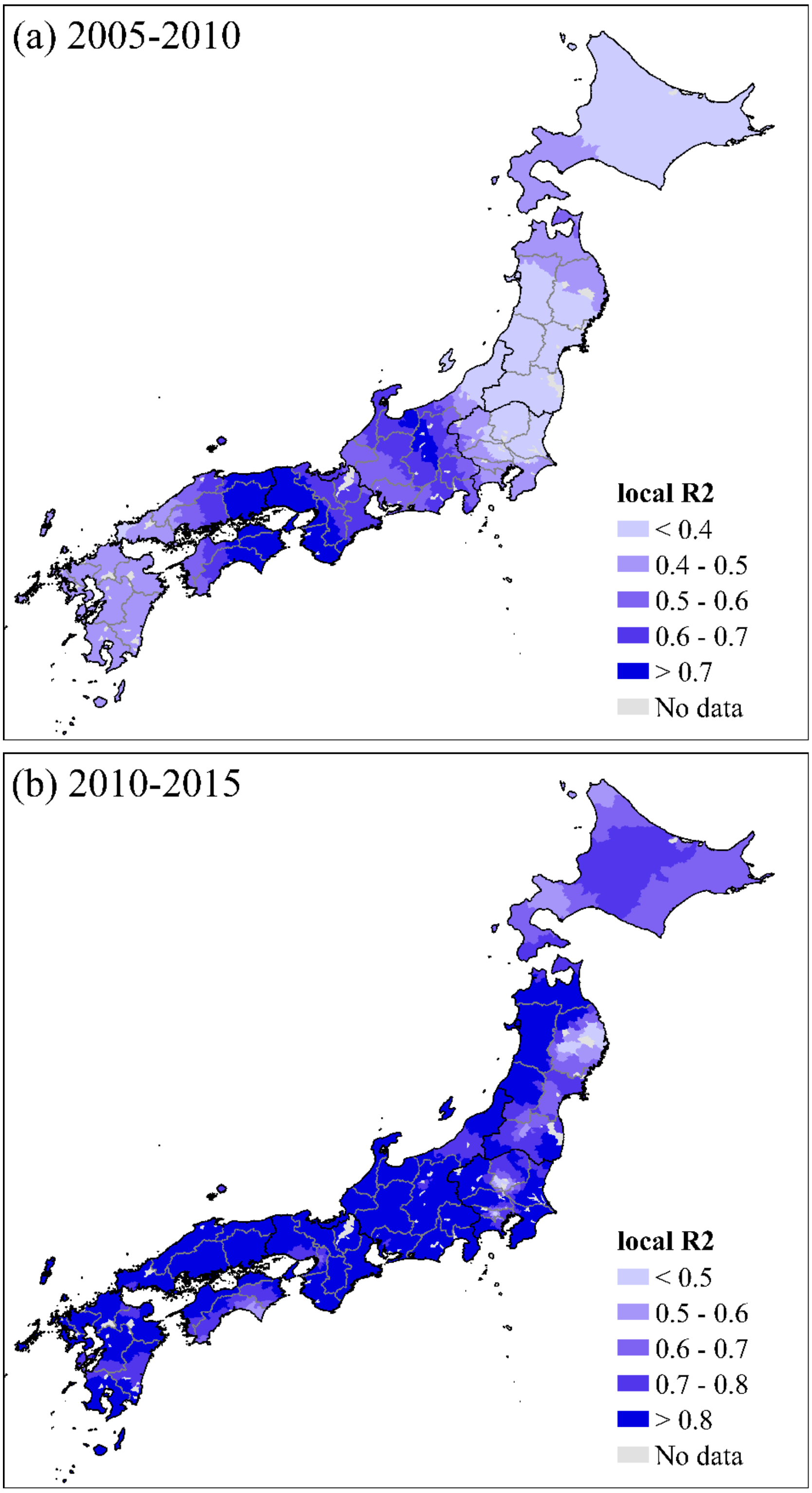

Fig. 4-6 Local R^2 of city shrinkage in Japan based on SGWR (a) from 2005 to 2010; (b) from 2010 to 2015.

As Fig. 4-6 shown the local R^2 of the SGWR models, for the first study period from 2005 to 2010, the values of local R^2 for Shikoku, Chugoku, Kinki, and Chubu were relatively larger, especially in and around the Osaka city cluster. However, the values of local R^2 for Tohoku and Hokkaido were relatively smaller, which can be explained by many municipalities in the two regions experienced mergers in the first study period. Due to policy directives and execution as a response to city shrinkage, the population of the city exploded because of the consolidation between municipalities, which make it very hard to explain the situation through population structure, economic structure, or social factors. Conversely, there was little change in municipalities from 2010 to 2015, which is an essential reason for the high value of local R^2 in most regions in Japan.

For UPR, APR, and ECR found to be non-stationary spatial correlates affect the population change, the local coefficients of each variable and the spatial characteristics of city shrinkage correlates were analyzed. The t-test was conducted to pick out the coefficients of the local variables which passed the significance level of 0.05.

Fig. 4-7 depicts the local coefficients of UPR from 2005 to 2010, and from 2010 to 2015, UPR had a significant positive effect in 1074 and 988 municipalities ($p < 0.05$) for the two study periods, respectively. The results indicated that from 2005 to 2010, the ratio of the underage population mainly affected the population change around Nagoya city cluster, whereas from 2010 to 2015, the underage-population-affected areas were scattered and extended to south Kinki, east Shikoku, and the boundary area between Chubu and Kanto, and the north and south parts of Kyushu. UPR remained correlated with the population change in most parts of Hokkaido and Tohoku from 2005 to 2015.

Different from the other countries facing city shrinkage, even countries in East Europe, city shrinkage is most strongly linked to demographic transition and process of an ultra-ageing society [34, 37]. The results indicated that low fertility rate could be the key factor influencing the city shrinkage and the ageing population [39, 40]. Since 2007, the fertility rates have continued decreasing and began to fall below death rates. City shrinkage in Hokkaido and Tohoku, where the underage population ratio was below the national average, have always been affected by low fertility rates. As the fertility rate continues to fall, it would become a main factor affecting the city shrinkage in the other regions.

Fig. 4-8 shows the coefficient of the ageing population effect on population change from 2005 to 2010 and from 2010 to 2015. In the first period from 2005 to 2010, only 10 municipalities did not pass the significance test, whereas the other municipalities were found to have a negative correlation between UPR and population change, which suggests the ageing population is correlated with driving city shrinkage nationwide. However, the estimated coefficient of UPR varied between regions. Kyushu and Kanto were the regions with the largest UPR estimated coefficients. The ageing phenomenon in Kyushu was serious, especially in the south, which has aggravated the city's shrinkage. Conversely, in Kanto, centered in Tokyo, the labor force continuously migrated inward and the proportion of the elderly population continued to decline, which has caused urban expansion in the region. The city shrinkage in the distant periphery and suburban areas occurred due to the ageing populations and infrastructure that has become inadequate. From 2010 to 2015, the area of the ageing population effect shrunk and negative coefficients were found in 935 municipalities mainly concentrated in Kyushu, Chubu, and Chugoku. However, positive coefficients were found in 45 municipalities in south Tohoku and south and north Hokkaido, which could be due to the aggregation of the elderly population and population ageing.

Fig. 4-9 shows the spatial distribution of the local ECR coefficient from 2005 to 2010 and from 2010 to 2015. The local ECR coefficient was found to be spatially non-stationary, and the differences between the two study periods in the region varied. Generally, the economic correlates less impacted city shrinkage than the demographic correlates. From 2005 to 2010, the local ECR coefficient for Kanto was the largest, followed by Kyushu, Shikoku, and Kinki, indicating the population changes in those four regions were strongly correlated with the number of enterprises. However, the non-significant correlation in Tohoku indicated that the population changes in the region were not correlated with the number of enterprises. Comparatively, from 2010 to 2015, the local ECR coefficient for 81.7% of municipalities in Tohoku was significantly positive. The number of enterprises decreased, which was an essential reason for population decline and city shrinkage in the region. The results revealed that the changing numbers of enterprises was significantly correlated with the population change in several main city clusters in Japan, which are also the economic centers, including Tokyo, Osaka, and Fukuoka, for both periods. Urban agglomerations benefit from the increase in the number of enterprises, which appeals to the working population and stimulates population agglomeration and urban expansion [40, 41], thus leading to the population loss and city shrinkage in small cities far from metropolises.

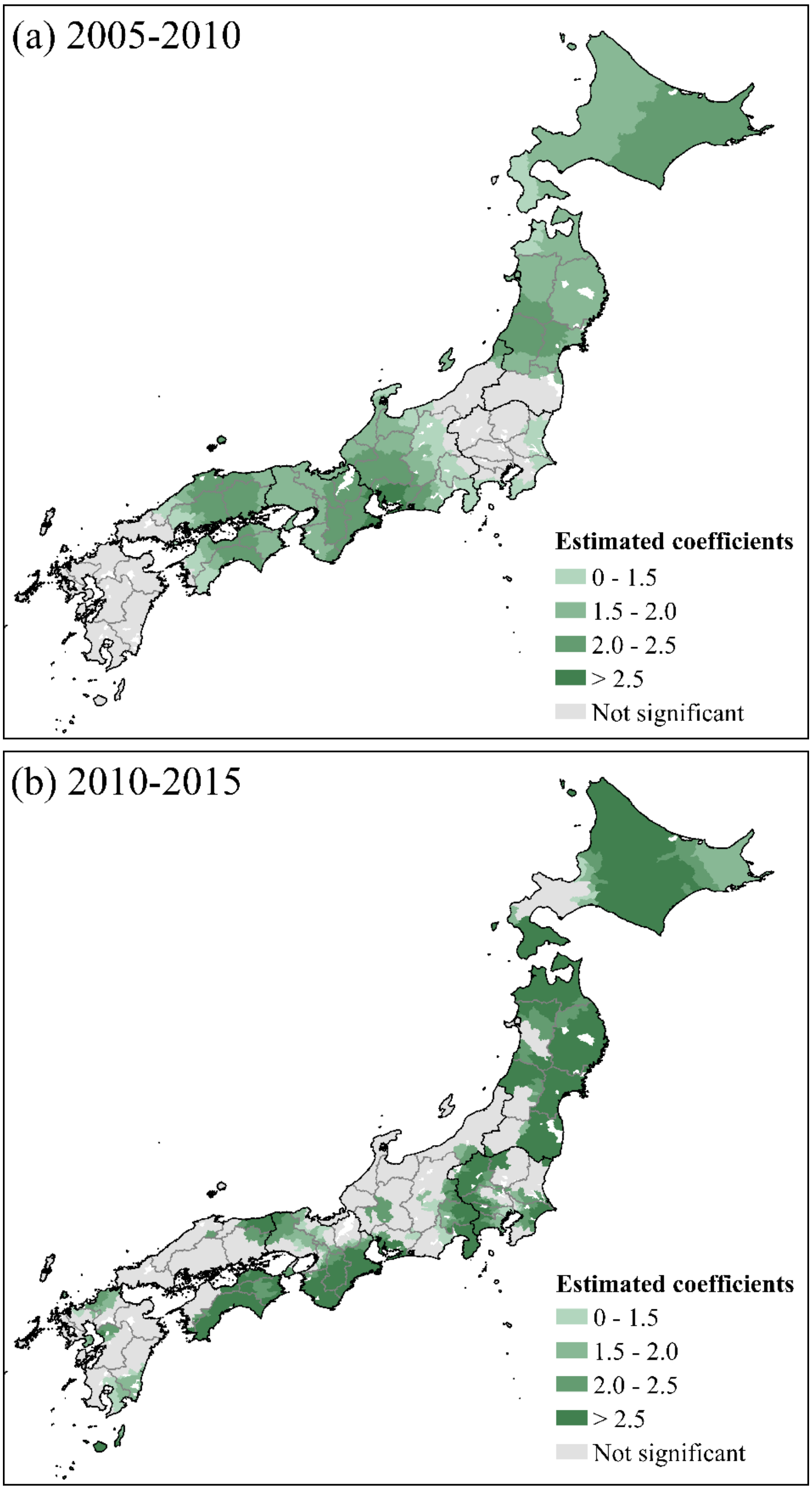

Fig. 4-7 Local estimated coefficient of underage population ratio (**a**) from 2005 to 2010 and (**b**) from 2010 to 2015.

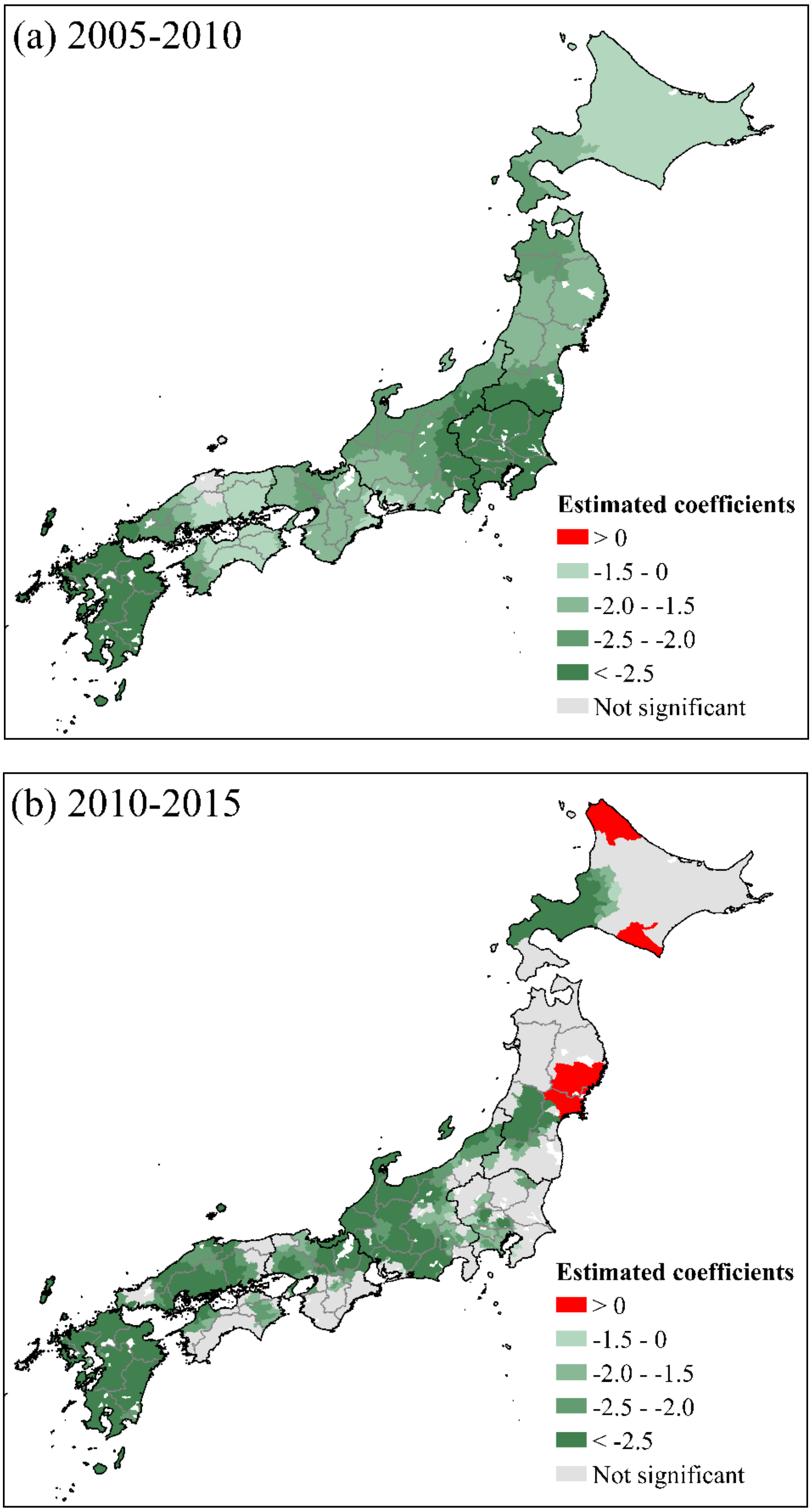

Fig. 4-8 Local estimated coefficient of ageing population ratio (**a**) from 2005 to 2010 and (**b**) from 2010 to 2015.

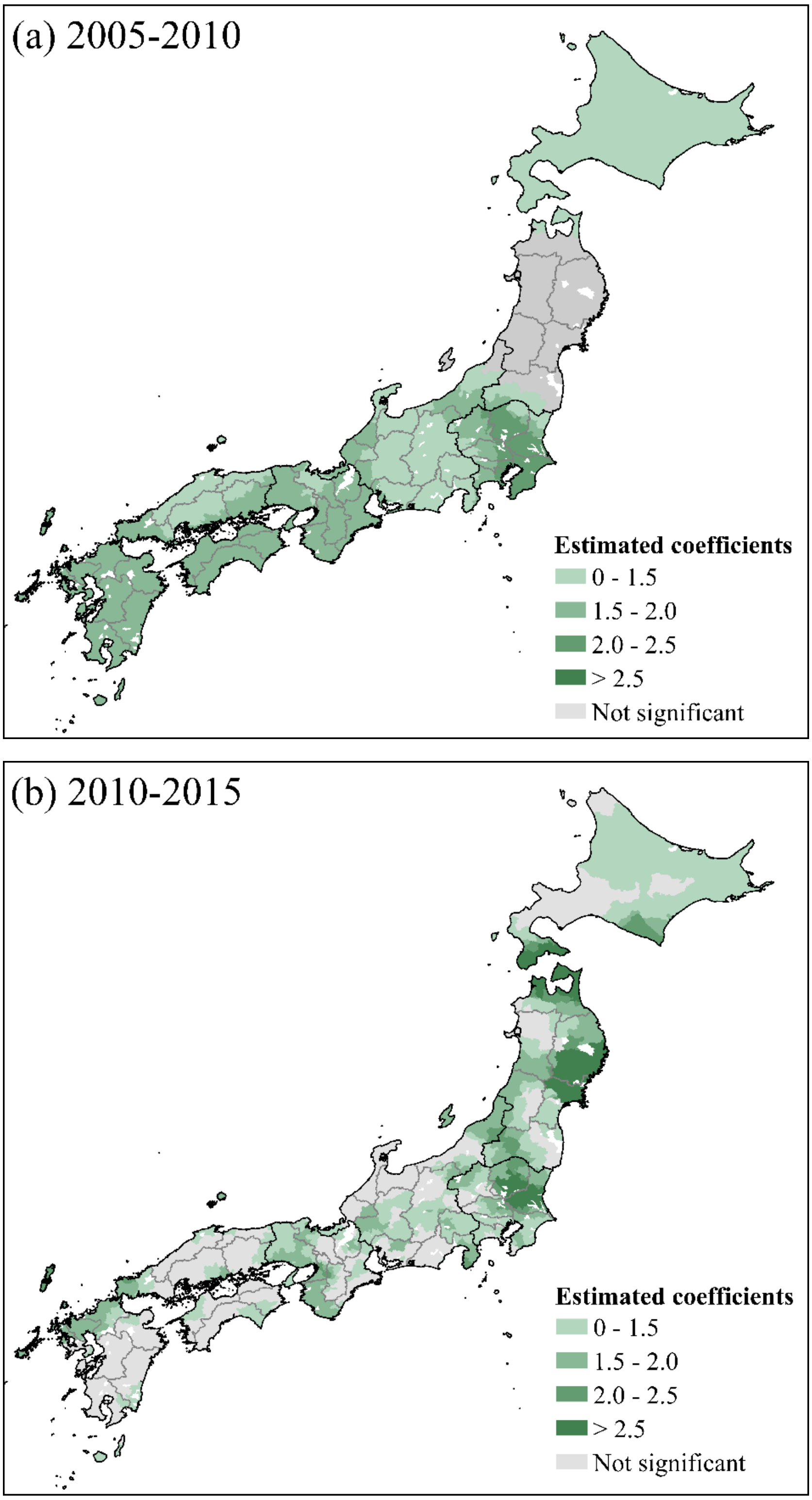

Fig. 4-9 Local estimated coefficient of enterprise change ratio (**a**) from 2005 to 2010 and (**b**) from 2010 to 2015.

Other studies explained city shrinkage in Japan as being due to the ageing population, low fertility, and de-industrialization at a global level [42, 43]. However, few studies focused on the quantitative differences of determinates that contribute to city shrinkage. As city shrinkage worldwide refers to the loss of population, it is a severe phenomenon accompanied by economic, social, and cultural decline [44, 45]. As the global and local Moran's I statistics showed spatial aggregation for the population change ratio, we considered the variables to have spatially stationary or non-stationary effects on city shrinkage in Japan, and encouraging us to explore the regional differences in city shrinkage from 2005 to 2015. The results revealed the spatial heterogeneity of shrinking cities, and showed UPR, which refers to low fertility, dominated city shrinkage in Hokkaido, Tohoku, and Kinki; APR, which refers to the ageing population, dominated in Chubu and Kyushu; and ECR had a significantly positive effect in Kanto. In the two study periods, the influence of the local variables in different regions were quite different. Generally, demographic indexes were found to be more correlated with city shrinkage in Japan, which validates that the demographic transition had more of an effect than economic transition. The results showed that APR have the largest absolute value of the estimated coefficients, which indicate ageing population could be a key factor influencing city shrinkage in most municipalities in Japan from 2005 to 2010, whereas low fertility could be the key factor influencing city shrinkage from 2010 to 2015.

4.5 Summary

In this chapter, we developed OLS, GWR, and SGWR models to capture the spatiotemporal differences in determinants affecting city shrinkage in Japan based on national census data from 2005 to 2015. The spatial dependence of the shrinking cities in Japan has been confirmed through both global and local Moran's I tests.

Our findings are as follows: (1) City shrinkage in Japan is a serious national problem, which showed a significant increasing positive spatial autocorrelation; Hokkaido, Tohoku, and Shikoku had the largest shrinking city clusters, and this phenomenon has already occurred in suburban areas around the Tokyo and Nagoya city clusters. (2) Compared with traditional OLS and GWR models, the SGWR models, which consider spatial dependence and heterogeneity, are more interpretive in the explanation of city shrinkage. (3) The correlation between the demographic, economic, and social indexes and city shrinkage was revealed through quantitative analysis. Low fertility, ageing population, and industry changes, expressed by APR, UPR, and ECR, were the critical spatially non-stationary correlates, with large estimated coefficients, affected the city shrinkage in different regions at different times. The findings contribute to improving our understanding of the situation and correlates of city shrinkage, and provide valuable information for governments and planners when developing effective coping strategies for city regeneration.

Due to low fertility and strict immigration policies in Japan, which mean city shrinkage may be an irreversible process [34], determining how to ensure the smart decline of city sizes is an essential issue [45]. The limitation of this study is that specific policies were not considered as an explanatory variable. Future studies are required to analyze the implementation of specific policies and their effect on city shrinkage, and to explore the characteristics of spatial patterns of city shrinkage in each city using more sophisticated data.

The limitation of this study is that specific policies were not considered as an explanatory variable. As dummy variables, it is difficult to quantitatively evaluate the impact of policy promulgation and implementation on city shrinkage through the SGWR model. As a complex system, the influence of policies can often be reflected by indicators from such as population, economy, and social aspects, so the specific policies were therefore not taken as explanatory variables in this study. However, from 1999 to 2010, there was a wave of merger activity called 'the great Heisei mergers' as a response to the low fertility and aging population. The number of municipalities decreased from 2395 in 2005 to 1727 in 2010. The merge between municipalities had led to a population explosion for those municipalities, while it could not reflect the real situation of city shrinkage from 2005 to 2010, but the interpretation of SGWR model for this period was affected and created a moderate result (adjusted R^2 = 0.532). As low fertility and strict immigration policies in Japan, which make city shrinkage being an almost irreversible process, how to make a smart decline of city shrinkage is an essential issue. Future studies are required for analyzing specific policies implementation and effect on city shrinkage, and exploring the characteristics of spatial patterns of city shrinkage in each city with more sophisticated data such as street-level population data.

Reference

[1] Nations U. 2018 revision of world urbanization prospects. United Nations Department of Economic and Social Affairs; 2018.
[2] Haase A, Rink D, Grossmann K, Bernt M, Mykhnenko V. Conceptualizing urban shrinkage. Environment and Planning A. 2014;46:1519-34.
[3] Mallach A, Haase A, Hattori KJC. The shrinking city in comparative perspective: Contrasting dynamics and responses to urban shrinkage. 2017;69:102-8.
[4] Hattori K, Seike Y, Yoshida Z, Hamaguchi S, Yamada H, Suzuki N, et al. Shrinkage of tokamak current channel by external ergodization. 1984;121:368-73.
[5] He SY, Lee J, Zhou T, Wu DJC. Shrinking cities and resource-based economy: The economic restructuring in China's mining cities. 2017;60:75-83.
[6] Hospers G-JJUdi. Coping with shrinkage in Europe's cities and towns. 2013;18:78-89.
[7] Großmann K, Bontje M, Haase A, Mykhnenko VJC. Shrinking cities: Notes for the further research agenda. 2013;35:221-5.
[8] Haase D, Haase A, Kabisch N, Kabisch S, Rink DJEM, Software. Actors and factors in land-use simulation: The challenge of urban shrinkage. 2012;35:92-103.
[9] Haase DJN, Culture. Urban ecology of shrinking cities: an unrecognized opportunity? 2008;3:1-8.
[10] Rieniets TJN, Culture. Shrinking cities: causes and effects of urban population losses in the twentieth century. 2009;4:231-54.
[11] Hospers G-JJEPS. Policy responses to urban shrinkage: From growth thinking to civic engagement. 2014;22:1507-23.
[12] Syssner JJARdEsDyDR. Planning for shrinkage? Policy implications of demographic decline in Swedish municipalities. 2016:7-31.
[13] Sadler RC, Lafreniere DJ. Racist housing practices as a precursor to uneven neighborhood change in a post-industrial city. Housing Studies. 2017;32:186-208.
[14] Wiechmann T, Pallagst KMJIjou, research r. Urban shrinkage in Germany and the USA: A comparison of transformation patterns and local strategies. 2012;36:261-80.
[15] Zhang Y, Fu Y, Kong X, Zhang FJSC, Society. Prefecture-level city shrinkage on the regional dimension in China: spatiotemporal change and internal relations. 2019;47:101490.
[16] Anselin L. The Moran scatterplot as an ESDA tool to assess local instability in spatial association: Regional Research Institute, West Virginia University Morgantown, WV; 1993.
[17] Anselin LJGa. Lagrange multiplier test diagnostics for spatial dependence and spatial heterogeneity. 1988;20:1-17.
[18] Brunsdon C, Fotheringham AS, Charlton MEJGa. Geographically weighted regression: a method for exploring spatial nonstationarity. 1996;28:281-98.
[19] Fotheringham AS, Brunsdon C, Charlton M. Geographically weighted regression: the analysis

of spatially varying relationships: John Wiley & Sons; 2003.
[20] Fotheringham AS, Charlton ME, Brunsdon CJE, A p. Geographically weighted regression: a natural evolution of the expansion method for spatial data analysis. 1998;30:1905-27.
[21] Van Donkelaar A, Martin RV, Spurr RJ, Burnett RTJEs, technology. High-resolution satellite-derived PM2.5 from optimal estimation and geographically weighted regression over North America. 2015;49:10482-91.
[22] Mei CL, He SY, Fang KT. A note on the mixed geographically weighted regression model. Journal of Regional Science. 2004;44:143-57.
[23] Jin C, Xu J, Huang ZJHI. Spatiotemporal analysis of regional tourism development: A semiparametric Geographically Weighted Regression model approach. 2019;87:1-10.
[24] Li W, Cao Q, Lang K, Wu JJSotTE. Linking potential heat source and sink to urban heat island: Heterogeneous effects of landscape pattern on land surface temperature. 2017;586:457-65.
[25] Zhao Q, Wentz EA, Fotheringham S, Yabiku ST, Hall SJ, Glick JA, et al. Semi-parametric Geographically Weighted Regression (S-GWR): a Case Study on Invasive Plant Species Distribution in Subtropical Nepal. 2016.
[26] Hattori K, Kaido K, Matsuyuki MJC. The development of urban shrinkage discourse and policy response in Japan. 2017;69:124-32.
[27] Frey WH. Migration and depopulation of the metropolis: regional restructuring or rural renaissance? American Sociological Review. 1987:240-57.
[28] Pallagst K. Shrinking cities in the United States of America. The Future of Shrinking Cities: Problems, Patterns and Strategies of Urban Transformation in a Global Context Los Angeles (University of California). 2009:81-8.
[29] Long Y, Wu KJE, A P. Shrinking cities in a rapidly urbanizing China. 2016;48:220-2.
[30] Beauregard RA. Urban population loss in historical perspective: United States, 1820–2000. Environment and planning A. 2009;41:514-28.
[31] Jacobs AJ. Japan's evolving nested municipal hierarchy: The race for local power in the 2000s. Urban Studies Research. 2011;2011.
[32] World Economic Situation and Prospects: United Nations Publications; 2018.
[33] Xie Y, Gong H, Lan H, Zeng S. Examining shrinking city of Detroit in the context of socio-spatial inequalities. Landscape and urban planning. 2018;177:350-61.
[34] Buhnik S. From shrinking cities to Toshi no Shukushō: Identifying patterns of urban shrinkage in the Osaka metropolitan area. Berkeley Planning Journal. 2010;23.
[35] Hair JF, Sarstedt M, Ringle CM, Mena JAJJotaoms. An assessment of the use of partial least squares structural equation modeling in marketing research. 2012;40:414-33.
[36] Yao J, Stewart Fotheringham AJTPG. Local spatiotemporal modeling of house prices: A mixed model approach. 2016;68:189-201.
[37] Feuillet T, Salze P, Charreire H, Menai M, Enaux C, Perchoux C, et al. Built environment in

local relation with walking: Why here and not there? Journal of Transport & Health. 2016;3:500-12.
[38] Fol S, Cunningham-Sabot E. Urban decline and shrinking cities: a critical assessment of approaches to urban shrinkage. Annales de géographie: Armand Colin; 2010. p. 359-83.
[39] SAKAMOTO K, IIDA A, YOKOHARI M. Spatial emerging patterns of vacant land in a Japanese city experiencing urban shrinkage. Urban and Regional Planning Review. 2017;4:111-28.
[40] Ye J. Stayers in China's "hollowed-out" villages: A counter narrative on massive rural–urban migration. Population, Space and Place. 2018;24:e2128.
[41] Tian Y, Kong X, Liu Y. Combining weighted daily life circles and land suitability for rural settlement reconstruction. Habitat International. 2018;76:1-9.
[42] Schwarz N, Haase D, Seppelt RJE, Planning PB, Design. Omnipresent sprawl? A review of urban simulation models with respect to urban shrinkage. 2010;37:265-83.
[43] Joo Y-M, Seo BJC. Dual policy to fight urban shrinkage: Daegu, South Korea. 2018;73:128-37.
[44] Zingale NC, Riemann DJUDI. Coping with shrinkage in Germany and the United States: A cross-cultural comparative approach toward sustainable cities. 2013;18:90-8.
[45] Hollander JB, Németh J. The bounds of smart decline: A foundational theory for planning shrinking cities. Housing Policy Debate. 2011;21:349-67.

Chapter 5. Comprehensive evaluation of urbanization process in Beijing city cluster

5.1 Introduction

During the past few decades, the world was undergoing fast pace urbanization, particularly in China [1, 2]. With the continuous rural-urban migration and urban expansion, more mega cities, large cities have emerged continuously in China. However, there are quite differences in urbanization level according to cities in China [3, 4]. Along with the rapid urbanization and modernization, built-up areas replaced with natural landscapes, and thus many environmental issues occurred, such as water and air pollution, increase in greenhouse gas, increase in fossil fuel energy consumption, and urban heat islands [5 - 7]. The most significant environmental implications of urbanization are water-air pollution, increase in energy consumption, and the urban heat island (UHI). Numerous studies have found that urbanization has a significant effect on the environment and urban quality [8 - 10]. With increasing closely economic and traffic connection among cities, three principal urban agglomerations emerged in China, including the Yangtze River Delta Region, the Peral River Delta Region, and the Beijing city clyster (also known as Beijing-Tianjin-Hebei Region) [11]. The urban built-up areas and the urban environment form a complex system with multiple feedback loops. Hence, it is essential to study the urbanization process and its impact on the urban environment on the urban agglomeration scale instead of a signal city for maintaining a good quality of urbanization and better urban planning strategies.

Within systems theory, a complex system refers to its constituent elements cannot explain the overall characteristics for their nonlinear links [12]. Previous studies showed urbanization process is a complex system which is inappropriate to evaluate only using population, such economy factors and social infrastructure factors are also essential parts for urbanization evaluation [13 - 16]. At present, there are several methods applied to assess urbanization including AHP, fuzzy comprehensive evaluation method, entropy method, gray relational analysis, and so on [14, 16 - 20]. The entropy method is a useful tool according to the abstraction and quantitative difficulty of urbanization impact factors. Information entropy is defined as the measurement of the degree of order that higher entropy indicates more information, and lower entropy indicates less information. The urbanization coupling coordination model treats demographic urbanization, economic development, and social development as three subsystems that interact with each other nonlinearly. The three subsystems are considered as independent but integrated systems. The coordination statement between subsystems is an indicator of sustainable development, providing a standard for judging whether the system is tending to higher-order [21].

With rapid urbanization, environmental implications become essential issues for urban planning. Panel data and monitoring stations data were the primary sources for evaluation of environmental implications such as water pollution and air pollution.

The Beijing city cluster, locating on the North China Plain, is the economic and cultural center in north China. There are in total 13 cities with quite differences in urbanization level in the region. This research is structured as follows: after presenting study area, data and methods, we will evaluate the urbanization process and it coupling coordination degree for the 13 cities in the Beijing city cluster from 2000 to 2017. Then, four cities in the core area of the region are selected for analyzing the impact of urbanization effect on SUHI. Finally, summarizes the conclusion.

5.2 Location and general information of Beijing city cluster

The study areas used in this study covered 13 cities in the Beijing city cluster, including Beijing, Tianjin, and 11 cities in Hebei prefecture (Shijiazhuang, Tangshan, Qinhuangdao, Baoding, Handan, Xingtai, Zhangjiakou, Chengde, Cangzhou, Langfang, and Hengshui). Beijing is the capital and the second largest city in China. Tianjin is the largest open city along the coastline in northern China. The other 11 cities belong to Hebei province which is one of the general provinces in China closely nearby Beijing and Tianjin. The Beijing city cluster which located within 36°2’-42°36’N and 113°53’-119°49’E shows the geographic location of the study area (Fig. 5-1). The Beijing city cluster as the economic and cultural center in north China was rapidly urbanizing during the past decades. The urban population of the Beijing city cluster increased from 26.17 million in 2000 to 44.33 million in 2017, an average annual increase rate of 2.6%, and the regional gross district product (GDP) increased from 0.95 trillion yuan in 2000 to 6.01 trillion yuan in 2017, an average annual increase rate of 10.8%. However, there are quite differences of the urbanization process for the cities in the city cluster. The region can be divided into 4 areas, including north-west area, coastal area, core area, and southern area. The north-west area is an ecological conservation area of high altitude where mainly covered by savannas and mountain area. Tianjin, Tangshan, and Qinhuangdao, locating in the coastal area, form the coastal economic development zone in the region. In the core area, Beijing and Tianjin act as the demonstration and radiating role in the urbanization development. Langfang and Baoding, which surrounding Beijing and Tianjin are at the forefront of urbanization radiation. With Beijing rapidly urbanized, Xiongan new area in Baoding established in 2017, acting as the hub of Beijing, Tianjin, and Hebei province, was targeting on building a highly urbanized city and representing the most advanced urbanization in China, which is good for promoting coordinated urbanization in the region and release the urban diseases and decentralize urban function in Beijing. Shijiazhuang is the capital of Hebei province which is the sub-central city in the southern part of Beijing city cluster to drive the urbanization development of cities in Hebei province.

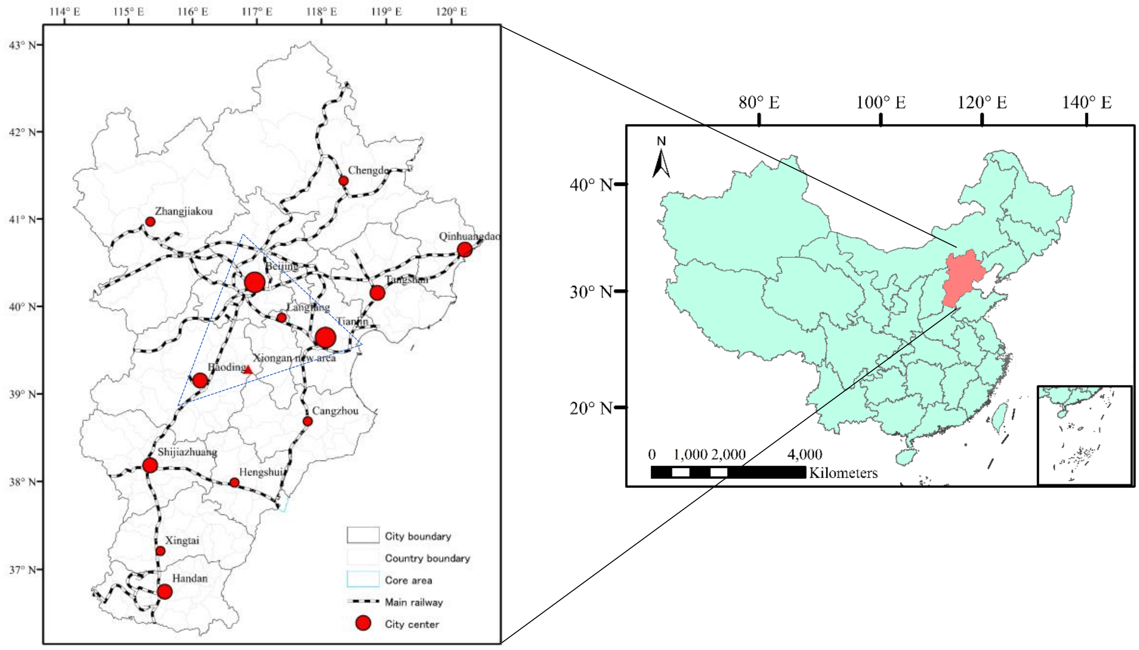

Fig. 5-1. Location of Beijing city cluster.

As Beijing and Tianjin directly under the jurisdiction of the central government, having a lot of political advantages, Beijing and Tianjin as 2 municipalities have edged ahead of Hebei province as the process of urbanization. The 13 cities are divided into 3 categories based on the urban population data from National Statistics data in 2015 (Table 1). The 3 categories are mega-city (urban population over 10 billion people), including Beijing and Tianjin, big-city (urban population over 1 billion people) including Shijiazhuang, Tangshan, Qinhuangdao, Baoding, and Handan, and mid-city (urban population over 0.5 billion people) including Xingtai, Zhangjiakou, Chengde, Cangzhou, Langfang, and Hengshui. The region is characterized by a warm temperature zone and has a typical continental monsoon climate with four distinct seasons, including a hot and rainy summer and a cold and dry winter.

Table 5-1. Outline of 13 cities in the Beijing city cluster. (The data come from the 2016 China City Statistical Yearbook)

Category	City	Urban population (10,000 people)	Land area (km^2)	Density (people/km^2)	GDP (billion yuan)	Country/District
Mega-city	Beijing	1345.2	16411	819.69	23014.59	0/16
	Tianjin	1026.9	11920	861.68	16538.19	0/16
Big-city	Shijiazhuang	410.33	15848	784.86	5440.60	18/4
	Tangshan	334.28	14341	560.37	6103.06	7/7
	Qinhuangdao	140.53	7803	378.86	1250.44	3/4
	Baoding	282.25	22185	541.89	3000.34	19/5
	Handan	175.71	12065	870.02	3145.43	12/6
Mid-city	Xingtai	88.14	12433	627.66	1764.73	17/2
	Zhangjiakou	91.24	36797	127.18	1363.54	10/6
	Chengde	59.65	39490	96.83	1358.73	8/3
	Cangzhou	54.97	14304	551.72	3320.63	14/2
	Langfang	85.06	6419	722.56	2473.86	8/2
	Hengshui	55.9	8837	513.01	1220.01	9/2

Due to the rapid development of economies, the growth of the population, the fast urbanization and modernization, numbers of the metropolis have emerged in the world. As one of the three largest city accumulation areas and economic cores in China (the other 2 are the Yangtze River Delta Region, and the Pearl River Delta Region), the scale of urbanization in the Beijing city cluster is without precedent since the application of the Reform and Open Policy in 1978 (Zhu et al., 2016, Chen and Zheng, 2014). Moreover, a high rate of urbanization also contributes to the change in the living environment, such as global warming, urban heat island, air pollution, etc. It possesses certain advantages in the aspect of the urban study for understanding urbanization process and environment implications for cities with different scale in China.

5.3 Data and methodology of urbanization evaluation

5.3.1 Statistics data pre-processing

The annual socio-economic and environment-related statistics data for cities in the Beijing city cluster from 2000 to 2017 were acquired from the China Statistical Yearbook (2001-2018) (http://www.stats.gov.cn/), the China City Statistics Yearbook (2001-2018) (http://www.stats.gov.cn/), Beijing Statistical Yearbook (2001–2018) (http://www.bjstats.gov.cn), Tianjin Statistical Yearbook (2001–2018) (http://stats.tj.gov.cn), and Hebei Economic Yearbook (2001–2018) (http://tjj.hebei.gov.cn). As the indicators selected for urbanization evaluation have the differences both in the dimension and the magnitude, the indicators were first divided into 2 categories, including positive indicator and negative indicator. A greater value of a positive indicator suggests better condition for the development of the system, and a greater value of a negative indicator suggests worse condition for the development of the system. Then all the indicators were normalized into nondimensional values using the following equations:

For positive indicators: $X_{ij} = \frac{x_{ij}-x_{jmin}}{x_{jmax}-x_{jmin}}$ (Eq. 5-1)

For negative indicators: $X_{ij} = \frac{x_{jmax}-x_{ij}}{x_{jmax}-x_{jmin}}$ (Eq. 5-2)

Where i is the year; j is the indicator; X_{ij} is the normalized value; x_{ij} is the original value; x_{jmax} is the maximum value of indicator j over the study years; x_{jmin} is the minimum value of the indicator j over the study years. The normalized values of all indicators ranged from 0 to 1.

5.3.2 The urbanization evaluation indicators

As urbanization being a complex system, which involves population, economy, society aspects, three sub-systems including demographic urbanization, economic development, and social development were evaluated to improve the comprehensive understanding of the urbanization process in the Beijing city cluster. The indicators selected for the 3 aspects were the most cited and simplest indicators which are easy for data collection, understanding, and dissemination [13 - 15, 22, 23]. The demographic urbanization system is made up of 5 indicators; the economic development system is made up of 5 indicators; the social development system is made up of 5 indicators (Table 5-2).

Table 5-2. Indicators for urbanization system

Urbanization system	Indicator	Indicator effect	Weight
Demographic urbanization	Urban population size (million people)	Positive	0.3148
	Urban population rates (%)	Positive	0.2743
	Urban population density (people/km2)	Positive	0.0954
	Proportion of the secondary and tertiary industry employed population to total employed population (%)	Positive	0.1839
	Number of college students per 10,000 people	Positive	0.1316
Economic development	Per capital GDP (Yuan/people)	Positive	0.2423
	GDP proportion of the secondary and tertiary industry (%)	Positive	0.1187
	Per unit land GDP (Yuan/km^2)	Positive	0.1705
	Income ratio of urban to rural residents (%)	Negative	0.1392
	Investment in fixed assets (Yuan/km^2)	Positive	0.3293
Social development	Per capital park and green areas (people/m^2)	Positive	0.1944
	Per capital road areas (people/m^2)	Positive	0.2255
	Per capital built up area (people/m^2)	Positive	0.3245
	GDP per unit water consumption (Yuan/m^3)	Negative	0.1393
	GDP per unit electricity consumption (Yuan/kWh)	Negative	0.1163

5.3.3 Urbanization evaluation methods

The entropy method was used to determine the weight of each indicator (Table 2). The information entropy represents the disorder of a system and varies by index. Compared to expert weighting model and analytic hierarchy process (AHP), the entropy method can avoid the effect by subjective weight determination [34, 35]. The steps for calculating the weights of the indicators are showing as follows:

The proportion P_{ij} of the indicator *j* in year *i*: $P_{ij} = \frac{X_{ij}}{\sum_{i=1}^{n} X_{ij}}$ (Eq. 5-3)

Information entropy E_j for the indicator *j*: $E_j = -\frac{1}{\ln n} \sum_{i=1}^{n} (P_{ij} \times \ln (P_{ij})$ (Eq. 5-4)

Entropy redundancy D_j: $D_j = 1 - E_j$ (Eq. 5-5)

Weight W_j of the indicator *j*: $W_j = \frac{D_j}{\sum_{j=1}^{m} D_j}$ (Eq. 5-6)

Evaluation of the indicator *j* in year *i*: $Y_{ij} = W_j \times X_{ij}$ (Eq. 5-7)

Index for composition systems in year *i*: $Y_i = \sum_{j=1}^{m} Y_{ij}$ (Eq. 5-8)

Where *n* is the total number of observations; *m* is the number of indicators.

As urbanization promote the urban population migration, economic growth, and social infrastructure development, coordinated development is a big issue in regional research. As urbanization is a multi-component process, the coupling coordination degree model was utilized to understand the comprehensive urbanization level (CUL) in the Beijing city cluster. Coupling coordination refers to two or more systems can influence each other through interactive mechanisms [21]. The CUL for cities were calculated as follows:

The coupling degree: $C = \left\{ \frac{Y_D \times Y_E \times Y_S}{\left[\frac{(Y_D + Y_E + Y_S)}{3}\right]^3} \right\}^{\frac{1}{3}}$ (Eq. 5-9)

Comprehensive coupling coordinated development evaluation index:

$$T = \alpha Y_D + \beta Y_E + \gamma Y_s \quad \text{(Eq. 5-10)}$$

The degree of coupling coordination: $D = \sqrt{C \times T}$ (Eq. 5-11)

Where *C* is the coupling degree of urbanization; Y_D is the index for demographic urbanization system; Y_E is the index for economic development system; Y_S is the index for social development system; *T* is the comprehensive coupling coordinated development evaluation index; α, β, and γ denote the contribution of demographic urbanization, economic development, and social development the comprehensive system, respectively; *D* is the coupling coordination degree which refers to CUL. In this study, the 3 systems were considered as equally important for urbanization (α = 1/3, β = 1/3, and γ= 1/3). The degrees of CUL were divided into 5 categories (Table 3) [20, 21, 24].

Table 5-3. Classification of coupling coordination degree

Category	CUL range
Non-coordination	$0 \le D < 0.2$
Barely coordination	$0.2 \le D < 0.4$
Medium coordination	$0.4 \le D < 0.6$
Good coordination	$0.6 \le D < 0.8$
Close coordination	$0.8 \le D \le 1$

5.3.4 Data Availability

The following data used during the study are available online and the models used during the study appear in the submitted article.

Table 5-4. Data availability

Data	Source	URL
Statistics data	China Statistical Yearbook (2001-2018)	http://www.stats.gov.cn/
	China City Statistics Yearbook (2001-2018)	http://www.stats.gov.cn/
	Beijing Statistical Yearbook (2001–2018)	http://www.bjstats.gov.cn
	Tianjin Statistical Yearbook (2001–2018)	http://stats.tj.gov.cn
	Hebei Economic Yearbook (2001–2018)	http://tjj.hebei.gov.cn

5.4 Data descriptive analysis of urbanization of Beijing city cluster

In this study, the statistics of urbanization and environmental indexes from statistics of China City Statistics Yearbook (2001-2018) including population, economy, society, and environment from 2000 to 2017 were used to state the situation of urbanization development and environmental change. As the rapid development of urbanization processing in the Beijing city cluster, the urbanization-related indexes of each city kept increasing over the past decades. However, the uneven urbanization process is an essential issue for local government. As regional urbanization could have both positive and negative impacts on the local environment, the regional environment change is a complex process which is affected by reasons combined by regional urbanization and natural environment.

The gradually urban population growth and population density growth were found in the Beijing city cluster (Fig. 5-2). No matter from the urban population or urban population density, Beijing and Tianjin were ahead of cities in Hebei province. The urban population of Beijing and Tianjin increased by 3.85 and 3.68 million, with an annual increase rate of 1.87% and 2.43%. Comparatively, an even faster increase in Hebei was found that the average increase rate of cities in Hebei was 4.49%. There were some changes in administration district around 2015 (such as Ji area in Tianjin changing from country to district in 2015, Luancheng area in Shijiazhuang changing from country to district in 2014, Xushui and Qingyuan area in Baoding changing from country to district in 2015), which make a significant expansion of urban population around 2015.

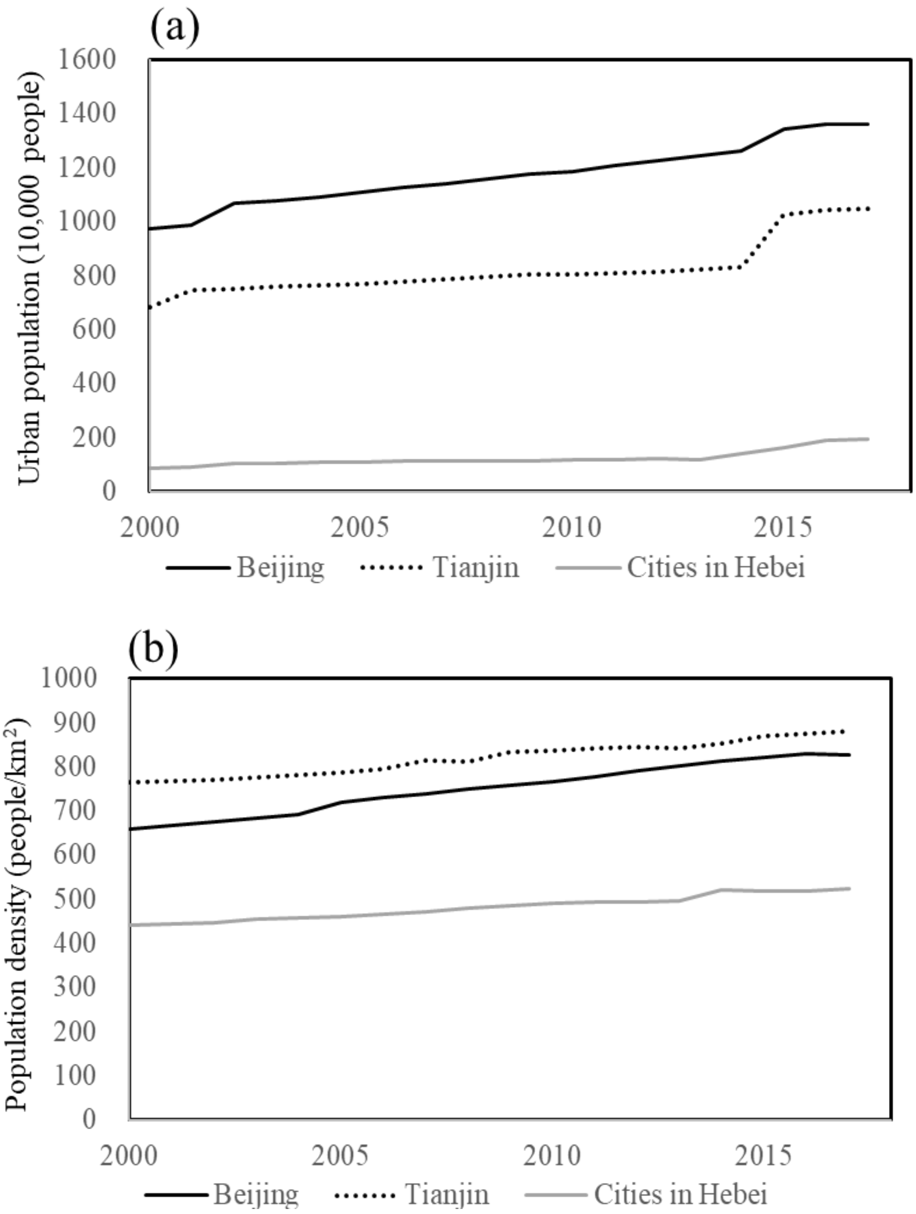

Fig. 5-2 Statistics of population indexes of cities in the Beijing city cluster from 2000 to 2017

(a) urban population (10,000 people) variation, (b) population density (people/km^2) variation

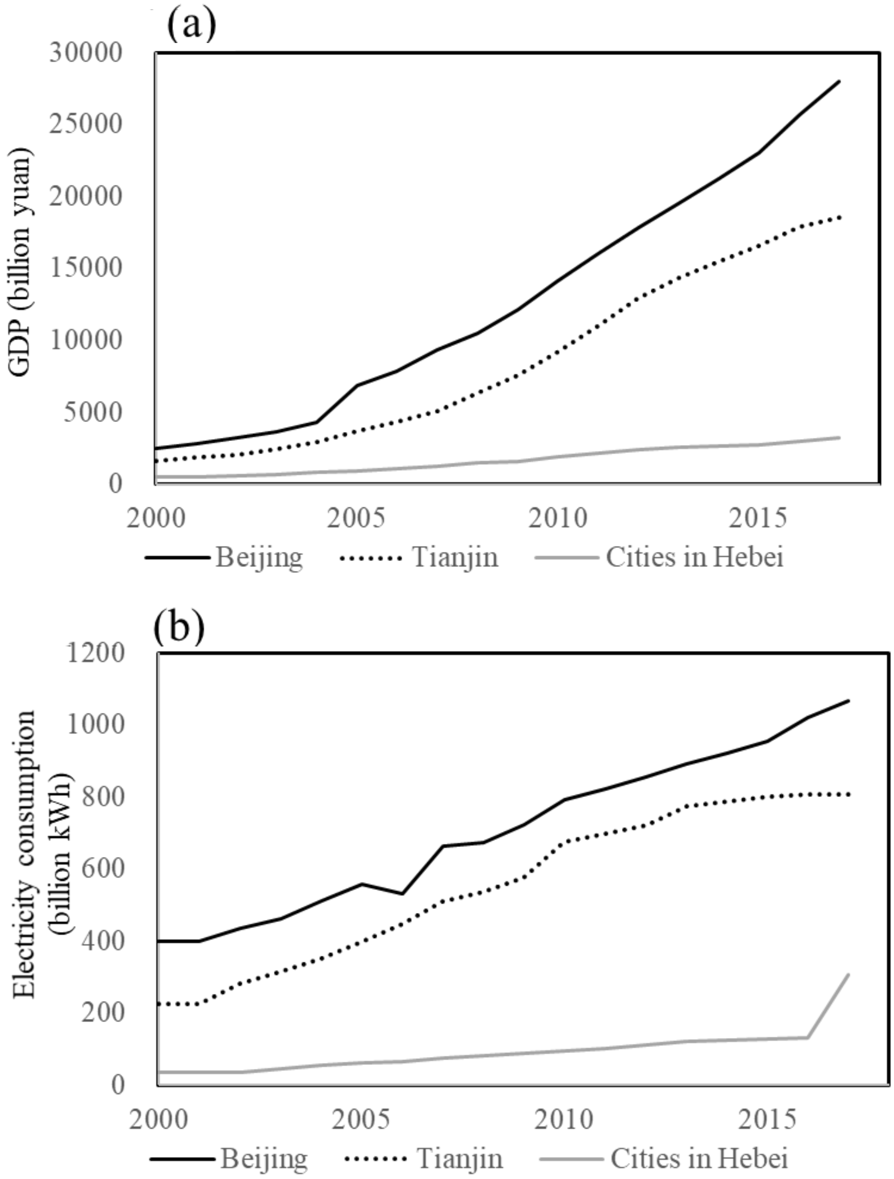

Fig. 5-3 Statistics of economy indexes of cities in the Beijing city cluster from 2000 to 2017 (a) GDP (billion yuan) variation, (b) electricity consumption (billion kWh) variation

Significant growth of GDP and electricity consumption for cities in the Beijing city cluster showed constant urbanization process, whilst the gap between cities was also expanding temporally, suggesting a tremendous regional discrepancy in the region (Fig. 5-3). In 2017, the GDP reached about 2.8 trillion yuan in Beijing, and 1.8 trillion yuan in Tianjin, which is 25.8 and 17.1 times as the same as average GDP for cities in Hebei. Similarly, electricity consumption in Beijing and Tianjin were about 1067 and 805 million kWh, 3.47 and 2.62 times than average of Hebei.

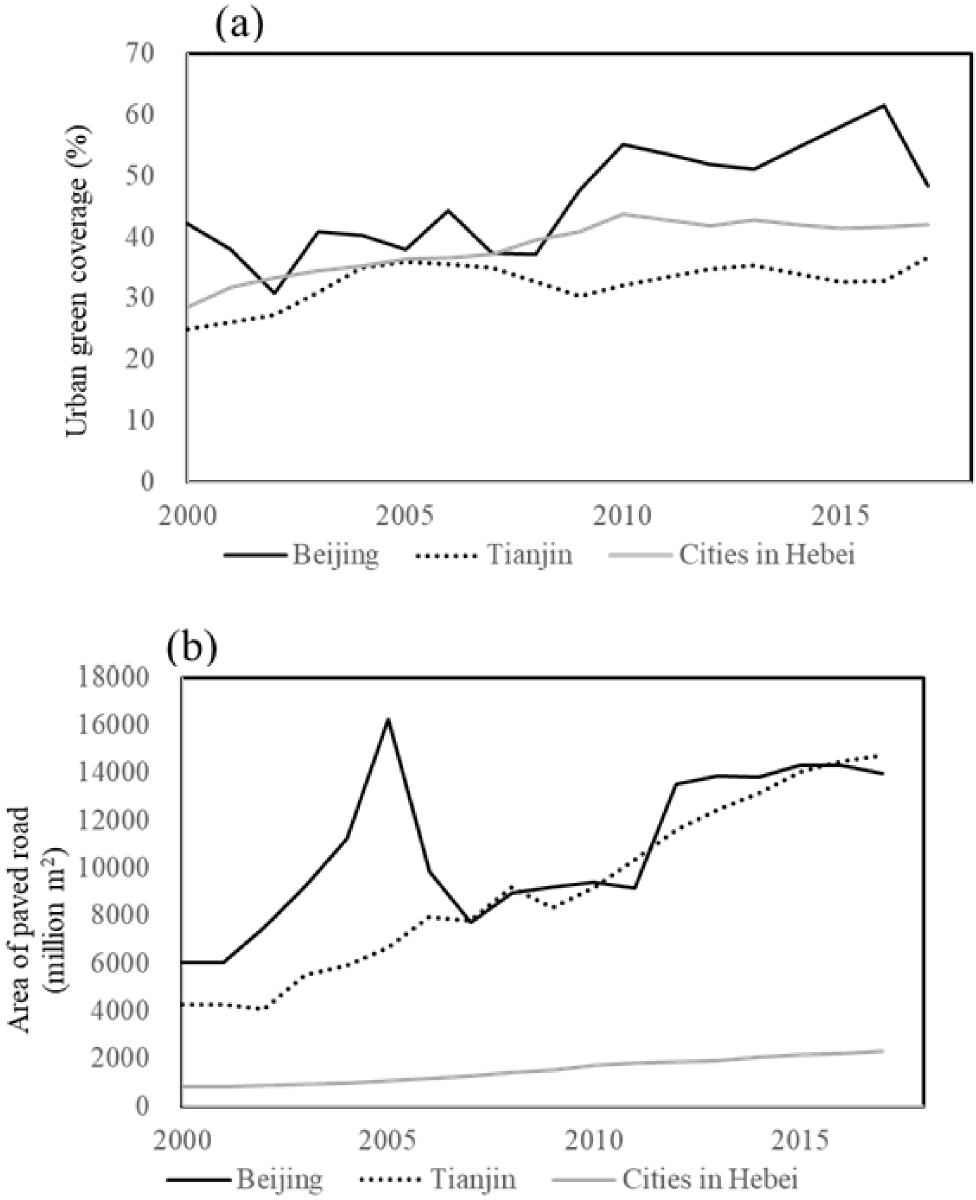

Fig. 5-4 Statistics of society indexes of cities in the Beijing city cluster from 2000 to 2017

(a) urban green ratio (%), (b) area of paved road (million m^2)

Urban greenery contributes to a healthy natural environment for city residents. Thus, the government has made continuous efforts to restrict the development of green space in the built-up area and convert empty lots to green space. Fig. 5-4 shows the ratio of urban green coverage and area of paved road in the region from 2000 to 2017. In 2017, the urban green coverage ratio reached 48.4%, 36.7%, and 42.1% for Beijing, Tianjin, and the average for cities in Hebei. Stable upward trends were found in Tianjin and cities in Hebei, while the broad variation range of urban green coverage in Beijing was owing to the continuous urban expansion and the periodical urban green construction such as Beijing Olympic Park (2008), which covers an area of 11.59 km^2. Roads are the facilities of urban structures, which provide spaces to meet the diversified traffic needs of citizens (Gao et al., 2004). Because of the problems in statistic practice and criterion, the road area in 2005 for Beijing was extreme. For Beijing and Tianjin, the area of paved road in 2017 were around 14,000 million m2, which is about 6 times as average for cities in Hebei.

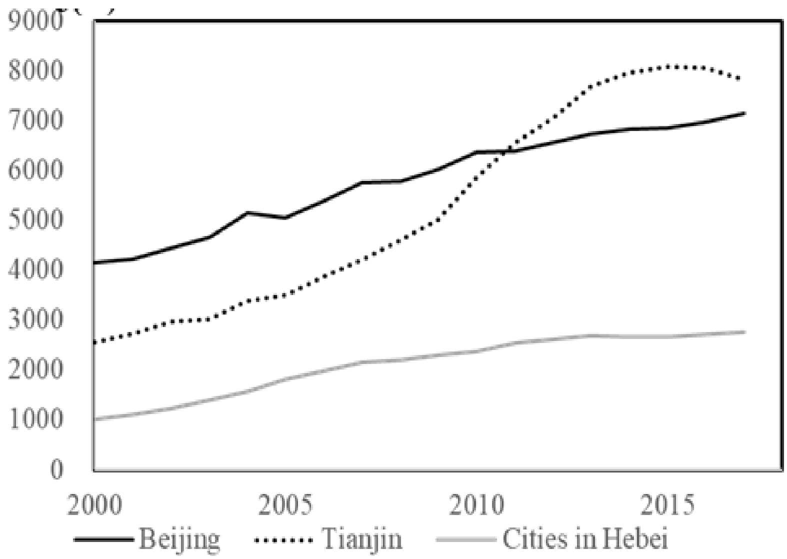

Fig. 5-5 Statistics of energy consumption (10,000 tons of SCE) of cities in the Beijing city cluster from 2000 to 2017.

In the Beijing city cluster, energy consumption rises rapidly (Fig. 5-5), as heavy industries such as iron-steel industry being the pillar industry which drives the industrialization and urbanization. Whilst the energy demand remains overwhelmingly dominated by fossil fuels, especially coal, accounting for 50% of the total energy consumption, large quantities of the pollution discharge is a serious problem which cannot be ignored.

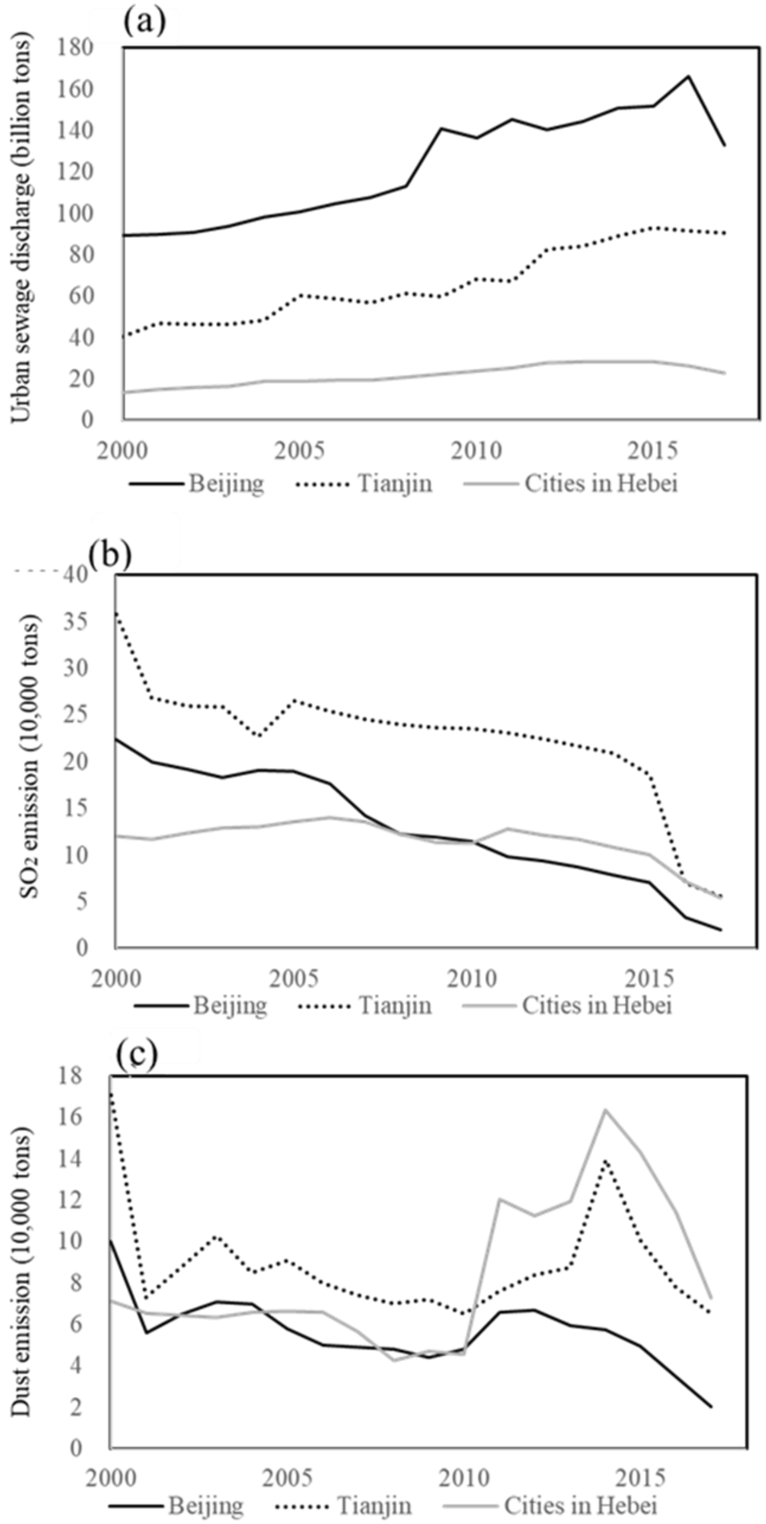

Fig. 5-6 Statistics of pollution indexes of cities in the Beijing city cluster from 2000 to 2017 (a) urban sewage discharge (billion tons), (b) SO_2 emission (10,000 tons) variation, (c) dust emission (10,000 tons).

Fig. 5-6 (a-c) show how the region's pollution emission has changed over time. The number of sewage discharge in Beijing was significantly higher than that in Tianjin and cities in Hebei, which is owing to the difference in the sewage discharge standards and the maximum allowable discharge concentration. Ambient air pollutants mainly including SO_2, NO_x, and particulate matter, before China released 'Ambient Air Quality Standard' in 2012, there was no mandatory monitoring for particulate matter such as pm2.5. Despite the severe air pollution caused by pm2.5 and pm10 in the region in recent years, the study chose SO_2 emission and dust emission to represent the ambient air pollution from 2000 to 2017. In general, the pollutants emissions were falling, which is due to the change in the energy structure and the increasing investment in emissions treatment.

5.5 Comprehensive evaluation of urbanization level of cities in Beijing city cluster

5.5.1 Time series variation of urbanization index for cities in the Beijing city cluster

The entropy method was applied to calculate the weights and the indexes values of demographic urbanization system, economic development system, and social development system. Figure 7 shows indexes values variations of the demographic urbanization system, economic development system, and social development system for the 13 cities in the Beijing city cluster.

The demographic urbanization system index (DUSI) values characterized by rapid linear growth for all cities from 2000 to 2017. Comparing with the other 11 cities, the demographic urbanization level in Beijing and Tianjin were significantly higher, suggesting the two cities are standing a leading position in the cluster. It is worth noting that benefitting from Langfang’s location, as the Beijing-Tianjin corridor, the DUSI value of Langfang was rapidly increasing and came third in 2017. Meanwhile, the difference between DUSI values of big-cities and mid-cities is getting smaller (0.07 in 2000, and 0.02 in 2017). The results showed that the gap of demographic urbanization level between megacities and big-mid cities was widening, and the development of demographic urbanization for big-mid cities tended to be balanced. The economic development system index (EDSI) values also characterized by rapid linear growth for all cities from 2000 to 2017. For the economic development level, Beijing and Tianjin were in the first echelon, Shijiazhuang, Tangshan, Cangzhou, and Langfang were in the second echelon, and the rest cites were in the third echelon. Except for Shijiazhuang, as the capital of Hebei province, Tangshan, Cangzhou, and Langfang are in the central area of Beijing city cluster, suggesting the economic development of Beijing and Tianjin has driven the development of surrounding cities. The social development system index (SDSI) values revealed an increasing trend for all cities from 2000 to 2017. The SDSI values of Tangshan, Qinhuangdao, Baoding, and Xingtai increased during the first few years then stabilized, and a linear growth characterized the SDSI values of the other cities.

Although the level of 3 urbanization systems for the cities in the Beijing city cluster increased between 2000 to 2017. Considerable differences between cities suggesting an uneven regional development phenomenon. Beijing was in the leading place, with Tianjin in the second place. Meanwhile, the urbanization development in mid-cities caught up that in big-cities, suggesting a balanced urbanization trend.

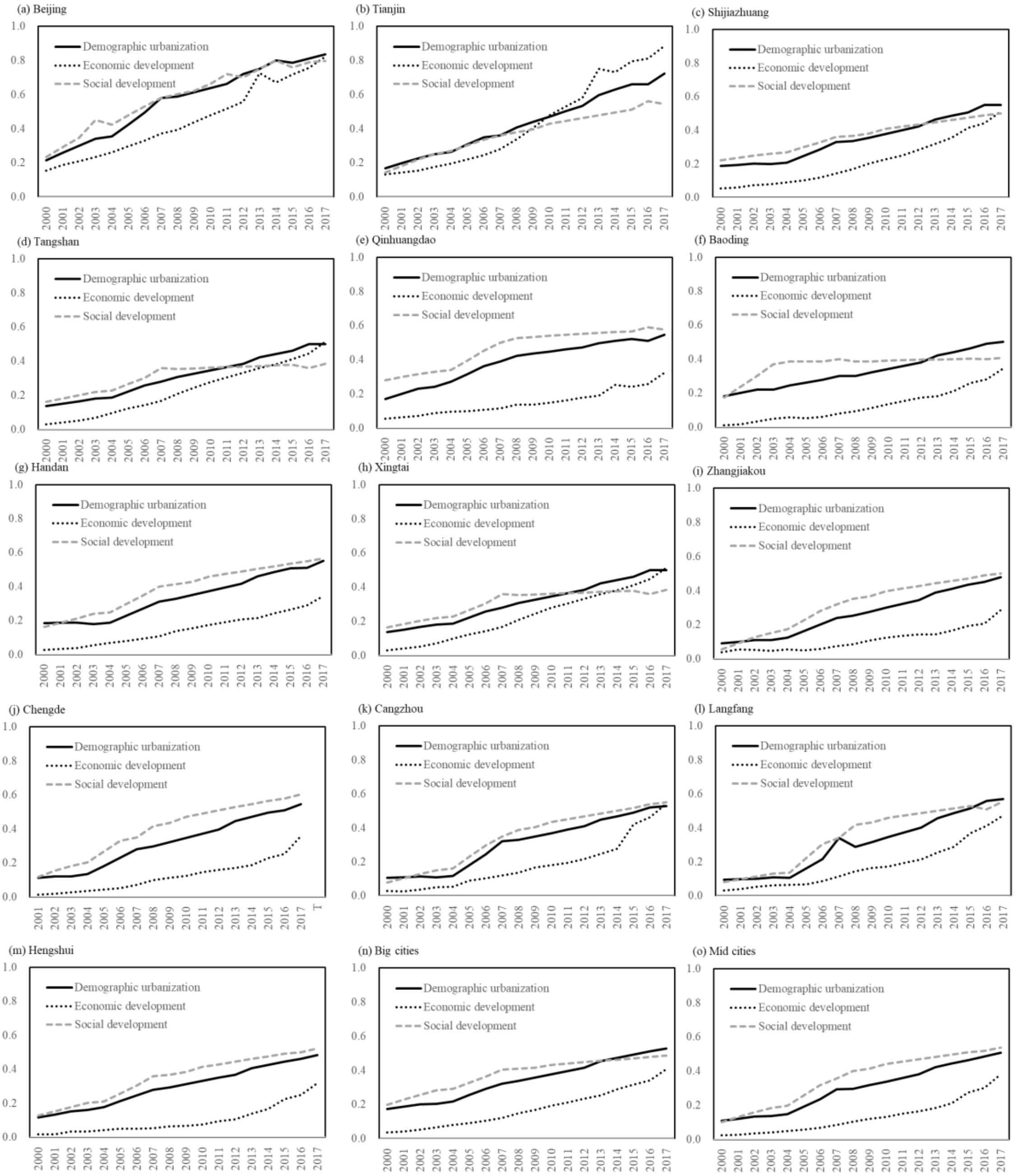

Fig. 5-7 Variations of 3 urbanization systems indexes for cities in the Beijing city cluster from 2000 to 2017 (a) Beijing, (b) Tianjin, (c) Shijiazhuang, (d) Tangshan, (e) Qinhuangdao, (f) Baoding, (g) Handan, (h) Xingtai, (i) Zhangjiakou, (j) Chengde, (k) Cangzhou, (l) Langfang, (m) Hengshui, (n) mean of big-cities, (o) mean of mid-cities.

5.5.2 Comprehensive urbanization level

The coupling coordination degree model was utilized to calculate the coupling coordination degree of the 3 urbanization systems for cities in the Beijing city cluster based on equation (9), (10), and (11). For the degree of coupling coordination reflects both the correlation and size of indexes among systems, it was select to represent the CUL of each city. Then the CUL were classified into 5 different (Table 5-3). Table 5-3 shows the CUL varied from 2000 to 2017 for cities in the Beijing city cluster based on coupling coordination degree model.

The CUL was mainly medium to good and showed an overall increasing trend within the Beijing city cluster from 2000 to 2017. The sequence of the coupling coordination degree varied spatially with a course of mega-city > big-city > mid-city, while cities in central area > cities in coastal area > cities in southern area > cities in the north-west mountain area. In 2007, all the cities made the CUL from barely coordination to medium coordination, while all cities made it from medium to good until 2017. However, only Beijing and Tianjin realized close coordination of CUL. Since 2005 Beijing entered a stage of good coordinated urbanization, and in 2012, it reached the close coordination stage showing Beijing far ahead of the other cities in the urbanization process. Tianjin lagged slightly, but it was clear that Tianjin exhibit strong competence in urbanization development. Langfang, as a corridor between Beijing and Tianjin, made a considerable increase of the CUL from 2000 to 2017. However, the CUL of Baoding city increased from 0.27 to 0.64, the weakest pace of growth among cities, but it is expected to develop rapidly as the Xiongan new area established in 2017.

The coupling coordination degree model was utilized to show the development of comprehensive urbanization in the Beijing city cluster, that can be helpful for the future development for the cities. As one of the most prominent city clusters in China, cities are quickly urbanized and closely linked, which make it essential to explore the coordination of urbanization for inclusive and sustainable urbanization. The results revealed the urbanization stage in the Beijing city cluster. Although all cities were urbanizing rapidly from 2000 to 2017, the vast differences between cities cannot be ignored.

Table 5-5. The CUL of cities in the Beijing city cluster from 2000 to 2017

	2000	2001	2002	2003	2004	2005	2006	2007	2008	2009	2010	2011	2012	2013	2014	2015	2016	2017
Beijing	0.45	0.49	0.53	0.57	0.58	0.63	0.67	0.71	0.72	0.74	0.77	0.79	0.81	0.86	0.87	0.87	0.89	0.91
Tianjin	0.38	0.41	0.44	0.47	0.49	0.52	0.55	0.58	0.61	0.64	0.68	0.70	0.72	0.77	0.78	0.80	0.82	0.84
Mean of big city	0.32	0.34	0.37	0.39	0.41	0.44	0.47	0.50	0.52	0.54	0.56	0.57	0.59	0.61	0.63	0.64	0.66	0.68
Mean of mid city	0.24	0.26	0.30	0.31	0.33	0.37	0.41	0.45	0.48	0.50	0.52	0.54	0.55	0.58	0.59	0.63	0.65	0.68
Shijiazhuang	0.36	0.38	0.39	0.40	0.41	0.44	0.47	0.51	0.52	0.55	0.57	0.59	0.61	0.64	0.66	0.68	0.70	0.72
Tangshan	0.30	0.32	0.35	0.37	0.40	0.44	0.47	0.51	0.53	0.55	0.57	0.59	0.60	0.62	0.63	0.64	0.66	0.68
Qinhuangdao	0.37	0.39	0.41	0.44	0.45	0.48	0.51	0.53	0.56	0.56	0.57	0.59	0.60	0.61	0.64	0.64	0.65	0.68
Baoding	0.27	0.30	0.36	0.40	0.42	0.41	0.43	0.46	0.47	0.49	0.51	0.53	0.54	0.56	0.58	0.60	0.62	0.64
Handan	0.31	0.32	0.34	0.36	0.38	0.42	0.45	0.49	0.51	0.53	0.56	0.57	0.59	0.61	0.63	0.64	0.66	0.69
Xingtai	0.19	0.27	0.32	0.35	0.38	0.40	0.43	0.45	0.49	0.50	0.51	0.53	0.54	0.55	0.57	0.59	0.60	0.64
Zhangjiakou	0.24	0.28	0.30	0.30	0.32	0.35	0.38	0.42	0.44	0.47	0.49	0.51	0.52	0.54	0.56	0.58	0.60	0.64
Chengde	0.24	0.23	0.27	0.29	0.31	0.36	0.40	0.44	0.48	0.50	0.52	0.55	0.56	0.58	0.60	0.63	0.65	0.70
Cangzhou	0.25	0.26	0.29	0.31	0.32	0.39	0.44	0.49	0.51	0.54	0.56	0.57	0.59	0.62	0.64	0.70	0.71	0.75
Langfang	0.25	0.27	0.29	0.31	0.31	0.37	0.42	0.49	0.51	0.53	0.55	0.57	0.59	0.62	0.65	0.68	0.70	0.73
Hengshui	0.25	0.27	0.31	0.32	0.34	0.37	0.39	0.42	0.44	0.45	0.47	0.49	0.51	0.54	0.57	0.61	0.62	0.66

Non-coordination	Barely coordinatio	Midium coordination	Good corrodination	Close coordination
[0,0.2)	[0.2,0.4)	[0.4,0.6)	[0.6,0.8)	[0.8,1]

5.6 Conclusion

Over the past 20 years, cities in the Beijing city cluster have experienced rapid urbanization. In this situation, urban population growth and urban sprawl are putting increasing pressure on the environment. In this study, we have discussed the urbanization process and its environmental implications in Beijing city cluster, considering the differences in cities, and the characteristics of coordinated development in the region. The coupling coordination degree model was applied to exanimate the comprehensive level of urbanization for cities from the demographic urbanization aspect, the economic development aspect, and the social development aspect. Meanwhile, descriptive analysis was performed to state the variation of water pollution, air pollution, and energy use in the Beijing city cluster.

The scale of urban expansion is in accordance with city classification. The increment of Beijing is the largest, but the increase rate is relative slow. Compared with impervious surface, urban area in Tianjin was relatively small, because a large area of impervious area is on the coast and the connection between the area and Tianjin downtown is not very close. As a result, the area on the coast was not classified into urban areas through machine recognition. Same with Tianjin city, urban area in Baoding was also relatively small, which is due to the developed counties in Baoding city. The increase rate of urban area and impervious surface area of Langfang city is quite high. However, the base is still too small compared Beijing, Tianjin, and Baoding.

Through the application of the entropy method, we found that: (1) the urban population size (31.48%), urban population rate (27.43%) are the primary indicators with significant effect on demographic urbanization system; (2) the investment in fixed assets (32.93%), and per capita GDP (24.23%) are the primary indicators with significant effect on economic development system; (3) per capita built-up areas (29.28%) is the primary indicator with significant effect on social development system. The coupling coordination degree model applied in the study make it possible to assess the comprehensive level of urbanization for cities in the Beijing city cluster from 2000 to 2017. The results suggest that those five indicators made the enormous contribution in evaluating the urbanization level, and determining the coupling coordination degree of urbanization. Besides, the results reveal that the coordinated urbanization in the region from ‘barely coordination’ to ‘medium coordination’ to ‘good coordination’. This study can provide useful information for understanding the current level of urbanization and promoting sustainable development in the future.

In the foreseeable future, the comprehensive urbanization process in the Beijing city cluster will be the main component of China’s urbanization. Our empirical analysis for the 13 cities in the Beijing city cluster illustrated that the coupling coordination urbanization model is a useful tool which contribute to improve the understanding of the urbanization process and help with management policies and strategies for comprehensive development of urbanization for cities and balanced development for the region. However, many environmental implications caused by urbanization were apparent, especially in mega cities. Compared to environment-related statistics, with the development of GIS and RS technologies, more environmental harms can be investigated based on GIS and RS data to reflect the immediate urban environmental phenomenon and make timely countermeasures.

References

[19] Hair JF, Sarstedt M, Ringle CM, Mena JAJJotaoms. An assessment of the use of partial least squares structural equation modeling in marketing research. 2012;40:414-33.

[1] J. Klugman, *A sourcebook for poverty reduction strategies*. World Bank Washington, DC, 2002.

[2] A. R. dos Santos *et al.*, "Spatial and temporal distribution of urban heat islands," *Science of the Total Environment,* vol. 605, pp. 946-956, 2017.

[3] Q. Chen and Z. Song, "Accounting for China's urbanization," *China Economic Review,* vol. 30, pp. 485-494, 2014.

[4] B. Qin and Y. Zhang, "Note on urbanization in China: Urban definitions and census data," *China Economic Review,* vol. 30, pp. 495-502, 2014.

[5] J. A. Foley *et al.*, "Global consequences of land use," *science,* vol. 309, no. 5734, pp. 570-574, 2005.

[6] L. Zhou *et al.*, "Evidence for a significant urbanization effect on climate in China," *Proceedings of the National Academy of Sciences,* vol. 101, no. 26, pp. 9540-9544, 2004.

[7] H.-M. Zhu, W.-H. You, and Z.-f. Zeng, "Urbanization and CO2 emissions: A semi-parametric panel data analysis," *Economics Letters,* vol. 117, no. 3, pp. 848-850, 2012.

[8] N. B. Grimm *et al.*, "The changing landscape: ecosystem responses to urbanization and pollution across climatic and societal gradients," *Frontiers in Ecology and the Environment,* vol. 6, no. 5, pp. 264-272, 2008.

[9] S. Peng *et al.*, "Surface urban heat island across 419 global big cities," *Environmental science & technology,* vol. 46, no. 2, pp. 696-703, 2011.

[10] D. Zhou, S. Zhao, L. Zhang, and S. Liu, "Remotely sensed assessment of urbanization effects on vegetation phenology in China's 32 major cities," *Remote Sensing of Environment,* vol. 176, pp. 272-281, 2016.

[11] X. Zhu *et al.*, "The inhabited environment, infrastructure development and advanced urbanization in China's Yangtze River Delta Region," *Environmental Research Letters,* vol. 11, no. 12, 2016.

[12] R. Gallagher and T. Appenzeller, "Beyond reductionism," *Science,* vol. 284, no. 5411, pp. 79-80, 1999.

[13] M. Chen, D. Lu, and L. Zha, "The comprehensive evaluation of China's urbanization and effects on resources and environment," *Journal of Geographical Sciences,* vol. 20, no. 1, pp. 17-30, 2010.

[14] M. Chen, D. Lu, and H. Zhang, "Comprehensive evaluation and the driving factors of China's urbanization," *Acta Geographica Sinica,* vol. 64, no. 4, pp. 387-398, 2009.

[15] L. Guo-ping, "The analysis and evaluation of the compatible relationship between industrialization and urbanization in China," *Areal Research and Development,* vol. 5, no. 002, 2008.

[16] Y. Sakieh, B. J. Amiri, A. Danekar, J. Feghhi, and S. Dezhkam, "Scenario-based evaluation of urban development sustainability: an integrative modeling approach to compromise between

urbanization suitability index and landscape pattern," *Environment, Development and Sustainability,* vol. 17, no. 6, pp. 1343-1365, 2015.

[17] A. Beskese, H. H. Demir, H. K. Ozcan, and H. E. Okten, "Landfill site selection using fuzzy AHP and fuzzy TOPSIS: a case study for Istanbul," *Environmental Earth Sciences,* vol. 73, no. 7, pp. 3513-3521, 2015.

[18] Y. Liu, R. Li, and X. Song, "Grey associative analysis of regional urbanization and eco-environment coupling in China," *Acta Geographica Sinica,* vol. 2, pp. 237-247, 2005.

[19] S. Wang, H. Ma, and Y. Zhao, "Exploring the relationship between urbanization and the eco-environment—A case study of Beijing–Tianjin–Hebei region," *Ecological Indicators,* vol. 45, pp. 171-183, 2014.

[20] G. Yan-bing, "Comprehensive assessment on ecological risk of Hexi Corridor urbanization based on normal cloud model and entropy weight," *Journal of Arid Land Resources and Environment,* vol. 26, no. 5, pp. 169-173, 2012.

[21] Y. Li, Y. Li, Y. Zhou, Y. Shi, and X. Zhu, "Investigation of a coupling model of coordination between urbanization and the environment," *Journal of environmental management,* vol. 98, pp. 127-133, 2012.

[22] C. Fang, H. Liu, and G. Li, "International progress and evaluation on interactive coupling effects between urbanization and the eco-environment," *Journal of Geographical Sciences,* vol. 26, no. 8, pp. 1081-1116, 2016.

[23] W. Gao, X. Wang, L. Haifeng, P. Zhao, J. Ren, and O. Toshio, "Living environment and energy consumption in cities of Yangtze Delta Area," *Energy and buildings,* vol. 36, no. 12, pp. 1241-1246, 2004.

[24] W. Zheng and Q. Tian, "The Application of Entropy Method and AHP in Weight Determining [J]," *Computer Programming Skills & Maintenance,* vol. 22, pp. p19-20, 2009.

Chapter 6. Correlation analysis of population change and urban vitality in Kitakyushu

6.1 Introduction

At present, Japan is considered as the country faces with the most serious urban shrinkage and it associated issues. More than 85% municipalities experienced population loss during 2005 to 2015 and were considered as shrinking cities. Therefore, a number of studies have contributed to explore the correlates and driving factors of urban shrinkage in Japan and concluded that the primary driving factor of urban shrinkage in Japan was relate to the demographic characteristics [3]. Different from shrinking cities in Europe or America, where the primary factor was considered to be the background of globalization and de-industrialization [13, 14]; and China or other fast-developing countries, where the primary factor was considered to be the urbanization led to population loss in less developed cities [15]. As we explored the spatial-temporal determinants of city shrinkage in Japan in Chapter four, Japan has an irrational demographic structure. As of 2018, the population of Japan is about 1.26 billion, while the aging population (age over 65) ratio reaches 28.1% and it keeps growing. In addition, the low birth rate keeps the population in a decline trend.

Among all the municipalities in Japan, Kitakyushu is the city kept shrinking for over 40 years, and it was the biggest shrinking cities in Japan. In 1963, Kitakyushu city was merged from five cities including Kokura city, Moji city, Yahata city, Tobata city, and Wakamatsu city. After the World War 2, the population of Kitakyushu increased rapidly and exceeded 1 million. And in the decade since the merger (1960s-1970s), the population growth has slowed. Since 1980, Kitakyushu's population began to decline, and in 2005, it dropped below 1 million for the first time.

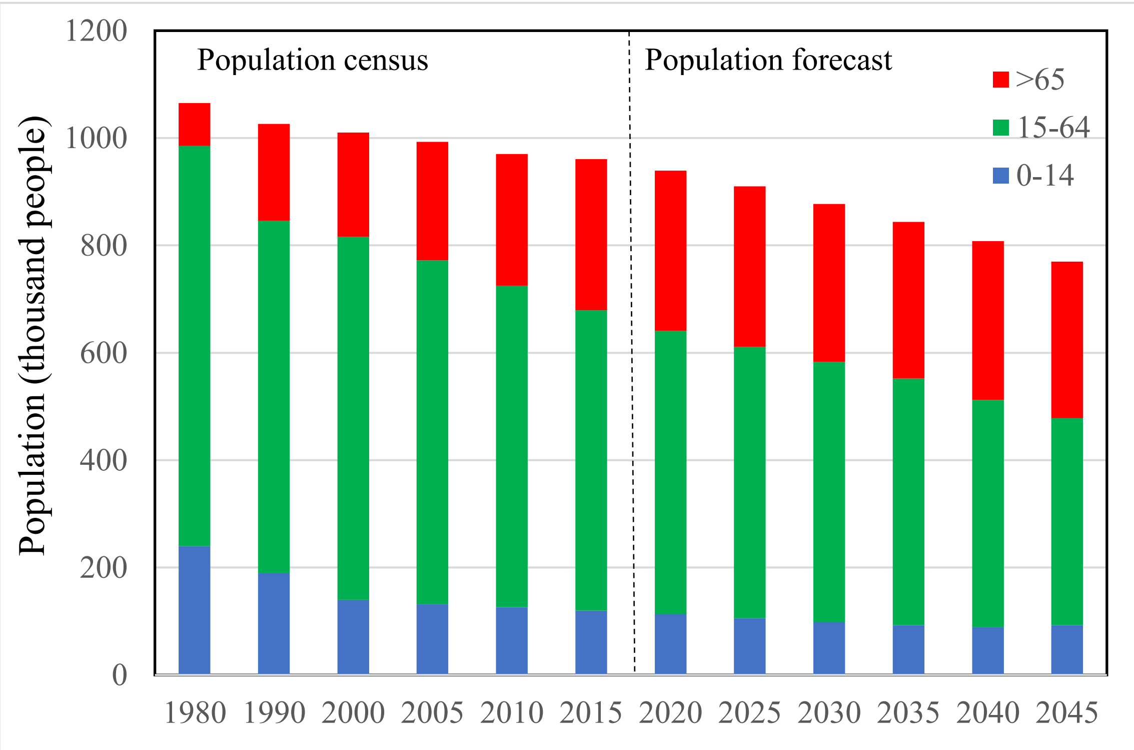

Fig. 6-1. Population forecast of Kitakyushu.

As Fig. 6-1 shows the population variation from 1980 to 2045, along with the population loss in the city, the aging population ratio kept a fast-increasing trend. The ratio was 7.5% in 1980, 29.3% in 2015, and it was forecast to be 37.9% in 2045. As this situation intensifies, social security systems, medical care and other aspects need to be considered. The aging of urban infrastructure and its impact on urban lifeline is likely to have a significant impact on future urban development.

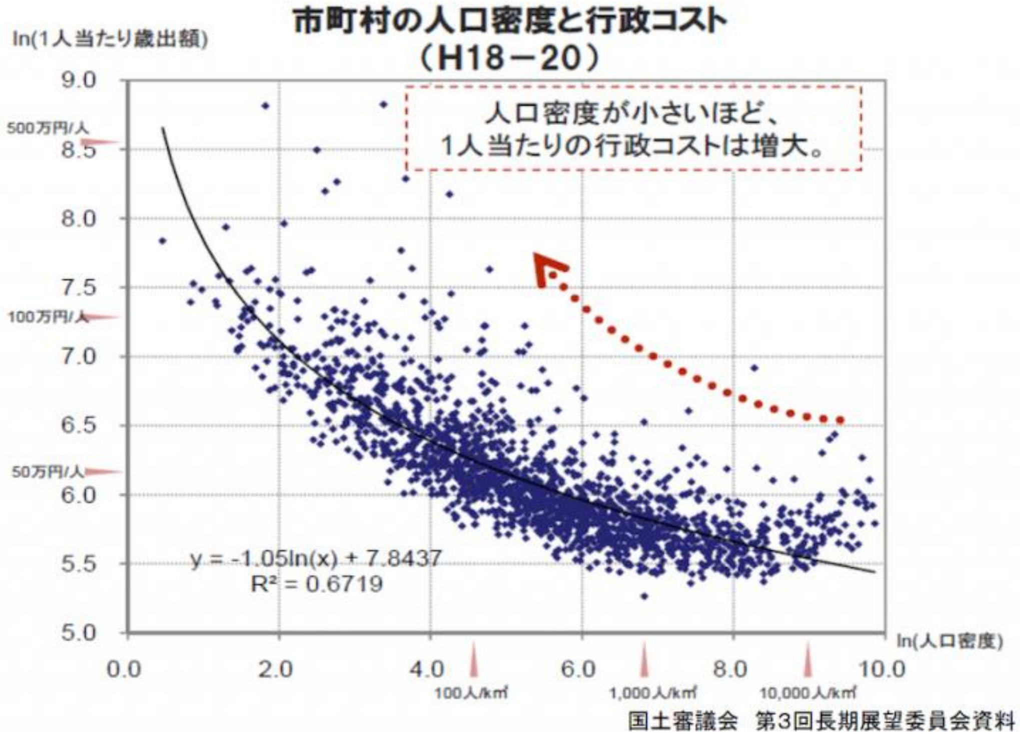

Fig. 6-2 Relation between population density and administrative per capita cost.

(Source: Ministry of Land, Infrastructure, Transport and Tourism)

To address this problem, the Japanese government has proposed such a measure as compact cities. Because of Japan's strict immigration policy and its current demographic characteristics, the phenomenon of shrinking cities in Japan is almost irreversible, so how to make this decline a smart decline is an essential issue. As Fig. 6-2 illustrates the relation between the population density and administrative per capita cost of municipalities in Japan, with the increase in the population density of a municipality, the administrative per capita cost tends to decrease. Which is to say, when a city become more compact, the costs of running a city are more likely to fall, which is more conducive to its sustainable development.

In this chapter, we explored the spatial population change patterns and its impact factors in Kitakyushu. As the first city plan based on the compact city idea was issued in 2003, the study period was selected from 2000 to 2015. The objectives of this study were to (1) investigate the spatiotemporal distributions and patterns of population change in Kitakyushu; (2) reveal the interrelationship between urban shrinkage and aggregation and demographic, economy, and social indexes on global and local scales; and (3) compare the determinants across different regions. The findings illustrate the local determinants of urban shrinkage in Kitakyushu, improve the understanding of the situation and the factors driving city shrinkage, provide valuable information for governments and planners developing effective coping strategies on the global and local levels, and hopefully will draw the attention of other cities to this possible future issue.

This chapter is organized as the following. In Chapter 6.2 the methods and the materials are introduced, and general information of Kitakyushu is discussed. The investigation of spatial distribution patterns of shrinking and aggregating patterns is presented in Chapter 6.3. And the spatial determinants of city shrinkage are explored through regression analysis in Chapter 6.4. The Chapter 6.5 is the summary.

6.2 Study area, materials, and methods

6.2.1 Study area and its general information

The study city, Kitakyushu, is located at the northernmost point of Kyushu on the Kanmon Straits, separating the island from Honshu. Kitakyushu is the second-largest city in both Fukuoka Prefecture and the island of Kyushu after the city of Fukuoka. It is one of Japan's 20 designated cities, one of three on Kyushu, and is divided into 7 wards (Fig. 6-3). As of 2018, the city had an estimated population of 945,595 and a total area of 491.95 km^2 [5]. The average population density is 1,922 persons /km^2. It is now the country's 15th most populated city and the biggest shrinking city.

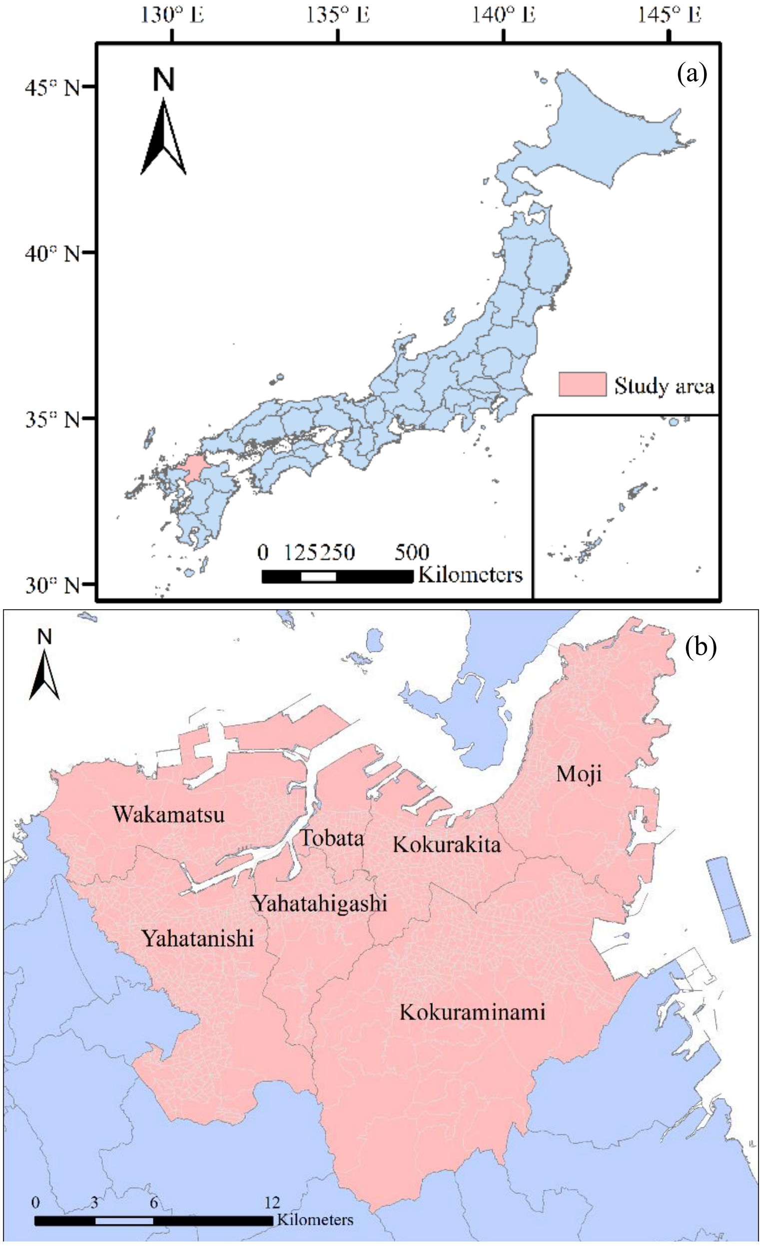

Fig. 6-3 Study area (a) location of Kitakyushu; (b) distribution of streets in Kitakyushu.

In this chapter, to further illustrate how the local government and residences work against depopulation in Kitakyushu, the study unit is street. Fig. 6-3(b) shows the distribution of streets in Kitakyushu in 2000. The data was downloaded from the Portal Site of official Statistics of Japan (https://www.e-stat.go.jp/). The total streets of Kitakyushu in 2000 is 1521.

6.2.2 Materials

Different from Chapter 3 and 4, where the dependent variable is the population change ratio, in this chapter, the number of population change (NPC) was selected as the dependent variable. In chapter 3 and 4, as the magnitude of population varies greatly between cities, the population change ratio is more suitable than NPC as dependent variable for it following a normal distribution. However, within a city, the NPC is more normally distributed than the population change ratio. In addition, there are some streets where there have been no residents, streets where there were residents and now there are no residents, and streets where there were no residents and now there are residents. Hence, the NPC was a more suitable choice as dependent variable.

The study period was selected as from 2000 to 2015. The compact city issue and its accompanied policies and strategies in Japan were first raised in 2003 and Kitakyushu is one of the first Japanese cities to push for compact city. We used the data in 2000 to represent the situation of the city before the compact city issue, and the data in 2015 is the closest to the current situation. To explore the inner correlates of NPC, we selected in total 29 variables from demographic system and urban vitality system. Moreover, the variables were divided into 2 kinds of situation including before "compact city" and variation since "compact city". The demographic factors were collected from the population census data in 2000 and 2015 from the Portal Site of official Statistics of Japan (https://www.e-stat.go.jp/). The elevation data of Kitakyushu was collected from the Advanced Spaceborne Thermal Emission and Reflection Radiometer (ASTER) Global Digital Elevation Model Version 3 (GDEM 003), it was downloaded through the USGS EARTHEXPLORER website (https://earthexplorer.usgs.gov/). The average elevation and average slope of each street were calculated using ArcGIS 10.8. The other urban vitality factors were based on the building data in Kitakyushu and calculated using ArcGIS 10.8.

Table 6-1. Description of explanatory variables for urban shrinkage in Kitakyushu.

System	Situation	Variable	Abbreviation
Demographic factors	Before "compact city"	Total population	TP
		Aging population ratio	APR
		Underage population ratio	UPR
		Total households	TH
		House ownership ratio	HOR
		Total employed staff and workers	TE
		Proportion of employees in secondary and tertiary industries	PESTI
	Variation since "compact city"	Change ratio of total population	CRTP
		Change ratio of aging population	CRAP
		Change ratio of underage population	CRUP
		Change ratio of total households	CRTH
		Change ratio of total employed staff and workers	CRTE
		Change ratio of proportion of employees in secondary and tertiary industries	CRPESTI
Urban vitality factors	Before "compact city"	Average building age	ABA
		Building coverage ratio	BCR
		Average floor area ratio	AFAR
		Total floor area of commercial buildings	TFACB
		Total floor area of residential buildings	TFARB
		Total floor area of educational welfare facility buildings	TFAEB
		Total floor area of office buildings	TFAOB
		Average elevation	AE
		Average slope	AS
	Variation since "compact city"	Change ratio of building coverage ratio	CRBCR
		Change ratio of floor area ratio	CRFAR
		Increase floor area of commercial buildings	IFACB
		Increase floor area of residential buildings	IFARB
		Increase floor area of educational welfare facility buildings	IFAEB
		Increase floor area of office buildings	IFAOB

6.2.3 Methods and research flow

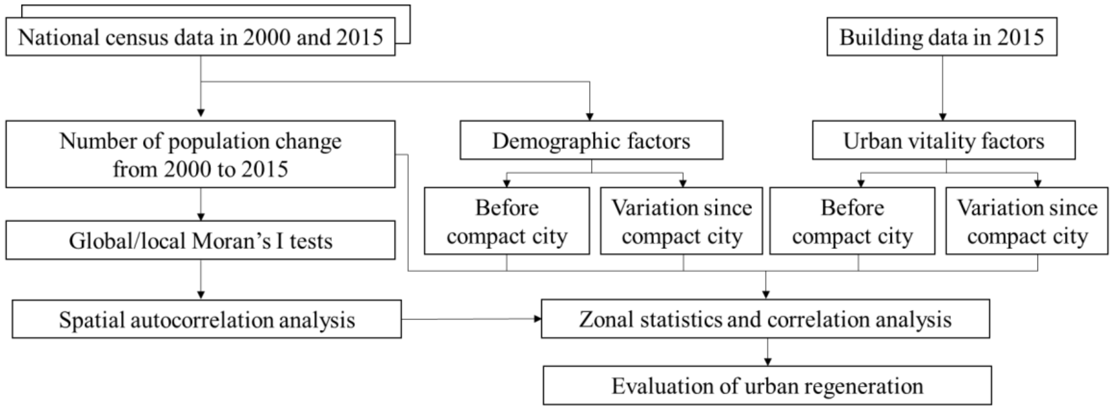

Fig. 6-4 Research flow of evaluating urban regeneration against depopulation in Kitakyushu.

In this chapter, the methods have mentioned were designed to model the correlation between number of populations change and its potential related demographic and urban vitality factors. We first applied both global and local Moran's tests to reveal whether the spatial dependency of depopulation in Kitakyushu. Because the global Moran's test result showed the overall spatial autocorrelation was not strong that the GWR and SGWR regression analysis may not suitable for this case. However, the local Moran's test showed that there were several streets clusters in Kitakyushu. So, we extracted those clusters and applied zonal statistics and correlation analysis to evaluate the urban regeneration in those regions.

The Moran's tests were applied to find whether the distribution of shrinking streets is concentrated in space. Spatial autocorrelation analysis, including Global Moran's I statistics and Local Moran's I statistics were performed to reveal the spatial dependence of population change. Global Moran's I, which is a rational number ranged from -1 to 1 after normalized variance was selected for spatial autocorrelation analysis for its widely used in revealing the global spatial autocorrelation. Global Moran's I >0 means positive spatial correlation, the larger the value, the more obvious the spatial correlation; Global Moran's I <0 means negative spatial correlation, the smaller the value, the greater the spatial difference; otherwise, Global Moran's I = 0, indicates a random space.

However, the Global Moran's I could only reflect on the spatial autocorrelation but do not identify the location and type of spatial clusters. The Local Moran's I can be applied to identify the local differences and similarities among neighboring streets. The Local Indicators of Spatial Association (LISA) can be determined using Local Moran's I. Generally, four clustering/outlier types are classified using the Local Moran's I including (1) high-high cluster (HH); (2) high-low outlier (HL); (3) low-high outlier (LH); (4) low-low outlier (LL). HH and LL reflect the positive spatial correlation; HL and LH reflect the negative spatial correlation. Therefore, both the Global and Local Moran's I statistics for analyzing the correlation of population variation between each street. In this chapter, as the size and scale of the streets were quite different and the streets were not normally distributed, we selected the adaptive bi-square as the kernel type, and the k was selected as 30. In this chapter, HH refers to an above-average number of populations increase in a local street, with the same characteristic exists in its neighboring streets. HL refers to an above-average number of populations increase in a local street, whilst the population decreased in the neighboring streets. LH refers to the shrinkage in a local street, whilst an above-average number of populations increases in the neighboring streets. LL refers to the shrinkage in a local street, and its neighboring streets have the same characteristics. Thus, we used ArcGIS 10.8 to statistic the Global/Local Moran's I, which shows the spatial relationship between the population change in a street and its neighbors for Kitakyushu.

Then the Pearson Correlation analysis was conducted to reveal the correlation between NPC and each explanatory variable. In statistics, the Pearson correlation coefficient is a statistic that measures linear correlation between two variables X and Y. It has a value between 1 and −1, where 1 is total positive linear correlation, 0 is no linear correlation, and −1 is total negative linear correlation. And it can be calculated through Eq. 6-1.

$$\rho_{X,Y} = \frac{cov(X,Y)}{\sigma_X \sigma_Y} \qquad (\text{Eq.} 6-1)$$

where cov is the covariance, X is NPC, Y is the explanatory variable in Table 6-1, σ is the standard deviation.

6.3 Spatial autocorrelation analysis of population change in Kitakyushu

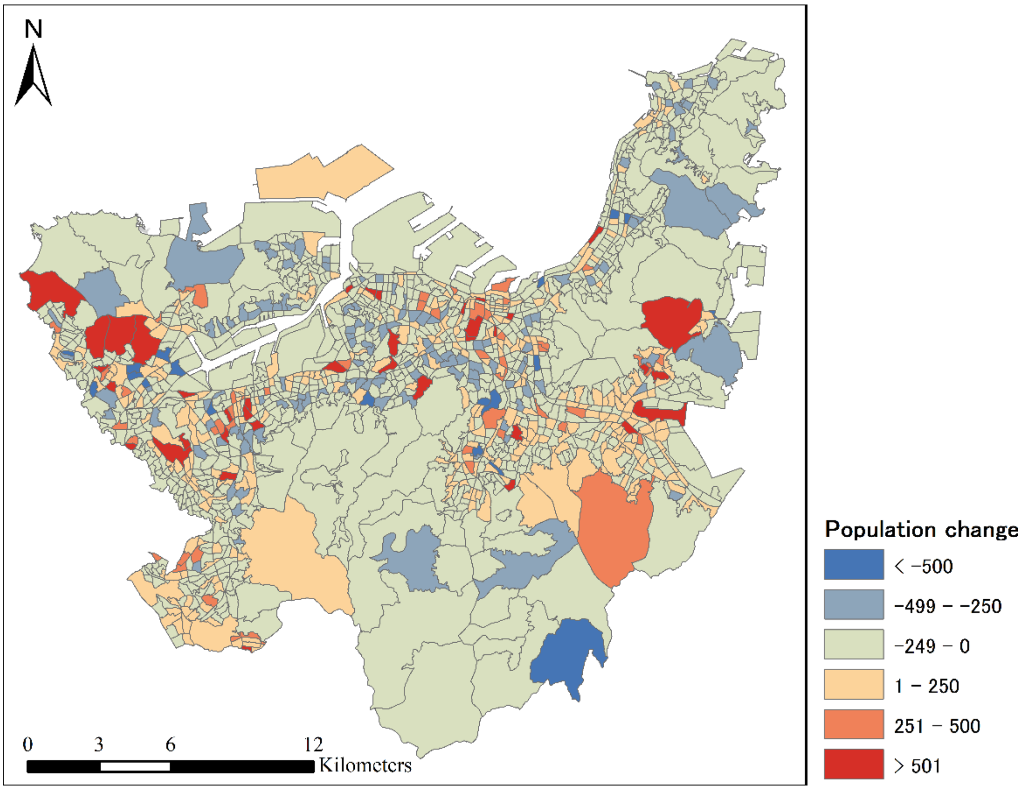

Fig. 6-5 Spatial distribution of number of populations change in each street from 2000 to 2015 in Kitakyushu.

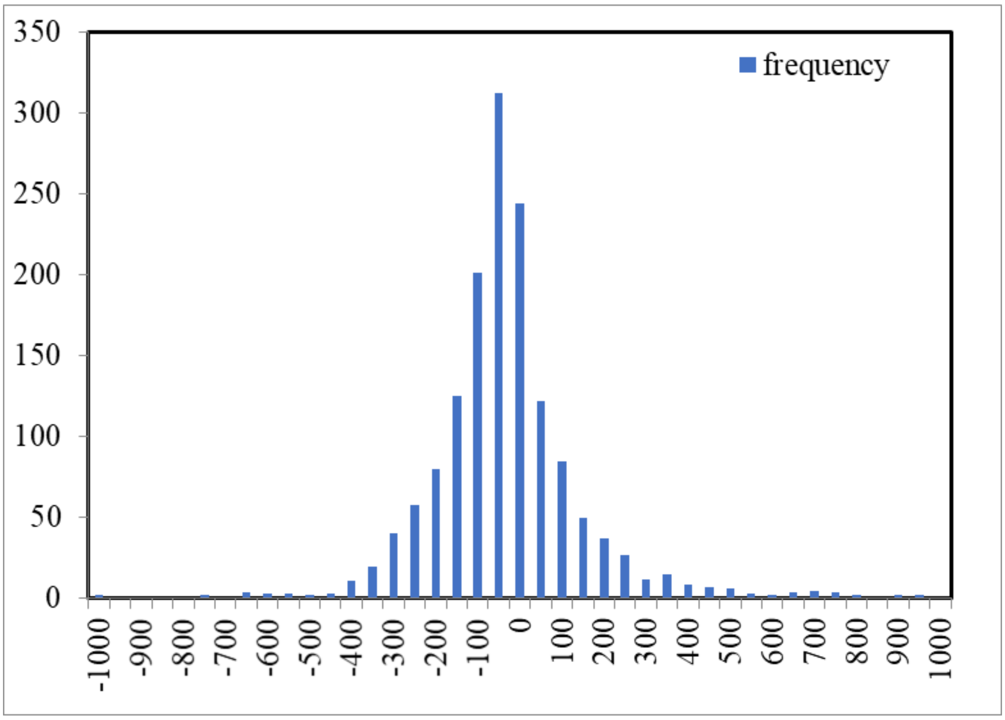

Fig. 6-6 Frequency distribution histogram of NPC from 2000 to 2015 in Kitakyushu.

As the city plan and evolution from 2000 to 2015, the number of streets increased from 1521 to 1590 from 2000 to 2015. We used the street data in 2000 as a baseline and calibrated the street data in 2015. Fig. 6-5 shows the spatial distribution of number of populations change in each street from 2000 to 2015 in Kitakyushu. From 2000 to 2015, the total population declined by about 49,000, and the average NPC for a street is about 32. Fig 6.6. shows the frequency distribution histogram of NPC from 2000 to 2015 in Kitakyushu. Due to there are some null value of the population for several streets, the NPC is more normally distributed than the population change ratio of each street. Thus, NPC was selected as dependent variable.

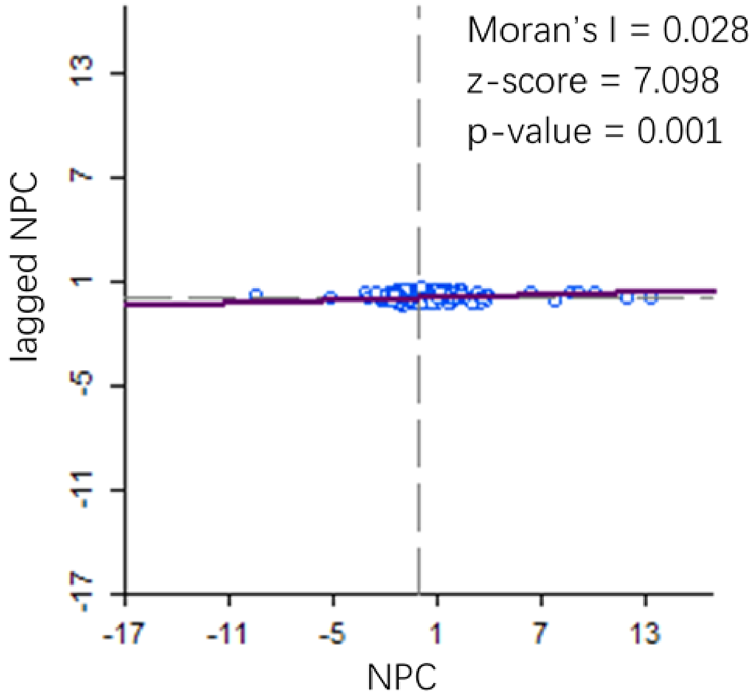

Fig. 6-7 Scatter plot of global Moran's I test for NPC

As Fig. 6-7 shows the result of global Moran's I test, the Moran's I is 0.028 which there is litter spatial correlation between NPC of a street and its location from a global view. The global Moran's I test result is quite different from the results in Chapter 3 and Chapter 4. Meanwhile, spatial regression analysis is not suitable for the case as we cannot validate the spatial dependence of NPC in Kitakyushu from 2000 to 2015.

However, the result of local Moran's I test shows that there are mainly 6 region clusters. Three of the clusters are urban aggregation areas, and other three clusters are urban shrinkage areas (Fig. 6-8). As the LISA map shows that in each aggregation cluster, a lot of streets belongs to LH outliers; whilst in each shrinkage cluster, a lot of streets belongs to HL outliers (Fig. 6-9). This may be the result of population movements with in those regions and statistical changing from zoning adjustments in those streets. We further selected the six clusters for further explore the characteristics of urban regeneration.

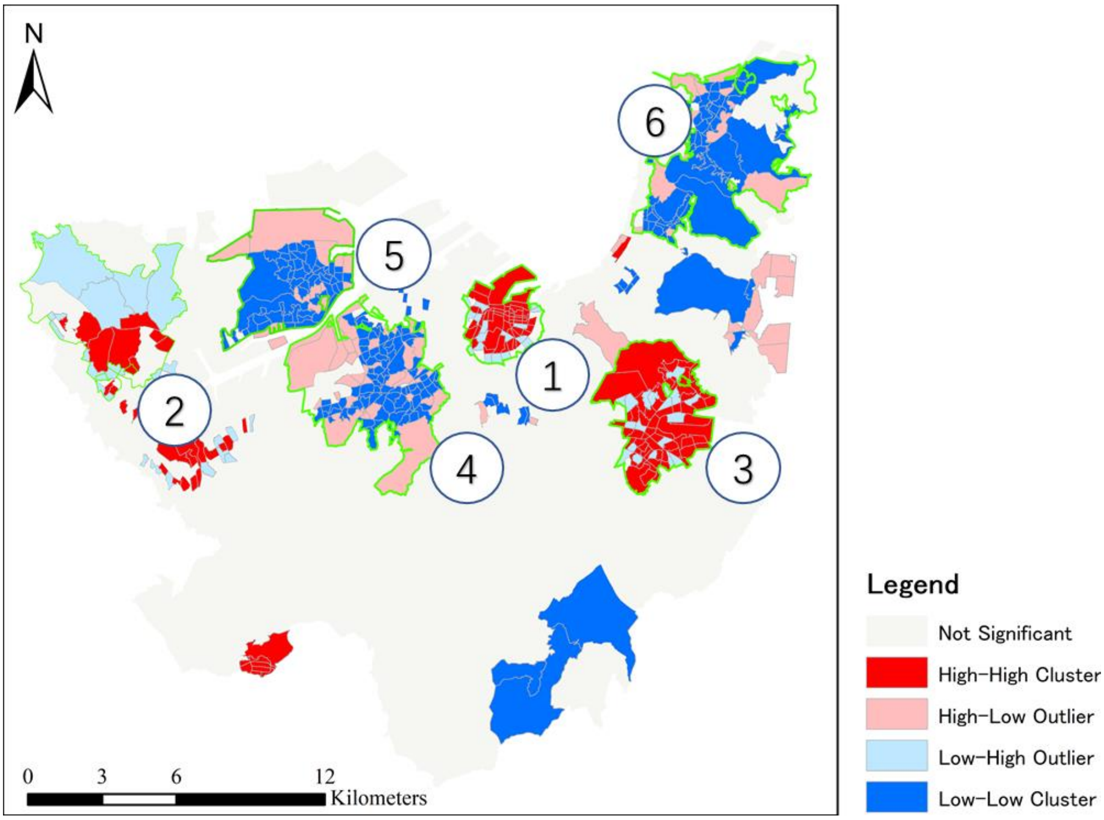

Fig. 6-8 LISA map of NPC from 2000 to 2015 in Kitakyushu.

6.4 Zonal statistics and correlation analysis of urban regeneration in Kitakyushu

6.4.1 Zonal statistics of the study areas

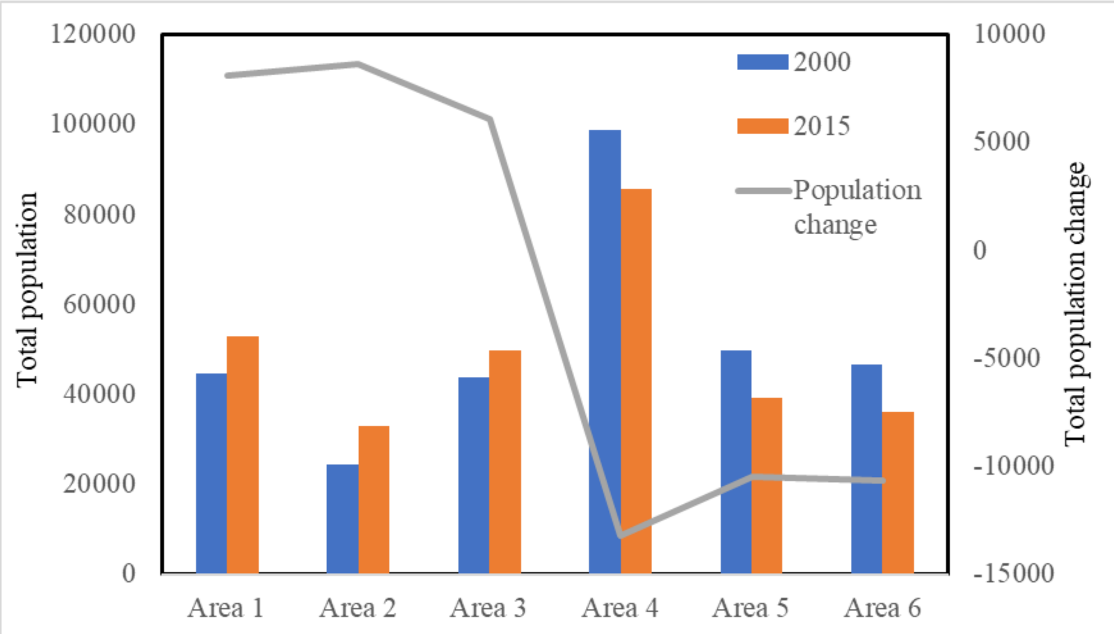

Fig. 6-9 Population and population change of the study areas.

As Fig. 6-9 shows the general population information of the six study areas, the population change from 2000 to 2015 were the most obvious in the six areas and thus the areas were further selected for analysis. The zonal statistics were conducted with four categories, namely 1) demographic factors – before “compact city”, 2) demographic factors – variation since “compact city”, 3) urban vitality factors – before “compact city”, and 4) urban vitality factors – variation since “compact city”.

1) Demographic factors – before “compact city”

As Fig. 6-10 illustrated, the characteristics of the six areas related to demographic factors – before “compact city” are as follows:

Firstly, the aggregation areas have less population, households, and employees, while the shrinkage areas have more population, households, and employees.

Secondly, the HH clusters in Area 2 and Area 3 have more underage population than the other areas in Kitakyushu, while in area 1, the underage population ratio is below than 6%.

Thirdly, in 2000, according to the population census, the aging population ratio is about 19% in Kitakyushu, whilst among all the shrinkage streets, aging population accounts for a large proportion, especially in the shrinkage clusters, the aging population ratio reach over 25%.

Fourthly, due to area 1 and 4 is and nearby the downtown areas of the city, the house ownership ratio is relatively low compared the city average value and the other areas.

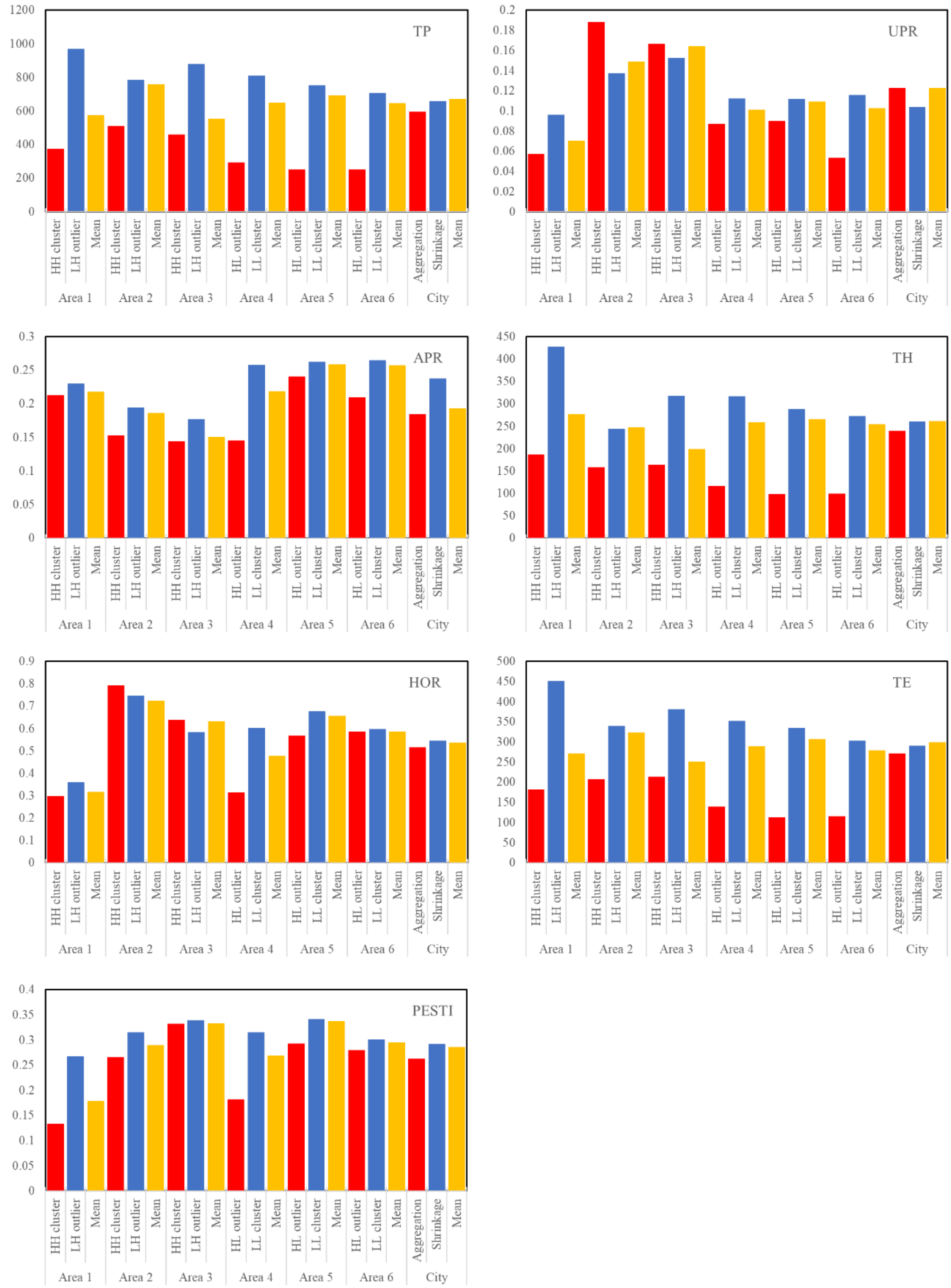

Fig. 6-10 Zonal statistics of demographic factors – before "compact city".

2) Demographic factors – variation since "compact city"

As Fig. 6-11 illustrated, the characteristics of the six areas related to demographic factors – variation since "compact city" are as follows:

Firstly, except the aggregation areas (HL outliers) in area 6, the population increased several times in the aggregation areas.

Secondly, there is a significant increase of underage population in area 1 and 4, while there is a significant increase of aging population in area 3.

Thirdly, the increase of aging population can be significantly observed in area 3.

Fourthly, the increase of employees can be significantly observed in area 2 and 3.

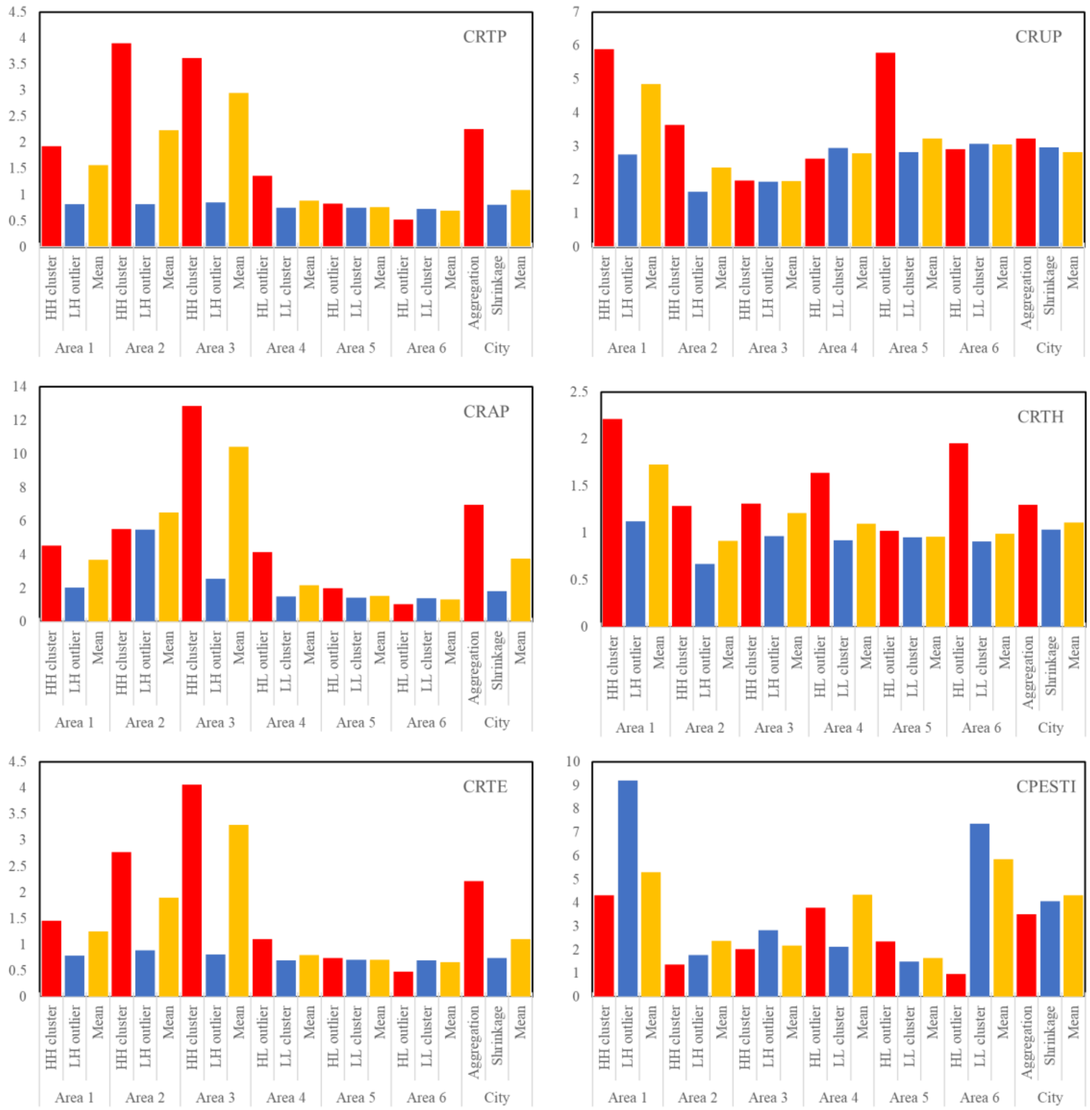

Fig. 6-11 Zonal statistics of demographic factors – variation since “compact city”.

1) Urban vitality factors – before "compact city"

As Fig. 6-12 illustrated, the characteristics of the six areas related to urban vitality factors – before "compact city" are as follows:

Firstly, the difference between the shrinkage of the streets or the aggregation of the streets of the building construction years is not obvious.

Secondly, the building coverage and floor area ratio of the aggregation area are larger than those of the shrinking area.

Thirdly, as the central area of the city, area 1 has larger commercial floor area, educational welfare floor area, and office educational floor area than other areas. Whilst the difference between the residential floor area was not obvious.

Fourthly, the average elevation and slope of area 4 and 6 are relatively big, indicating that the terrain conditions of the area may be a factor that affects the area shrinking.

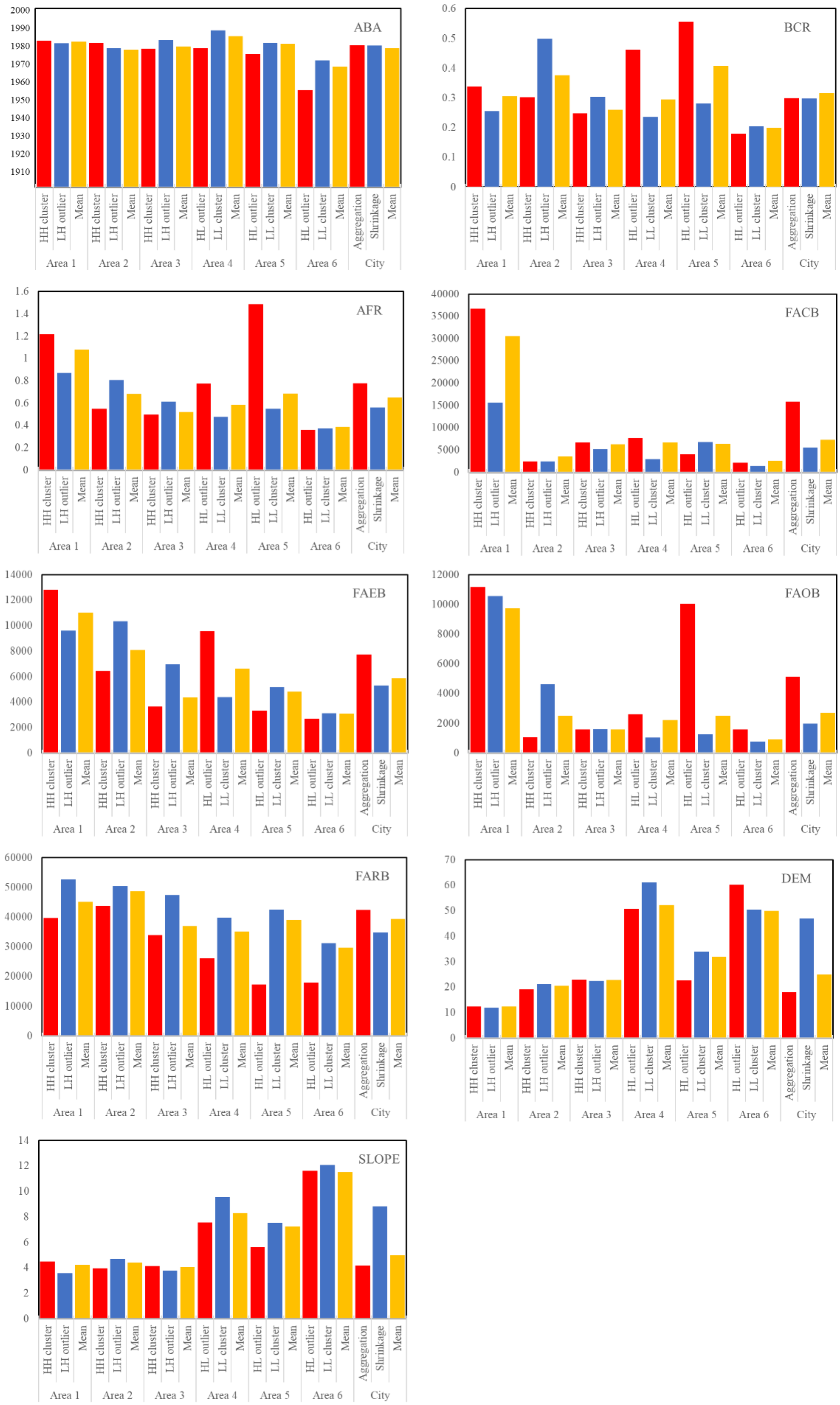

Fig. 6-12 Zonal statistics of urban vitality factors – before “compact city”.

2) Urban vitality factors – variation since "compact city"

As Fig. 6-13 illustrated, the characteristics of the six areas related to urban vitality factors – variation since "compact city" are as follows:

Firstly, the increase of building coverage and floor area ratio of the aggregation area are larger than those of the shrinking area.

Secondly, the increase of commercial buildings is more obvious in aggregation streets in area 1 and 4.

Thirdly, the increase of educational welfare facilities buildings is more obvious in aggregation streets in area 1, 2 and 4.

Fourthly, the increase of office buildings is more obvious in aggregation streets in area 1, 4 and 5.

Fifthly, the increase of residential buildings is more obvious in aggregation streets in area 1, 2, 3 and 4.

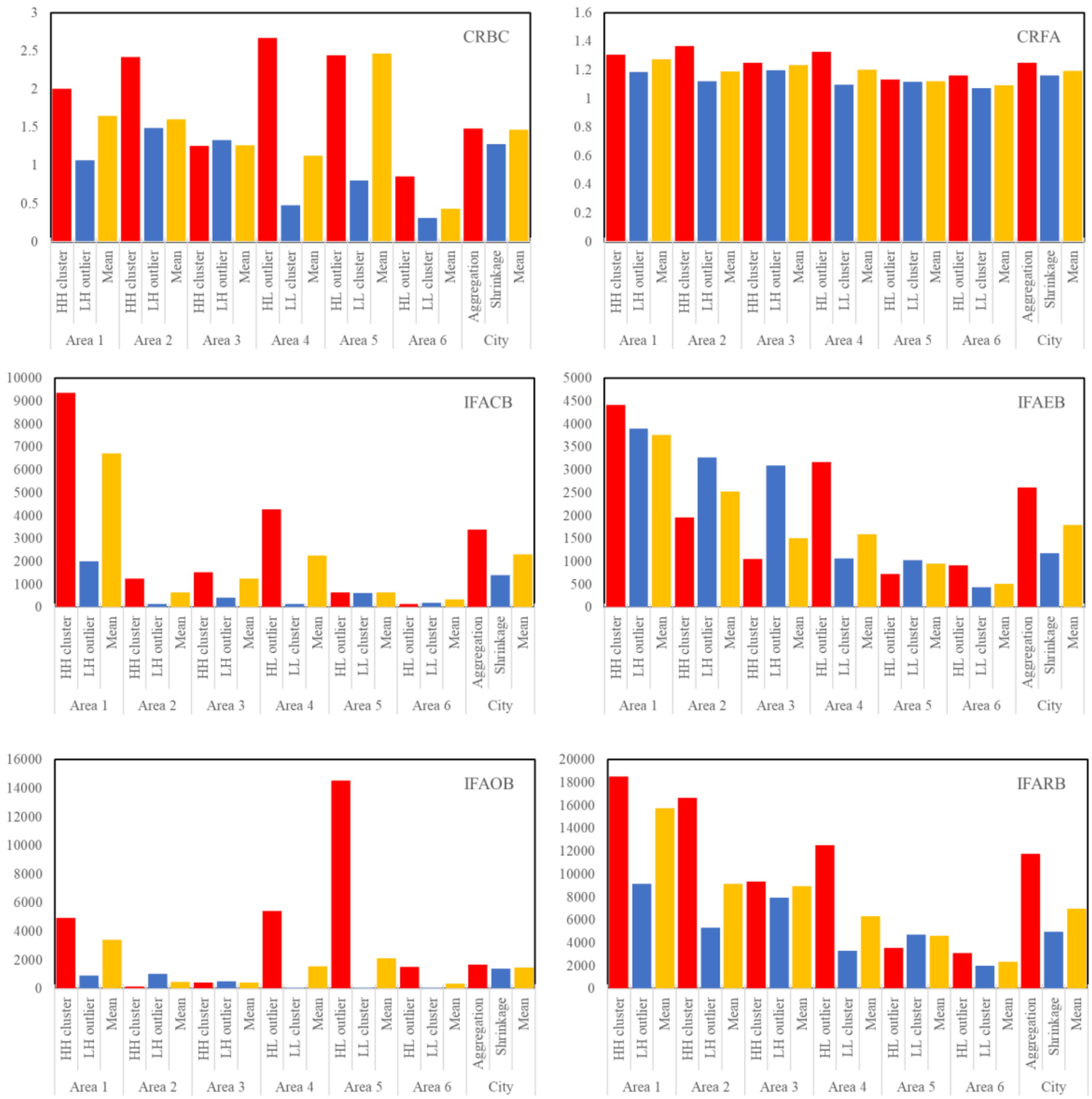

Fig. 6-13 Zonal statistics of urban vitality factors – variation since “compact city”.

6.4.2 Pearson correlation analysis between population change and demographic-urban vitality factors

Table 6-2 shows the Pearson correlation analysis result between the NPC and the demographic factors – before "compact city". Firstly, NPC is significantly related to TP, TH, and TE in all the study areas. However, the significant positive correlation is only found in area 1 that R^2 are 0.704, 0.646, and 0.690 respectively. In the other areas, the negative correlation indicates that the street with more population, households, or employees are tend to loss population during 2000 to 2015. Secondly, NPC is significant relate to UPR in area 3 and 6. However, the correlation is positive in area 3 while negative in area 6. Thirdly, significant negative correlation between NPC and APR was only showed in area 4 which indicates the streets with higher aging population ratio tends to loss more population from 2000 to 2015. Fourthly, positive correlation between NPC and HOR were found in area 4 and 6, which means the streets with higher house ownership ratio have lost fewer population from 2000 to 2015. Fifthly, PESTI have shown significant correlation with NPC in area 4, 5 and the city. However, the correlation coefficient is not high compared with other demographic factors.

Table 6-2. Coefficient of determinant R^2 between NPC and demographic factors – before "compact city".

Area	TP	UPR	AP	TH	HOR	TE	PESTI
Area 1	.704**	0.22	0.02	.646**	-0.2	.690**	0.038
Area 2	-.367*	-0.192	0.281	-.342**	0.202	-.362*	0.25
Area 3	-.314**	.316**	-0.137	-.296**	0.145	-.310**	0.051
Area 4	-.470**	-0.015	-.300**	-.444**	-.265**	-.443**	-.265**
Area 5	-.665**	-0.165	-0.054	-.693**	0.075	-.650**	-.241*
Area 6	-.721**	-.281*	-0.029	-.706**	.273*	-.704**	-0.134
City	-.308**	-0.006	-0.045	-.278**	0.011	-.290**	-.086**

Note: * refers a 0.05 significance level; ** refers a 0.01 significance level.

Table 6-3 shows the Pearson correlation analysis result between the NPC and the demographic factors – variation since "compact city". Firstly, all the demographic factors – variation since "compact city" are significantly correlated to NPC in the city from a global view. However, there are significant differences in the correlation variables and their correlation coefficients in different regions, indicating that the factors affecting regional contraction and expansion are quite different. Secondly, in area 1, there is no significant correlation between the variables and NPC, which indicate the population increase in the area is more effect by the original demographic characteristics than the application of

Table 6-3. Coefficient of determinant R^2 between NPC and demographic factors – variation since "compact city".

Area	CTP	CUP	CAP	CTH	CTE	CPESTI
Area 1	0.161	0.1	0.17	-0.269	0.275	-0.021
Area 2	.254*	.270*	.247*	-0.191	.253*	0.065
Area 3	.816**	.359**	.866**	0.121	.814**	-0.034
Area 4	.572**	0.067	.433**	-.316**	.466**	0.046
Area 5	.254*	.270*	.247*	-0.191	.253*	0.065
Area 6	0.019	0.023	-0.026	-.372**	0.046	-0.199
City	.379**	.175**	.263**	-.081**	.409**	-.064*

Note: * refers a 0.05 significance level; ** refers a 0.01 significance level.

demographic related compact city policies. Thirdly, the characteristics of area 2 and 3 are similar, that the NPC is significantly positive relate to CTP, CUP, CAP, and CTE. Fourthly, in area 4, NPC is correlated to CTP, CAP, CTH, and CTE. Fifthly, in area 5, NPC is correlated to CTP, CUP, CAP, CTE. Sixthly, NPC is only correlated to CTH in area 6.

Table 6-4 shows the Pearson correlation analysis result between the NPC and the urban vitality factors – before "compact city". Firstly, except BCR and AFARB, the other urban vitality factors – before "compact city" are significantly correlated to NPC in the city from a global view. However, there were significant differences between the study areas. Secondly, in area 1, NPC is significantly correlated to AFAR, AFAEB, and AFARB. Thirdly, in area 2, there is no significant correlation between the variables and NPC, which indicate the population increase in the area is not affected by the original effect by the original urban vitality characteristics. Fourthly, similar with area 2, except ABA which showed significant negative correlation with NPC, the other variables showed non-significant relation with NPC. Fifthly, area 4 is only area which shows significant negative correlation between AS and NPC. The elevation and slope vary greatly in the area. And many houses are built on steep slopes. Populations in these areas are more likely to decline as residents age and demand for transportation increases. Fifthly, different positive correlation between AFARB and NPC in area 1, negative correlation is found in area 5 and 6. As area 1 is urban aggregation area, and area 5 and 6 are urban shrinkage areas, with the advance of the compact city policy, population aggregation and loss also mainly occur in areas with dense residential buildings. Sixthly, NPC is significant correlated to ABA, AFAOB, AFARB in area 5. Seventhly, NPC is significant correlated to ABA, BCR, AFAR,

Table 6-4. Coefficient of determinant R^2 between NPC and urban vitality factors – before “compact city”.

Area	ABA	BCR	AFAR	AFACB	AFAEB	AFAOB	AFARB	AE	AS
Area 1	0.013	0.098	.620**	0.058	.463**	0.203	.902**	0.131	0.059
Area 2	-0.309	-0.195	-0.246	-0.176	0.113	-0.146	-0.246	-0.101	0.115
Area 3	.359**	-0.151	-0.018	0.213	-0.192	0.017	-0.152	-0.019	0.062
Area 4	0.147	0.034	0.137	.187*	0.138	0.095	0.021	-0.123	-.190*
Area 5	.320**	0.142	0.118	-0.026	-0.016	.327**	-.592**	0.03	-0.046
Area 6	0.177*	-.254*	-.347**	-.278*	0.043	0.098	-.481**	0.164	0.127
City	.109**	-0.003	.058*	.085**	.069**	.077**	0.024	-.077**	-.089**

Note: * refers a 0.05 significance level; ** refers a 0.01 significance level.

AFACB, AFARB in area 6.

Table 6-5 shows the Pearson correlation analysis result between the NPC and the urban vitality factors – variation since “compact city”. Firstly, except IFAOB, the other urban vitality factors – variation since “compact city” are significantly correlated to NPC in the city from a global view. However, there were significant differences between the study areas. Secondly, in area 1, NPC is significantly correlated to CAFAR, and IFARB. Thirdly, in area 2, NPC is significantly correlated to CRBC, CRAFR, IFAEB and IFARB, which indicate the population increase in the area is affected by the urban vitality characteristics. Fourthly, similar with area 2, the population increase in area 3 is correlated to the urban vitality characteristics especially the increase of commercial areas. Fifthly, in area 4, the population change has a certain trend from existing residential areas to new residential areas and commercial areas. Sixthly, NPC is not significantly correlated to the urban vitality variation from 2000 to 2015, which indicate the responses to the urban shrinkage are not effective in the regions. And the population of area 5 and 6 are more likely to move out of the areas and keep decline.

Table 6-5. Coefficient of determinant R^2 between NPC and urban vitality factors – variation since "compact city".

Area	CRBC	CRAFR	IFACB	IFAEB	IFAOB	IFARB
Area 1	0.159	.685**	0.045	0.141	-0.036	.965**
Area 2	.450**	.440*	0.19	.241*	-0.149	.517**
Area 3	0.016	0.136	.228*	-0.154	-0.084	0.162
Area 4	.334**	.625**	.254**	0.148	0.058	.784**
Area 5	0.212	0.227	-0.028	-0.014	0.025	-0.029
Area 6	0.101	0.151	-0.12	0.162	0.124	0.054
City	.085**	.222**	.098**	.100**	0.014	.520**

Note: * refers a 0.05 significance level; ** refers a 0.01 significance level.

6.4.3 Analysis of the characteristics of the study areas

Table 6-6. Population change characteristics of the study areas.

<table>
<tr><td>Area</td><td>Overall generality</td><td>Regional characteristics</td></tr>
<tr><td>Area 1
(urban aggregation)</td><td rowspan="6">• Relate to the existing demographic and urban vitality properties of the street
• Negative correlation with most demographic factors
• Positive correlation with most urban vitality factors</td><td>Positively correlated to previous population
Non-significant correlation with demographic change
Positively correlated to the floor area residential building</td></tr>
<tr><td>Area 2
(urban aggregation)</td><td>Positively correlated to the demographic change
Non-significant correlation with previous urban vitality properties
Positively correlated to the urban vitality change</td></tr>
<tr><td>Area 3
(urban aggregation)</td><td>Positively correlated to underage population and the demographic change
Positively correlated to building construction year
Positively correlated to increase of commercial buildings</td></tr>
<tr><td>Area 4
(urban shrinkage)</td><td>Negatively correlated to aging population and house ownership ratio
Positively correlated to the increase of aging population
Significantly correlated to the slope
Positively correlated to increase of commercial and residential building</td></tr>
<tr><td>Area 5
(urban shrinkage)</td><td>Nonsignificant correlation with previous age structure properties while significantly correlated to the variation of age structure
Positively correlated to building construction year
Positively correlated to floor area of office building
Nonsignificant correlation with the variation of urban vitality factors</td></tr>
<tr><td>Area 6
(urban shrinkage)</td><td>Negatively correlated to aging population
Non-significant correlation with most demographic changes
Significantly correlated to building construction year, area of commercial and residential building
Nonsignificant correlation with urban vitality variation</td></tr>
</table>

As Table 6-6 summaries the population change characteristics of the study areas, several overall generalities have been found showing as follows: 1) Relation with the existing demographic and urban vitality properties of the street; 2) Negative correlation with most demographic factors; 3) Positive correlation with most urban vitality factors.

Moreover, there were also quite differences of the regional differences. Among urban aggregation areas, area 1, located in the center of the city, the location advantage is obvious, attracting the population aggregation. The regional characteristics are (1) positively correlated to previous population, (2) non-significant correlation with demographic change, (3) positively correlated to the floor area residential building. Besides, in area 2 and 3, population change has little correlation with the pervious demographic and urban vitality properties. Area 2 attracted population aggregation through increase of education welfare facilities, while area 3 attracted population aggregation through increase of commercial buildings. The characteristics of area 2 are (1) positively correlated to the demographic change, (2) non-significant correlation with previous urban vitality properties, and (3) positively correlated to the urban vitality change. The characteristics of area 3 are (1) positively correlated to underage population and the demographic change, (2) positively correlated to building construction year, and (3) positively correlated to increase of commercial buildings.

Among urban shrinkage areas, area 4, located in the sub-center of the city, the characteristics are (1) negatively correlated to aging population and house ownership ratio, (2) positively correlated to the increase of aging population, (3) significantly correlated to the slope, and (4) positively correlated to increase of commercial and residential building. The movement of population has a certain trend: 1) from existing residential areas to new residential areas; 2) from high slope to low slope; 3) The aging population dominated the population movement.

The characteristics of area 5 are (1) nonsignificant correlation with previous age structure properties while significantly correlated to the variation of age structure, (2) positively correlated to building construction year, (3) positively correlated to floor area of office building, and (4) nonsignificant correlation with the variation of urban vitality factors. The characteristics of area 6 are (1) negatively correlated to aging population, (2) non-significant correlation with most demographic changes, (3) significantly correlated to building construction year, area of commercial and residential building, and (4) nonsignificant correlation with urban vitality variation. In area 5 and 6, population change has little correlation with the demographic and urban vitality variation that population decline is more disorderly and comprehensive. This situation also means the responses to the urban shrinkage are not effective against depopulation in the region. The population of area 5 and 6 are more likely to move out of the areas and keep decline.

6.5 Summary

In this chapter, we first applied global and local Moran's tests to investigate the population change since the city plan with the concept of compact city come out. The results showed the type of population change in a street is not related to its location. That is to say, the change is not spatially dependent. However, according to the results of local Moran's I statistics, there are six main regions with their own characteristics of population shrinkage and expansion.

The government wish the compact city model to creates benefits that are attractive to modern urbanites. The desired benefits include shorter commute times, reduced environmental impact of the community, and reduced consumption of fossil fuels and energy.

Our findings are as follows: (1) The shrinkage and expansion of the six main regions in Kitakyushu have some similarities, but the differences are larger. (2) Among urban aggregation areas, area 1, located in the center of the city, the location advantage is obvious, attracting the population aggregation. in area 2 and 3, population change has little correlation with the pervious demographic and urban vitality properties. Area 2 attracted population aggregation through increase of education welfare facilities, while area 3 attracted population aggregation through increase of commercial buildings. (3) Among urban shrinkage areas, area 4, located in the sub-center of the city, the movement of population has a certain trend: from existing residential areas to new residential areas; from high slope to low slope; The aging population dominated the population movement. In area 5 and 6, population change has little correlation with the demographic and urban vitality variation that population decline is more disorderly and comprehensive. This situation also means the responses to the urban shrinkage are not effective against depopulation in the region. The population of area 5 and 6 are more likely to move out of the areas and keep decline.

Reference

[1] Nations U. 2018 revision of world urbanization prospects. United Nations Department of Economic and Social Affairs; 2018.

[2] Haase A, Rink D, Grossmann K, Bernt M, Mykhnenko V. Conceptualizing urban shrinkage. Environment and Planning A. 2014;46:1519-34.

[3] Mallach A, Haase A, Hattori KJC. The shrinking city in comparative perspective: Contrasting dynamics and responses to urban shrinkage. 2017;69:102-8.

[4] Hattori K, Seike Y, Yoshida Z, Hamaguchi S, Yamada H, Suzuki N, et al. Shrinkage of tokamak current channel by external ergodization. 1984;121:368-73.

[5] Population News of Major Cities. City of Yokohama. Oct 1, 2018.

[6] Hospers G-JJUdi. Coping with shrinkage in Europe's cities and towns. 2013;18:78-89.

[7] Großmann K, Bontje M, Haase A, Mykhnenko VJC. Shrinking cities: Notes for the further research agenda. 2013;35:221-5.

[8] Haase D, Haase A, Kabisch N, Kabisch S, Rink DJEM, Software. Actors and factors in land-use simulation: The challenge of urban shrinkage. 2012;35:92-103.

[9] Haase DJN, Culture. Urban ecology of shrinking cities: an unrecognized opportunity? 2008;3:1-8.

[10] Rieniets TJN, Culture. Shrinking cities: causes and effects of urban population losses in the twentieth century. 2009;4:231-54.

[11] Hospers G-JJEPS. Policy responses to urban shrinkage: From growth thinking to civic engagement. 2014;22:1507-23.

[12] Syssner JJARdEsDyDR. Planning for shrinkage? Policy implications of demographic decline in Swedish municipalities. 2016:7-31.

[13] Sadler RC, Lafreniere DJ. Racist housing practices as a precursor to uneven neighborhood change in a post-industrial city. Housing Studies. 2017;32:186-208.

[14] Wiechmann T, Pallagst KMJIjou, research r. Urban shrinkage in Germany and the USA: A comparison of transformation patterns and local strategies. 2012;36:261-80.

[15] Zhang Y, Fu Y, Kong X, Zhang FJSC, Society. Prefecture-level city shrinkage on the regional dimension in China: spatiotemporal change and internal relations. 2019;47:101490.

[16] Anselin L. The Moran scatterplot as an ESDA tool to assess local instability in spatial association: Regional Research Institute, West Virginia University Morgantown, WV; 1993.

[17] Anselin LJGa. Lagrange multiplier test diagnostics for spatial dependence and spatial heterogeneity. 1988;20:1-17.

[18] Brunsdon C, Fotheringham AS, Charlton MEJGa. Geographically weighted regression: a method for exploring spatial nonstationarity. 1996;28:281-98.

[19] Fotheringham AS, Brunsdon C, Charlton M. Geographically weighted regression: the analysis of spatially varying relationships: John Wiley & Sons; 2003.

[20] Fotheringham AS, Charlton ME, Brunsdon CJE, A p. Geographically weighted regression: a natural evolution of the expansion method for spatial data analysis. 1998;30:1905-27.

[21] Van Donkelaar A, Martin RV, Spurr RJ, Burnett RTJEs, technology. High-resolution satellite-derived PM2.5 from optimal estimation and geographically weighted regression over North America. 2015;49:10482-91.

[22] Mei CL, He SY, Fang KT. A note on the mixed geographically weighted regression model. Journal of Regional Science. 2004;44:143-57.

[23] Jin C, Xu J, Huang ZJHI. Spatiotemporal analysis of regional tourism development: A semiparametric Geographically Weighted Regression model approach. 2019;87:1-10.

[24] Li W, Cao Q, Lang K, Wu JJSotTE. Linking potential heat source and sink to urban heat island: Heterogeneous effects of landscape pattern on land surface temperature. 2017;586:457-65.

[25] Zhao Q, Wentz EA, Fotheringham S, Yabiku ST, Hall SJ, Glick JA, et al. Semi-parametric Geographically Weighted Regression (S-GWR): a Case Study on Invasive Plant Species Distribution in Subtropical Nepal. 2016.

[26] Hattori K, Kaido K, Matsuyuki MJC. The development of urban shrinkage discourse and policy response in Japan. 2017;69:124-32.

[27] Frey WH. Migration and depopulation of the metropolis: regional restructuring or rural renaissance? American Sociological Review. 1987:240-57.

[28] Pallagst K. Shrinking cities in the United States of America. The Future of Shrinking Cities: Problems, Patterns and Strategies of Urban Transformation in a Global Context Los Angeles (University of California). 2009:81-8.

[29] Long Y, Wu KJE, A P. Shrinking cities in a rapidly urbanizing China. 2016;48:220-2.

[30] Beauregard RA. Urban population loss in historical perspective: United States, 1820–2000. Environment and planning A. 2009;41:514-28.

[31] Jacobs AJ. Japan's evolving nested municipal hierarchy: The race for local power in the 2000s. Urban Studies Research. 2011;2011.

[32] World Economic Situation and Prospects: United Nations Publications; 2018.

[33] Xie Y, Gong H, Lan H, Zeng S. Examining shrinking city of Detroit in the context of socio-spatial inequalities. Landscape and urban planning. 2018;177:350-61.

[34] Buhnik S. From shrinking cities to Toshi no Shukushō: Identifying patterns of urban shrinkage in the Osaka metropolitan area. Berkeley Planning Journal. 2010;23.

[35] Hair JF, Sarstedt M, Ringle CM, Mena JAJJotaoms. An assessment of the use of partial least squares structural equation modeling in marketing research. 2012;40:414-33.

[37] Yao J, Stewart Fotheringham AJTPG. Local spatiotemporal modeling of house prices: A mixed model approach. 2016;68:189-201.

[38] Feuillet T, Salze P, Charreire H, Menai M, Enaux C, Perchoux C, et al. Built environment in local

relation with walking: Why here and not there? Journal of Transport & Health. 2016;3:500-12.
[39] Fol S, Cunningham-Sabot E. Urban decline and shrinking cities: a critical assessment of approaches to urban shrinkage. Annales de géographie: Armand Colin; 2010. p. 359-83.
[40] SAKAMOTO K, IIDA A, YOKOHARI M. Spatial emerging patterns of vacant land in a Japanese city experiencing urban shrinkage. Urban and Regional Planning Review. 2017;4:111-28.
[41] Ye J. Stayers in China's "hollowed-out" villages: A counter narrative on massive rural–urban migration. Population, Space and Place. 2018;24:e2128.
[42] Tian Y, Kong X, Liu Y. Combining weighted daily life circles and land suitability for rural settlement reconstruction. Habitat International. 2018;76:1-9.
[43] Schwarz N, Haase D, Seppelt RJE, Planning PB, Design. Omnipresent sprawl? A review of urban simulation models with respect to urban shrinkage. 2010;37:265-83.
[44] Joo Y-M, Seo BJC. Dual policy to fight urban shrinkage: Daegu, South Korea. 2018;73:128-37.
[45] Zingale NC, Riemann DJUDI. Coping with shrinkage in Germany and the United States: A cross-cultural comparative approach toward sustainable cities. 2013;18:90-8.
[46] Hollander JB, Németh J. The bounds of smart decline: A foundational theory for planning shrinking cities. Housing Policy Debate. 2011;21:349-67.

Chapter 7. Spatial temporal analysis of thermal environmental implications based on remote sensing

7.1 Introduction

The urban heat island (UHI) in which the atmospheric or surface temperature of an urban area is significantly higher than its surrounding rural areas is known as one of the most significant environmental implications of the urbanization [1]. This phenomenon has raised great attention for it causes a great impact on the energy use, thermal comfort, people health's, etc [2-5]. Moreover, UHI widely affects the cities across the world [6] and is being aggravated all the time [7]. Hence, numbers of research have been conducted to investigate the UHI effects and develop mitigation strategies or countermeasures [8-10].

Different from investigating the UHI using air temperature data from the local meteorological observations or in-situ measurements, the land surface temperature (LST) is another critical parameter for the investigation and assessment of the UHI [11, 12]. The LST could be obtained or retrieved from the thermal infrared remote sensors, which enables surface urban heat island (SUHI) studies over large-scale spaces [13]. However, for the quite differences between the spatial and temporal resolution, the remote sensors have their respective characteristics and applicability. In general, the high spatial resolution sensors have a low temporal resolution, whilst the low spatial resolution sensors have a high temporal resolution [14]. For example, the spatial resolution of Landsat TIRS is 100 m but the temporal resolution is 16 day; The spatial resolution of the Moderate Resolution Imaging Spectroradiometer (MODIS) LST images is 1 km but the temporal resolution is twice a day [15]. Hence, downscaling the spatial resolution of LST images from coarser to finer resolution became a mainstream method to improve the application of the LSTs [16].

So far, various downscaling methods have been developed to downscale the spatial resolution of LSTs. Based on remote sensing technology, a number of the UHI studies introduced vegetation indices such as Normalized Difference Vegetation Index (NDVI), surface reflectance, or land use and land cover (LULC), which is easy to calculate from remote sensing data as evaluation indices for the UHI. Traditional downscaling methods such as Temperature Sharpening (TsHARP) [17] and multiple linear regression [18] bases on building linear correlation between predictors and LST. However, in a highly dense urban area, the UHI study should give priority to the effect of artificial heat source, aerodynamic roughness length, wind speed, and sky view factor [19, 20], which suggest the UHI mechanism is complex. As a result, with the development of machine learning technology, various machine learning methods such as support vector regression and random forests (RF) regression have been developed and applied to improve the downscaling performance [21].

In this study, one of the most urbanized areas, Fukuoka prefecture (Japan) was selected as the study area. Fukuoka prefecture has a population of approximately 5.1 million and covers an area of approximately 4986.4 km^2. The main objectives are first to investigate the UHI in this area during summer and winter both in the daytime and nighttime; second to explore the spatial correlation between the population, the LULC and the LSTs; and third to explore the urban cooling effect of the urban blue-green spaces. For the following reasons, we developed RF models to downscale the LSTs in the area with MODIS LST products from 1 km spatial resolution to 250 m: (1) the area is cloudy and rainy during the years that remote sensors with the low temporal resolution are not applicable for this area for the discontinuous time-series observations for the same area and high possibility of the images with high cloud cover; (2) various studies concluded the urban cooling effect of the water bodies and green spaces was relate to its size, and the affected distance is less than 1 km [18]; and (3) the RF models for downscaling LSTs have better fitting performance than the other methods [22]. The study contributes to illustrate the spatial correlates of LSTs, improve the understanding of the situation and the factors driving UHI, provide valuable information for governments and planners developing effective coping strategies on the UHI, and hopefully will draw the attention of the urbanizing cities.

7.2 General information of study area

Fukuoka prefecture, Japan is chosen as the study area which is located in the west of Japan and domains ranging from 130.0°N, 33.0°E to 131.19°N, 33.97°E, with an approximate area of 4986.4 km^2 (Fig. 7-1). Mixed landscapes characterize this area with a various climate, that it faces the sea on three sides, whilst the primary terrain is mountain and hills, and cities are mainly distributed in the plain area along the coast. The temperature in this area peaks in August and reaches its minimum in January. The area has a humid climate throughout the year, mainly rainy and cloudy days. The dominating land cover types were forest (44.6%), urban and built-up (21.9%), cropland (16.6%), and others (15.1%) in 2019.

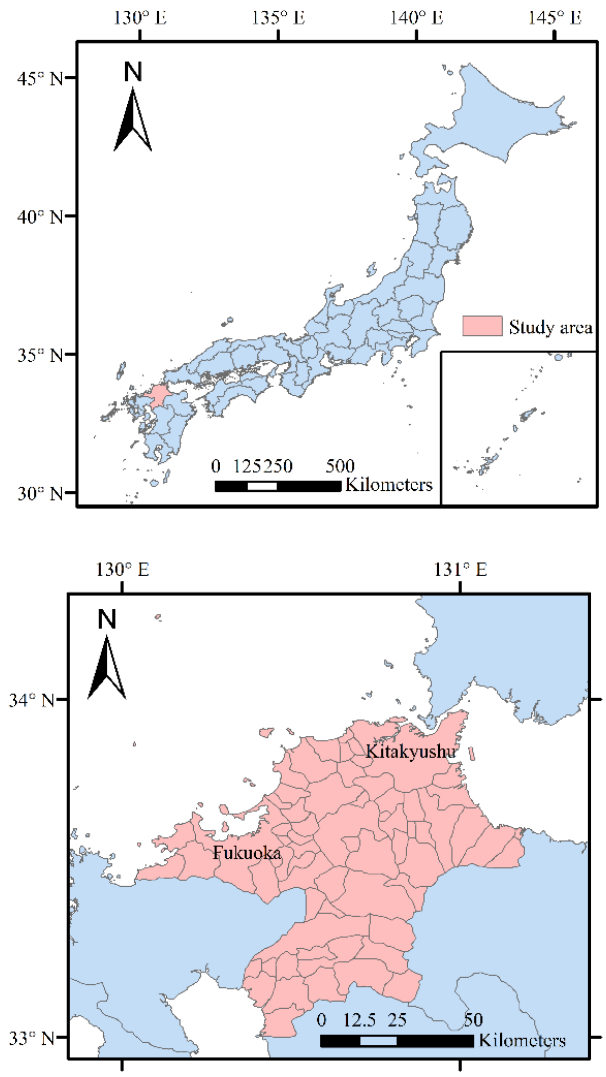

Fig. 7-1 Location of study area.

In this area, over 50% residents live in the two coastal cities Fukuoka and Kitakyushu, which both are the designated cities of Japan with more functions than other cities, including civil affairs, urban planning, culture, education, and other public administrative affairs. The two cities have experienced significant urbanization [23], and formed the Kitakyushu-Fukuoka metropolitan area, which is the fourth largest metropolitan area after Tokyo, Osaka, and Nagoya [24]. After a rapid rate of urbanization since 1950s in Japan, the process of urbanization has been slowed since the 21st century. However, the population of Fukuoka keeps a fast-growing rate and increased from 1.34 million to 1.57 million; Conversely, Kitakyushu has become the biggest shrinking city in Japan with about 50 thousand population loss since 2000. To further explore the spatial-temporal variation of SUHI in an expanding city and a shrinking city, the two cities were therefore selected as comparisons.

7.3 Data sources and methods for UHI investigation

7.3.1 Satellite data

Multiple remote sensing data were used in this study. First, the Terra MODIS daily LST products (MOD11A1) in 2005 and 2015 at 1 km (960.3 m) spatial resolution were collected from the NASA EARTHDATA website (https://search.earthdata.nasa.gov/). The daytime (local time 10:30) LST and nighttime (local time 22:30) LST layers were reprojected into WGS 1984 (World Geodetic System 1984) and resampled to 1km resolution. In the study area, summer was the period from June to August, and winter was the period from December to February. The LST images with large missing pixels or cloud cover were excluded, and the other images were composited to seasonal LST images. Second, vegetation indices, bands surface reflectance, and sun zenith angle, which are correlated with the LST were extracted from MODIS products (MOD13Q1). The data at 250 m spatial resolution were also collected from the NASA EARTHDATA website, including the following: (1) Normalized Difference Vegetation Index (NDVI), (2) Enhanced Vegetation Index (EVI), (3) red reflectance, (4) near infrared (NIR) reflectance, (5) blue reflectance, (6) middle infrared (MIR) reflectance, and (7) sun zenith angle. Third, the digital elevation data with 30 m spatial resolution from the Advanced Spaceborne Thermal Emission and Reflection Radiometer (ASTER) Global Digital Elevation Model Version 2 (GDEM V2) were downloaded from the NASA EARTHDATA website. These data were all reprojected to WGS 1984 and resampled to 1 km and 250 m spatial resolution respectively to match the LST images and for the downscaling process.

7.3.2 Land numerical data and population data

The land use and land cover of Fukuoka prefecture in 2006 and 2016 at 100 m spatial resolution were downloaded from Japan National Land Numerical Information website (http://nlftp.mlit.go.jp/ksj/). We then recalcified it into 6 categories namely: urban, grassland, forest, bare land, coast, and water body (Fig. 7-2). The data were also resampled to 250 m spatial resolution. Besides, to find interrelationship between population with SUHI, population distribution data with 250 m spatial resolution in 2005 and 2015 based on Japan National Population Census in 2005 and

2015 were collected from Japanese Government Statistics Website (https://www.e-stat.go.jp/).

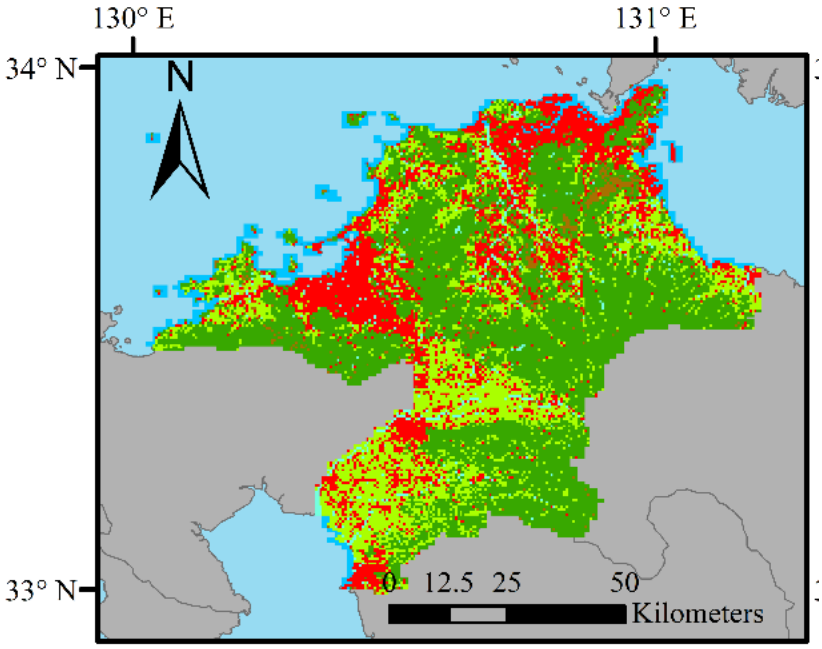

(a) 2006

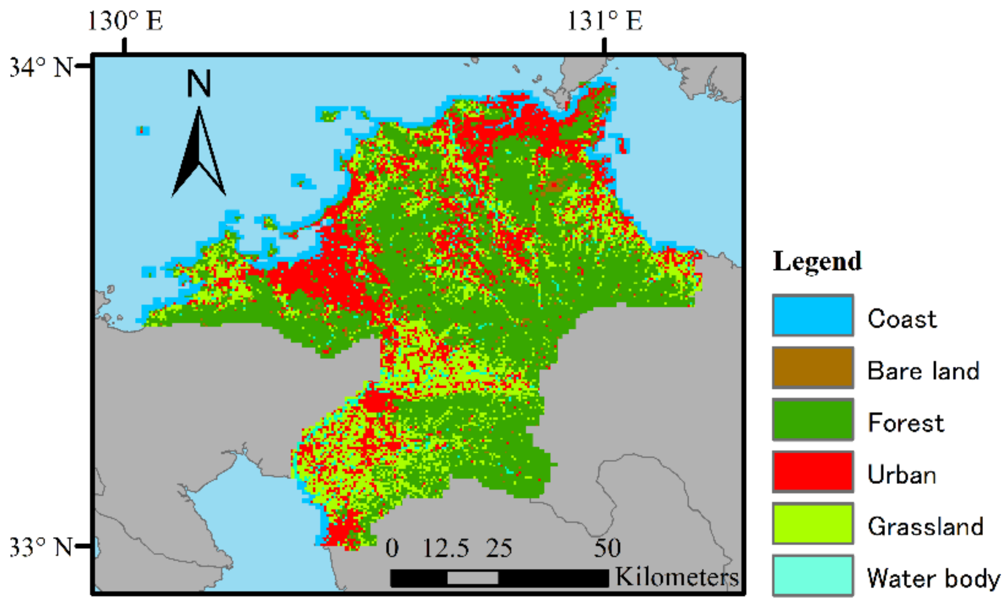

(b) 2016

Fig. 7-2 Land use and land cover of Fukuoka in (a) 2006, and (b) 2016.

7.3.3 Downscaling LST based on random forests

The random forest (RF) method is a widely used ensemble machine learning method for classification, regression, and other tasks [25]. The framework of RF regression is showed in Fig. 7-3. The method is a nonlinear statistical ensemble method which constructs large numbers of de-correlated decision trees during the training time, and outputs the mean prediction of the individual trees. RF has the advantage of modeling the complex nonlinear relationships between responding variable and predictive variables. Compared to other downscaling methods, the RF method has higher precision in downscaling LST [21, 22].

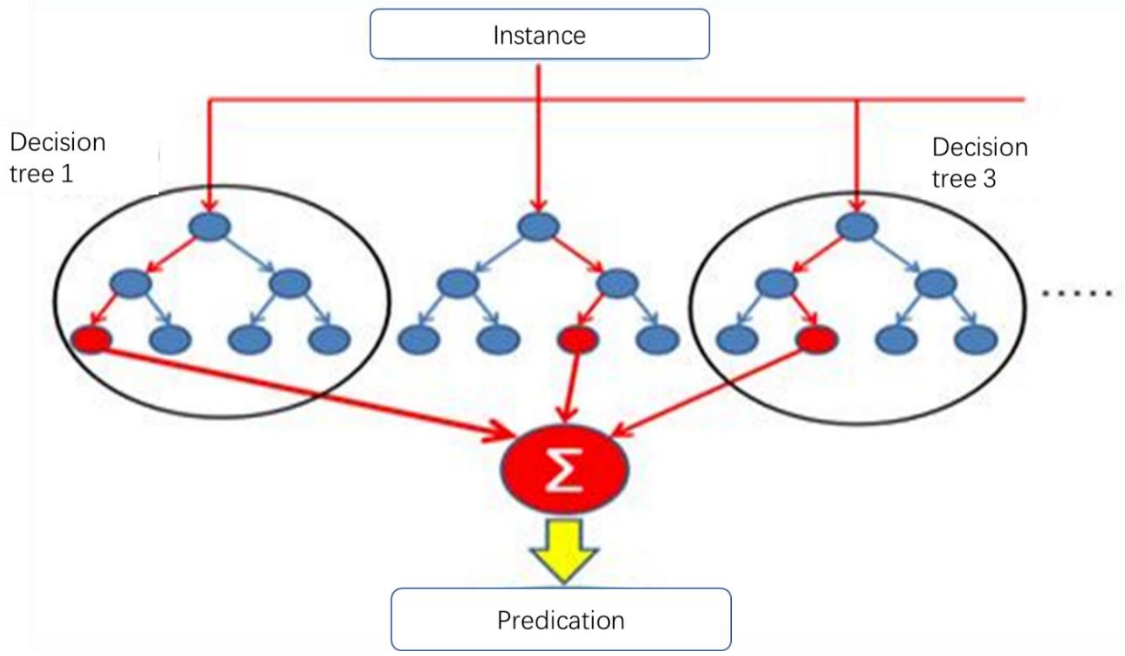

Fig. 7-3 Sample of a RF regression model.

Fig. 7-4 shows the downscaling LST process. Firstly, to find the correlates of LST, the following variables were selected as predictors for the RF model: digital elevation (h_{DEM}); vegetation indexes (i_{VI}), surface reflectance (ρ_i), and sun zenith angle (θ_{SZA}). The land use and land cover and population distribution were not regarded as the predictors to avoid endogeneity and to facilitate the recognition of the influence of LULC and population on the LST in the future. The bootstrap aggregation strategy was applied with each decision tree built from a bootstrap sample contains 70% of the input data. The bootstrap aggregation strategy that the model is trained by in-bag data and validated by out-of-bag (OOB) data significantly helps to avoid overfitting in commonly used machine learning procedures. The model with the highest coefficient of determination (R^2), which refers to the highest fitting degree was chosen as the optimal model based on a number of iterative testing results using scikit-learn in Python. Meanwhile, the coefficient of determination (R^2) and the root mean square error (RMSE) were calculated for downscaling accuracy assessment in the future. Therefore, the corresponding model between LST and these predictors is written as follows:

$$LST_{prediction}^{1km} = f(h_{DEN},\ i_{VI}, \rho_i, \theta_{SZA}) \qquad (1)$$

where $LST_{prediction}^{1km}$ represents the estimated LST at 1 km resolution, f refers to a nonlinear function based on RF, h_{dem} represents the digital elevation, i_{VI} represent the vegetation indexes including NDVI and EVI, ρ_i represent the surface reflectance of red, NIR, blue, and MIR bands, θ_{SZA} represents the sun zenith angle.

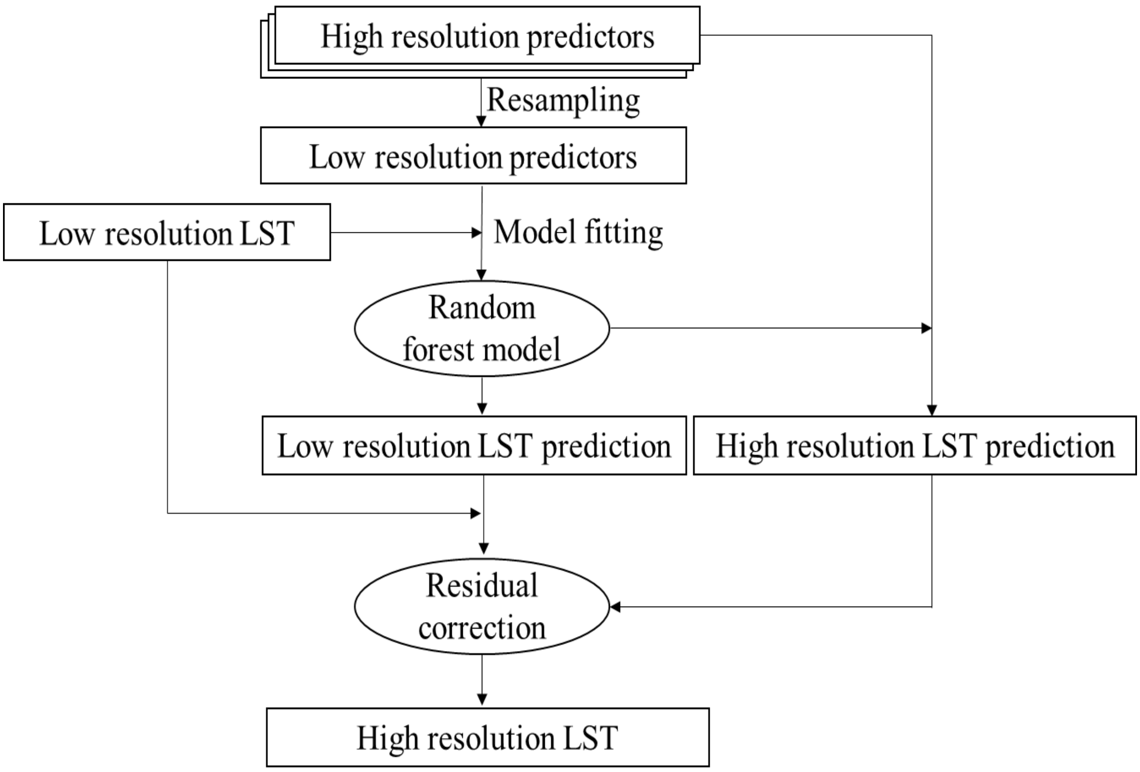

Fig. 7-4 Flow chart of downscaling MODIS LST products based on random forests.

Secondly, as the RF models cannot interpret the total distribution of LSTs, a residual correction process was conducted. This process could correct the LSTs that could not be predicted by the RF model and ensures the reaggregated downscaled LSTs match the original LSTs data. The residual error ($\Delta LST_{residual}^{1km}$) between LST^{1km} and $LST_{prediction}^{1km}$ was calculated with equation (2). Then, the residual was interpolated to a 250 m resolution ($\Delta LST_{residual}^{250m}$) by simple spline interpolation method.

$$\Delta LST_{residual}^{1km} = LST^{1km} - LST_{prediction}^{1km} \qquad (2)$$

Thirdly, the RF models were applied to estimate the LSTs at fine scale ($LST^{250m}_{prediction}$) using the predictors at 250m spatial resolution. Then the calibrated LSTs (LST^{250m}) was calculated using the sum of the $LST^{250m}_{prediction}$ and $\Delta LST^{250m}_{residual}$, shown as Equation (3):

$$LST^{250m} = LST^{250m}_{prediction} - \Delta LST^{250m}_{residual} \qquad (3)$$

7.3.4 Data analysis

Traditional statistical analysis methods usually focus on statistical relationship between population, LULC and UHI at the same site. However, to further explore the spatial impact of population distribution and the LULC on the UHI, bivariate spatial correlation analysis was conducted to identify spatial association patterns of the LSTs with the population and the LULC. In this study, the bivariate spatial autocorrelation, including global Moran's I statistics and local Moran's I statistics were performed to reveal the spatial dependence of LSTs with population and LULC.

The global Moran's I, which is a rational number ranged from -1 to 1 after normalized variance could reflect the global spatial. Positive value of global Moran's I represents positive spatial correlation, the larger the value, the more obvious the spatial correlation; negative value represents negative spatial correlation; otherwise, Global Moran's I = 0, indicates a random space. Meanwhile, the Local Moran's I could identify the local differences and similarities among neighboring pixels [26]. The Local Indicators of Spatial Association (LISA) can be determined using Local Moran's I [27]. Five clustering/outlier types are classified using the Local Moran's I including (1) high-high cluster (HH); (2) high-low outlier (HL); (3) low-high outlier (LH); (4) low-low outlier (LL); (5) not significant (at 0.05 significance level). The bivariate global and local Moran's I tests were conducted for the LSTs of the eight studying periods with the population and the LULC. The number of people within a pixel was used as the unit of population variable. And the area of each land use type within a pixel was used as the unit of LULC variable for the spatial correlation analysis. For example, among the LISA types between the urban land and LST during 2005 summer daytime, HH refers to a high proportion of urban land of a pixel and high LSTs of its neighbouring pixels; HL refers to a high proportion of urban land of a pixel while low LSTs of its neighbouring pixels; LH refers to a low proportion of urban land of a pixel while high LSTs of its neighbouring pixels; and LL refers to a low proportion of urban land of a pixel and low LSTs of its neighbouring pixels. For the other variables, the same interpretation was followed.

Meanwhile, the spatial weight matrix can significantly affect the results of Moran's I. Fixed kernel bandwidth is constant, while adaptive kernel bandwidth varies from the density of observations [28].

As the pixels were uniformly distributed and to further explore the urban cooling effect potential of each LULC type, we selected the fixed Gaussian kernel for the weighting matrix. We used Geoda 1.14 (http://geodacenter.github.io/index.html) to generate the spatial weight matrix and then calculate the bivariate global/local Moran's I, which demonstrated the spatial relationship between the LSTs with the population and LULC in the area.

After global/local Moran's I tests, the pixels at 0.05 significance level were extracted for each bivariate test result. And we calculated the mean surface urban heat island intensity (SUHII) for the population distribution (gradient 10 people), and Euclidean distance to each LULC type (gradient 100 m). In this study, the SUHII was defined as the urban LST subtracts the average LST of surrounding rural areas. Densely Inhabited Districts (DID) are the urban areas designated based on the Japan National Population Census statistical data. The urban boundaries of Fukuoka city and Kitakyushu city were extracted based on the distribution of DID, which is downloaded from Japan National Land Numerical Information (http://nlftp.mlit.go.jp/ksj/) (Fig. 7-5).

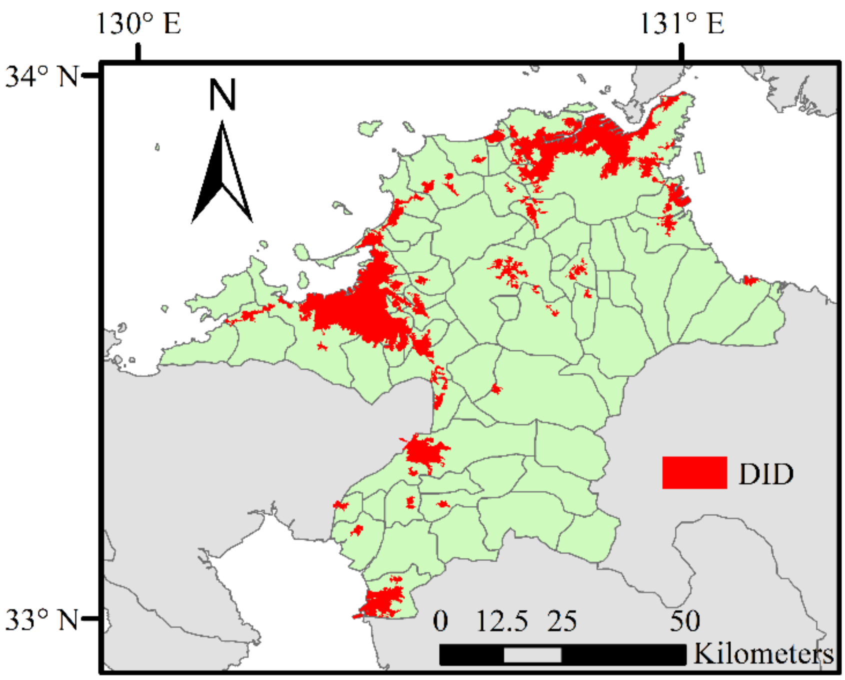

Fig. 7-5 The distribution of Densely Inhabited Districts in the study area.

The urban areas of the 2 cities were extracted by the DID distribution and 3 km buffer zones surrounding the DID in the two cities were then selected as the urban boundary area. Zonal statistics were used to calculate the mean LST value of the urban boundary area. The SUHII of a pixel at location i,j ($SUHII_{(i,j)}$) is the difference between the LST of the pixel ($LST_{(i,j)}$) and the mean LST value of the urban boundary area ($LST_{boundary}$), shown as Equation (4).

$$SUHII_{(i,j)} = LST_{(i,j)} - LST_{boundary} \qquad (4)$$

Then, zonal statistics were conducted to reveal the correlation between the mean SUHII and each LULC type to evaluate the urban cooling effect of each LULC type from LST and distance.

7.4 Downscaling LST results

7.4.1. Random forests variable importance

Table 1 shows the variable importance scores of the RF regression of each study period. The score of each predictor refers to the contribution of the predictor in the RF regression. The contributions of DEM rank high over the study scenes, which might occur due to the topography and land use characteristics of the area. Large topographic have great impacts on solar incident radiation and longwave surface cooling along mountainous surfaces [29]. Moreover, as one of the most urbanized areas in Japan, the urban and built-up areas almost cover the coastal plain, whilst the mountain and hills area is mainly covered by forest due to the policy of forest protection. It implies that there are greater differences in solar radiation absorption and heat transfer capacity with the change of topography. In addition, during winter nighttime, the contributions of vegetation index and NIR band surface reflectance are higher than the other study periods. However, the importance scores do not represent the correlation between the predictors and LST. It could only represent the contributions in the model, which means the change in the predictors will affect the contribution of each predictor.

Table 7-1. Random forests variable importance scores for each scene

Study periods	h_{DEM}	i_{NDVI}	i_{EVI}	ρ_{red}	ρ_{NIR}	ρ_{blur}	ρ_{MIR}	θ_{SZA}
2005SD	0.21	0.09	0.11	0.09	0.14	0.11	0.14	0.12
2005SN	0.22	0.11	0.12	0.10	0.12	0.12	0.15	0.06
2005WD	0.20	0.12	0.11	0.11	0.10	0.15	0.14	0.07
2005WN	0.15	0.22	0.19	0.01	0.17	0.03	0.15	0.06
2015SD	0.17	0.15	0.09	0.10	0.12	0.12	0.13	0.12
2015SN	0.15	0.09	0.07	0.13	0.16	0.15	0.14	0.10
2015WD	0.14	0.11	0.14	0.10	0.16	0.15	0.13	0.07
2015WN	0.18	0.10	0.13	0.13	0.16	0.15	0.11	0.05

Note: summer daytime (SD); summer nighttime (SN); winter daytime (WD); winter nighttime (WN).

7.4.2 Downscaled results

Due to the largest seasonal difference of heat and moisture between winter and summer, the SUHI in both seasons was investigated to illustrate the temporal variation of thermal environment in this area. Furthermore, daytime and nighttime SUHI were conducted in this study. As Fig. 7-6, 7-7, 7-8, and 7-9 show the downscaled LST images, the thermal environment is similar during the same study periods in 2005 and 2015. Significant UHI effect could be observed during summer daytime, summer nighttime, and winter daytime. Specifically, the UHI effect exists during the study period for the high LST in the urban area. However, during winter nighttime, the distribution of LSTs showed a trend of gradually decreasing from the north coastal area to the south mountain and hills area. The LSTs of the coastal area in the northern part of Fukuoka prefecture were low in the daytime, and high in nighttime both in summer and winter, which showed the urban cooling effect potential.

The accuracy of the downscaling LST based on RF regression is presented in Table 7-2. In general, the results showed good performance of RF regression. The RF models for the downscaled LST during summer daytime have the best fitting performance, that the R^2 and RMSE for the RF model are 0.831 and 1.271 K in 2005, whilst 0.925 and 0.845 K in 2015. Meanwhile, the models for the study periods during summer nighttime and winter daytime also had resulted in high fit degree that the overall R^2 varied from 0.781 to 0.874, and the overall RMSE varied from 0.430 to 1.244 K. However, the lack of topographic factors might be the account for the relatively poor fitting degree in winter nighttime, that the R^2 of winter nighttime in 2005 and 2015 were 0.507 and 0.492 respectively.

Table 7-2. Downscaled LST results based on random forests regression, R^2 is the determination coefficient, RMSE is the root-mean-square error (K).

Index	2005 SD	2005 SN	2005 WD	2005 WN	2015 SD	2015 SN	2015 WD	2015 WN
R^2	0.831	0.781	0.843	0.507	0.925	0.865	0.874	0.492
RMSE	1.271	0.682	1.117	0.871	0.845	0.430	1.244	1.186

Note: summer daytime (SD); summer nighttime (SN); winter daytime (WD); winter nighttime (WN).

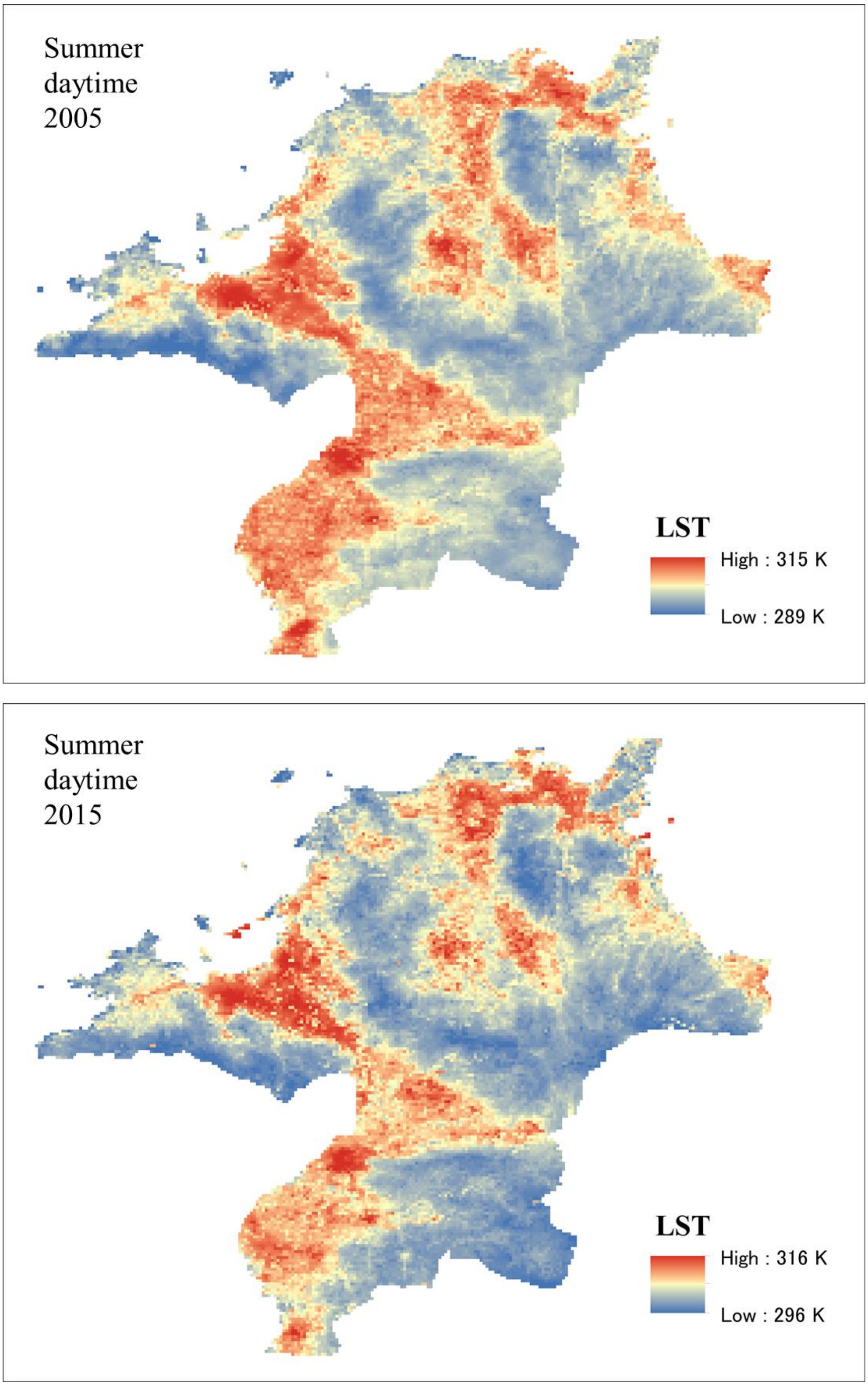

Fig. 7-6 250 m downscaled LST using random forests regression during summer daytime

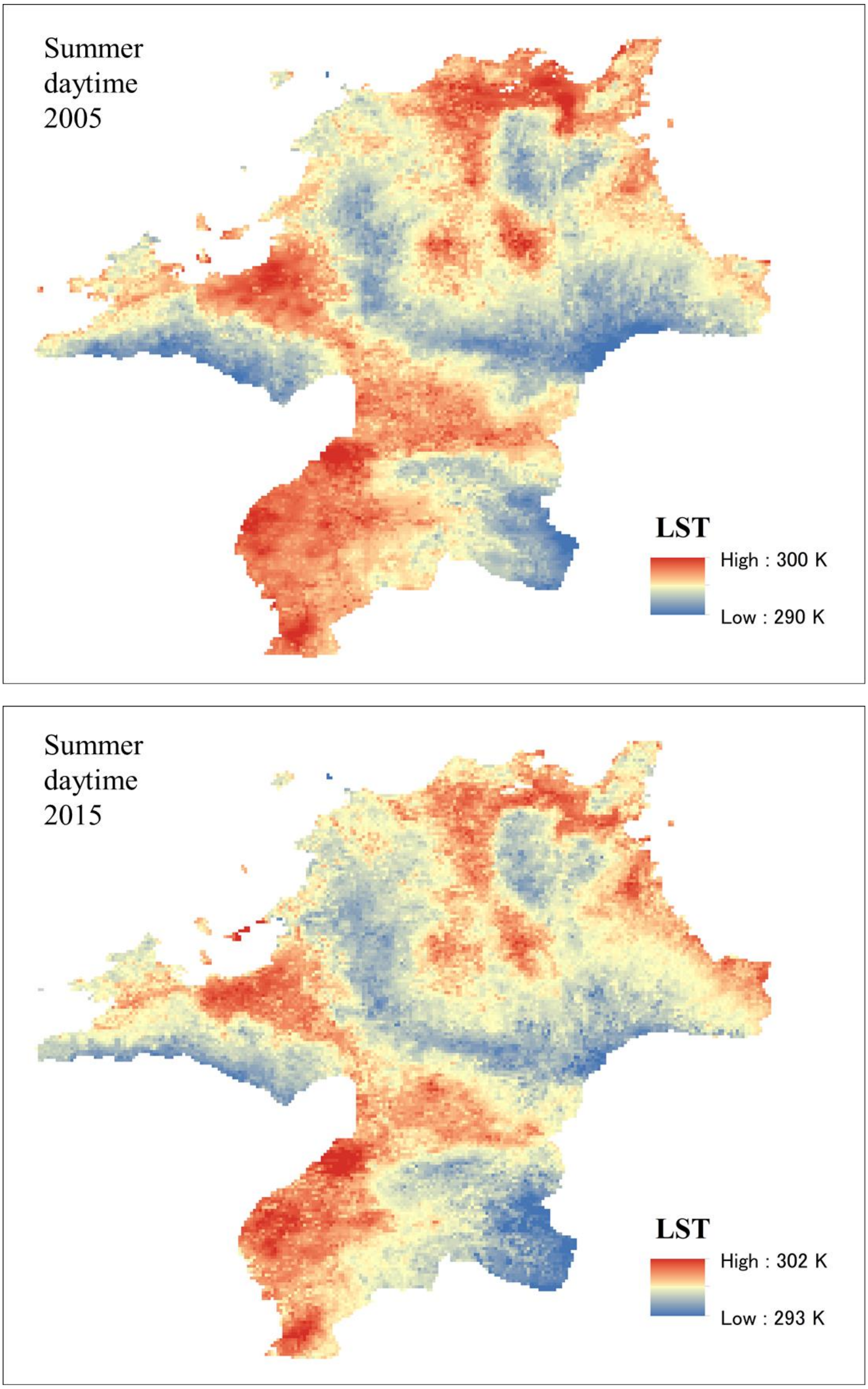

Fig. 7-7 250 m downscaled LST using random forests regression during summer nighttime

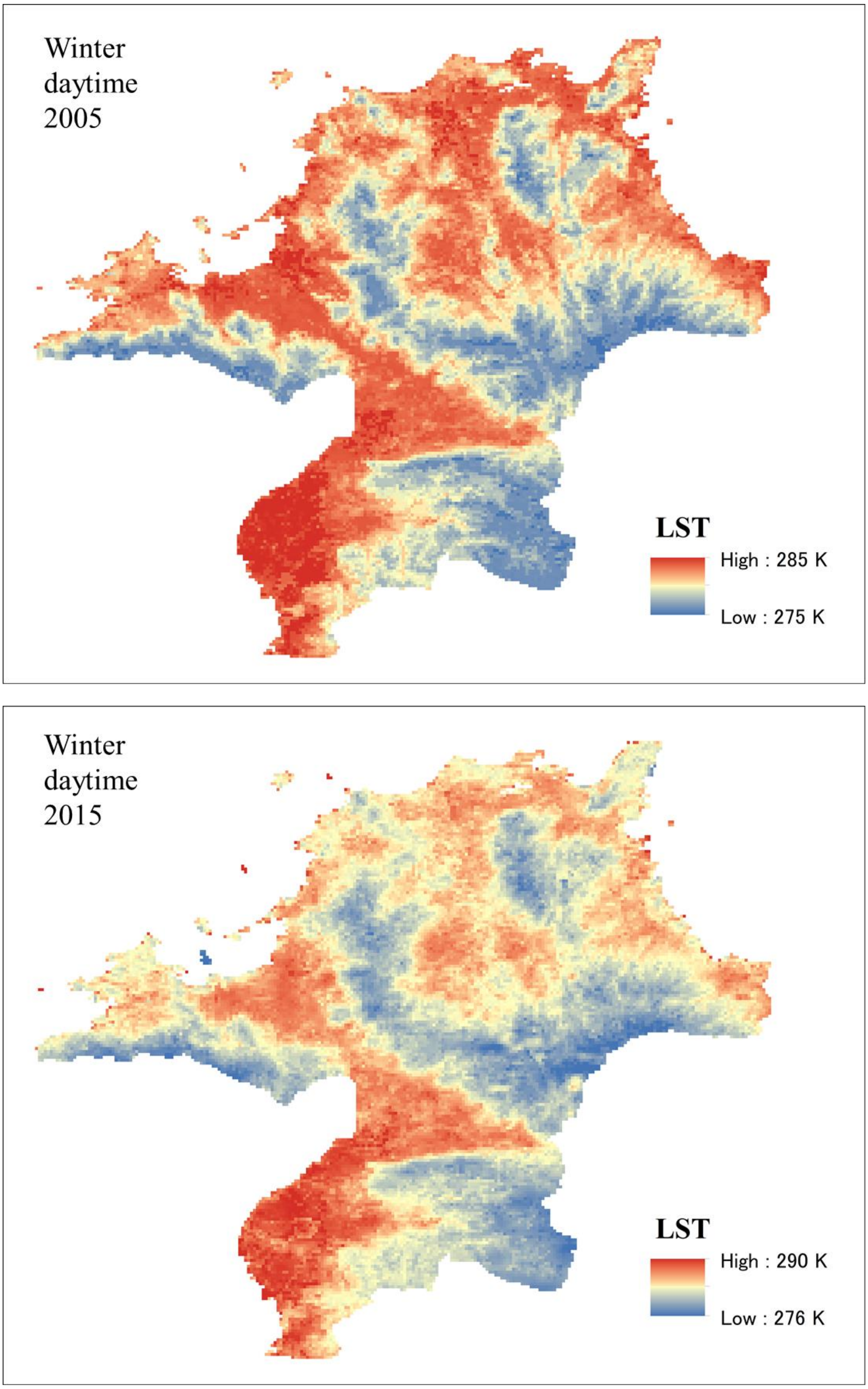

Fig. 7-8 250 m downscaled LST using random forests regression during winter daytime

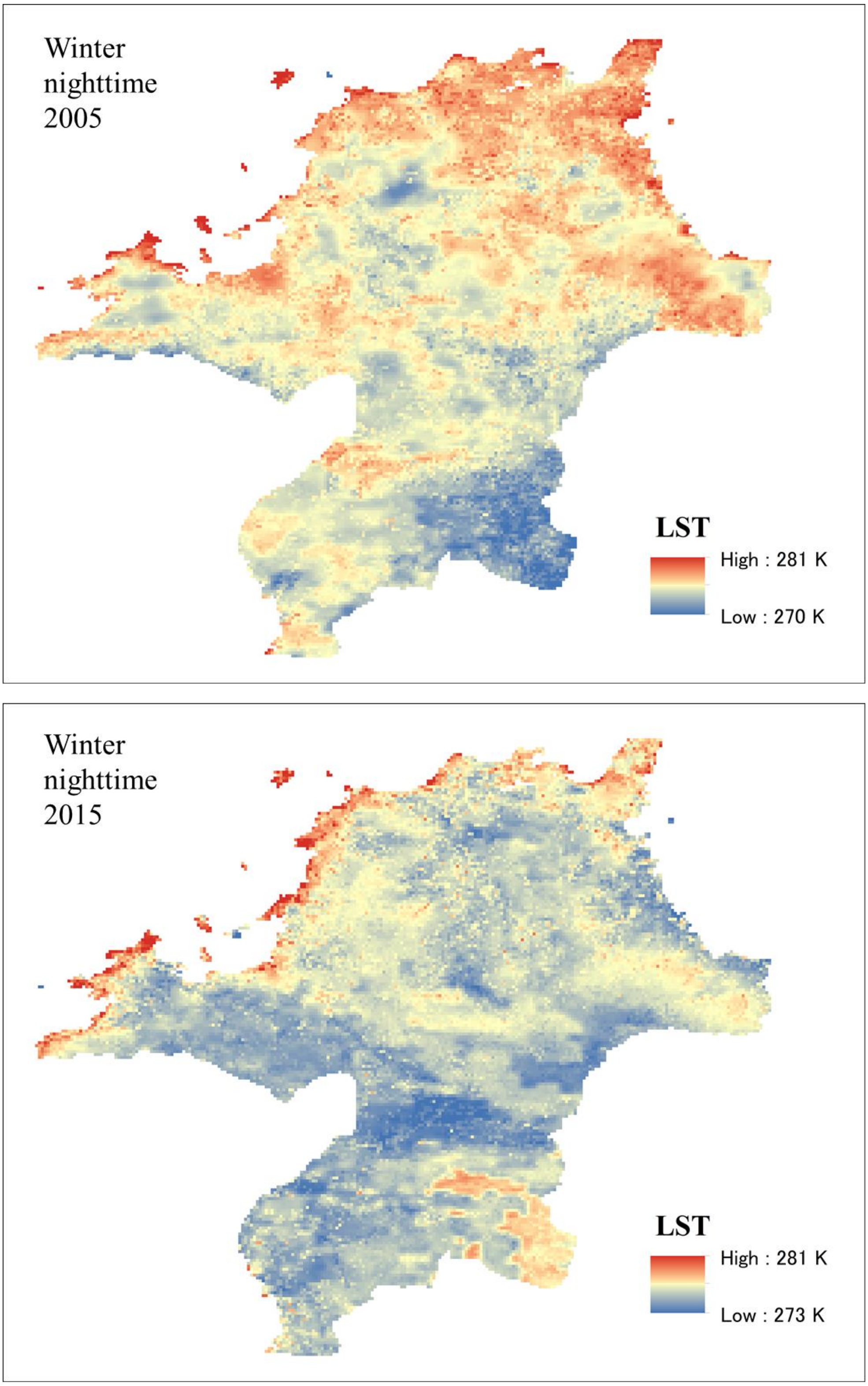

Fig. 7-9 250 m downscaled LST using random forests regression during winter nighttime

7.4.3 Bivariate spatial analysis

The results from the bivariate global Moran's I are presented in Table 7-3. The results revealed that the LSTs have similar spatial patterns with the population and the LULC in some parts area. Specially, significant positive spatial correlations were found between the LSTs and the number of populations during the four study periods (all p-values < 0.01 and Moran's I > 0). Moreover, the degree of the spatial correlation is substantial in summer or during the daytime. Meanwhile, the effect and the degree of the spatial correlation varied with LULC type. It showed that the area of urban land, coastal area, and grassland have a positive spatial correlation with LSTs. The positive correlation was strongest between LSTs and urban area, followed by that between LSTs and coast area, LSTs and grassland. Whilst the area of water, forest, and bare land have negative spatial correlation with LSTs. The negative correlation was strongest between LSTs and forest, followed by that between LSTs and bare land, and LSTs and water bodies. However, the spatial correlation only refers to a similar spatial pattern, which does not imply a linear correlation between the spatial variables.

Table 7-3. Bivariate global Moran's I value for the variables and downscaled LSTs.

Variables	Summer daytime		Summer nighttime		Winter daytime		Winter nighttime	
	2005	2015	2005	2015	2005	2015	2005	2015
Population	0.535*	0.566*	0.475*	0.537*	0.403*	0.469*	0.091*	0.072*
Urban	0.493*	0.511*	0.477*	0.486*	0.446*	0.457*	0.123*	0.124*
Coast	0.135*	0.102*	0.091*	0.101*	0.082*	0.121*	0.072**	0.080*
Water	-0.091*	-0.133*	-0.072*	-0.175*	-0.064*	-0.171*	0.054**	-0.132*
Forest	-0.457*	-0.466*	-0.476*	-0.438*	-0.473*	-0.481*	-0.172*	-0.142*
Bare land	-0.144*	-0.155*	-0.201*	-0.137*	-0.183*	-0.134*	-0.150*	-0.054**
Grassland	0.062**	0.107*	0.082*	0.075*	0.161*	0.171*	0.105*	0.061**

Note: * represents 0.01 significance level, ** represents 0.05 significance level.

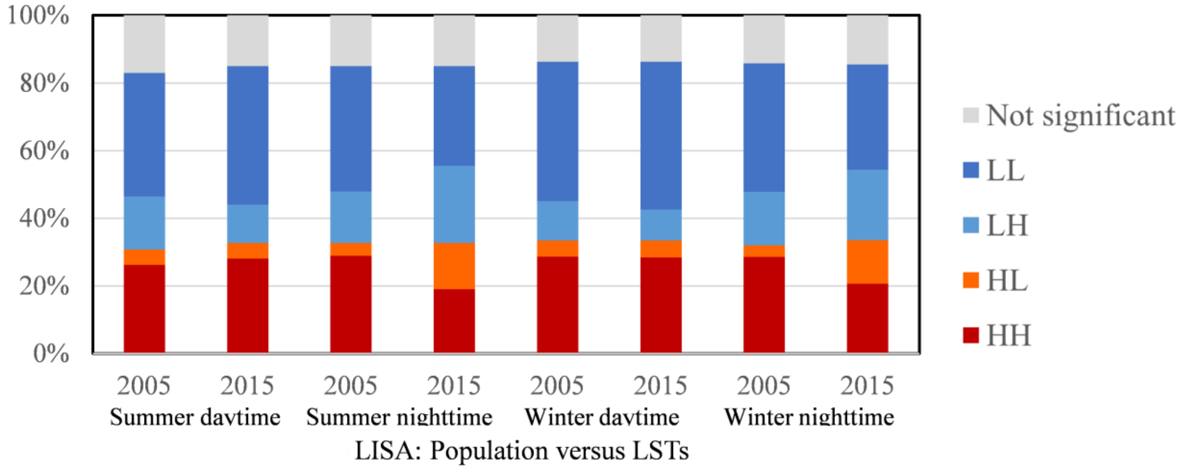

Fig. 7-10 LISA cluster statistics between population and the LSTs during the eight study periods

The bivariate LISA statistical results indicate the differences of the spatial correlations between the LSTs and the population and the LULC types (Fig. 7-10, 7-11, 7-12). The population and the urban area have similar spatial correlations with the LSTs. The significant spatial correlation could be observed over 80% areas (ranging from 82.98% to 88.11%), while the main LISA types are the HH cluster and LL cluster, which indicate the population and the urban area are positive spatial correlates of the LSTs. Conversely, the HL outlier and LH outlier are the main components (ranging from 50.65% to 73.87%) of the LISA types between the forest and LSTs. Besides, as the water area, the coastal area, the grassland, and the bare land in the study area is relatively small and distributed, we observed that the spatial correlations are not significant in most areas, which are consistent with the low global Moran's I results. However, according to the LISA results between the water and grassland and the LSTs, the HL and LH outliers are the main parts for the significant spatial correlated areas, indicating a cooling potential of these LULC types on the SUHI. More remarkably, the high proportions of the HH cluster and LH outlier between the coast area and the LSTs are found. As the cities are built along the coast and sprawled towards inland, the LSTs of the inland urban areas could still be high.

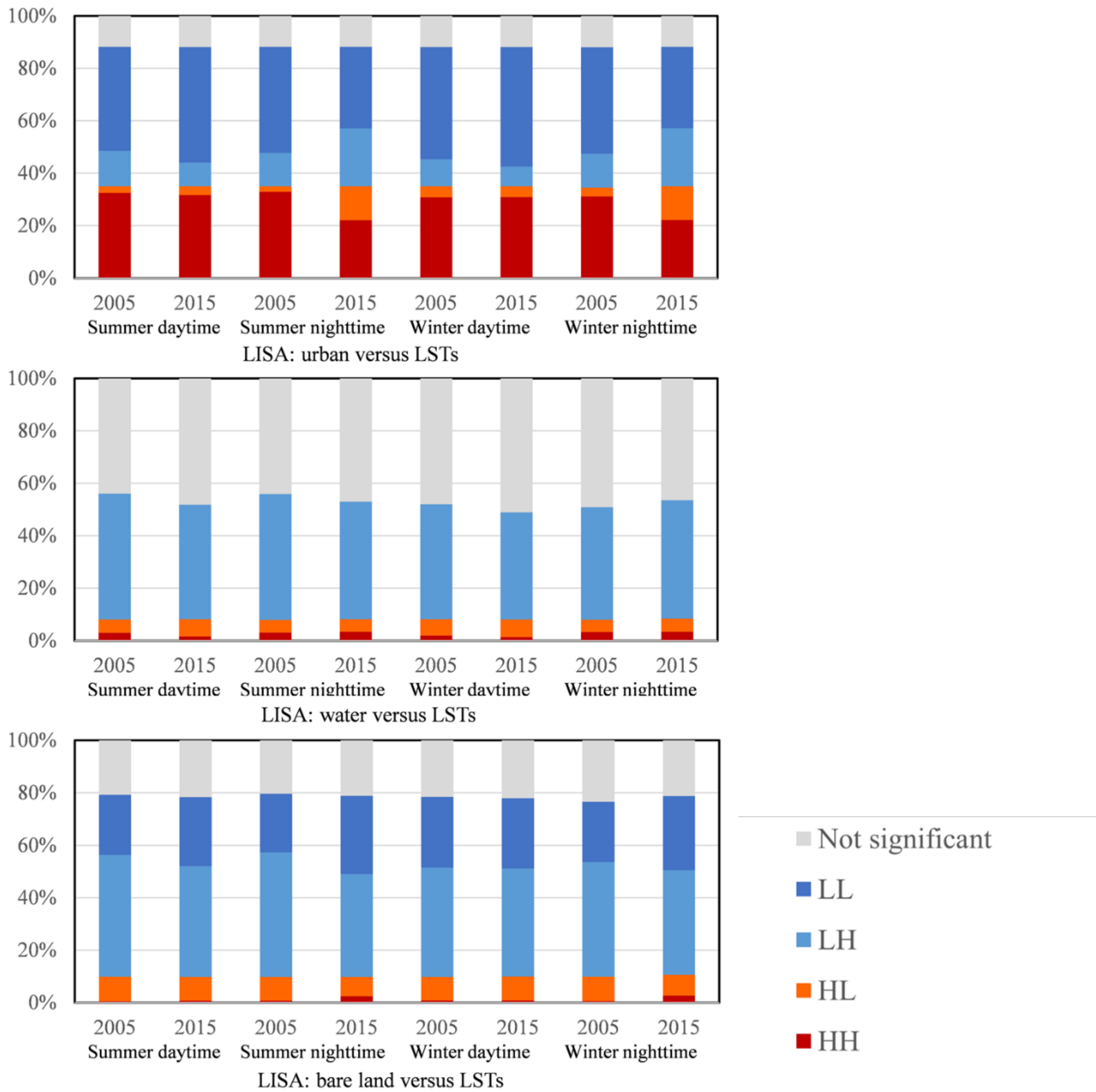

Fig. 7-11 LISA cluster statistics between urban, water, bare land and the LSTs during the eight study periods

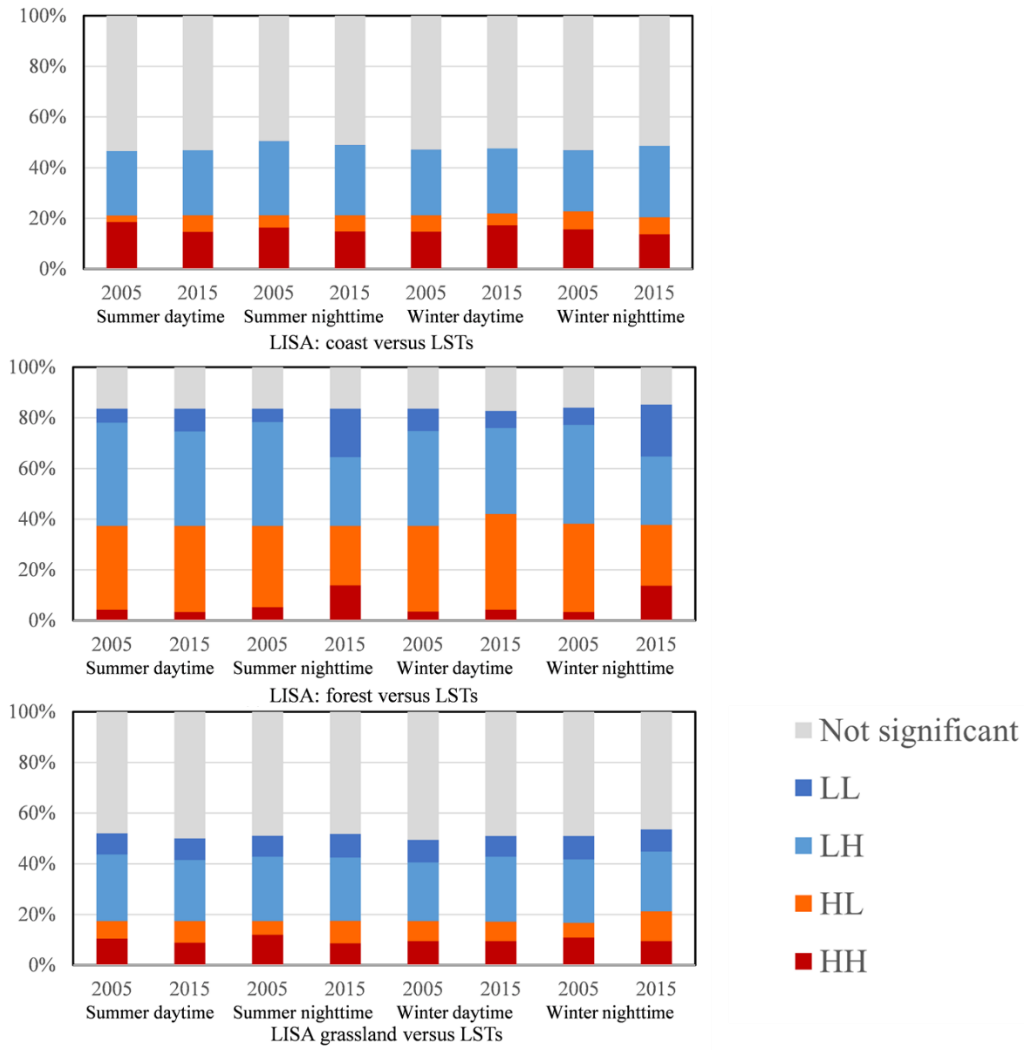

Fig. 7-12 LISA cluster statistics between coast, forest, grassland and the LSTs during the eight study periods

7.4.4 Zonal statistics results

As Fig. 7-13 illustrates the SUHII variation for Fukuoka and Kitakyushu during eight study periods. In general, the SUHI is more influential in summer and daytime. Specifically, the SUHII during summer daytime is the highest for both two cities, while in winter nighttime, the SUHI is the least significant. Meanwhile, the SUHI in Fukuoka is more intense than that in Kitakyushu, and the SUHII increased in Fukuoka and decreased in Kitakyushu. This result also implied the positive correlation between SUHI and city size and evolution types.

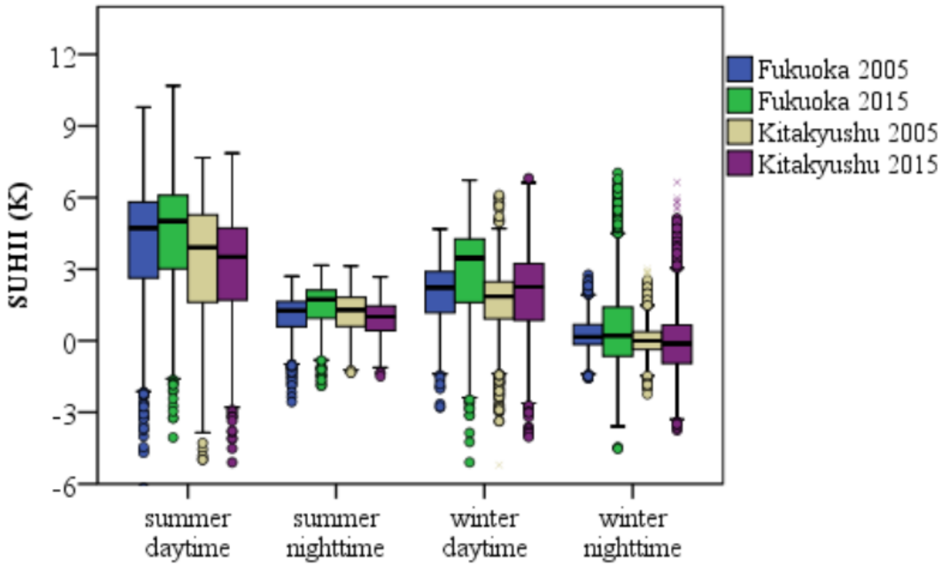

Fig. 7-13 The variation of the SUHII during the eight study periods in Fukuoka and Kitakyushu.

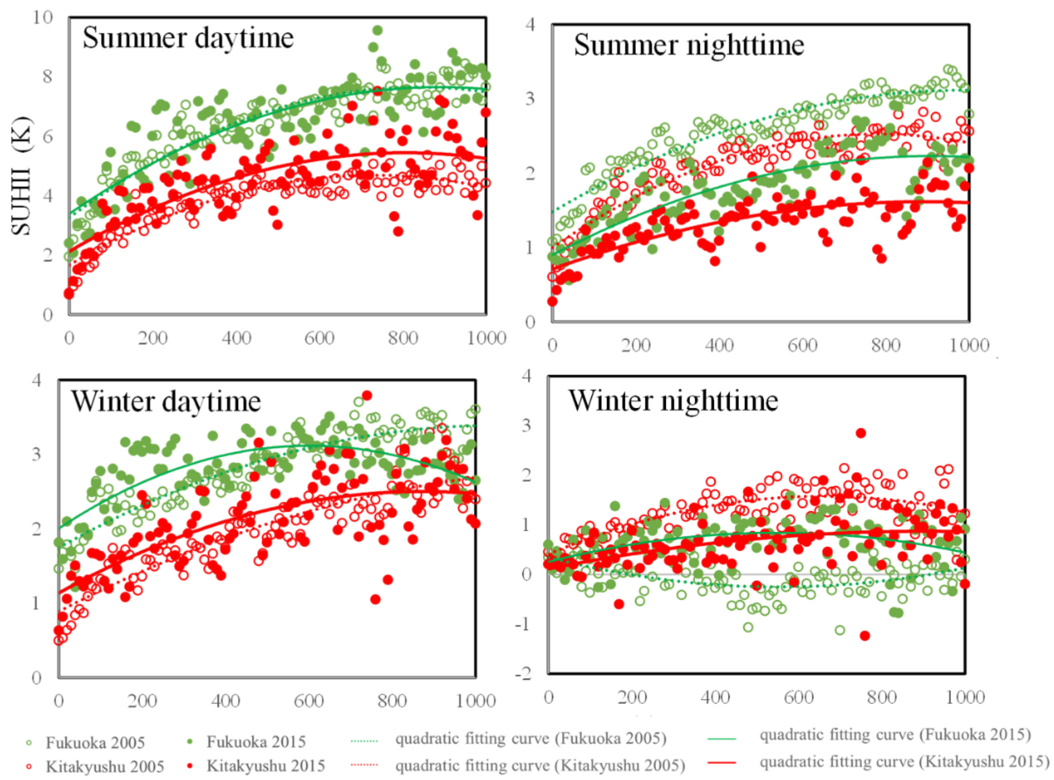

Fig. 7-14 Relationship between mean SUHII and population

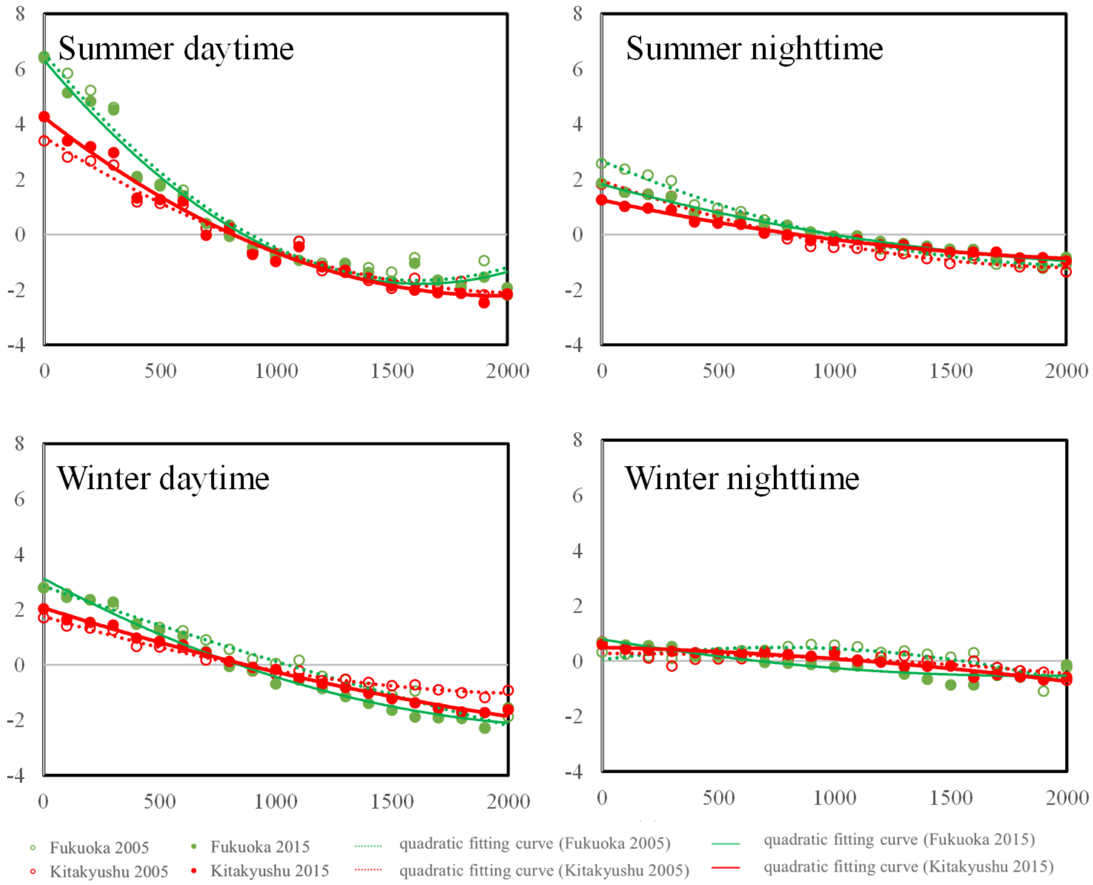

Fig. 7-15 Relationship between mean SUHII and distance to urban area

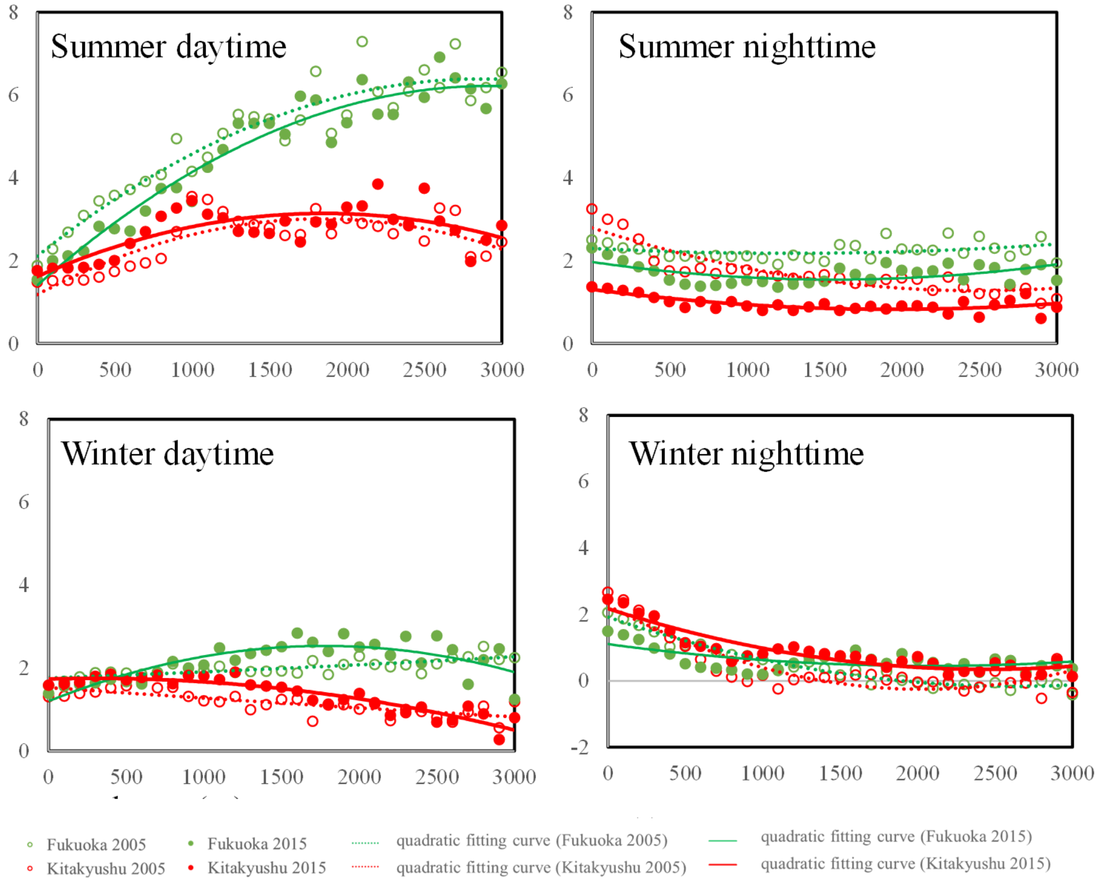

Fig. 7-16 Relationship between mean SUHII and distance to coastal area

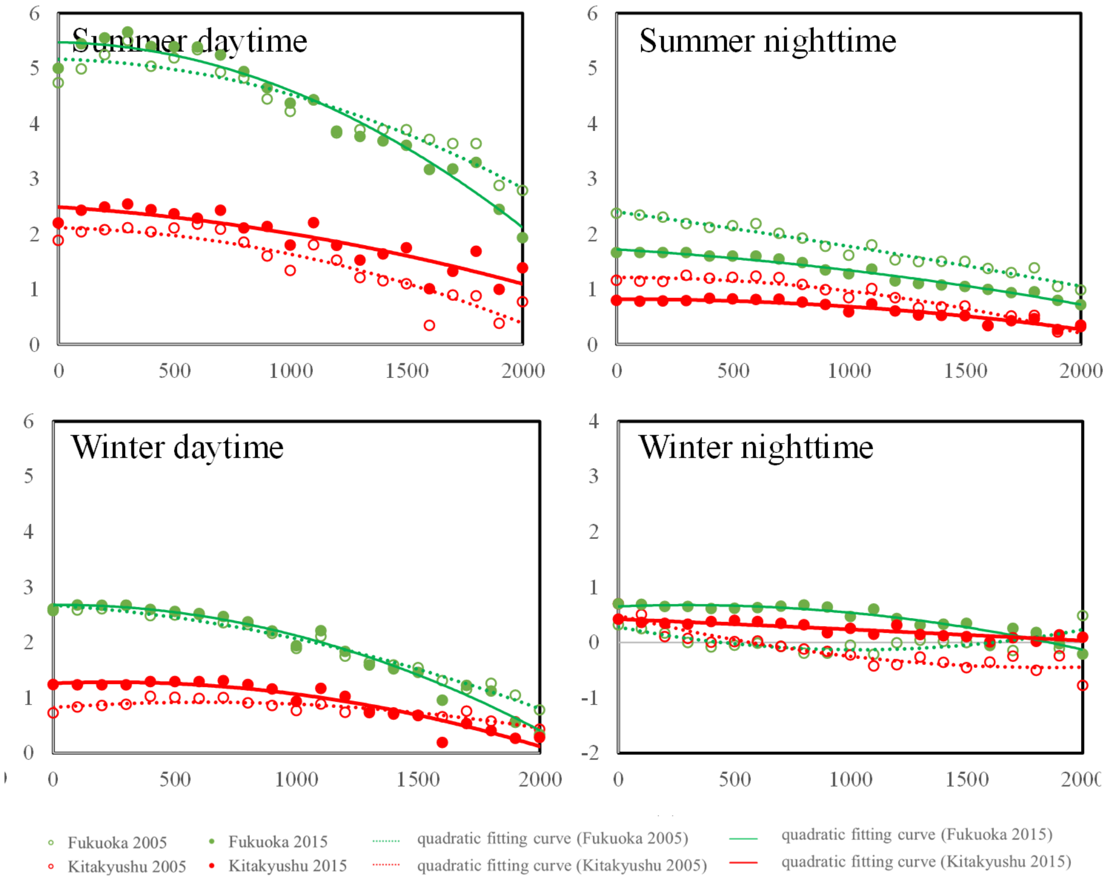

Fig. 7-17 Relationship between mean SUHII and distance to water area

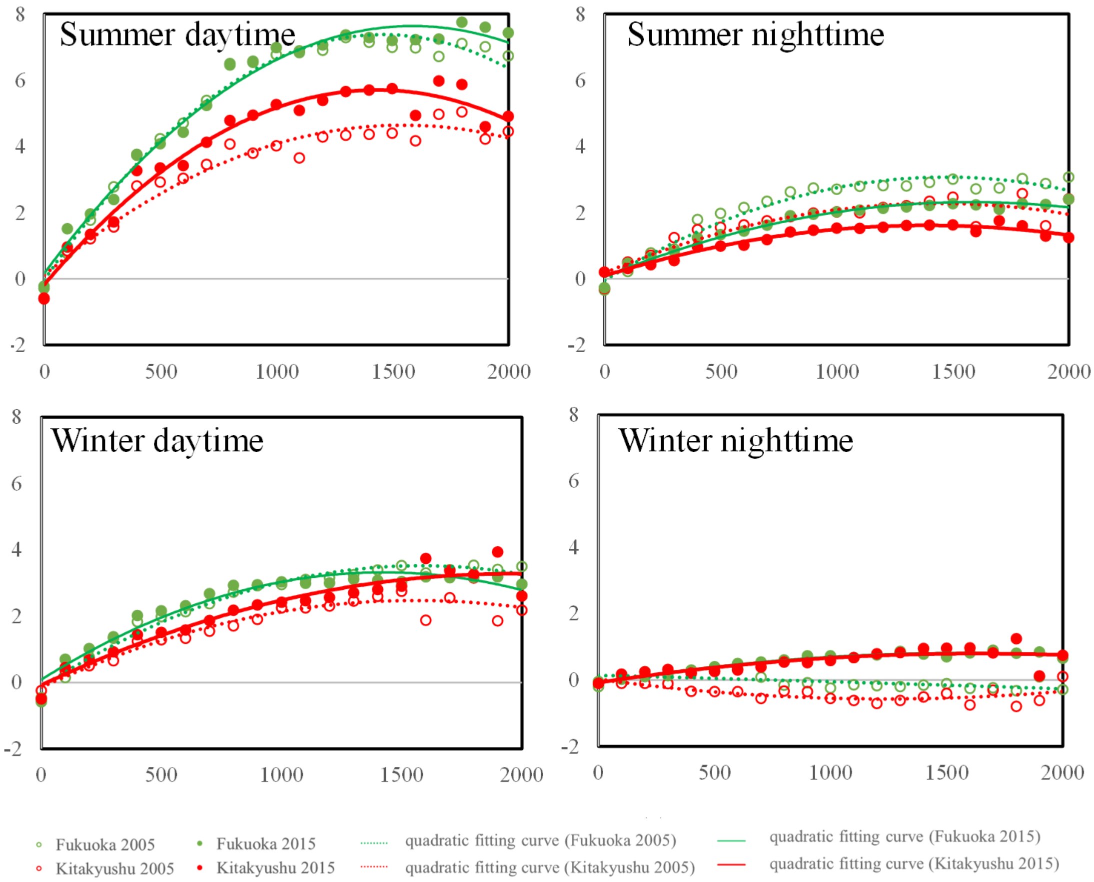

Fig. 7-18 Relationship between mean SUHII and distance to forest

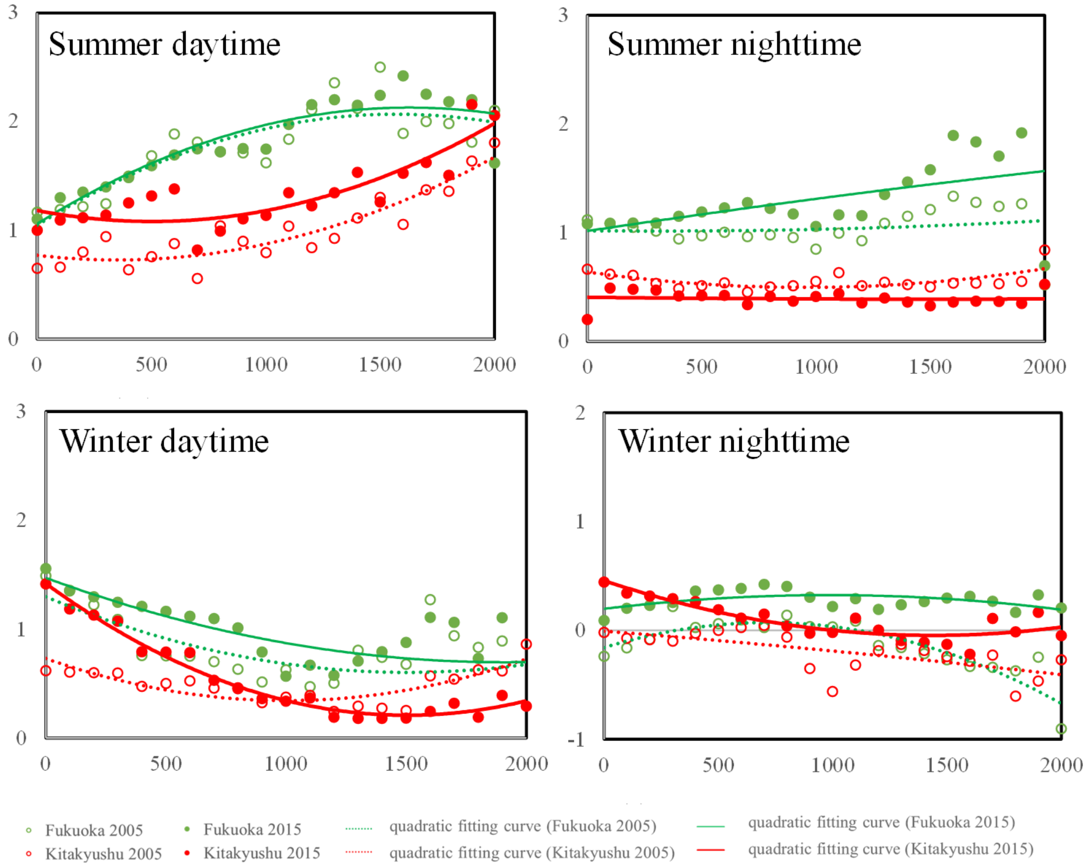

Fig. 7-19 Relationship between mean SUHII and distance to grassland

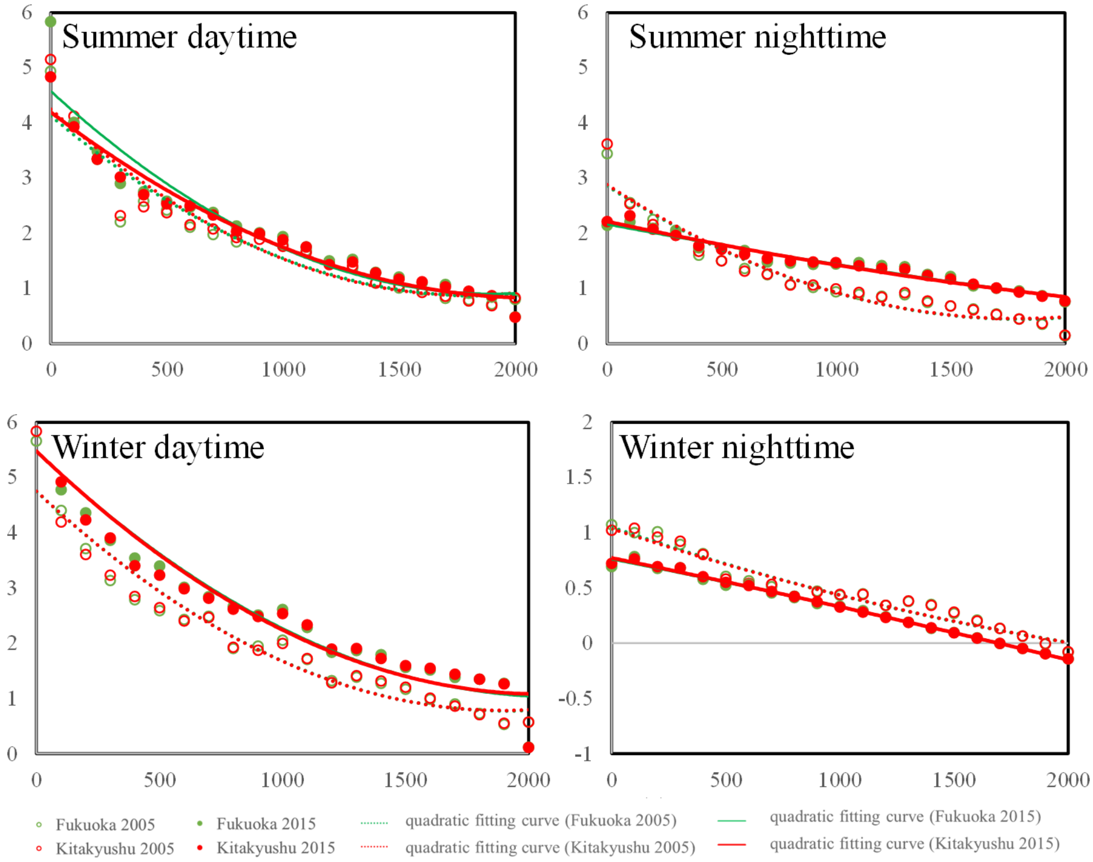

Fig. 7-20 Relationship between mean SUHII and distance to bare land

Then, we extracted the pixels at 0.05 significance level of each LISA map, and the results of the mean SUHII variation with the increase in the population and the distance to each LULC type are shown in Fig. 7-14 to 7-20. The mean SUHII variation with the increase of the populations shows the strong linear correlation between urban population and urban thermal environment, especially during the summer daytime, summer nighttime, and winter daytime. In contrast, the population effect on SUHII is not obvious in winter nighttime. The mean SUHII increased rapidly first then slowed down when the populations in a gird reaches about 800. However, the not obvious effect of the population during winter nighttime might due to the effect of the high LST of the coast area.

For the LULC effect on the SUHI, in general, the sea and the forests have strong cooling potential, then comes to water and grassland; On the contrary, urban area and bare land will increase the SUHI. Meanwhile, we observed that there are significant differences in the effects of LULC on the SUHI in different study periods. More specifically, at first, with the distance to the urban area increased to the mean SUHII dropped rapidly, and when it is below -1 K, the variation of mean SUHII is not apparent. The fitting curves in winter nighttime are different from the other periods, which could be explained by the high LSTs in the coastal areas. Meanwhile, the SUHII variation trends for the bare land are similar to that for the urban area. The great decrease of mean SUHII with the distance to the urban area or bare land increases implies that the aggregation of the urban area or the bare land could be a significant factor for the SUHI. Secondly, the results show the converse trends between the SUHII variation with the distance to the coastal area increase during the daytime and that during nighttime.

Table 7-4. The cooling effect of the LST and distance for the urban blue-green spaces.

LULC type	Area	summer daytime		summer nighttime		winter daytime		winter nighttime	
	(ha)	LST (K)	Distance (km)	LST (K)	Distance (km)	LST (K)	Distance (km)	LST (K)	Distance (km)
Coast	988.89	2.79	1.0-1.3	-0.95	1.1-1.3	0.48	0.6-0.8	-1.9	0.8-1.0
Forest	5267.48	6.32	1.0-1.3	2.32	0.9-1.3	3.71	1.0-1.4	0.37	0.5-0.7
Water	299.25	0.61	0.3-0.4	-0.08	0.2-0.4	0.12	0.3-0.4	-0.3	0.3-0.6
Grassland	2734.88	0.51	0.3-0.7	0.03	0.4-0.7	-0.27	0.3-0.4	0.08	0.3-0.7

During the daytime, although the mean SUHII of the coastal areas is about 2 K, the SUHII increased rapidly with the distance to coast increases, which indicates a substantial urban cooling effect benefits from the coastal areas. Thirdly, the first turning point of the mean SUHII variation with the increase in the distance to the water is found at about 300 m during the four study periods. The seasonal characteristics are clear that the variation of the mean SUHII is the largest during summer daytime. Fourthly, the cooling effect of the forests on the surrounding is clear during the eight periods, especially in summer daytime. The daytime characteristics for the SUHII variation for the forest are similar to the coast area, while the nighttime characteristics are the opposite. The mean SUHII change is occurring at about 1.5 km to the forest area with about 6 K SUHII variation in the summer daytime, 2 to 3 K SUHII variation in the summer nighttime and winter daytime, 0.5 K SUHII variation in the winter nighttime. Fifthly, the SUHII changes of green areas vary from 300 m to 600 m. However, the cooling potential is relatively small for the small changing scale of the SUHII variation and flat fitting curves.

Previous studies have intensively focus on the urban cooling effect of the urban green-blue spaces

[30-33].

However, the spatial heterogeneity of the cooling effect was often ignored. In this study, considering the spatial heterogeneity, we extracted the pixels which showed significant spatial correlation with neighboring pixels through the bivariate spatial correlation analysis and then explored the cooling effect of the urban green-blue spaces. The size and the type of urban blue-green spaces have great differences in the cooling potential for the UHI. In general, with the increase in the area of urban blue-green spaces, the increase in the temperature and the distance of urban cooling effect could be observed. We summarized the average urban cooling effect of the LST and the distance in the area for the sea, forest, water body, and grassland, shown in Table 7-4. The cooling effect of forest and sea (evaluated through coast area) are stronger than that of water and grassland both in LST and distance. The topography of the area, which is characterized by sea surrounding on three sides and over 40% forest cover, could be an essential reason account for the sea and forests to play significant roles in relieving urban heat island, while grassland and water bodies have relatively small roles.

7.5 Summary

In this study, we developed RF models to downscale the MODIS LST products during eight periods in Fukuoka, Japan. Then we captured the spatial correlation between the population, the LULC, and the LSTs, and explored the cooling effect potential of the urban blue-green spaces. Our findings are as follows: (1) The downscaled LST results showed good fitting performance of the RF model. With such downscaling methods, analysis on the SUHI and its correlates could be spatial-temporal precisely in a cloudy, rainy area using remote sensing data. (2) Through the bivariate global and local Moran's I tests, the number of population and the LULC were found significantly spatial correlated with the LSTs in summer and winter both in day and night. This finding implied that the LULC could have an impact on the LST of its surrounding neighbors, and which also is the basis for investigating the cooling effect of the urban blue-green spaces. (3) Through zonal statistics, the forest and sea could significantly mitigate the UHI in its approximate 1 km buffer zone, while the mitigation effect of the water and the grassland on the UHI are less spectacular compared with the forest and sea. The urban land in the area is mainly distributed in the coastal areas, and the policies of restricting the development of forests have been adopted, which is an important reason for the relatively low SUHII during summer nighttime and winter daytime, and no obvious SUHI during winter nighttime. The findings contribute to improving our understanding of the spatial temporal variation and the correlates of UHI, and provide valuable information for governments and planners to developing effective coping migration strategies for the UHI considering the perspective of the local environment.

References

[1] T. R. Oke, "The energetic basis of the urban heat island," Quarterly Journal of the Royal Meteorological Society, vol. 108, no. 455, pp. 1-24, 1982.

[2] A. Qaid, H. B. Lamit, D. R. Ossen, and R. N. R. Shahminan, "Urban heat island and thermal comfort conditions at micro-climate scale in a tropical planned city," Energy and Buildings, vol. 133, pp. 577-595, 2016.

[3] X. Yang et al., "Impact of urban heat island on energy demand in buildings: Local climate zones in Nanjing," Applied Energy, vol. 260, p. 114279, 2020.

[4] A. Aboelata and S. Sodoudi, "Evaluating urban vegetation scenarios to mitigate urban heat island and reduce buildings' energy in dense built-up areas in Cairo," Building and Environment, vol. 166, p. 106407, 2019.

[5] J. Tan et al., "The urban heat island and its impact on heat waves and human health in Shanghai," International journal of biometeorology, vol. 54, no. 1, pp. 75-84, 2010.

[6] T. R. Oke, "City size and the urban heat island," Atmospheric Environment (1967), vol. 7, no. 8, pp. 769-779, 1973.

[7] Q. Meng, L. Zhang, Z. Sun, F. Meng, L. Wang, and Y. Sun, "Characterizing spatial and temporal trends of surface urban heat island effect in an urban main built-up area: A 12-year case study in Beijing, China," Remote Sensing of Environment, vol. 204, pp. 826-837, 2018.

[8] J. Corburn, "Cities, climate change and urban heat island mitigation: Localising global environmental science," Urban studies, vol. 46, no. 2, pp. 413-427, 2009.

[9] A. Onishi, X. Cao, T. Ito, F. Shi, and H. Imura, "Evaluating the potential for urban heat-island mitigation by greening parking lots," Urban forestry & Urban greening, vol. 9, no. 4, pp. 323-332, 2010.

[10] A. Synnefa, A. Dandou, M. Santamouris, M. Tombrou, and N. Soulakellis, "On the use of cool materials as a heat island mitigation strategy," Journal of Applied Meteorology and Climatology, vol. 47, no. 11, pp. 2846-2856, 2008.

[11] H. Tran, D. Uchihama, S. Ochi, and Y. Yasuoka, "Assessment with satellite data of the urban heat island effects in Asian mega cities," International journal of applied Earth observation and Geoinformation, vol. 8, no. 1, pp. 34-48, 2006.

[12] Q. Weng, D. Lu, and J. Schubring, "Estimation of land surface temperature–vegetation abundance relationship for urban heat island studies," Remote sensing of Environment, vol. 89, no. 4, pp. 467-483, 2004.

[13] A. R. dos Santos et al., "Spatial and temporal distribution of urban heat islands," Science of the Total Environment, vol. 605, pp. 946-956, 2017.

[14] Q. Weng, P. Fu, and F. Gao, "Generating daily land surface temperature at Landsat resolution by fusing Landsat and MODIS data," Remote sensing of environment, vol. 145, pp. 55-67, 2014.

[15] F. Gao, J. Masek, M. Schwaller, and F. Hall, "On the blending of the Landsat and MODIS surface reflectance: Predicting daily Landsat surface reflectance," IEEE Transactions on Geoscience and Remote sensing, vol. 44, no. 8, pp. 2207-2218, 2006.

[16] K. Zakšek and K. Oštir, "Downscaling land surface temperature for urban heat island diurnal cycle analysis," Remote Sensing of Environment, vol. 117, pp. 114-124, 2012.

[17] N. Agam, W. P. Kustas, M. C. Anderson, F. Li, and C. M. Neale, "A vegetation index based technique for spatial sharpening of thermal imagery," Remote Sensing of Environment, vol. 107, no. 4, pp. 545-558, 2007.

[18] L. Cheng, D. Guan, L. Zhou, Z. Zhao, and J. Zhou, "Urban cooling island effect of main river on a landscape scale in Chongqing, China," Sustainable Cities and Society, vol. 47, p. 101501, 2019.

[19] H. Swaid, "Urban climate effects of artificial heat sources and ground shadowing by buildings," International Journal of Climatology, vol. 13, no. 7, pp. 797-812, 1993.

[20] Y. Kikegawa, Y. Genchi, H. Kondo, and K. Hanaki, "Impacts of city-block-scale countermeasures against urban heat-island phenomena upon a building’s energy-consumption for air-conditioning," Applied Energy, vol. 83, no. 6, pp. 649-668, 2006.

[21] S. Mukherjee, P. Joshi, and R. Garg, "A comparison of different regression models for downscaling Landsat and MODIS land surface temperature images over heterogeneous landscape," Advances in Space Research, vol. 54, no. 4, pp. 655-669, 2014.

[22] C. Hutengs and M. Vohland, "Downscaling land surface temperatures at regional scales with random forest regression," Remote Sensing of Environment, vol. 178, pp. 127-141, 2016.

[23] H. Ikemi, "Geologically constrained changes to landforms caused by human activities in the 20th century: A case study from Fukuoka Prefecture, Japan," Applied Geography, vol. 87, pp. 115-126, 2017.

[24] Y. Kawamoto, "Effect of land-use change on the urban heat island in the Fukuoka–Kitakyushu metropolitan area, Japan," Sustainability, vol. 9, no. 9, p. 1521, 2017.

[25] L. Breiman, "Random forests," Machine learning, vol. 45, no. 1, pp. 5-32, 2001.

[26] L. J. G. a. Anselin, "Local indicators of spatial association—LISA," vol. 27, no. 2, pp. 93-115, 1995.

[27] E. Forey, C. J. Lortie, and R. Michalet, "Spatial patterns of association at local and regional scales in coastal sand dune communities," Journal of Vegetation Science, vol. 20, no. 5, pp. 916-925, 2009.

[28] J. Tu, "Spatial variations in the relationships between land use and water quality across an urbanization gradient in the watersheds of northern Georgia, USA," Environmental management, vol. 51, no. 1, pp. 1-17, 2013.

[29] R. C. Deo and M. Şahin, "Forecasting long-term global solar radiation with an ANN algorithm coupled with satellite-derived (MODIS) land surface temperature (LST) for regional locations in Queensland," Renewable and Sustainable Energy Reviews, vol. 72, pp. 828-848, 2017.

[30] Z. Xue et al., "Quantifying the cooling-effects of urban and peri-urban wetlands using remote sensing data: Case study of cities of Northeast China," Landscape and urban planning, vol. 182, pp. 92-100, 2019.

[31] X. Cheng, B. Wei, G. Chen, J. Li, and C. Song, "Influence of park size and its surrounding urban landscape patterns on the park cooling effect," Journal of Urban Planning and Development, vol. 141, no. 3, p. A4014002, 2015.

[32] F. Kong, H. Yin, P. James, L. R. Hutyra, and H. S. He, "Effects of spatial pattern of greenspace on urban cooling in a large metropolitan area of eastern China," Landscape and Urban Planning, vol. 128, pp. 35-47, 2014.

[33] R. Sun and L. Chen, "How can urban water bodies be designed for climate adaptation?," Landscape and Urban Planning, vol. 105, no. 1-2, pp. 27-33, 2012.

Chapter 8. Comparison of urban development and thermal environment in China and Japan

8.1 Introduction

Urban development was first proposed from a population perspective. Specifically, urbanization refers to the inflow of population from rural areas to large cities and the concentration of population in cities. It refers to the increase in the proportion of population in urban areas. On the other hand, city shrinkage refers to the decrease in the population of cities.

However, the urban development contains many aspects, so its interpretation has begun to extend to other aspects. From social aspects, urban development refers to changes in the lifestyles of urban and rural residents. From geographical aspects, it refers to the organization and development of existing cities, streets, and regions, changes in urban areas, the formation and changes of relationships between cities, and the formation of large cities. From economic aspects, the essence of urban development is the transformation of the city's economic structure [1-4].

Hence, due to the multi-dimensional characteristics of urban development, the classification of the urban development type (urbanization or shrinkage) of city may be different. For example, a number of Chinese cities, such as Nantong, Zhoushan, Zhongshan, the variation of the GDP, economic structure, built-up area, city infrastructure all show that the cities were in the stage or urbanization from 2000 to 2010, while the population decreased in the period. Because China is now in a period of rapid development, such socio-economic related data of cities may still be growing with a lower than the regional or national average growth rate. Previous studies on urban development using hysteresis effect showed that the urban indicators often lags behind population change.

On the other hand, due to differences in statistical indicators and differences in statistical calibers of the same indicators, the use of demographic, social and economic indicators may lead to incomparable urban development between China and Japan. Therefore, this study takes population change of a city as the criterion for judging the stage of urban development, and establishes a numerical regression relationship between population and other indicators to comprehensively evaluate and compare urban development between China and Japan.

With the process of urbanization, air pollution in the city, large-scale sinking of the ground, damage to the ground landscape, domestic garbage, urban heat island effect and other urban environmental problems have affected the normal life and health of urban residents. In the past, the Japanese government neglected the health of residents in pursuit of economic development, resulting in many urban pollution problems, and some of them have now been resolved. On the contrary, China is now in a period of rapid development, and there are also many urban pollution problems that need to be solved, such as pm2.5, garbage problems, and water pollution.

This study compared the urban heat island between China and Japan cities to compare the environmental implications of cities in different urban development stages. There are several reasons for choosing the heat island as a comparison. Firstly, the heat island effect is a problem faced by all cities in China and Japan. It is accompanied by potential impacts on urban energy consumption, human health, and urban structure. Secondly, the heat island can be directly obtained through remote sensing data, and conduct large-scale and high-precision temporal-spatial analysis combined with GIS technology. Thirdly, for example, the comparison of water pollution and air pollution needs to base on local measured data. There are differences in statistical calibers and standards. These data are difficult to obtain and are less comparable. Fourthly, due to the different strategies and experiences of urban development, the urban environmental problems experienced are quite different, and the reference for comparison may not be significant.

8.2 Comparison of urban development between China and Japan

8.2.1 Urban development in China

The urbanization process of modern China started after the Opium War in 1840. However, due to the social nature of China in a semi-feudal and semi-colonial era at that time, China had no sovereignty outside and no independence at home, so urbanization was in its infancy for a long time until the founding of the People's Republic of China in 1949. Since 1949, the urbanization level of China has continued to increase, with urban population ratio increasing from 10.6% in 1949 to 59.1% in 2018 (Fig. 8-1). Although during this period, the social turmoil caused by the Great Leap Forward and the Cultural Revolution caused the level of urbanization to stagnate or lag behind. After the implement of Reform and Opening up Policy, China's economy and urbanization developed rapidly. Later, after the socialist market economic system in China was determined in 1992, the development of the economy and urbanization entered a faster development phase. Until now, China is still in a rapid urbanization phase. In various time periods, due to the influence of factors such as policy, economy, and era background, the urban development process has its own characteristics, so it is necessary to explain the development process of modern urbanization in China.

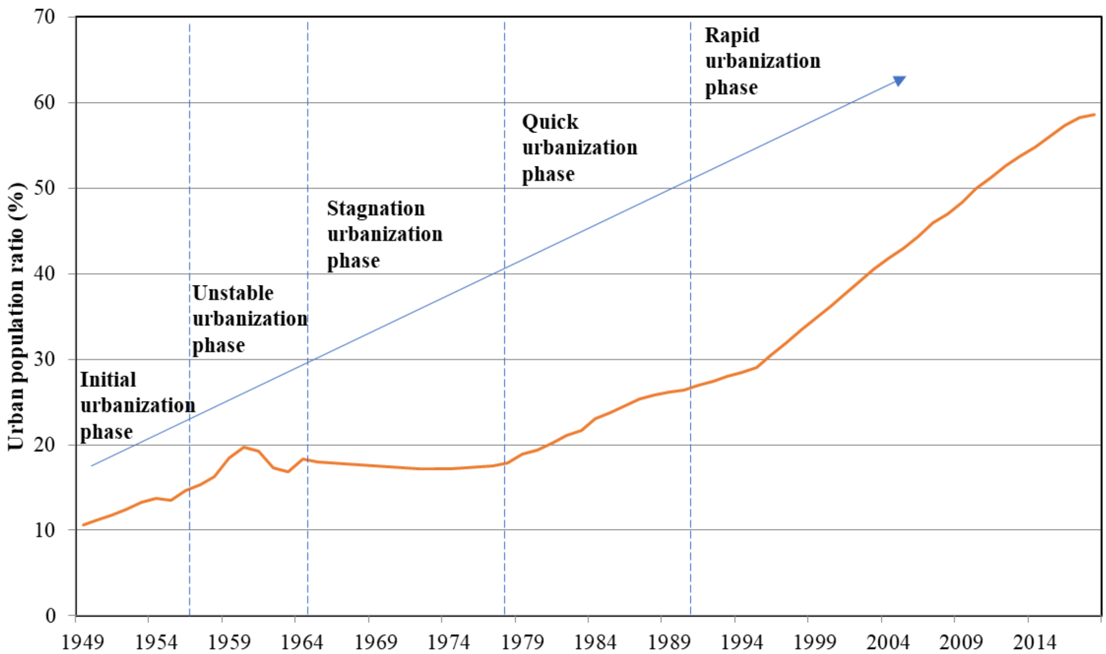

Fig. 8-1 Urban population ratio and urban development phases of China since 1949.

Initial urbanization stage (1949-1957)

Since 1949, the foundation of the People’s Republic of China, China enters its initial urbanization stage. During this period, China mainly develops the coal industry, and some cities with rich coal resources have been established, such as Jiaozuo, Pingdingshan, and Anshan. In addition, the original old cities continued to develop and improve urban functions, such as Taiyuan, Wuhan, and Lanzhou.

At the same time, a number of large and medium cities also appeared. From 1949 to 1957, the urban population ratio increased from 10.6% to 15.4%, and the urban population increased from 57.7 million to 98.9 million. During this time, the Chinese development strategy proposed was to shift from agriculture to heavy industry. At this stage, the development of major urbanization is also concentrated in cities that are dominated by heavy industry. These cities and their heavy industrial enterprises attract large numbers of rural migrants.

Unstable urbanization phase (1958-1965)

Since 1958, China began its second five-year plan. From 1958 to 1960, China entered a period of great leap forward. At this stage of urban development centered on heavy industry and steel industry. However, due to the people's commune movement, agricultural development has shrunk dramatically, and grain output has been greatly reduced.

In this context, the government did not adopt a timely and effective confrontation strategy. During this period, the rural population still flooded into urban for employment, resulting in an increasing urban population and increasing the burden on urban public facilities and infrastructure. In addition to the tight supply of grain and other developmental disorders of industry and agriculture. During this time, the population also showed negative growth. Since 1961, the government has adopted certain strategies to deal with such mistakes. That is to adjust the economic structure, mobilize new rural residents who have entered the city to return to the countryside, and let some urban residents go to the countryside. During this time, the urban population decreased by about 10.5 million, and the urban population ratio also dropped from 19.3% to 16.8%.

Stagnation urbanization phase (1966-1978)

The background of this period was the Cultural Revolution. Under this background, China's urbanization process was severely hindered. This was also a period of dis-urbanization or urban shrinkage, with the urban population ratio reduced from 17.9% in 1966 to 17.6% in 1977. During this period, over 15 million urban youth were forced to immigrate to rural areas. Moreover, the government contributed to construct cities in the northwest, central, southwest parts where is less developed. These regions have not attracted labor from rural areas, and the process of urbanization has also been relatively stagnant.

Quick urbanization phase (1979-1991)

With the effective implementation of the reform and opening policy, Chinese cities have begun to enter a quick urbanization phase. Due to the export-oriented economic development strategy, the aggregation effect led to the concentration of people and material resources in the city. The city began to expand in size and began to appear as a prototype of the urban agglomeration. The central city began to show some radiation to the surrounding cities. The urban population ratio reached 26.9% in 1991.

Rapid urbanization phase (1992-now)

In 1992, China government defined the framework of the socialist market economic system. As the center of economic development, cities have entered a stage of rapid development. After that, coordinated development between large, medium and small cities was also proposed. This gradually developed the Beijing urban agglomeration centered on Beijing, the Yangtze River Delta urban agglomeration centered on Shanghai, and the Pearl River Delta urban agglomeration centered on Guangzhou and Shenzhen.

8.2.2 Urban development in Japan

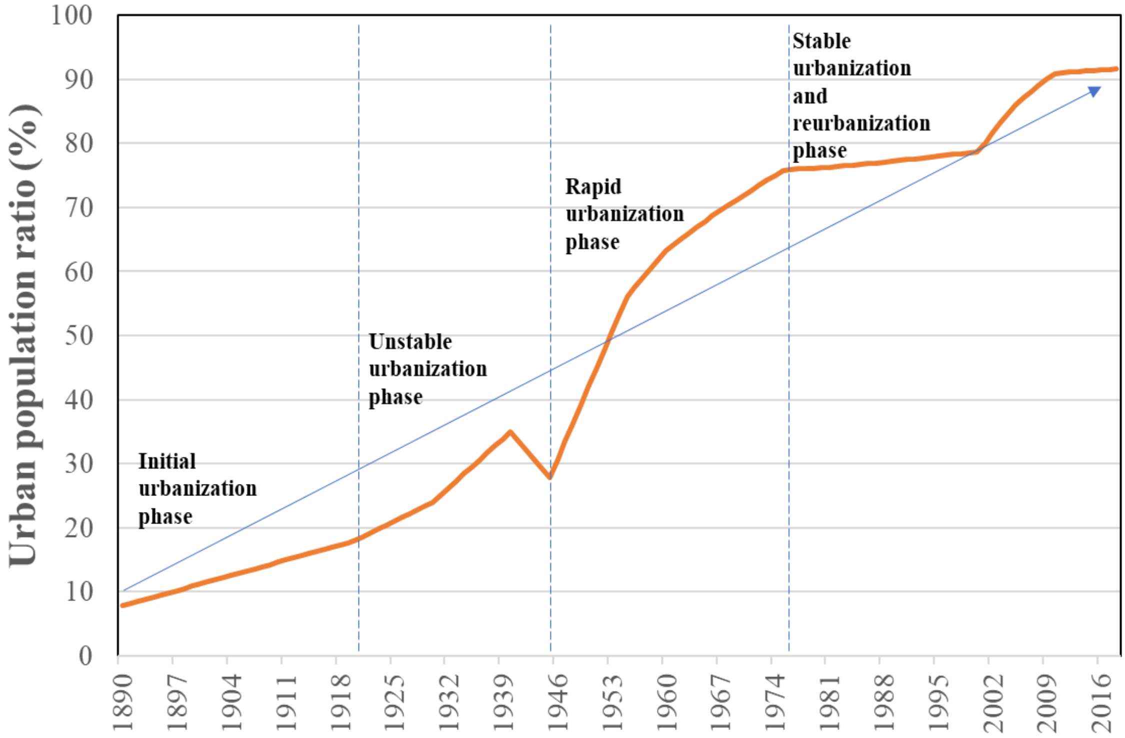

Fig. 8-2 Urban population ratio and urban development phases of Japan since 1890.

Now, as a developed country, Japan 's urbanization rate has exceeded 90%, and it has entered a stable urbanization stage. The urbanization process can be divided into the following four stages. Japan's industrialization began with the Meiji Restoration in 1868. The development of industrialization drove the process of urbanization. Although urbanization began to develop during this period, it still lags behind the European and American industrialized countries in the same period. After the World War 2, Japan's economy grew rapidly and entered a period of rapid urbanization, which reached the urbanization and industrialization process of European and American developed countries that lasted more than 100 years within 30 years.

Initial urbanization stage (1868-1920)

Japan's industrialization began with the Meiji Restoration in 1868. Since Meiji Restoration, Japan 's economic structure has shifted from agriculture-based to industry-based. The cities were inoculated with a large population, and the urban population ratio has increased to about 25% in 1930s.

Unstable urbanization phase (1920-1945)

The rapid development of industry at this stage has greatly driven the migration of rural population to cities, and the characteristics of population migration to heavy industrial cities have become more obvious. Until 1940, Japan's urbanization rate reached 35%. However, during World War II, in order to restore agriculture, a large amount of labor was relocated to the countryside, and the process of urbanization was delayed.

Rapid urbanization phase (1946-1977)

Since 1950, Japan has entered a stage of rapid economic growth and rapid urbanization after the war. During the golden period of Japanese industrial development from 1956 to 1973, industrial production grew at an average annual rate of 13.6% during 18 years.

During the World War 2, many cities in Japan have been destroyed. Unemployment has skyrocketed, people's living standards have declined, and the achievements of industrialization since the Meiji Restoration have been destroyed. The turning point of Japan's development appeared in the Korean War that began in the 1950s. During the period, as a material base, Japan took advantage of this opportunity to start rapid urban development.

After 1955, due to Japan's one-sided pursuit of the speed of industrial development, the city's environmental protection issues were not taken seriously, and residents' lives and physical health were in crisis. From 1966 to 1970, with the rapid development of industry, serious environmental pollution and public hazards occurred in Japan, which endangered the health of residents. Environmental pollution in Japan includes mercury poisoning, cadmium poisoning, air pollution, water pollution, noise problems, garbage pollution and so on. The Japanese government has also formulated various environmental protection laws and regulations to strictly improve environmental hygiene.

Stable urbanization and reurbanization phase (1978-now)

During the period, Japan 's economic growth has slowed, the output value of the secondary industry in the GDP has declined year by year, and the tertiary industry has gradually become the most important part of the national economy. In the 1970s, due to the collapse of the Bretton Woods system and the two oil crises, Japan 's economic development was greatly affected. The economic growth rate was reduced from two digits to one digit, and the Japanese government had to make corresponding adjustments. The factory is still moving from the city to the countryside and from the country to the Asian countries. Japanese industries have also shifted from industries such as automotive steel to emerging industries such as electronics.

Japan 's economic growth has slowed, the output value of the secondary industry in the GDP has declined year by year, and the tertiary industry has gradually become the most important part of the national economy. In the 1970s, due to the collapse of the Bretton Woods system and the two oil crises, Japan 's economic development was greatly affected. The economic growth rate was reduced from two digits to one digit, and the Japanese government had to make corresponding adjustments. The factory is still moving from the city to the countryside and from the country to the Asian countries. Japanese industries have also shifted from industries such as automotive steel to emerging industries such as electronics.

After 2000, due to the low birth rate and strict immigration system, Japan began to enter the ageing era, and the population began to decline. In this era, a large number of shrinking cities appeared in Japan. To deal with this phenomenon, the government proposed the concept and strategy of compact cities for urban regeneration. A number of cities including Sapporo, Wakkanai, Aomori, Sendai, Toyam, Toyohashi, Kobe, and Kitakyushu, adopted compact city as a policy.

8.2.3 Comparison of urban development

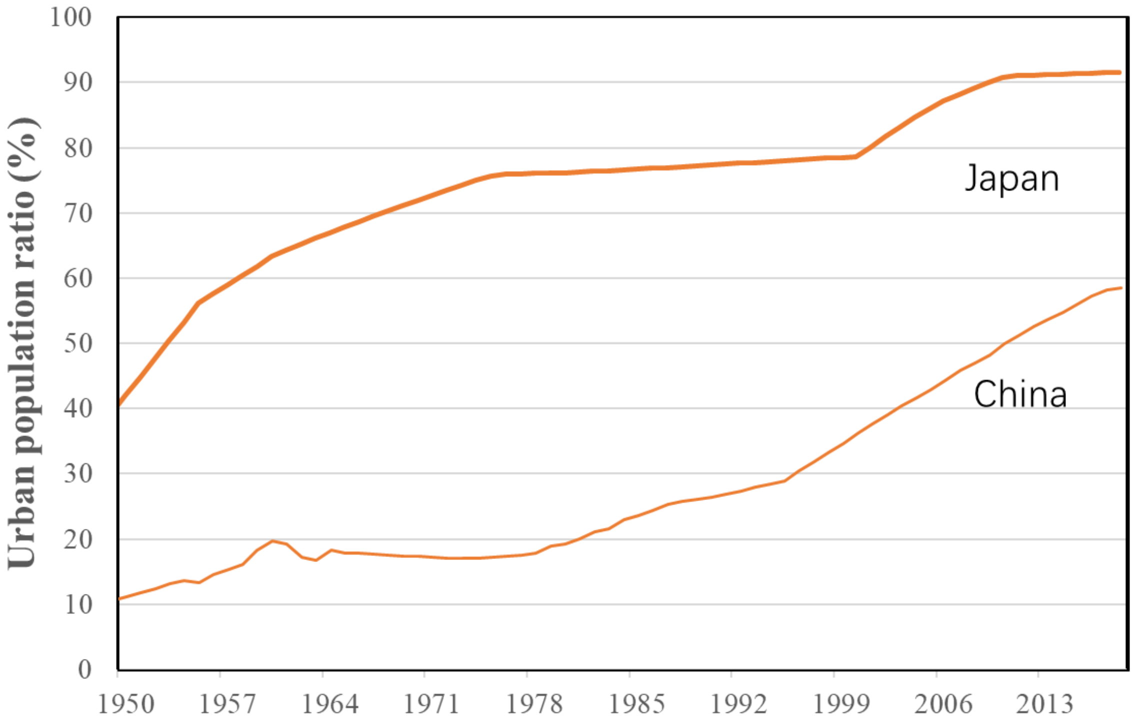

Fig. 8-3 Urban population ratio between China and Japan from 1950 to 2018

As Fig. 8-3 shows, the urban population ratio of China and Japan all show increasing trends. However, Japan's urban population ratio has always been significantly ahead of China. Now Japan's urban population ratio has exceeded 90%, while China's urban population ratio is only 59%. In the process of urban development, both countries have experienced unstable development and reverse urbanization, all due to the social background at the time. In the period of rapid urbanization phase, the social environment of China and Japan was relatively stable at that time, and during this period, large urban aggregations began to appear, such as Tokyo Metropolitan Area, Osaka Metropolitan Area, and Nagoya Metropolitan Area in Japan, the Yangtze River Delta, Pearl River Delta, and Beijing city cluster in China.

At present, the stages of urban development in China and Japan are very different. In chapter 3 and

4, we discussed the urbanization of China and the city shrinkage in Japan. According to the China City Statistical Yearbook data in 2005, 2010, and 2015, 51.6% cities experienced continuous population increase, and 28.6% cities experienced temporal population increase during 2005 to 2015, while only 19.8% cities population continuously decrease during the period. While in Japan, 71.9% municipalities experienced continuous shrinkage, and 13.6% municipalities experienced temporal shrinkage, while only 14.5% municipalities population continuously increased during the period (Table 8-1.). Meanwhile, the shrinkage is more likely to happen in smaller cities or municipalities both for China and Japan while urbanization is more likely to happen in larger cities.

Table 8-1. Percent of city type in China and Japan from 2005 to 2015

Country	Urbanization	Unstable	Shrinkage
China	51.6%	28.6%	19.8%
Japan	14.5%	13.6%	71.9%

With the SGWR models, the urban development type of a city showed significant correlation with demographic-social-economic factors in previous chapters. Specifically, the demographic factors have a great spatially non-stationary impact on urban shrinkage of cities in Japan, while have a little spatially stationary impact on urbanization in China. The economic factors have a little spatially stationary impact both in China and Japan. In addition, the social factors have great spatially non-stationary impact on urbanization of cities in China while the effect is global and little in Japan.

8.3 Environmental implications between China and Japan

Japan has experienced high growth at the expense of the environment during the urbanization process. However, as the environment deteriorated and environmental awareness increased, Japan took effective measures to overcome environmental constraints and became a model country with significant environmental protection effects. China's long-term high-input and low-output production method also ignores the protection of the environment, causing a lot of waste of resources and environmental pollution. In recent years, environmental problems have gradually become a factor restricting China's development. China's long-term high-input and low-output production method also ignores the protection of the environment, causing a lot of waste of resources and environmental pollution. In recent years, environmental problems have gradually become a factor restricting China's development.

With increasing closely economic and traffic connection among cities, three principal urban agglomerations emerged in China, including the Yangtze River Delta Region, the Peral River Delta Region, and the Beijing city clyster (also known as Beijing-Tianjin-Hebei Region) [5]. The urban built-up areas and the urban environment form a complex system with multiple feedback loops. Hence, it is essential to study the urbanization process and its impact on the urban environment on the urban agglomeration scale instead of a signal city for maintaining a good quality of urbanization and better urban planning strategies.

With rapid urbanization, environmental implications become essential issues for urban planning. Panel data and monitoring stations data were the primary sources for evaluation of environmental implications such as water pollution and air pollution. However, remote sensing (RS) and GIS technologies enable large-scale research of the UHI which are increasingly used in recent UHI studies [6]. Compared with the traditional method for UHI studies of observing meteorological data, which has the limitation that the local meteorological observation points are not able to represent the whole study region, the RS based studies provided high resolution of spatial-temporal information. There are several RS datasets used in UHI studies, including NOAA AVHRR [7-9], ASTER [10, 11], MODIS [12], and Landsat series [13, 14]. However, there are many limitations of the satellite remote sensing approach. One of the most significant weaknesses of remote sensing data is that the data accuracy could affect by could cover. Therefore, two possible solutions including choosing cloud-free images or constructing temporally composited data are mainly adopted to decrease the impact of clouds [7, 15, 16]. Hence, Moderate Resolution Imaging Spectroradiometer (MODIS) LST products have become an increasingly important source in UHI studies for providing land surface temperature (LST) images with 1 km spatial resolution and high temporal resolution (per day) which decrease the clouds impact and make temporal UHI studies available.

In this chapter, in total 60 cities were selected as study area to compare the thermal environment and to further explore the surface urban heat island variation course. The selected 33 Chinese cities and 27 Japanese cities were the most populated cities for the two countries with over at least 0.5 million population (Fig. 8-4).

8.3.1 Urban heat island data source

As urbanization process, natural landscapes were replaced by built-up areas, and thus many environmental problems occurred. The UHI is one of the biggest environmental problems. In this study, the MODIS (Moderate-resolution Imaging Spectroradiometer) LST products were acquired to illustrate the distribution of SUHI and the interrelationship between urbanization and SUHI in the target cities.

The MODIS instrument is located on both the Terra and Aqua NASA satellites. The Terra satellite was launched in December 1999, and TERRA/MODIS LST data were used to investigate the SUHI in the study area from 2000 to 2017. A total of 361 8-day composite (MOD11A2) MODIS LST scenes from 2000 to 2017 at 1 km (930.3 m) spatial resolution were downloaded from the NASA EARTHDATA website (https://search.earthdata.nasa.gov/). The daytime (local time 10:30) LST and nighttime (local time 22:30) LST layers were reprojected into WGS 1984 Transverse Mercator projection and resampled to 1km resolution using the MODIS Reprojection Tool (MRT). Then the summer daytime, summer nighttime, winter daytime, winter nighttime LST maps from 2000 to 2015 were mosaiced by the downloaded scenes. We have used LST data in June, July, and August to describe the summer SUHI and the data in December, January, and February to describe the winter SUHI. Table 8-2. SUHI indicator and its definition

Indicator	Units	Definition in the study
SUHII	°C	Average SUHII of the urban pixels

In this chapter, the indicator was the same for SUHI evaluation in Chapter 7 (Table 8-2). The indicator SUHII uses the mean LST between urban and suburban area. As the UHI can affect an area of 150% of the urban area [17] and excluding the effect by water, the study extracted the urban area of the selected cities from the MODIS land cover product (MCD12Q1) with 500 m spatial resolution were downloaded from the EARTHDATA website (https://search.earthdata.nasa.gov/), and 150% of the urban area excluding water as the urban boundary. The following figure shows the sample of urban boundary extracted from MODIS land cover product (Fig. 8-5).

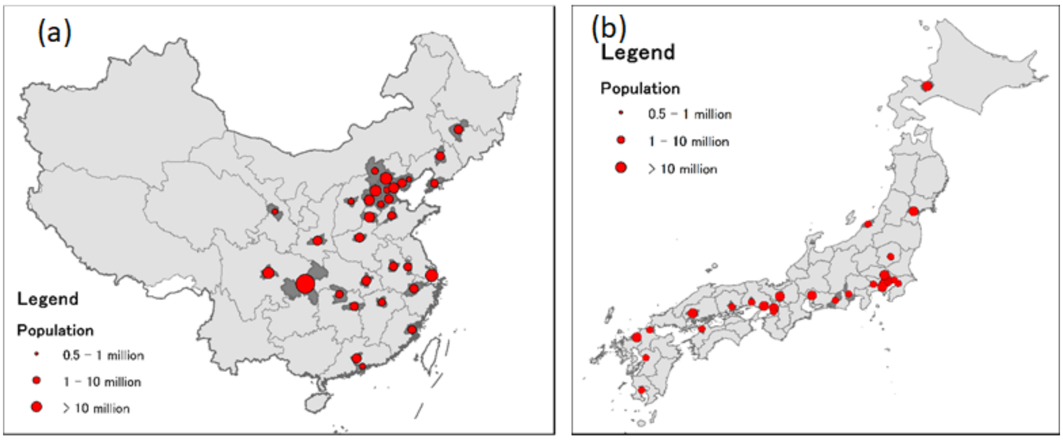

Fig. 8-4 Location of study cities in (a) China, (b) Japan.

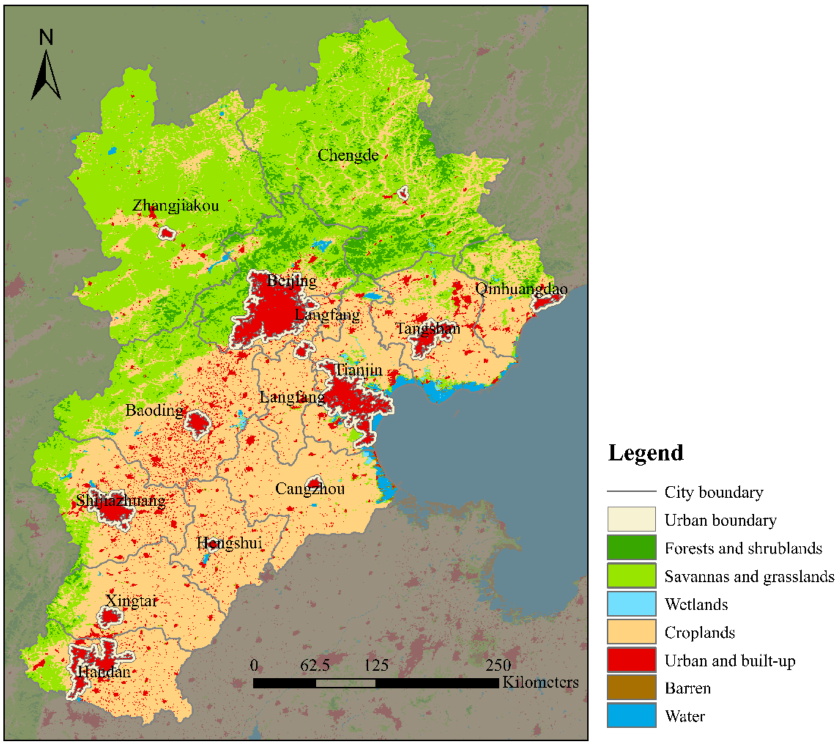

Fig. 8-5 Urban land distribution and urban boundary extraction of the Beijing city cluster in 2015

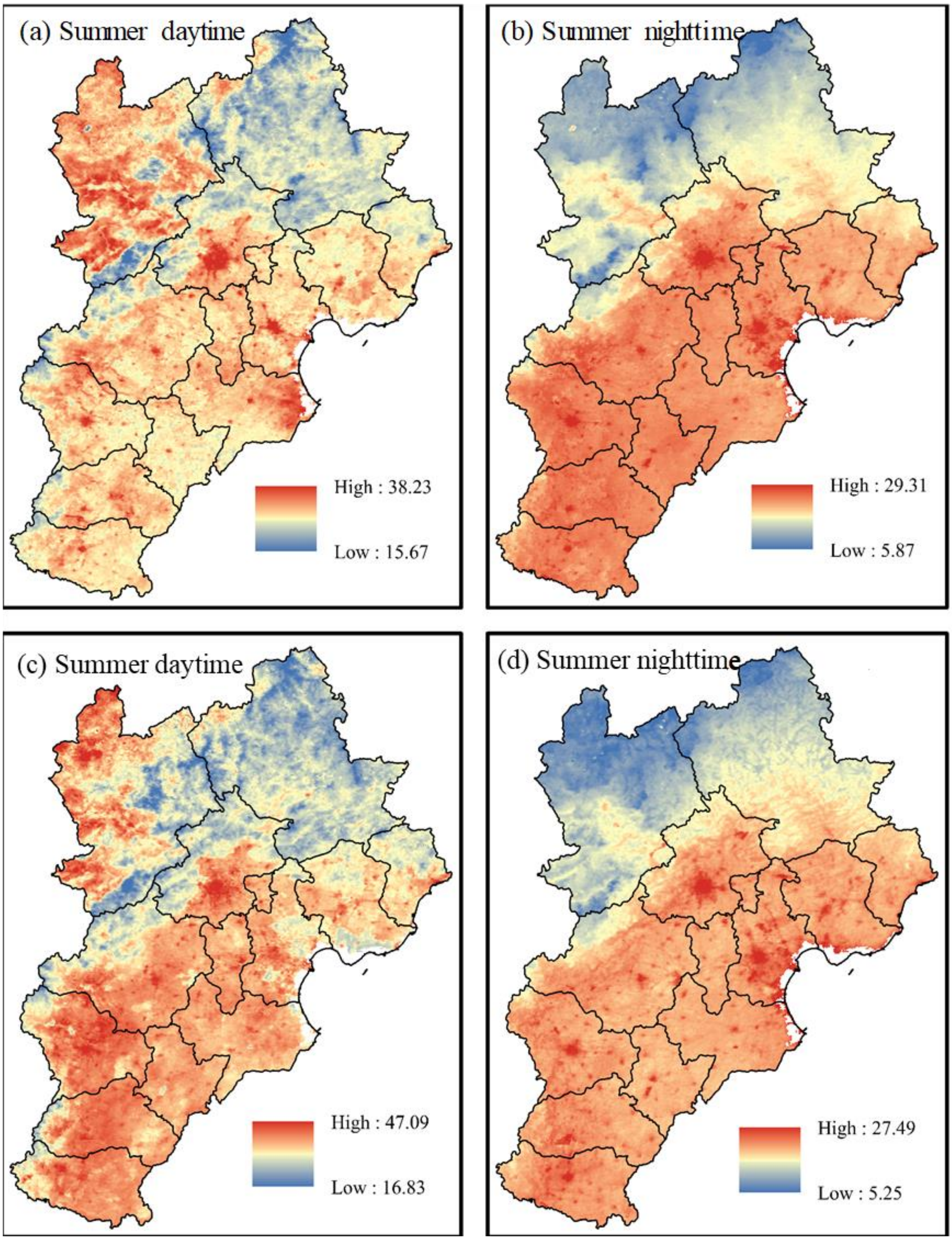

Fig. 8-6 Spatial distribution of LST in Beijing city cluster in 2005 and 2015 (a) LST in summer daytime of 2005, (b) LST in summer nighttime of 2005, (c) LST in summer daytime of 2015, (d) LST in summer nighttime of 2015.

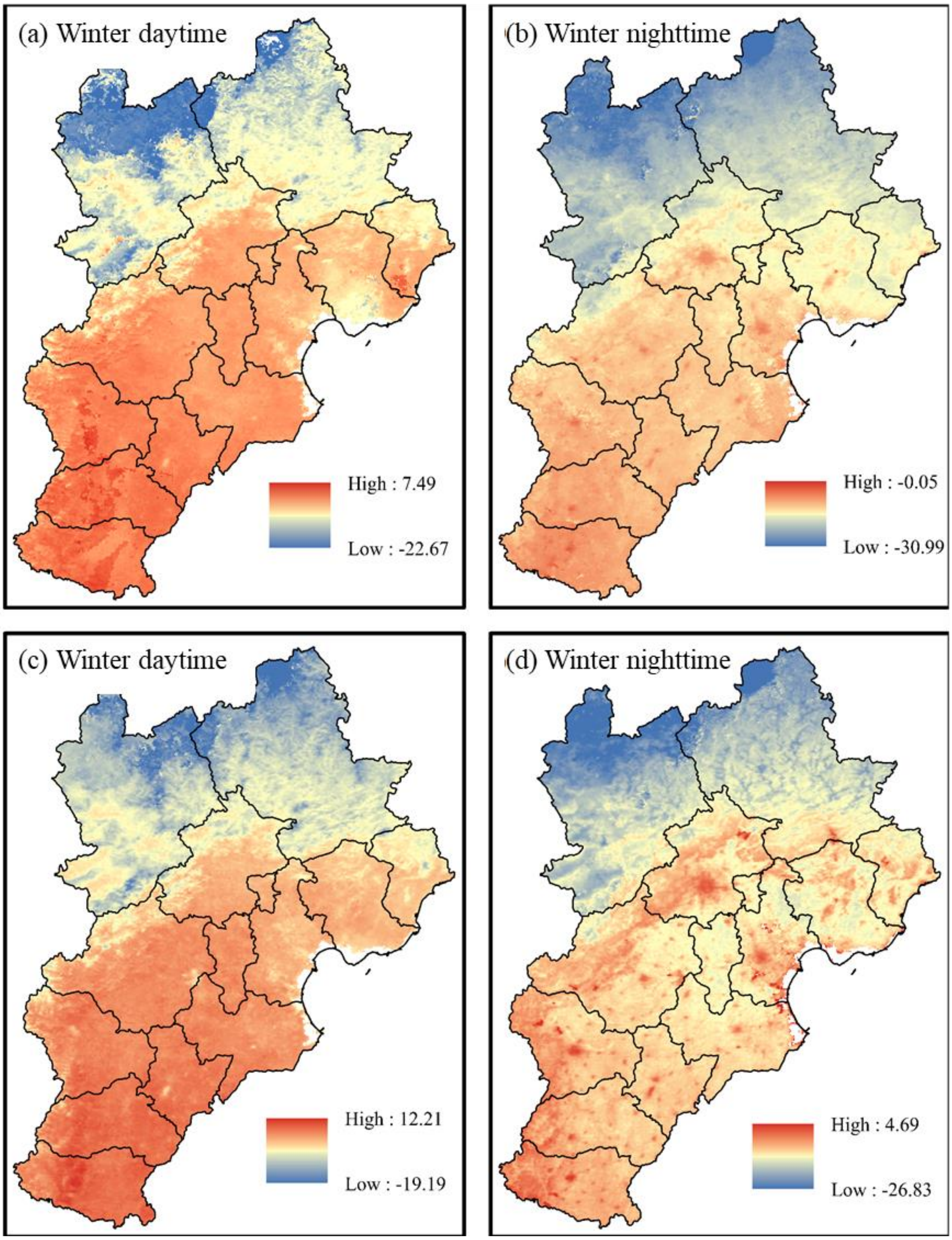

Fig. 8-7 Spatial distribution of LST in Beijing city cluster in 2005 and 2015 (a) LST in winter daytime of 2005, (b) LST in winter nighttime of 2005, (c) LST in winter daytime of 2015, (d) LST in winter nighttime of 2015.

8.3.2 Urban heat island distribution analysis

8-day composite LST scenes from MODIS TERRA LST products were utilized to map the summer and winter LST distribution both in daytime and nighttime from 2005 to 2015. Fig. 8-6 and Fig. 8- show the LST maps in Beijing city cluster in 2005 and 2015. In general, the LST varied temporally and increased with increasing latitude with an extensive range. Specifically, the urban heat island is not significant for cities in the region during winter daytime. While except during winter daytime, the LST in urban areas were significantly higher than that in surrounding rural areas where evident SUHI phenomenon were observed. Meanwhile, the LSTs in 2015 were higher than that in 2005, which indicate a warming phenomenon in the areas.

Fig. 8-8 gives the SUHII of the 60 cities during summer daytime, summer nighttime, winter daytime and winter nighttime in 2005 and 2015. In winter daytime, there is no Gaussian surface can match the LST images for most Chinese cities. The absence of a diacritical SUHI during winter daytime and strong SUHI during winter nighttime in most cities could owe to several reasons. One is related to the coal consumption for heating in north China during winter [18], and another one is related to decrease the incoming short wave solar radiation in urban areas relative to surrounding suburbs [19], which might artificially result in the absent SUHI winter daytime. The results showed increasingly strong SUHI effect in the region as the SUHII of almost all the cities increased, whilst the SUHII had a correlation with the city size. The SUHII in Beijing was the largest. Besides, the SUHII in Chengde was significantly smaller than that in the other cities, which can be explained by the main urban land to the town is located near mountain areas which could results in a mitigation effect of UHI by the forest.

Meanwhile, the results showed all the cities are under significant SUHI phenomena in summer daytime, summer nighttime, and winter nighttime, and the results were consistent with the previous study [20, 21].

The major cities in Japan are located near the sea, and the selected research objects Fukuoka and Kitakyushu have no heat island phenomenon in winter nights, and the heat island intensity in summer nights is much less than that of Chinese cities. On the contrary, during winter days A heat island of intensity appeared. This difference is more related to the geographical environment of the city. The vastness of China has caused few cities to be built entirely near the sea. Even in a port city like Tianjin, the city center is quite far from the sea. However, due to topographical factors, the development of the urban coastal plains caused by the sea breeze, the heat island effect is far weaker than that of Chinese cities. In addition, from the perspective of urban development, as urbanization progresses, the heat island effect will often increase year by year, and the heat island effect of shrinking cities will be relieved to some extent.

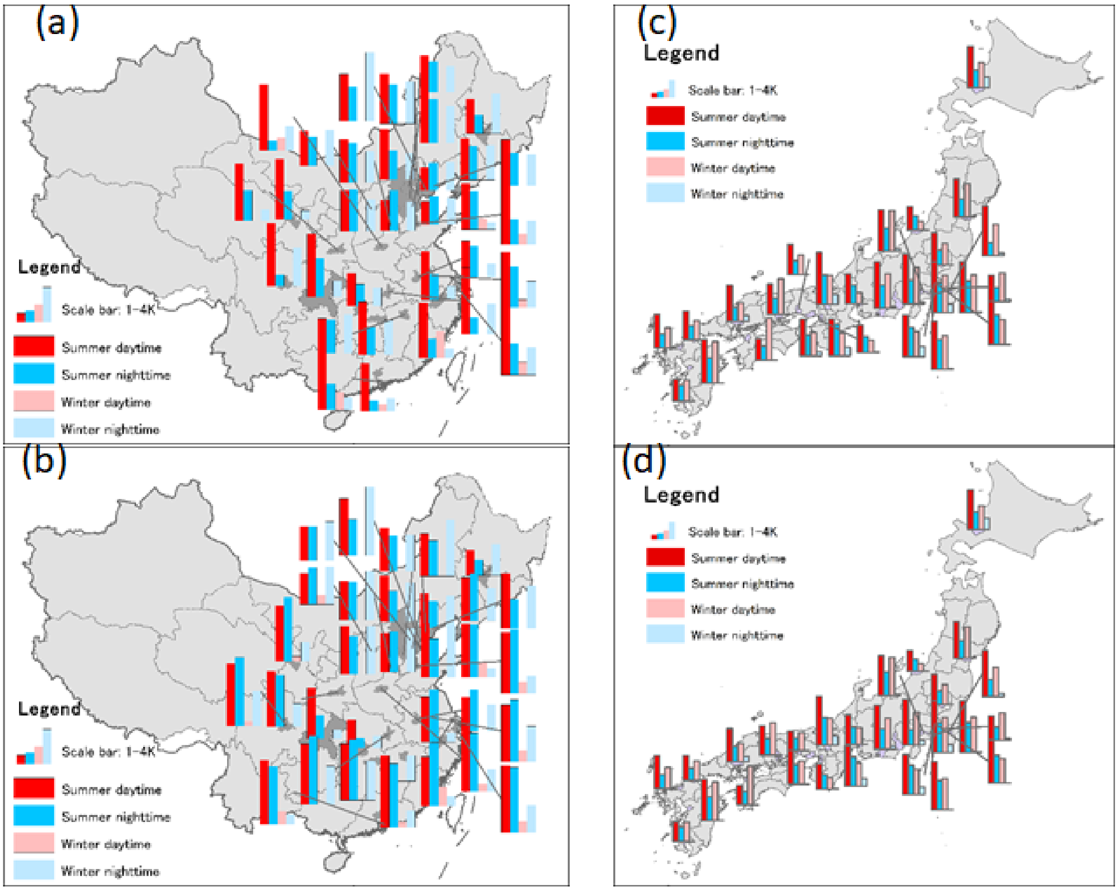

Fig. 8-8 SUHII of selected cities of (a) China in 2005, (b) China in 2015, (c) Japan in 2005, (d) Japan in 2015.

Numerous studies focused on the correlation between UHI and urban configurations including land use and land cover (LULC), indicators related to LULC, such as Normalized Difference Vegetation Index (NDVI), Normalized Difference Building Index (NDBI), Normalized Difference Water Index (NDWI), and indicators related to urban activity such as nighttime light (NTL) [10, 22-25]. With large populations shifting from rural to urban, the rapid development of economy, and improvement of social infrastructure, the increase of built-up areas density and human activity within a city and the urban sprawl are the main reasons for increasing SUHI phenomenon. As a countermeasure, the increase in vegetation cover area was an effective way to buffer environment temperature in a city [26-28]. However, in an urban center, the setbacks such as damage to buildings by roots and other dangerous compounds were required when considering vegetation planting in urban areas [28, 29].

8.4 Conclusion

In this chapter, the history of urban development process in China and Japan is summarized. The cities of China and Japan are developing steadily. However, the current urban population ratio in China still lags far behind Japan. In addition, both countries have periods of unstable development and periods of dis-urbanization in the process of urban development, mostly because of the social environment and corresponding government policies. Now, the demographic factors have a great spatially non-stationary impact on urban shrinkage of cities in Japan, while have a little spatially stationary impact on urbanization in China. The economic factors have a little spatially stationary impact both in China and Japan. In addition, the social factors have great spatially non-stationary impact on urbanization of cities in China while the effect is global and little in Japan.

In addition, time-series of MODIS LST data were used to compare the UHI phenomena in the cities within different urban development phase and sizes from 2005 to 2015, and strong SUHI were found among the cities. Through the SUHII quantified by estimation for each LST composition of the individual cities for comparison. There was a piece of strong evidence showing that SUHI was related to city size based on the SUHII results that SUHI vary spatially with a sequence of mega-city > large-city > mid-city; whilst SUHI vary temporally with a course of summer > winter and daytime > nighttime through differences of SUHI through time. Also, significant increases both in extent and magnitude of SUHI were observed for the 60 cities.

The major cities in Japan are located near the sea, and the selected research objects Fukuoka and Kitakyushu have no heat island phenomenon in winter nights, and the heat island intensity in summer nights is much less than that of Chinese cities. On the contrary, during winter days A heat island of intensity appeared. This difference is more related to the geographical environment of the city. The vastness of China has caused few cities to be built entirely near the sea. Even in a port city like Tianjin, the city center is quite far from the sea. However, due to topographical factors, the development of the urban coastal plains caused by the sea breeze, the heat island effect is far weaker than that of Chinese cities. In addition, from the perspective of urban development, as urbanization progresses, the heat island effect will often increase year by year, and the heat island effect of shrinking cities will be relieved to some extent.

In the foreseeable future, the comprehensive urbanization process in the Beijing city cluster will be the main component of China's urbanization. While Japan will face increasing urban shrinkage phenomena.

Reference

[1] Lockwood WW. Economic development of Japan: Princeton University Press; 2015.

[2] Wu F, Xu J, Yeh AG-O. Urban development in post-reform China: State, market, and space: Routledge; 2006.

[3] Bai X, Shi P, Liu Y. Society: Realizing China's urban dream. Nature News. 2014;509:158.

[4] Sorensen A. The making of urban Japan: cities and planning from Edo to the twenty-first century: Psychology Press; 2002.

[5] Zhu X, Gao W, Zhou N, Kammen DM, Wu Y, Zhang Y, et al. The inhabited environment, infrastructure development and advanced urbanization in China's Yangtze River Delta Region. Environmental Research Letters. 2016;11.

[6] dos Santos AR, de Oliveira FS, da Silva AG, Gleriani JM, Gonçalves W, Moreira GL, et al. Spatial and temporal distribution of urban heat islands. Science of the Total Environment. 2017;605:946-56.

[7] Gallo KP, Owen TW. Satellite-based adjustments for the urban heat island temperature bias. Journal of applied meteorology. 1999;38:806-13.

[8] Sobrino JA, Jiménez-Muñoz JC, Zarco-Tejada PJ, Sepulcre-Cantó G, de Miguel E. Land surface temperature derived from airborne hyperspectral scanner thermal infrared data. Remote Sensing of Environment. 2006;102:99-115.

[9] Streutker DR, Glenn NF. LiDAR measurement of sagebrush steppe vegetation heights. Remote Sensing of Environment. 2006;102:135-45.

[10] Liu L, Zhang Y. Urban heat island analysis using the Landsat TM data and ASTER data: A case study in Hong Kong. Remote Sensing. 2011;3:1535-52.

[11] Pu R, Gong P, Michishita R, Sasagawa T. Assessment of multi-resolution and multi-sensor data for urban surface temperature retrieval. Remote Sensing of Environment. 2006;104:211-25.

[12] Quan J, Chen Y, Zhan W, Wang J, Voogt J, Wang M. Multi-temporal trajectory of the urban heat island centroid in Beijing, China based on a Gaussian volume model. Remote Sensing of Environment. 2014;149:33-46.

[13] Fu P, Weng Q. Consistent land surface temperature data generation from irregularly spaced Landsat imagery. Remote Sensing of Environment. 2016;184:175-87.

[14] Weng Q, Fu P. Modeling annual parameters of clear-sky land surface temperature variations and evaluating the impact of cloud cover using time series of Landsat TIR data. Remote Sensing of Environment. 2014;140:267-78.

[15] Holben BN. Characteristics of maximum-value composite images from temporal AVHRR data. International journal of remote sensing. 1986;7:1417-34.

[16] Sellers PJ, Tucker CJ, Collatz GJ, Los S, Justice C, Dazlich D, et al. A global 1 by 1 NDVI data set for climate studies. Part 2: The generation of global fields of terrestrial biophysical

parameters from the NDVI. International Journal of Remote Sensing. 1994;15:3519-45.

[17] Peng S, Piao S, Ciais P, Friedlingstein P, Ottle C, Bréon Fo-M, et al. Surface urban heat island across 419 global big cities. Environmental science & technology. 2011;46:696-703.

[18] He K, Huo H, Zhang Q. Urban air pollution in China: current status, characteristics, and progress. Annual review of energy and the environment. 2002;27:397-431.

[19] Sang J, Liu H, Liu H, Zhang Z. Observational and numerical studies of wintertime urban boundary layer. Journal of Wind Engineering and Industrial Aerodynamics. 2000;87:243-58.

[20] Zhou D, Zhao S, Liu S, Zhang L, Zhu C. Surface urban heat island in China's 32 major cities: Spatial patterns and drivers. Remote Sensing of Environment. 2014;152:51-61.

[21] Yao R, Wang L, Huang X, Niu Z, Liu F, Wang Q. Temporal trends of surface urban heat islands and associated determinants in major Chinese cities. Science of the Total Environment. 2017;609:742-54.

[22] Weng Q, Lu D, Schubring J. Estimation of land surface temperature–vegetation abundance relationship for urban heat island studies. Remote sensing of Environment. 2004;89:467-83.

[23] Lu D, Weng Q. A survey of image classification methods and techniques for improving classification performance. International journal of Remote sensing. 2007;28:823-70.

[24] Lu D, Weng Q. Use of impervious surface in urban land-use classification. Remote Sensing of Environment. 2006;102:146-60.

[25] Buyantuyev A, Wu J. Urban heat islands and landscape heterogeneity: linking spatiotemporal variations in surface temperatures to land-cover and socioeconomic patterns. Landscape ecology. 2010;25:17-33.

[26] Yu C, Hien WN. Thermal benefits of city parks. Energy and buildings. 2006;38:105-20.

[27] Tran H, Uchihama D, Ochi S, Yasuoka Y. Assessment with satellite data of the urban heat island effects in Asian mega cities. International journal of applied Earth observation and Geoinformation. 2006;8:34-48.

[28] Anyanwu E, Kanu I. The role of urban forest in the protection of human environmental health in geographically-prone unpredictable hostile weather conditions. International Journal of Environment Science and Technology. 2006;3:197-201.

[29] Doick KJ, Hutchings T. Air temperature regulation by urban trees and green infrastructure: Forestry Commission; 2013.

Chapter 9. Conclusion

9.1 Conclusion

The development of the city is the current main theme. However, the development stages of cities in the world are very different. China is mainly faced with uncoordinated development caused by rapid urbanization, large environmental problems, and obvious regional differences. And Japan is facing a serious problem of shrinking cities.

This study compares the urban development of China and Japan and its environmental impact, and analyzes the development of the city from large scale and medium-small scale. In addition, this study focused on exploring the role of spatial independence and spatial heterogeneity in urban development and its inner correlation with environment implications.

The main works and results can be summarized as follows:

In *chapter one*, PREVIOUS STUDY AND PURPOSE OF THE STUDY, research background and significance of urban development and environmental implications is demonstrated. In addition, the importance of plan and evaluation of urban environment is analyzed and the previous study about this research is reviewed. Then the purpose of the study is proposed.

In *chapter two*, THERIES AND METHODS OF URBAN DEVELOPMENT ASSESSMENT, firstly, the concept and application of GIS and RS is introduced. In addition, theory, development history and application methods for ESDA are described. Finally, this thesis presents a loose-coupled urban development evaluation method considering the strength and weakness of both the GIS and RS. The requirement, conceptual framework and integration component for the association between GIS and RS is discussed.

In *chapter three*, SPATIAL TEMPORAL ASSESSMENT OF URBANIZATION IN CHINA, we developed OLS, GWR, and SGWR models to capture the spatiotemporal differences in determinants affecting urbanization in China based on national statistics data from 2005 to 2015. The correlation between the demographic, economic, infrastructure and social indexes and urbanization was revealed through quantitative analysis. PCGDP, GDPS, AFC, and EMBC, which refer to the economy development and urban infrastructure, were the critical spatially non-stationary correlates, with large estimated coefficients, affected the urbanization in different regions at different times. UPR, HIRE which refer to the demographic structure and educational resources with large estimated coefficients, affected the urbanization spatially stationary. The findings contribute to improving our understanding of the situation and correlates of urbanization, and provide valuable information for governments and planners when developing effective coping strategies for sustainable city development.

In *chapter four*, SPATIAL TEMPORAL DETERMINANTS OF CITY SHRINKAGE IN JAPAN, we developed OLS, GWR, and SGWR models to capture the spatiotemporal differences in determinants affecting city shrinkage in Japan based on national census data from 2005 to 2015. City shrinkage in Japan is a serious national problem, which showed a significant increasing positive spatial autocorrelation; Hokkaido, Tohoku, and Shikoku had the largest shrinking city clusters, and this phenomenon has already occurred in suburban areas around the Tokyo and Nagoya city clusters. The correlation between the demographic, economic, and social indexes and city shrinkage was revealed through quantitative analysis. Low fertility, ageing population, and industry changes, expressed by APR, UPR, and ECR, were the critical spatially non-stationary correlates, with large estimated coefficients, affected the city shrinkage in different regions at different times. The findings contribute to improving our understanding of the situation and correlates of city shrinkage, and provide valuable information for governments and planners when developing effective coping strategies for city regeneration.

In *chapter five*, COMPREHENSIVE EVALUATION OF URBANIZATION PROCESS IN BEIJING CITY CLUSTER, the coupling coordination degree model make it possible to assess the comprehensive level of urbanization for cities in the Beijing city cluster from 2000 to 2017. The results suggest that those five indicators made the enormous contribution in evaluating the urbanization level, and determining the coupling coordination degree of urbanization. Besides, the results reveal that the coordinated urbanization in the region from ‘barely coordination’ to ‘medium coordination’ to ‘good coordination’. This study can provide useful information for understanding the current level of urbanization and promoting sustainable development in the future. In the foreseeable future, the comprehensive urbanization process in the Beijing city cluster will be the main component of China’s urbanization. Our empirical analysis for the 13 cities in the Beijing city cluster illustrated that the coupling coordination urbanization model is a useful tool which contribute to improve the understanding of the urbanization process and help with management policies and strategies for comprehensive development of urbanization for cities and balanced development for the region.

In *chapter six*, CORRELATION ANALYSIS OF POPULATION CHANGE AND URBAN VITALITY IN KITAKYUSHU, we first applied global and local Moran’s tests to investigate the population change since the city plan with the concept of compact city come out. According to the results of local Moran’s I statistics, there are six main regions with their own characteristics of population shrinkage and expansion. The shrinkage and expansion of the six main regions in Kitakyushu have some similarities, but the differences are larger. The government wish the compact city model to creates benefits that are attractive to modern urbanites. The desired benefits include shorter commute times, reduced environmental impact of the community, and reduced consumption of fossil fuels and energy.

In *chapter seven*, SPATIAL TEMPORAL ANALYSIS OF THERMAL ENVIRONMENTAL IMPLICATIONS BASED ON REMOTE SENSING, we developed random forest models to downscale the MODIS LST products during eight periods in Fukuoka, Japan. Then we captured the spatial correlation between the population, the LULC, and LSTs, and then we explored the cooling effect potential of the urban blue-green spaces. The downscaled LST results showed good fitting performance of the RF model. With such downscaling methods, analysis on the SUHI and its correlates could be spatial-temporal precisely in a cloudy, rainy area using remote sensing data. We found the LULC could have an impact on the LST of its surrounding neighbors, and which also is the basis for investigating the cooling effect of the urban blue-green spaces. Through zonal statistics, the forest and sea could significantly mitigate the UHI in its approximate 1 km buffer zone, while the mitigation effect of the water and the grassland on the UHI are less spectacular compared with the forest and sea. The findings contribute to improving our understanding of the spatial temporal variation and the correlates of UHI, and provide valuable information for governments and planners to developing effective coping migration strategies for the UHI considering the perspective of the local environment.

In *chapter eight*, COMPARISON OF URBAN DEVELOPMENT AND THERMAL ENVIRONMENT IN CHINA AND JAPAN, the history of urban development process in China and Japan is summarized. The economic factors have a little spatially stationary impact both in China and Japan. In addition, the social factors have great spatially non-stationary impact on urbanization of cities in China while the effect is global and little in Japan. Moreover, strong evidence showing that SUHI was related to city size based on the SUHII results that SUHI vary spatially with a sequence of mega-city > large-city > mid-city; whilst SUHI vary temporally with a course of summer > winter and daytime > nighttime through differences of SUHI through time. Also, significant increases both in extent and magnitude of SUHI were observed for the 15 cities. In the foreseeable future, the comprehensive urbanization process in the Beijing city cluster will be the main component of China's urbanization. While Japan will face increasing urban shrinkage problems.

In *chapter nine*, CONCLUSION, the whole summary of each chapter has been presented.